# Injectable biodegradable carriers for the delivery of therapeutic agents and tissue engineering

**Author: Riccardo Levato**
**Universitat Politècnica de Catalunya, Barcelona, España**
**Director: Dr. Miguel Ángel Mateos-Timoneda**
**UPC tutor: Dr. Elisabeth Engel**

**Programa de Doctorat en Enginyeria Biomédica**

**Departament de Enginyeria Biomédica**

**Universitat Politècnica de Catalunya**

**Barcelona, 2014**

**Tesis presentada per obtenir el títol de Doctor per la Universitat Politècnica de Catalunya**





**Vol. I**

*A mio padre e mia madre, Domenico e Maria Carla*

*Until you attain the truth, you will not be able to amend it.*
*But if you do not amend it, you will not attain it.*
*In the meanwhile, do not give up.*

*(José Saramago, Book of Advices, in "History of the Siege of Lisbon")*

# INDEX

# ABSTRACT

The design of smart biomaterial devices plays a key role to improve the way conventional therapies are being administered, as well as to promote the development of new approaches for advanced therapies, such as regenerative medicine and targeted drug release. Injectable biodegradable materials, such as those consisting of suspensions of polymeric particles, are highly versatile devices that can be delivered through minimally-invasive injections. The physic-chemical properties of the particles can be engineered to obtain smart scaffolds for tissue engineering, carriers for drug release and cell culture and therapy. The aim of this Thesis is to develop a novel class of biodegradable and injectable particulate carriers based on polylactic acid (PLA), that are capable to trigger and guide specific responses from the cells and the biological milieu. First, a novel route to fabricate PLA-based microcarriers (MCs) is set and characterized. This production method involves green, non-harmful chemicals and it is easy to scale-up. Such technique allows controlling key MC parameters, such as size and size distribution, which can be tuned in the range suitable for drug and cell delivery applications. The favorable regulatory status of the materials and reagents used to fabricate the MCs, may also be beneficial for the translation of the produced particles from bench to bedside. The principles guiding this fabrication procedure can inspire also techniques to generate nanocarriers for controlled drug delivery. Recent studies point out the importance of drug-loaded and submicron-sized biomaterials in the treatment of severe clinical conditions, such as persistent biofilm infections. These nanoparticles (NPs) can also be endowed with smart functionalities to enhance drug delivery through the biofilm matrix. In this way, NPs encapsulating the antibiotic ciprofloxacin have been produced and functionalized with DNase I. These carriers target and degrade directly the biofilm matrix, thus improving antimicrobial activity of the encapsulated drug and promoting established biofilm eradication. On the other hand, larger particles such as MC, display a suitable surface area for cell expansion. MCs can also be used to deliver cells with therapeutic potential as "living drugs", ideally in a spatio-temporal controlled fashion. This is especially important, as cell injection in standard cell therapies, often renders the treatment ineffective, as it is accompanied by massive cell mortality. PLA MCs modified with different functionalization approaches and suitable to support homing and survival of Mesenchymal Stromal Cells (MSCs) have been produced. The physic-chemical properties of the MCs and biofunctionalized coatings play an important role on cell adhesion, proliferation and migratory potential in response to chemokines that are fundamental in controlling MSC tissue localization, like SDF-1α. The results highlight the importance of carriers design to control cell release and delivery, and provide important considerations to instruct a new generation of efficient cell carriers. Another exciting application of injectable MCs is to use cell-laden particles as building blocks to fabricate living tissues *in vitro*. Combination of MC technology with 3D bioprinting is an appealing strategy to generate grafts of multimaterial tissues with controlled architectures. The suspension of injectable PLA cell-laden MCs within hydrogel-forming, gelatin-based materials generated an extrudable, composite bioink. MCs can be used as mechanical reinforcement for soft hydrogels and as means for cell expansion (for instance in a spinner flask bioreactor) to encapsulate high cell payload. MSCs on surface functionalized PLA

MCs were shown to form MC-MSCs aggregates, with enhanced cell-to-cell contact, and were shown to differentiate towards the osteogenic lineage. This result suggests potential applications of MC-MSCs laden bioinks for bone tissue engineering, and the composite material is proposed as component to build 3D printed osteochondral graft models. Taken together, the injectable devices developed in the Thesis constitute a promising biomaterial platform for biomedical applications with high versatility, which can be employed in a wide array of tissue engineering, and cell and drug delivery strategies.

# RESUMEN

El diseño de dispositivos basados en biomateriales inteligentes, juega un papel fundamental a la hora de mejorar las terapias convencionales, así como en el desarrollo de nuevas estrategias para la medicina regenerativa y la liberación controlada de fármacos. Materiales inyectables biodegradables, tales como las suspensiones de partículas poliméricas, constituyen dispositivos versátiles, que se pueden suministrar por medio de inyecciones mínimamente invasivas. Las propiedades físico-químicas de las partículas pueden ser modificadas para obtener andamios inteligentes para la ingeniería de tejidos, transportadores para liberación de fármacos y cultivo y terapia celular. El objetivo de esta Tesis es el desarrollo de una nueva clase de partículas transportadoras inyectables y biodegradables, basadas en ácido poliláctico (PLA), que sean capaces de desencadenar y guiar respuestas específicas por parte de las células y del entorno biológico. Primero, se ha creado y caracterizado una nueva ruta para fabricar microstransportadores (MCs) basados en PLA. Este método de producción utiliza reactivos verdes y no-tóxicos, y es sencillo de adaptar para la fabricación a gran escala. Esta técnica permite controlar parámetros fundamentales en las MCs, tales como su tamaño y dispersión, que pueden ser controlados dentro de los rangos adecuados para aplicaciones de liberación de fármacos y células. El hecho que los materiales y reactivos utilizados están bien aceptados por las agencias reguladoras, puede favorecer el traslado de las partículas fabricadas desde la investigación hasta la práctica clínica. Los principios de este método pueden adaptarse a otras técnicas de fabricación para generar nanotransportadores (nanopartículas, NPs) de fármacos. Estudio recientes subrayan la importancia de biomateriales submicrométricos cargados con compuestos bioactivos en el tratamiento de enfermedades, tal como las infecciones provocadas por biofilms. Estas NPs pueden ser modificadas con funcionalidades inteligentes, para mejorar la distribución del fármaco en la matriz del biofilm. De esta manera, se han producido NPs que encapsulan el antibiótico ciprofloxacino, modificadas superficialmente con DNasa I. Estos transportadores tienen como diana la matriz que compone el biofilm y pueden degradarla, incrementando la actividad antibacteriana del ciprofloxacino y promoviendo la erradicación de los biofilms. Por otra banda, las partículas más grandes, como las MCs, poseen una superficie adecuada para la expansión celular. Las MCs se pueden usar para transportar "drogas vivas", es decir células con potencial terapéutico, posiblemente controlando su distribución espacial y su cinética de liberación. Esto es de particular importancia, porque la ineficiencia de muchas terapias celulares actuales se debe a la gran cantidad de células que no sobreviven una vez inyectadas *in vivo*. Se han producido MCs de PLA modificadas por diferentes estrategias de funcionalización y aptas para suportar en su superficie células madres mesenquimales (MSCs). La biofuncionalización y las propiedades físico-químicas de las MCs juegan un papel fundamental en la adhesión y proliferación célular, así como la capacidad de las MSCs de migrar en respuesta a estímulos quimiotácticos, que regulan su localización en los tejidos, tal como el SDF-1α. Los resultados subrayan la importancia del diseño de las MCs para controlar la liberación de las células, y a la vez aportan información para desarrollar una nueva y más eficiente generación de transportadores de células. Otra aplicación prometedora de las MCs inyectables es su uso como bloques de construcción para fabricar

tejidos vivos *in vitro*. La combinación de la tecnología de las MCs con la bioimpresión 3D constituye una estrategia atractiva para obtener injertos de tejidos multimateriales con arquitectura controlada. Se han obtenido biotintas compuestas y capaces de ser extruidas mezclando materiales basados en hidrogeles de gelatina con las MCs de PLA cargadas con células. Las MCs actúan de refuerzo mecánico para el hidrogel y como vehículo para la expansión celular (por ejemplo, en un bioreactor "spinner flask") para encapsular elevadas cantidades de células. Las MSCs forman agregados células-particulas, una vez sembradas en las superficies de las MCs, y estos complejos, ricos en contactos célula-célula, se demostraron capaces de suportar la diferenciación osteogénica de las MSCs. Este resultado sugiere potenciales aplicaciones de las biotintas cargadas de agregados de MCs y MSCs para la ingeniería del tejido óseo. Esta biotinta ha sido también utilizada como componiente para generar un modelo de injerto osteocondral, por medio de una técnica de impresión 3D. El conjunto de dispositivos inyectables desarrollados en esta Tesis constituyen una plataforma muy versátil y prometedora para aplicaciones biomédicas, en particular en estrategias de ingeniería de tejidos, y liberación de células y fármacos.

# List of Figures

Figure 2.24: (A) Liquid jets are experienced every day, for instance, as water flowing from a faucet. Fluids at a nozzle tip can generate (B) large drops by dripping or stretch into laminar jets that will eventually break-up into a train of similarly-sized droplets. (D) Turbulent flows, for instance those generated by high pressures, can break into a spray of polydispersed droplets. Jet stability and break-up also depend of the flow speed,

# List of Tables

# List of Abbreviations

2D – Two dimensional

3D – three dimensional

ACC – Adrenal chromaffin cells

ACI – Autologous chondrocytes transplantation

ADMEM – Advanced Dulbecco's modified Eagle medium

AFSC – Amniotic fluid stromal cells

ALP – Alkaline phosphatase

AM – Additive manufacturing

AR S – Alizarin Red Staning

ASC – Adipose derived stromal cells

ATCC – American type culture collection

BSA – Bovine serum albumin

CAD/CAM – Computer-aided design and manufacturing

CaP – Calcium Phosphate

CC – Collagen covalent

CD – Cluster of differentiation

CECT – Spanish type culture collection

CLSM – Confocal laser scanning microscope

CP – Collagen physisorbed

CPX – Ciprofloxacin

CXCL12 – Chemokine (C-X-C motif) ligand 12

CXCR4 – Chemokine (C-X-C motif) receptor 4

DN – Dual nozzle

DNA – Deoxyribonucleic acid

DSC – Differential scanning calorimetry

ECM – Extracellular matrix

EDC – 1-Ethyl-3-(3-dimethylaminopropyl)carbodiimide

ELISA – Enzyme-linked immunosorbent assay

EPC – Endothelial progenitor cells

ESC – Embryonic stem cells

FACS – Fluorescence activated cell sorting

FBS – Fetal bovine serum

FDA – Food and Drug Administration

GAG – Glycosaminoglycan

GelMA – Gelatin methacrylamide

GG – Gellan Gum

GMP – Good manufacturing practice

HSC – Hematopoietic stem cells

IL – Interleukin

iPSC – Induced pluripotent stem cells

IVD – Intervertebral disc

LBL – layer-by-layer

LDH – lactate dehydrogenase

LS – Low serum medium

MBEC – Minimal biofilm eradication concentration

MCP – Monocyte chemoattractant protein

MCs – Microcarriers

MIAMI – Marrow-isolated adult multilineage inducible cells

MIC – Minimum inhibitory concentration

Micro BCA – Micro bicinchoninic acid assay

MPs – Microparticles

MSCs – Mesenchymal stromal cells

Mw - Molecular weight

MWCO – Molecular weight cut-off

NCs – Nanocarriers

NHS – N-Hydroxysuccinimide

NIPS – non-solvent induced phase separation

NPs – Nanoparticles

OCN – Osteocalcin

OPF – Oligopropylene fumarate

PAM – Pharmacologically active microcarrier

PBS – Phosphate buffered saline

PCL – Polycaprolactone

PDMS – Polydimethylsiloxane

PEG – Polyethylene glycol

PEGdA – Polyethyleneglycol diacrylate

PEO – Polyethylene oxide

PFA – Paraformaldehyde

PGA – Polyglycolic acid

PHBV – Poly(hydroxy butyrate-co-valerate)

PL – Polylysine

PLA – Polylactic acid

PLGA – Poly(lactic-co-glycolic) acid

PPF – Polypropylenefumarate

PSCs – Pluripotent stem cells

PTFE – Polytetrafluoroethylene

PVA – Polyvinyl alcohol

RC – RGD covalent

RGD – Arginine-Glycine-Aspartic acid

RP – RGD physisorbed

RPE – Retinal pigment epithelium cells

SCF – Supercritical fluid

SD – Standard deviation

SDF – Stroma cell-derived factor

SEM – Scanning electron microscopy

SMC – Smooth muscle cells

TCP – Tricalcium phosphate

TCPS - Tissue culture polystyrene

TE – Tissue engineering

Tg – Glass transition temperature

TGF – Tumor growth factor

TIPS – Thermally induced phase separation

Tm – Melting temperature

TNF – Tumor necrosis factor

UV – Ultraviolet

VEGF – Vascular endothelial growth factor

μCT – Micro-computed tomography

# Chapter 1

# General Introduction

## 1.1 General introduction, motivation and aim of the Thesis

The latest years have been characterized by significant progresses in biology, pharmacology and medicine. Significant advances in the knowledge of biological systems, their pathologies and regenerative processes, go along with the understanding of cell and tissue behavior, as well as the development of novel pharmaceutical compounds. This progress are paving the way for new paradigms in medicine, centered on personalized, regenerative therapies and routes for specific and controlled delivery of therapeutic compounds [1]. A great push in this direction comes from the field of biomedical engineering, which applies the principles of engineering to biological systems to obtain predictive models for cells, tissues and organs, and to design technological solutions to diagnose the status –health/disease- of such systems and restore, maintain or improve their functionality. As this definition suggests, biomedical engineering covers a wide variety of applications and is intrinsically multidisciplinary. In this field, the tools and the scientific lore of "classical" engineering (structural, mechanical, electronic and chemical, to mention some), are used to understand, model and solve problems related to a highly complex and yet not fully understood system: the human body. This challenge certainly makes biomedical engineering an extremely fascinating field of research: the possibility to apply its knowledge to prevent or cure pathologies and to improve life conditions of patients is a driving force for scientific research. Moreover, the potential to design and implement devices capable to translate this knowledge into clinical practice provides strong motivation for this investigation.

A multitude of technologies - pacemakers, devices for dialysis and extracorporeal circulation, medical imaging techniques, substitute heart valves, hip prosthesis, to name a few- have been solidly implemented in medicine in the past century, and are nowadays part of common clinical practice. Research in bioengineering is strongly oriented to provide new answers to health issues. Personalized therapies, computational predictive models, advanced drug delivery and regenerative medicine are a few keywords indicating the current directions of scientific research that promise to describe the medical practice of the next future.

The field of *Biomaterials* plays an important role in this direction. Biomaterials are required whenever there is a need for a *physical* component of a device that enters in contact with a biological system, may it be inside the body such as prosthesis or outside (i.e. components of a heart-lung machine in contact with the blood, sensors in equipments to analyze biological fluids).

There is a continuous crosstalk between novel therapies and developments in biomaterials, and the need of new approaches to biomaterials sciences and engineering goes together with the need of healthcare for society; which is increasing, due the aging of the population in the developed countries [2].

Biomaterials need to be designed as smart devices, capable i) to improve the way conventional therapies are being administered, ii) to trigger specific responses once in contact with the biological milieu, iii) as well as to promote the development of new approaches for advanced therapies, such as tissue engineering and cell delivery [3]. Following these guidelines, for instance, biomaterials can be used as drug delivery devices, carriers for cell therapy, scaffolds for tissue engineering and platforms to build 3D tissue models for in *vitro*

drug screening. Furthermore, biomaterials meant to be administered into the body should be biodegradable, in order to be safely removed or metabolized by the organism, once their function is fulfilled [4].

Furthermore, biomaterials devices should be easy to apply, possibly with minimally invasive injections and no need for surgical intervention. This specification is greatly appealing, as it improves the compliance of patients to the treatment and facilitates the translation of the biomaterial device to the clinical practice [5].

Among the various classes of injectable materials, **this Thesis focuses on the development of injectable and biodegradable polymeric micro- and nanoparticles. Versatility is a key advantage of micro- and nanocarriers, which can address a wide range of applications, alone or in combination with other materials, such as the delivery of therapeutic agents, to act as culture supports and as cell-instructive components in regenerative medicine strategies. The aim of this work is to study novel approaches to generate and design such carriers, as well as how to control and choose the material properties in order to generate effects on specific biological targets. In this way, antibacterial as well as cell-fate guiding materials can be obtained. Moreover, these injectable materials are studied as components to build living tissues *in vitro* by means of biofabrication and tissue engineering strategies.**

## 1.2    Outline of the Thesis

The outline of the Thesis is schematized in Figure 1.1.
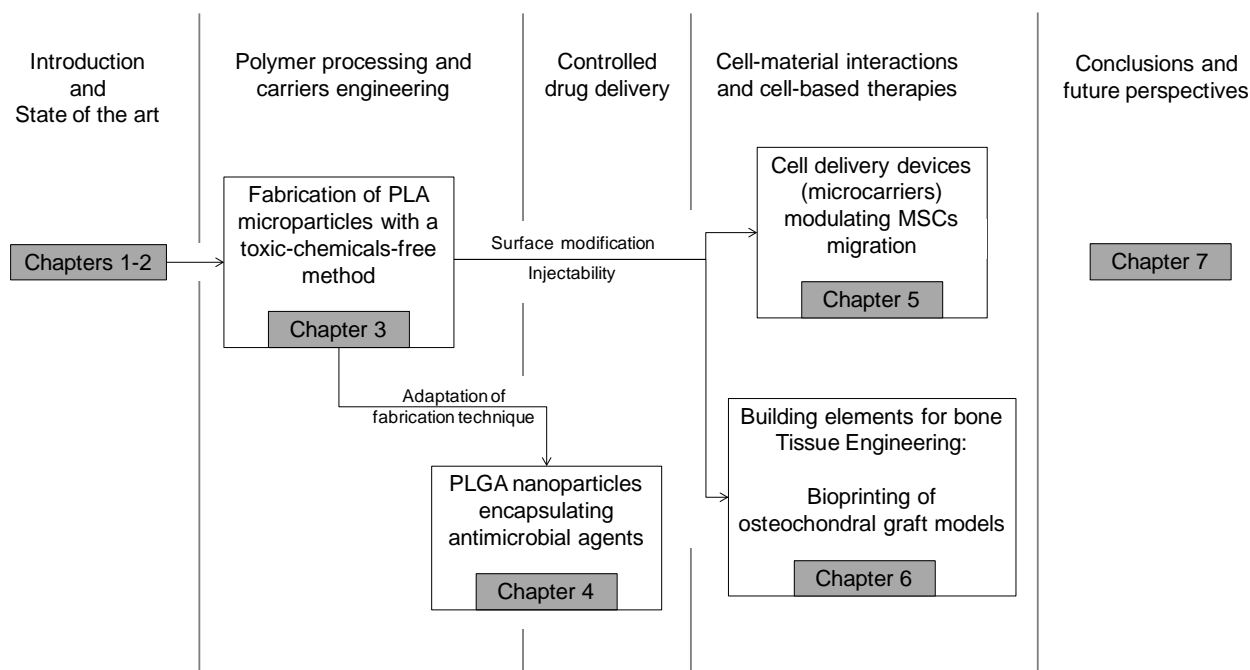


**Figure 1.1: Outline of the Thesis**

In *Chapter 2* a general introduction to the most important topics developed in the Thesis is provided. A review about biomaterials, with a special focus on biodegradable polymers and their chemical modification to tune their biological activity is provided, together with a description of classes of injectable polymers, and their application in controlled drug delivery, cell therapy and tissue engineering. The main concepts belonging to such areas of biomedical research and clinics are also described and summarized. Moreover, Chapter 2 provides an overview of the state-of-the-art concerning biodegradable injectable micro- and nanocarriers. The review covers topics ranging from the fabrication of such devices, their interaction with the biological environment and application in bioengineering. Furthermore the main research trends and open perspectives in the area of polymeric particulate carriers are discussed.

In *Chapter 3* a novel method to produce microparticles (MPs) made of polylactic acid (PLA) is described. This technique, based on the generation and break-up into droplets of a polymer solution jet by means of hydro- and aerodynamic forces, was set using no toxic chemicals. The most important engineering parameters involved in polymer processing and MPs fabrication are analyzed, in order to set a straight-forward, clean, scalable technique to generate MPs with controlled size. The method was also designed to allow the possibility to encapsulate bioactive compounds into the fabricated MPs. Morphology of the MPs is extensively studied, and potential biomedical applications of the particles generated with this method are discussed.

*Chapter 4* presents a modification of the method described in Chapter 3 to fabricate Nanoparticles (NPs). NPs were characterized as controlled drug delivery devices, and used to encapsulate ciprofloxacin, a broad-spectrum antibiotic. The results of NPs *in vitro* application to treat bacterial infection, with particular attention to their ability to eradicate biofilm infections, are also presented. The issue of surface modification of NPs is also introduced and studied. NPs were endowed with specific functionalities to interact actively with their target, the biofilm extracellular matrix, using different coatings.

In *Chapter 5* the MPs obtained with the technology introduced in Chapter 3, were evaluated as delivery vehicles for cell therapy applications. In particular, the potential of these MPs to act as microcarriers (MCs) for the controlled release of Mesenchymal Stromal Cells (MSCs) is assessed. These MCs were submitted to two different surface treatments and modified with recombinant collagen and RGD peptide coatings, and the role of such functionalization techniques on MSCs behavior in terms of homing, adhesion, proliferation and migratory potential is described through *in vitro* assays. Particularly, the specific migratory response triggered by SDF-1α, a key chemokine in stem cells recruitment *in vivo* is studied. Injectability of MSC-laden MCs is also discussed. The results collected with this research can offer guidelines for the choice and design of more efficient cell carriers, capable to guide MSCs therapeutic activity.

In *Chapter 6* MCs selected based on the results obtained in Chapter 5 are tested as elements to build living tissue grafts using a biofabrication technique, for innovative applications in Tissue Engineering. MCs are used to generate MC-MSCs complexes, via static and dynamic culture in a spinner flask. MSC-laden MCs

are suspended into a gelatin(methacrylamide)/gellan gum hydrogel to generate an injectable composite material. The potential of the MCs to improve the gel mechanical properties, as well as to act as a homing material to guide MSCs fate and promote osteogenic differentiation are analyzed. Using MSC-laden MCs, the hydrogel-MCs composite is employed as a bioink, and through a bioprinting technique, 3D constructs are built. Clinically-relevant size models of an osteochondral graft are also generated with such technology. The implications of MCs culture combination with bioprinting are also discussed.

Finally, *Chapter 7* summarizes the overall conclusions to the topics described in the experimental work, and provides future perspectives for the continuation and application of the research developed in this Thesis.

## 1.3    References

[1]    Mhashilkar AM, Atala A. Advent and maturation of regenerative medicine. Curr Stem Cell Res Ther. 2012 7(6):430-45.

[2]    Zippel N, Schulze M, Tobiasch E. Biomaterials and mesenchymal stem cells for regenerative medicine. Recent Pat Biotechnol. 2010 4(1):1-22.

[3]    Holzapfel BM, Reichert JC, Schantz JT, Gbureck U, Rackwitz L, Nöth U, Jakob F, Rudert M, Groll J, Hutmacher DW. How smart do biomaterials need to be? A translational science and clinical point of view. Adv Drug Deliv Rev. 2013 65(4):581-603.

[4]    Place ES, Evans ND, Stevens MM. Complexity in biomaterials for tissue engineering. Nat Mater. 2009 8(6):457-70.

[5]    Dreifke MB, Ebraheim NA, Jayasuriya AC. Investigation of potential injectable polymeric biomaterials for bone regeneration. J Biomed Mater Res A. 2013 101(8):2436-47.

# Chapter 2

# Introduction and state of the art

## 2.1    Introduction to Biomaterials

Since the beginning of the use of materials as implants or devices in contact with the human body, a long road has already been walked down. Materials such as metals, glass and ceramics have been sporadically used as tissue grafts through history, and since the first decades of the 20th century pioneering physicians started to use plastics as well. However, most of these experiments were doomed to fail, due to the lack of understanding in matters of toxicology and foreign body reaction [1]. After 1960, a so-called first generation of biomaterials was developed for use as medical devices. They were mostly based on bioinert metals, ceramics and polymers, and aimed to minimize adverse host response after implantation and thus be tolerated by the human body. Despite of the development of these successful implants, such as artificial joints, heart valves, stents and ocular lenses, the understanding of biological repair and regeneration mechanisms, as well as of the interaction between materials and tissues was limited. Thus, the design of these devices was still mostly due to the choice of commodity products the surgeons could easily find, rather than being driven by biocompatibility issues [2].

It was not until the second half of the 20th century that biomaterials science and engineering became an important and recognized field of study, and from 1980s, the focus of the field moved towards the need of improving integration between (artificial) materials and living tissues. A second generation of bioactive materials, capable of promoting tissue ingrowth and device-tissue interlocking were produced. In this period, studying of phenomena at the biomaterial-tissue interface became fundamental, and lead to an increase in implants lifetimes [3]. In such context, biodegradable and bioresorbable materials acquired more and more importance, as they break into non-toxic compound, capable of being eliminated gradually from the body once their *in vivo* function is completed [4]. This scientific and cultural context is reflected in the by then accepted definition of the term "biomaterials" as "nonviable [materials] used in a medical device, intended to interact with biological systems" [5]. In the following years and up to recently, the increasing crosstalk between the fields of materials science and cellular, molecular and developmental biology has, instead, lead to expand and analyze in detail what that "interact with biological systems" implied, leading to a third generation of devices, that aimed to guide and promote the body regenerative/repairing processes, interacting directly with cells and providing physic-chemical signals to trigger the activation of genes implicated in ECM synthesis and tissue repair, for instance [6]. The wide spectrum of "interactions" that a biomaterial may establish with the biological milieu, together with the fact that several devices are nowadays composed by a combination of supporting materials and living cells at the same time, lead to the affirmation of more comprehensive definitions. Current biomaterials can be generally defined as "substances that have been engineered to take a form which, alone or as part of a complex system, is used to direct, by control of interactions with components of living systems, the course of any therapeutic or diagnostic procedure, in human or veterinary medicine" [7].

To date, biomaterials to improve human life have become key elements in medicine, and are growing more and more important. With the aging of population, the need for replacement and repair of degenerated or

diseased tissue and organ is also increasing. The consequences of this need for society are reflected by the size of the biomaterials industry, estimated around 28 billion US dollars, and by its growing market, which is expected to worth 58.1 billion US dollars by the present year [8].These impressive data and previsions go along with the increment in clinical demand and patient expectations.

Holding its footstep on this foreground, biomaterials science is moving forward from the research directions followed in the past decade, and aims to fabricate smart and biomimetic materials. Biological materials show an intimate relationship between shape and microstructure, as they both originate during the growth of the tissue and development of the organism [9]. This implies that form and structure are created in the same, self-assembly process, and such structures are able to remodel themselves and dynamically adapt to the different stimuli provided by the surrounding environment. Unlike engineered materials, the final result is not an *a priori* design, but rather the result of a dynamic evolution, and thus biological materials and tissues display high functional flexibility and adaptability. The concept of biomimicry in materials engineering follows the idea that matrices can be fabricated, which reproduce nature hierarchical structures and its simple and elegant mechanisms conserved through genera and species [8]. A summary of the different properties of biological, engineered and smart materials is presented in Table 2.1. However, since we are still long way from recreating exactly natural tissues and their full functionality, a key challenge in biomaterials design is to determine how and to which degree artificial devices should recreate the complexity of native tissues (i.ei, in terms of structure, morphology, biochemistry). Common strategies to generate smart materials include, for instance: modification of surface properties [11], design of advanced 3D architectures [12], pH/temperature responsiveness [13]. In general, such properties should provoke instructive effects over cells and tissues. However, the required degrees of complexity, the type of response the biomaterial needs to trigger, and the method to endow the device with smart functionalities, depend, of course, on the type of application that the material is designed for, as well as on the type of material. The generation of smart materials, is necessary for most regenerative therapies strategies -which include tissue engineering, cell therapy and gene therapy-since biomaterials can be actuators in directing cell and tissue behavior rather than passive spectators. Analogously, smart functionalities are keys to improve drug delivery devices, for example, by permitting triggered drug release under certain stimuli, creating drug carriers capable of targeting certain cells/tissue or mimicking some enzyme activity. Biodegradable polymers are the preferred choice for these applications, which require devices that are gradually removed during the timescale of the healing process [14].

**Table 2.1 Filling the gap. Biomimicry can help to design engineered materials that can reduce the difference between biological, living, materials, imitating their properties (adapted from [10])**

| Biological Materials | Engineered Materials | Smart Materials |
|---|---|---|
| Growth by biological controlled self-assembly | Fabrication (exact design) | Fabrication (exact design). Self-assembly techniques can be implemented |
| Hyerarchical structuring, from the nano- to the macroscale | Forming of the part, and after that, microstructuring of the material | Bottom-up assembly of units, or self-assembly strategies to induce a degree of hyerachical structure |
| Adaptation of form and structure to the application | Selection of the material(s) according to the function | Selection of the material(s) according to the function |
| Healing and Remodeling according to signal received from the environment | Secure design | Stimuli-responsive Cell-instructive |

## 2.2 Biomaterials in Regenerative Medicine

### 2.2.1 Tissue Engineering

One of the most promising fields of medicine is the substitution of damaged or diseased tissues, and the necessity of adequate tissue replacements is increasing as the population ages. Many current clinical strategies to treat tissue defects rely on autologous, heterologous or even xenogenic transplantation. However, such approaches are far from optimal. Autotransplantation is only possible for limited tissues, and implicates donor site morbidity. On the other hand, the difficulty in finding compatible donors, lack of a complete recover of tissue functionality and immunogenicity are the main drawbacks of heterologous transplantation. Furthermore, also xenogenic tissues and organ have important donor-host compatibility issues and expose the recipient to the risk of cross-species transmission of pathologies. Donor compatibility, in particular, often requires the patient to undergo pharmacological treatments (e.g. immunosuppression) that may have important side consequences, so that while the damaged tissue is restored, other physiological functions may be significantly hampered. Another well established possibility is the implantation of inert biomaterials specifically processed to possess properties similar to those of the natural tissue. The field of

biomaterials in medicine is lively and brought to the realization of widely used artificial prosthesis, as reviewed in the previous paragraph. Despite of the success of these devices in accomplishing the anatomical and structural role of the original tissue/organ, artificial devices, usually fail to recreate all the complex physiological functionalities of biological materials. In fact, biological materials, that are the main constituents of living organisms and build up tissues, cover a variety of roles and functions, such as structural support, protection, insulation, metabolites and ions storage, signals generation and transmission, and production and conversion of energy, among others [10]. Therefore, it is evident the need for the evolution of such an approach towards the full restoration of all the biological functionality of native tissues.

This need constituted a turning point in the development of biomaterials with bioactive properties and capable of positively interact with the host organism and therefore guide cell activity. Strategies that aim at this objective belong to the field of regenerative medicine, which includes all the therapies directed towards the regeneration of tissue or organs affected by damages or diseases.

In this area are included Tissue Engineering (TE), Cell Therapy and Gene Therapy. Tissue Engineering can be defined as proposed during the 2005 Satellite Consensus Conference of the European Society of Biomaterials (ESB):

*"Tissue Engineering is the creation of new tissues for therapeutic reconstruction of the human body through the controlled stimulation of properly chosen cells with a combination of molecular and mechanical signals [15]"*

It is evident how tissue engineering is a highly interdisciplinary field and a crossover of knowledge from engineering, biology, materials science and medicine. In its paradigm, tissue engineering includes the utilization of adequate cells seeded on a biodegradable structure (the scaffold), which acts as a temporary artificial extracellular matrix (ECM). The cell-biomaterial construct is induced to maturate under specific environmental conditions, providing biochemical (growth factors or chemical cues given by the same scaffold) or physical signals (dynamic culture condition, mechanics of the scaffold) whose nature depends on the type of tissue that has to be recreated (fig. 2.1).
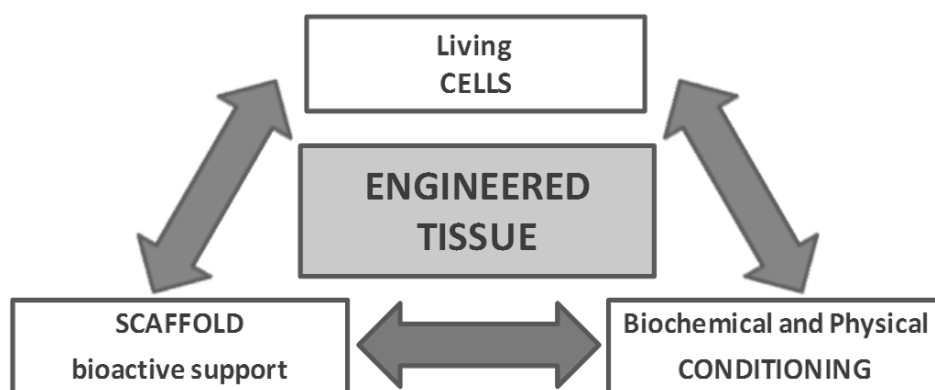


**Figure 2.1: Schematic representation of the paradigm of tissue engineering**

Cell culture conditions can be regulated through the use of a bioreactor, a system capable of maintaining the environmental parameters under control, while providing several stimuli (e.g. mechanical and electric) to induce tissue formation. The classical TE approach is given in Figure 2.2.
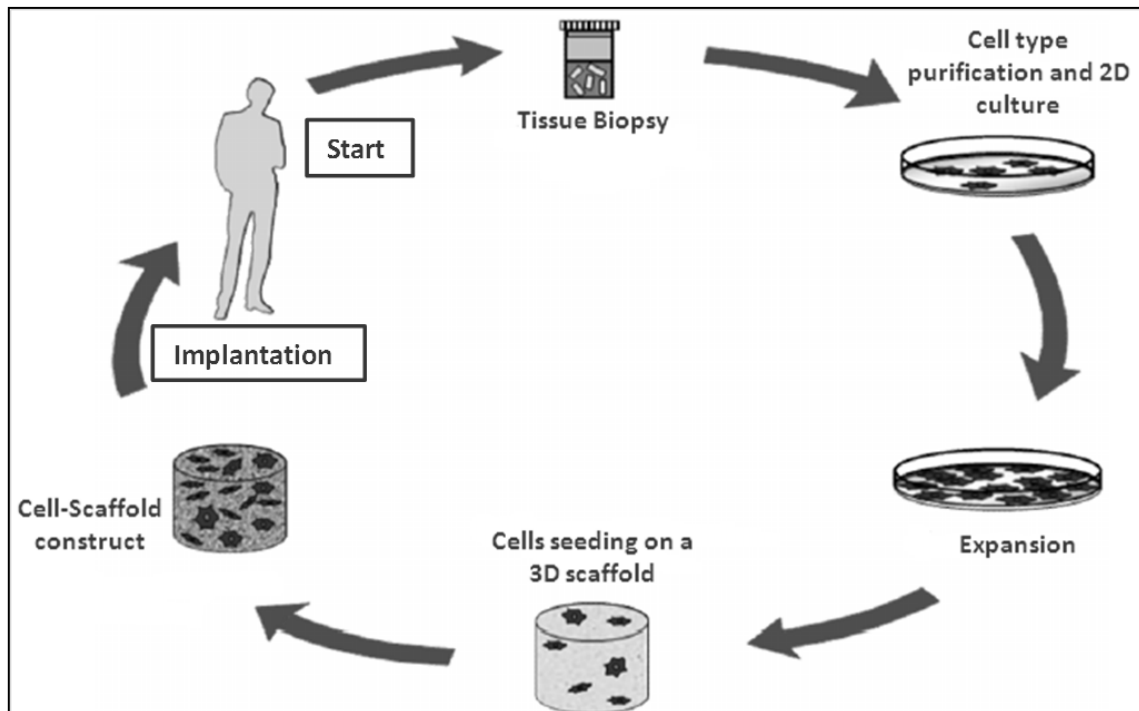


**Figure 2.2: Formation of a regenerated tissue from autologous cells.**

A sample of autologous tissue is taken from the patient to isolate the needed cells (usually pluripotent or progenitor cells, such as mesenchimal stem cells) that are afterwards cultured to increase their number. Cells are then seeded onto a scaffold (either 3D or 2D, according to the application) to be further cultured in an appropriate environment (static or dynamic) and the construct is afterwards implanted into the patient. The result is the gradual formation of newborn fully functional tissue together with the degradation and bioresorption of the scaffold [16]. More generally, it is possible to classify tissue engineering strategies as histoconductive, if the scaffold promotes the formation of the tissue through previously seeded cells, or histoinductive if the implanted construct promotes neovascularization and tissue regeneration is driven by cells recruited from the surrounding tissues [17]. The first strategy usually allows the production of limited volumes of tissue-like structures, while in the latter may be unsuccessful if the cells recruited in vivo are damaged by the tissue defect [18]. Histoconductive strategies may be also roughly classified between *top-down* and *bottom-up* (Figure 2.3) approaches [19]. In the first case, cells are required to home on a prefabricated scaffold, and from that to create the engineered tissue and its microarchitecture. In bottom-up techniques, instead, a modular, "tissue unit" is generated, and a multitude of these units is used to build a 3D

structure either by biological self assembly or by imposing a certain spatial distribution to the unit using microfabrication or rapid prototyping techniques. Such modules can be composed by cells alone or cells and biomaterials, such as gels and particles.
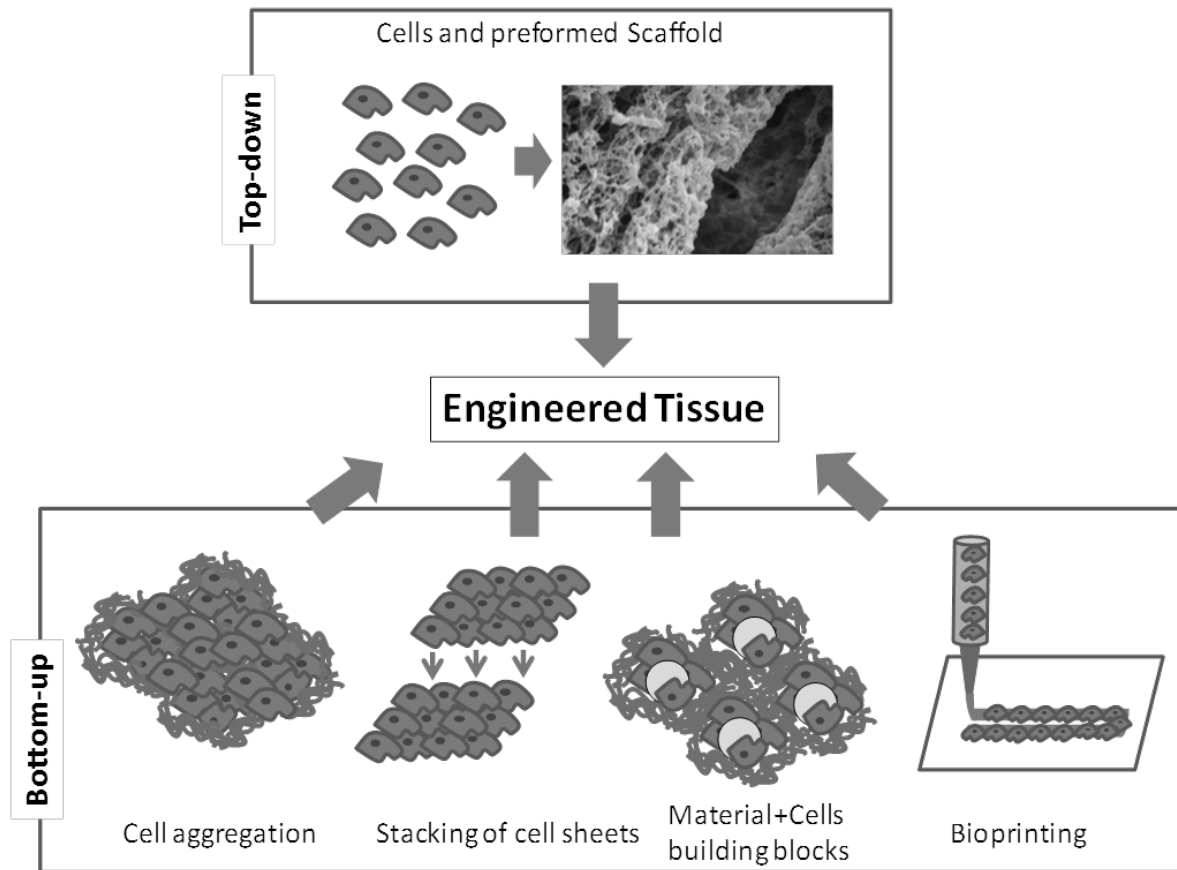


**Figure 2.3: Graphical representation of *top-down and bottom-up* Tissue Engineering.**

While the final aim of engineered tissue is to obtain devices that can recapitulate the complexity and the functionality of living tissues (and organs), such objective can be achieved by trying to replicate tissues *ex vivo,* already during the scaffold-cells construct design, or rather to develop devices that, thanks to their smart functionalities and physic-chemical properties, are able to replicate complex biological effects using "simplified" signals that can "establish key interactions with cells in ways that unlock the body's innate powers of organization and self repair" [20].

Additionally, tissue engineering provides a set of tools that can be used for regenerative medicine, but whose potential application goes beyond the only scope of tissue replacement, healing or enhancement, and can benefit other fields of biomedical research. Tissue engineering constructs, in fact, can also be used as *in vitro* models of living tissue, with potential applications as disease models, developmental biology studies and drug testing 3D platforms [21]. Nowadays, most of biological research is conducted on 2D cell culture on Petri dishes, an oversimplified model, uncapable of fully recapitulate cell behavior *in vivo*, and on animal models, which demand expensive facilities and have non-negligible ethical implications [22]. Tissue

engineering constructs can help to bridge the huge gap between 2D cell culture and animal models, and thus reducing the cost of animal experimentation, introducing a new class of *in vitro* models, one step closer to living tissues, 3D cell-to-cell communication.

Given this overview of the TE approach, four critical elements that are the backbone of the design and implementation of TE strategies can be identified:

a) A **cell** source is required. The choice of the type of cell (stem cells, differentiated cells) and their origin (i.e. autologous/heterologous), poses some limitation on cell availability, and how to expand those cells to a sufficient number to achieve tissue regeneration. In the case of histoconductive strategies, it should be clear which type of cells need to be recruited *in vivo*.

b) A **scaffold**, capable of supporting the regenerative process, home cells and/or recruit cells from the patient and act as an active matrix to guide cells fate. Several design aspects such as type of material, desired structure, inclusion of bioactive/smart cues, and method of application of implantation of device have to be taken into account.

c) 3D, *in vitro*, **tissue culture** on the scaffold. To generate a construct composed by cells cultured on the biomaterial. The culture can be done under static or dynamic conditions, in devices known as **bioreactors**.

d) A **stimulation**, to guide cell behavior and tissue deposition and maturation. This can be provided by the chemical composition of the culture medium (i.e. growth factors), by the scaffold (drug release, mechanical, physical and chemical properties) and bioreactors as well (i.e., mechanical and electrical stimulation, improved diffusion of nutrients).

### 2.2.1.2 Cells in Tissue Engineering

Cells are the main actors in tissue organization and functionality. They build up the ECM and direct its architecture, produce factors and signals that regulate tissue activity. Cells are also in charge for inducing tissue healing and remodeling, thus being the principal responsible of living materials homeostasis, adaptive behavior and responsiveness to environmental stresses [22]. It is no wonder that a huge effort in regenerative medicine and tissue engineering is directed towards the choice, isolation and purification of cells capable of inducing tissue regeneration, as well as developing strategies to control their biological activity [23]. Generally speaking, cells used in tissue engineering need to i) proliferate to and adequate amount, in order to colonize scaffolds and ii) being able to produce ECM and pro-regenerative factors (chemokines and other instructive molecules) adequate to the target tissue. Other mechanisms involving cell migration, sensing of the environment and communication are also fundamental in determining tissue regeneration. Considering the two necessary requirements mentioned above, two types of cells sources can be identified and used: already differentiated cells from the target tissue (e.g. osteoblasts for bone, chondrocytes for cartilage,

cardiomiocytes for the heart, and so on), or cells retaining the potential to differentiate towards the desired phenotype, such as progenitor cells [24]. The second approach has several advantages, especially when stem cells are considered. Stem cells are defined by their capability of self-renewal and multilineage differentiation. Self-renewal implies that these cells can proliferate without losing their phenotype, and thus continuously preserve their pool, while the differentiation potential consists in that stem cells, given the appropriate physic-chemical signals, can commit towards certain fully mature and tissue-specific cell types [25]. Stem cells can be classified into *toti-, pluri-* and *multipotent*, based on the different possible lineages that they can give rise to. *Totipotent* cells are able to differentiate into any cell type of the organism (such as a zygote and the cells following its very first divisions), while *pluripotent* cells are found in the inner cell mass of the blastocyst, and are defined as embryonic stem cells [26]. Although these cells hold great promise in tissue engineering, as they can differentiate in a wide spectrum of lineages, their usage raises several ethical and safety concerns [27]. On the other hand, several adult tissues, such as bone marrow, skin and adipose tissue, have been demonstrated to home a niche of *multipotent* stem cells, more limited in their differentiation potential, but also easier to retrieve and use in clinics and research, without sharing the same limitations of embryonic cells. It has also been inferred that every tissue may host a pool of stem and progenitor cells, which take part in healing and regeneration processes [28], and may be sometimes implicated also in cancerous diseases [29].

One of the most investigated and promising cell type in regenerative medicine are Mesenchymal Stem Cells (MSCs), that can be retrieved, for instance, from the bone marrow and the adipose tissue, and are known to be able to differentiate towards osteogenic, chondrogenic and adipogenic lineages [30]. For most of MSCs that are currently under investigation, although their multipotency is confirmed, their actual stemness and characterization is controversial [31]. For this reason, these cells are more correctly defined as Mesenchymal Stromal Cells (also abbreviated as MSCs), even though it should be noted that in the literature both terminologies can be found, and are often interchangeable [32]. In this Thesis, this second nomenclature to indicate MSCs will be used. MSCs are adherent-dependent cells, displaying a fibroblast-like morphology, once plated on tissue culture plastic. They are characterized by the *in vitro* expression of CD105, CD73 and CD90, and are negative for CD45, C34, CD14 or CD11b, CD79α or CD19 and HLA-DR surface molecules, and their in vitro adipogenic, chondrogenic and osteogenic differentiation ability [32]. Moreover, there have been reports of induction of MSCs differentiation towards additional phenotyopes, including myogenic [33] and neuronal lineages [34], which considerably expand the potential of MSCs for regenerative therapies. A scheme of MSCs differentiation potential is represented in Figure 2.4.
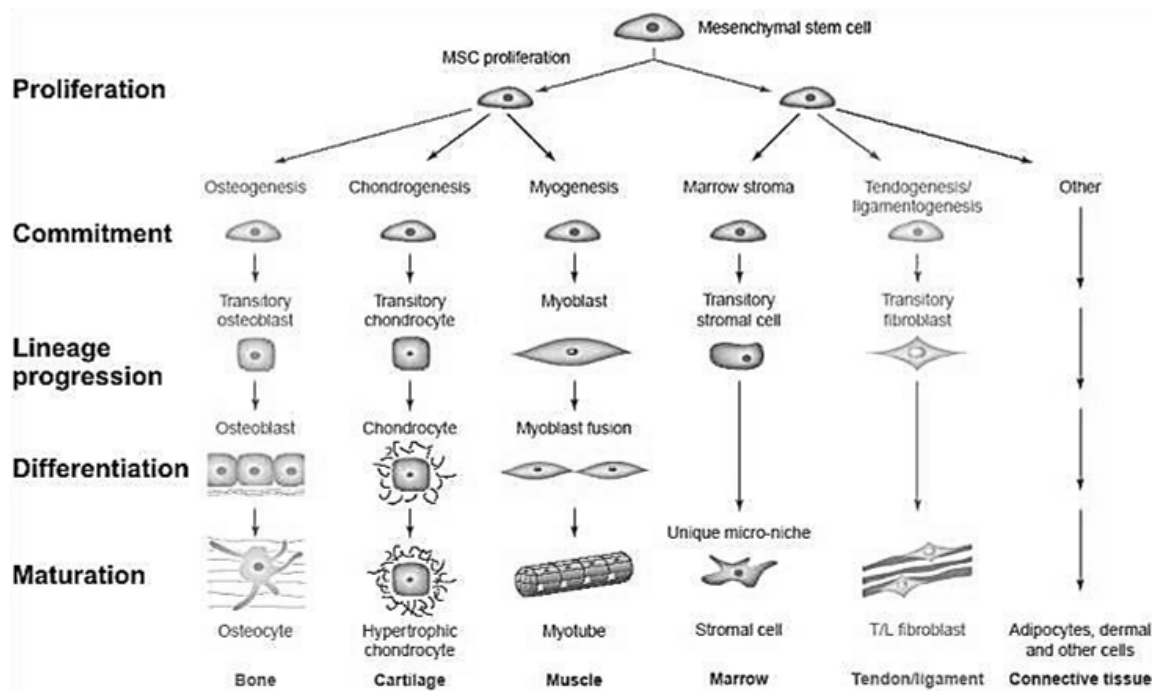
**Figure 2.4: Multilineage commitment of MSCs, adapted from [35].**

MSCs can be retrieved from different tissues (including umbilical cord blood and placenta), although the most common (and easier to access) sources are the bone marrow and the adipose tissue. In bone marrow biopsies about the 0.002% of the cellular fraction is composed by MSCs [36], while lipoaspirates can have up to a 2% of MSCs [37]. Once these cells are isolated and purified from the tissue sample, they need to be expanded to relevant numbers to be used in clinical settings, and, at the same time, cells have to preserve their "stem" phenotype, before being induced to differentiate towards the required cell type. Additionally, cell expansion and culture should be performed in rapid ways, compatible with the clinical needs of the patient. Knowledge of the biological mechanisms underlying these processes is fundamental in any regenerative therapy strategy and establishing and providing cues capable of guiding them can be provided by soluble factors, dynamic culture and by an accurate design of biomaterial scaffolds.

In the recent years, the discovery that adult, differentiated cells can be reprogrammed to dedifferentiate into an embryonic-like state, and from this state be expanded and differentiated again into a new cell phenotype, has risen a lot of attention. These cells, called induced-Pluripotent Stem cells (iPSC), possess the potential of tissue regeneration of embryonic cells, without sharing the ethical drawback and difficulties in retrieval [38]. Although it is foreseeable that these cells will play a key role in the next future of regenerative medicine and open new therapeutic perspectives, to date the lack of knowledge on their biological response and the risk of teratogenesis that they carry, limits their application as constituents for *in vitro* disease models [39].

### 2.2.1.3 Scaffolds

The ECM, together with the cells that produce it, makes up the 3D composition of a tissue, providing structural integrity and support. Far from being only a mechanical component, the ECM is a complex and

hierarchically organized source of signals, capable of determining cell fate. ECM macromolecules bear chemical functionalities that cells can recognize, are anchoring points for growth factors, can be pulled and stretched by cells to transmit mechanical signals and can be degraded to allow tissue remodeling and cell migration [40]. In addition that cells growth and tissue organisation are strictly dependent on mechanical, physical and biochemical signaling provided by the complex background in which those structures are involved: biological response to these pathways can determine the success or the failure of the wound healing process. Considering these cell-ECM interactions, it is evident that scaffolds for tissue engineering should be fabricated to act as a temporary ECM substitute, able to replicate its functions. Moreover, scaffolding materials are usually implanted at sites of tissue defects incapable to heal themselves, or in tissues with poor regenerative capabilities (such as cartilage and neuronal tissue). Advanced scaffolds must provide the molecular and physical information coded within the extracellular milieu, in order to establish specific interaction with cells, and thus unlocking their potential for tissue regeneration and organisation. For this reason, they have to be able to trigger specific cellular responses and regenerative processes, which the damaged organism may not be able to put into action. Of course, as the term scaffold itself suggests, they have to sustain mechanically the neo-tissue growth. Some of the most important specifications to design scaffolds can be summarized as follows [41]:

• *Biocompatibility* of the materials used to fabricate the device, meaning that the material does not exert a toxic effect on its environment, nor provoke any uncontrolled immunological or foreign body reaction;

• *Bioresoption*: the materials must possess a degradation kinetics paired with the rate of tissue regeneration. Degradation products must satisfy the specification of biocompatibility;

• Highly interconnected *porosity*. Pore dimensions should be adequate to allow cell colonization of the scaffold, tissue growth and mass transport (biological fluids, metabolic and catabolic substances);

• *Surface properties* favorable to cell adhesion and targeted to provide stimuli, also through the release or the exposure of bioactive molecules (e.g. growth factors). It is generally acknowledged that biomaterial-cells interactions are mediated by phenomena occurring on material surfaces, especially dynamic protein adsorption, and that engineering surface properties is a powerful tool to guide protein-biomaterials interactions, and cell reaction to biomaterials [42].

• *Mechanical properties* compatible to those of the tissue to regenerate. Scaffold should resist physiological loads typical of the native tissue and, during degradation, and gradually transfer them to the forming tissue;

• Promote *vascularization* (when necessary). Every living cell needs access to a nutrient and oxygen supply, for this reason, generation of functional vascular networks is fundamental for tissue survival. In absence of such mass transfer system, tissue engineered construct size is limited by oxygen diffusion

distance, which is too low to allow the fabrication of grafts with clinically relevant dimensions [43]. Certain tissues, such as cartilage, are naturally avascular, therefore nutrients should be provided through other means (for instance, using hydrogel scaffolds allowing proper diffusional rates) [44].

• Inclusion and release of *bioactive molecules*, to act as chemical signals to guide cell response;

• *Sterilizability*. A scaffold to be used in the biological milieu must be sterile, and the sterilization procedure should pose no relevant harm to the device (i.e. should not induce degradation of the material and its properties);

• Ease of handling and *suitability to be implanted* with common surgical practice, possibly even with minimally invasive procedures;

• Adequate *shelf-life*;

• The fabrication and the processing procedures should be respectful of the specifications cited above.

In order to address these specifications, scaffold design and tuning of the properties of the device is fundamental. Furthermore, cells can respond in specific manners even to certain morphological feature, scaffolds geometry and shape, biomolecules coating, and chemical composition [45]. Following this step, the device must undergo a rigorous characterization in order to be validated (Figure 2.5).
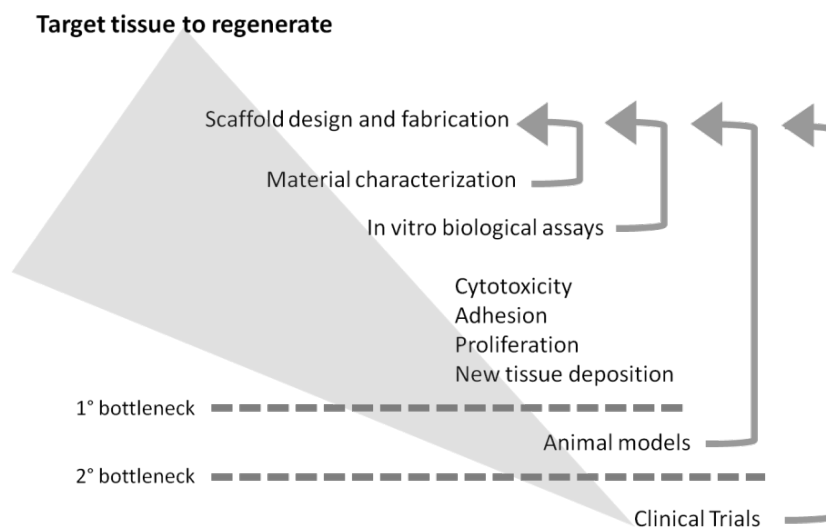


**Figure 2.5: Example of a workflow of scaffold design and device validation. Although only few materials are reaching applications in humans, each step in the development of such devices can provide new insight and information to improve scaffolds in regenerative medicine.**

*2.2.1.4 In vitro culture, bioreactors and environmental stimulation*

While the scaffold can provide a regeneration-promoting 3D microenvironment, another key necessity for tissue engineering is how to recapitulate the dynamic environment of cells. *In vivo*, cells receive stimulation from each other, from the extracellular milieu, but also from other tissues and organs, as well as from biomechanical and biochemical actors, both in space in time. This is especially important when considering the *in vitro* culture step on 3D scaffolds. Standard culture techniques are mostly oriented to expand cells in the bidimensional surface of a plastic well, and rely on simple diffusion of metabolites from the medium to a film of cells directly exposed to it. Although they can be used also to generate cell-laden scaffolds, this approach is far from being efficient. When moving from a 2D to a 3D environment it is necessary to: i) guarantee homogenous distribution of cells and neo-deposited tissue through the scaffold volume, ii) permit efficient mass exchange in the construct, allowing removal of catabolites, provision of oxygen, nutrients and bioactive compounds and iii) recapitulate the effect of external stimuli to induce maturation of the construct (i.e. mechanical stresses, electric signals). A technical solution to this need is the implementation of bioreactors, devices where biochemical processes can develop under closely monitored and controlled conditions [46]. Several types of bioreactors exist, and many of them are custom-made in order to meet the type of mechanical/electrical stress that the target tissue requires. Figure 2.6 reports a few examples of possible bioreactors.
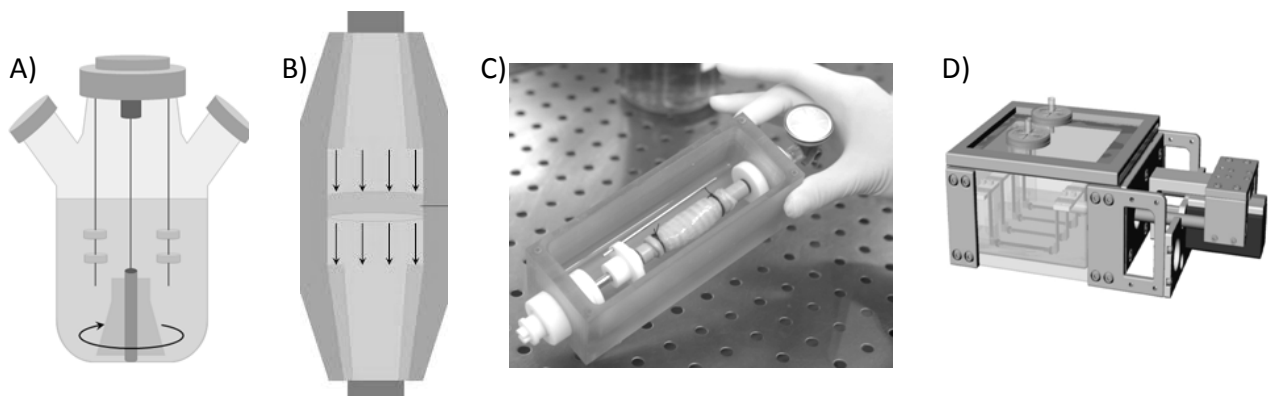


**Figure 2.6: Examples of bioreactors. A) spinner flask, B) perfusion bioreactor, C) rotating system [47], D) system to exert a mechanical tensile loading on the construct [48].**

Systems that are able to generate culture medium flows, such as spinner flasks, roller bottles and perfusion bioreactors, respond to the need generated by the point i) and ii) of the specifications described above. Additionally, perfusion systems, can apply beneficial shear stresses onto cells, which are also profitable to guide seeded cells fate and differentiation [49]. Flow systems combined with porous scaffolds, have also been demonstrated to enhance cell proliferation and ECM production, in comparison to static culture [50]. Furthermore, application of physical stimulations, such as cyclic mechanical loading has been shown to

participate in cell maturation and improvement of the quality of the neo-tissue formation. For instance, smooth muscle cell-laden constructs exposed to time-controlled series of tensile stresses were proven to increase their expression of myosin heavy chain, a marker for myogenic phenotype, and subsequent muscle matrix synthesis [48]. Devices combining sets of different stimuli can be also be designed; for instance, Tandon et al. have proposed a bioreactor allowing for construct perfusion and electrical stimulation to engineer cardiac tissue [51].

Indeed, bioreactor systems are key components in tissue engineering, as they produce a controlled environment, profitable to induce cells to generate efficient matrices. At the same time, development of bioreactor technology that can reduce risks of culture contamination and generation of more reproducible outcomes, also provides an automatization of the cell culture procedure, which is fundamental to permit scaling-up of the graft generation and thus its clinical application [52].

### 2.2.1.5 General remarks on tissue engineering and its current state

Nowadays, tissue engineering is considered a discipline in its maturity. TE products are already used in clinical settings, mostly in the area of skin (i.e. TransCyte, Apligraft, Oasis Wound Matrix), bone (INFUSE is a clear example of a successful TE product) and cartilage (i.e. Hyalograft C, Bioseed C, MACI), with few devices having obtained a regulatory green-light for other applications such as blood vessels, nerves, heart valves and bladder, among the others. These commercially available products have been summarized in the literature [20]. Despite of the central role of skin and orthopedic devices, current estimations foresee that cardiac TE products will become increasingly more central, due to the fact that cardiovascular diseases are the principal cause of death in the industrialized countries [8]. Additionally, to date, there are 41 clinical trials registered in the USA, as obtained by searching the words "Tissue Engineering" in the *clinicaltrials.gov* database. Despite of this, still too many tissue engineering strategies that showed promising results in preclinical studies, fail to reach the clinical practice. The problem of generating large grafts with functional vasculature and guarantees their survival, has been one of the main topics of the past and present decade, and still remains a fundamental bottleneck for many TE devices [53]. In the last years, many successful cell-free TE products, which rely on supporting the body's ability to self-heal, have reached the market and the clinics, especially for bone, cartilage and skin repair. Regulatory approval of cell-based products (in Europe falling under the regulation of the Advanced Therapies Medicinal Products, EC regulation No 1394/2007) is also a long and challenging route, and there is a crescent push for the applied research area to design and study TE grafts with such legislation in mind [54]. Additionally, to date, among the most important examples of engineered tissues, cell-seeded, tissue cultured *in vitro*, successfully implanted in humans and with higher-impact in the generalistic media two notable cases can be cited: the bladder constructs developed by Atala et al. (2006) [55] and the engineered airway, from a donor trachea decellularized, implanted by Macchiarini and coworkers (2008) [47]. These devices, as well as many others

designed according similar guidelines, still remain of limited application and with them other products as well, since they mostly respond to the need of a patient-specific/on demand implant, and can be better applied in hospitals or clinics that have available a Good Manufacturing Practice (GMP) facility for the treatment of cell culture constructs. Although such approaches are very appealing, they do not easily match the requirement of a conversion of the device fabrication from a bench-scale to a clinical and industrial scale, providing at the same time GMP, at affordable costs.

The design of new, smart biomaterials, devices with improved functionalities and cell-instructive properties also goes in the direction of facing and overcoming some limitations. Furthermore, as an additional requirement, these biomedical devices should be as easily as possible implantable with standard surgical practice, in order to improve their acceptance by most of the clinicians that will have to handle them. For these reasons, making TE strategies more effective and at the same time easier to translate towards the biomedical industry and the medical practice is a great challenge, whose reward will be a benefit for health and society.

### 2.2.2   Cell Therapy

Unlike tissue engineering approaches, which imply the *de novo* generation of the damaged tissue on a scaffolding support, cell therapy focuses on the *in vivo* delivery of cells as "living drugs", for disease treatment and tissue regeneration. Such therapeutic activity can be exerted via progenitor cell differentiation, ECM deposition and regeneration of a new tissue or by secretion of biomolecules that act as drug or as promoters to enhance healing and physiological processes in the host. Depending on the type of cell chosen and their potential biological activity, cell therapy has been proposed to tackle a wide variety of tissues and pathologies, such as tumors, heart dysfunctions and degenerative diseases. To do so, as for tissue engineering, the choice of adequate cell and their expansion technique are key issues, and will determine the type of therapy to be performed. Both stem and differentiated cells as autografts or allografts are potential candidates as therapeutic agents, and both cell types are already in use in the clinical practice.

According to a recently published survey on cellular therapies, only in 2011, 1759 treatments were applied on patients, for the treatment of cardiovascular, musculoskeletal, neurological, and gastrointestinal diseases, and tumors, skin and cornea defects and diabetes, among others. Among those procedures, the majority involved the transplantation of MSCs (autologous in 659 cases and allogenic in other 320), Haematopoietic Stem Cells (HSC, autologous in 397 cases, allogenic in 14) and chondrocytes (214 autografts) [56].

Two notable examples of cell therapy in clinics are HSCs transplants for the treatment of leukemia or myeloma and Autologous Chondrocytes Implantation (ACI), a treatment to repair articular cartilage damage. The first case is probably one of the clearest examples of the use of stem cells and their proliferation and differentiation ability to regenerate a tissue. HSCs, which reside in the bone marrow, are transplanted, usually in patients whose compromised cancerous bone marrow or blood cells have been treated with radio-

and chemotherapy, and they proliferate and give rise to a new, donor-derived healthy bone marrow and cells. Such procedure is able to replace the host cells with (compatible) donor cells (i.e. leukocytes). Additionally, in case of allogenic white blood cells may be prone to attack and eliminate residual cancer cells that the host immune system was not able to target. Despite potential side effect of this approach, including graft-vs.-host disease, the procedure is well established, leading to high survival rates especially in young patients [57]. On the other hand, ACI (Figure 2.7) is the golden standard of knee cartilage transplant procedures.
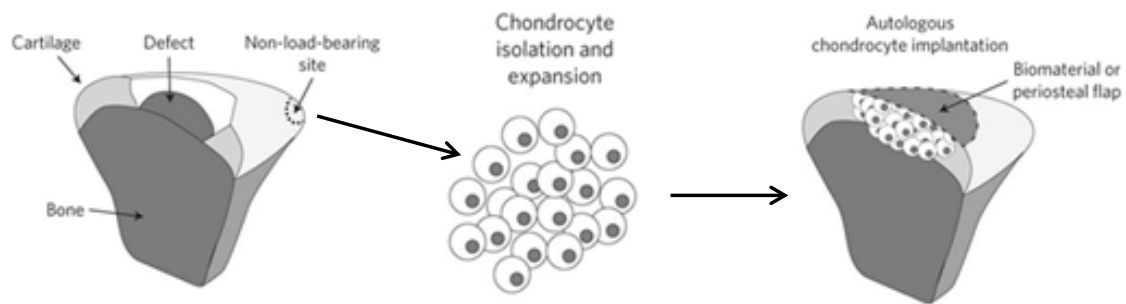


**Figure 2.7: Example of an ACI procedure, adapted from [58].**

Chondrocytes from a healthy site are harvested, can be expanded *in vitro* to achieve a sufficient quantity, and injected in the site of the cartilage defect. Such approach, which relies on the ability of differentiated chondrocytes to synthesize neo-cartilage ECM, has however some limitiations: it is an expensive and time-consuming procedure, due to the cell culture steps; moreover, chondrocytes are often prone to dedifferentiation during the expansion, and this generally leads to the repair of the cartilage defect with fibrocartilage, having lower quality, compared to native cartilagineous tissue [59].

For tissue engineering applications, adult stem cells and especially MSCs are a very promising therapeutic vector in cell therapy [56]. Indeed, the fast proliferative nature of MSCs, ease of harvesting and their multilineage differentiation, already discussed earlier in this chapter, are the reasons for the high expectation raised by these cells. While the interest around these cells has been for long time mostly focused on multipotency and tissue engineering, comparatively little is understood regarding the anatomical localization of these cells and their natural role in tissue homeostasis [60]. However MSCs display a wide spectrum of biological functions that open the way for their application in many pathology treatments, and a deeper comprehension of the elusive nature of MSCs, may help improving cell therapy. Most of the experiments using transplantation of cultured MSCs into animals, led to the observation that MSCs therapeutic effects could not be explained by differentiation into tissue specific cells alone. For instance MSCs injected to the infarcted myocardium successfully reduced fibrosis, contractile strain alterations, and cardiomyocyte apoptosis, while improving angiogenesis [61]. These effects are mostly due to the so-called "bystander" or paracrine effects". MSCs are known to secrete trophic factors, with angiogenic and antiapoptotic properties, as well as cytokines to support the cells of the damaged tissue and push them to work more efficiently, improving their biological activity. This role goes along with the secretion of immunomodulatory and anti-

inflammatory factors, which can reduce the environmental stress imposed by an overinflammated sorrounding on the native cells of the tissue. Such activity is exerted both via cell-to-cell contacts with immune cells, such as T-lynfocytes and dendritic cells, and production of soluble biomolecules (i.e. IL-10, interferon-γ)[62].

MSCs have also been proven to support haematopoiesis, as well as HSCs and Endothelial Progenitor Cells (EPCs) recruitment (secreting VEGF and SDF-1α, for instance) [63]. Additionally, MSCs appear to contribute to the stabilization and maturation of neo-blood vessels, localizing themselves around the vessel and acting as pericyte-like cells [64]. Indeed, there is increasing evidence that perivasculature may be an *in vivo* niche for MSCs and that perycyte may be among the biological progenitors of MSCs [65].

Another important ability of MSCs that can be beneficial to devise cell therapy strategy is MSCs high and selective migratory capability. *In vivo* MSCs where found to be mobilized from their niches in response to certain tissue injuries, such as tumor development and myocardial infarction, this migration and increased tissue localization seem to be mediated by the secretion from tumoral cells and cells resident in ischemic tissues of potent chemoattractors like SDF-1α, VEGF, MCP-1, among others [66]. MSCs, following gradients of these molecules are able to home into the diseased tissue, migrate through it and specifically localize at the site of the injury [67].

Using this potential, MSCs are even recruited by tumoral cells that are secreting such factors, possibly to stabilize their vascular network. MSCs injected in glioma where found to be localized inside the main tumoral mass, at the site of injection, but also to be able to track satellite cells in process of migration that were evading from the main tumoral mass, and to establish cell-to-cell contacts with them [68]. Such specific migration makes MSCs interesting candidates as controlled delivery vehicles for antitumoral agents. This is particularly appealing when thinking of applying MSCs therapy to tissues whose surgical treatment is too difficult, such as to the brain. Alieva et al., for instance, have engineered MSCs to express Herpes Simplex Tyrosine Kinase, deliver it to aggressive gliomas, and then trigger tumor cells death with the systemic administration of the drug ganciclovir. This enzyme/pro-drug therapy, coupled with delivery using MSCs, has been proven successful in strongly reducing glioma mass in mices [69].

The extent of this MSC versatility, depends on the subsets of cells used (i.e. STRO-1 positive MSCs display higher support to HSCs activity and higher colony-forming tendency than other subsets [70]), and the tissue from which the cells are harvested. However, more research is needed to correctly purify extracted MSCs and define the nature to fully understand these functional differences between these cells and their actual role *in vitro* [71]. Current knowledge seems to indicate that MSCs are prone to lose or have altered expression of certain membrane receptors and several of these trophic factors, once plated *in vitro* [72]. Therefore, the definition of alternative culture protocols to preserve optimal MSCs functions are subjects of great interest in the field of cell therapy. Furthermore, it should be taken into account, that under the current regulatory framework, the approval of new cell therapeutic products, especially those derived from cells cultured *in vitro* and altered by mean of cell engineering (such as gene therapy) must undergo stringent safety trials [73].

As such, straightforward strategies to control MSCs phenotype and receptors/cytokines expression should be sought.

The most important limitation of cell therapy (independently of the cell type to be delivered) is poor cell grafting and efficiency of transplantation. Injected cells are usually required to home in a highly inflammated, sometimes necrotic or scar tissues. Massive cell death, as well as cell dispersion by biological fluids, occurs within a few days post-implantation, so that only less that 1% of the injected cells survives and is localized at the desired site [74].

Biomaterials are still important actors in cell therapy, but as delivery vehicles, rather than structures were cells have to deposit the newly synthesized tissue, as it is for tissue engineering. With the advances in biomedical sciences, the borders between cell therapy, tissue engineering and gene therapy have become blurred, and often regenerative approaches, apart from being performed using a combination of the three, are not that easy to distinguish. Indeed, cell therapy has adopted many principles from scaffold-based TE, as well as concepts from the field of controlled drug delivery. Biomaterials carriers can be designed with appropriate topography, shape and smart functionality to improve cell homing, and have been demonstrated to dramatically increase cell survival after grafting in the host [75]. These carriers can be either in the form of macroscale delivery devices (hydrogels or porous scaffolds) or as suspension of particles, called microcarriers. The role, advantages and limitations of these types of biomaterials devices in cell delivery will be expanded later on in this Chapter. In any case, cell survival alone may not be enough for the required therapy. As discussed about MSCs, cells can lose much of their healing/trophic potential before reaching the damaged tissues, for example during the expansion steps or the delivery itself. Novel, successful therapies should take into account the multiple mechanisms that cells have to put into action, and be designed to enhance or at least preserve them (i.e. selective migratory capability, paracrine factor secretion and immunomoldulation, for MSCs). Similarly to what discussed about scaffolds for TE, biomedical engineers need to fabricate instructive materials that can, with their properties and simplified signals, guide cell functionality towards this goal.

## 2.3    Biomaterials and advanced drug release

Another field of medicine where biomaterials technology is a key component is the delivery of therapeutic agents. As seen in the previous paragraph, since cells can be considered a living drug, the term therapeutic agents can be used to group together both cells and drugs. Regarding non-living drugs, there are plenty of bioactive compounds that are researched, marketed and make part of the current pharmacological treatment of diseases. They range from classical synthetic drugs, to vaccines, proteins and growth factors. However, classical ways to deliver these compounds -such as oral, intravenous or intramuscular injections- are inherently inefficient, as they do not allow control of the spatial and temporal distribution of the free drug. This fact has four notable consequences: i) the drug has to be taken multiple times in order to maintain its

concentration in the therapeutic window, meaning the range of concentration at which it has the desired biological effect, ii) doses must be relatively high, since most of the compound will not be able to reach only the target tissue, but instead will be also unnecessarily distributed in other parts of the body, iii) side effect of the compound (especially systemic ones), are more likely to be experienced by the patient, and iv) labile drugs can quickly undergo degradation or inactivation, compromising their therapeutic potential [76]. This last point should be especially taken into account when dealing with harmful compounds, such as chemotherapeutic agents. In order to overcome these limitations, strategies for controlled drug delivery have been devised (as depicted in Figure 2.8). As for temporal control, biomedical devices that can be loaded with a drug and then permit a constant, nearly zero-order release to the organism have been developed since 1960s, when it was demonstrated that the diffusion rate from a drug reservoir, could be tuned using a silicon rubber membrane [77].
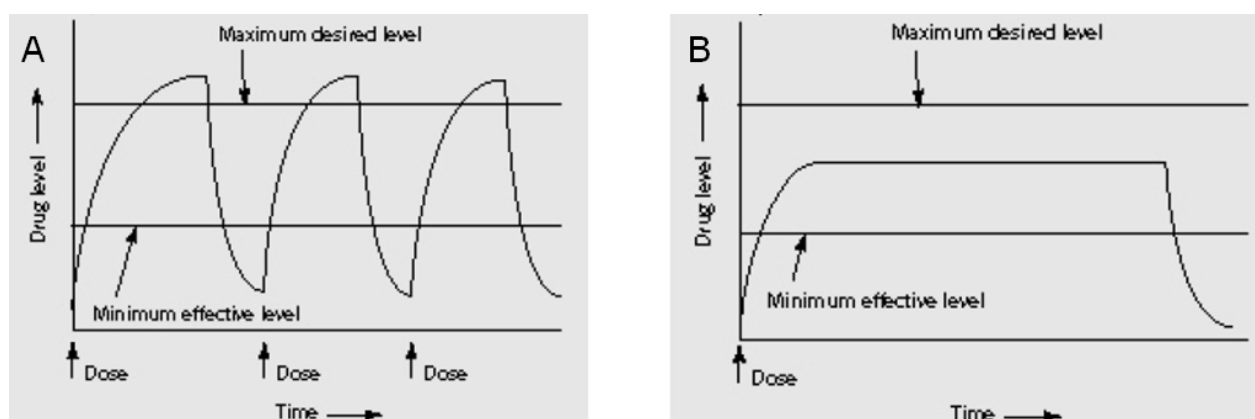


**Figure 2.8: A) Standard delivery of therapeutic compounds vs. B) Controlled release, with an initial burst and then a zero-order release profile.**

Biodegradable materials, especially polymers, soon became fundamental in this area, since they are able to release loaded compound both by means of passive diffusion through the polymer matrix and gradually, as the material degrades and is reabsorbed by the organism: tuning the degradation kinetics adds a degree of control over the liberation of the drug. Polylactic acid and its copolymers are among the most notable examples of polymers for drug delivery responding to these characteristics, as demonstrated by their use in devices used in medicine, such as Zoladex (PLA-PLGA device releasing anticancer treatment) and Absorb (PDLA coronary stent medicated to prevent re-stenosis). Degradation-mediated release can be controlled, choosing a polymer that undergoes surface erosion (such as certain polyanhydrides [78]) or bulk degradation. Besides using passive mechanisms, smart and stimuli-responsive materials have been used to control temporal release, in order to achieve an "on-demand delivery", most often in response to physiological conditions such as pH, temperature and ionic concentrations [79] (see also Figure 2.9 and 2.10). The crosslinks that prevent the delivery device to release the drug are based on reversible interactions such as ionic bonds, hydrogen bond, hydrophobic and van der Waals interactions. For instance, pH-responsive

materials, including hydrogels, can be used to improve the oral availability of drugs, or to protect labile compounds that have to be released in the intestine, such as proteins, once they enter the acidic environment of the stomach.
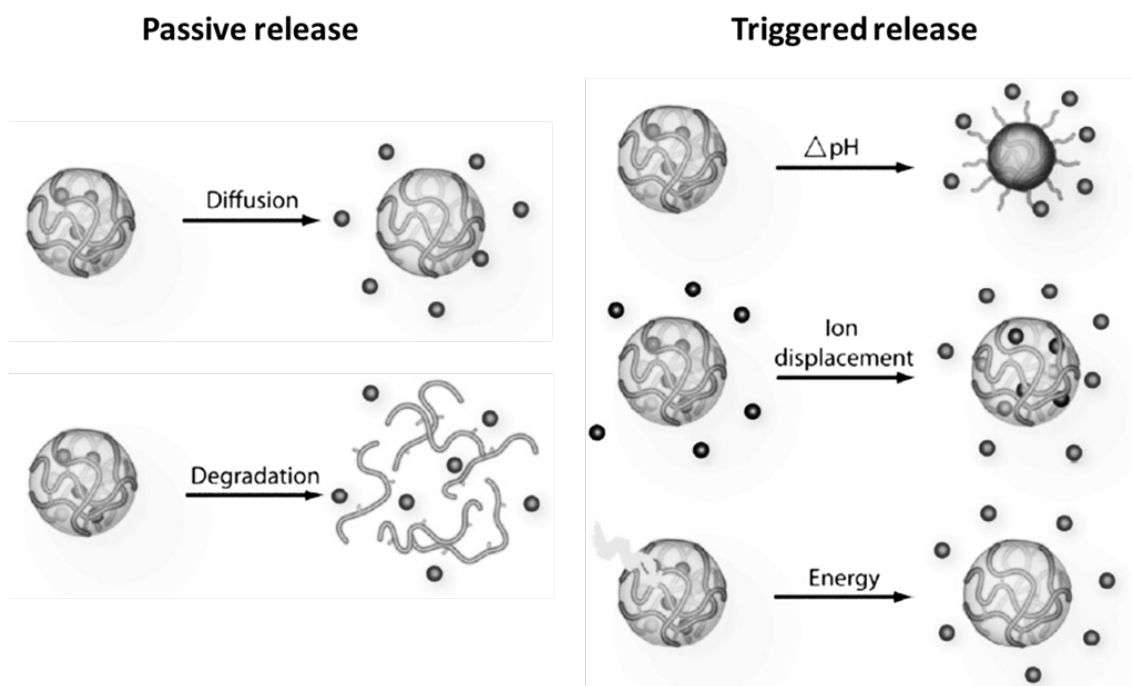


**Figure 2.9: Passive drug release vs. active stimuli-triggered release, from a carrier biomaterial.**
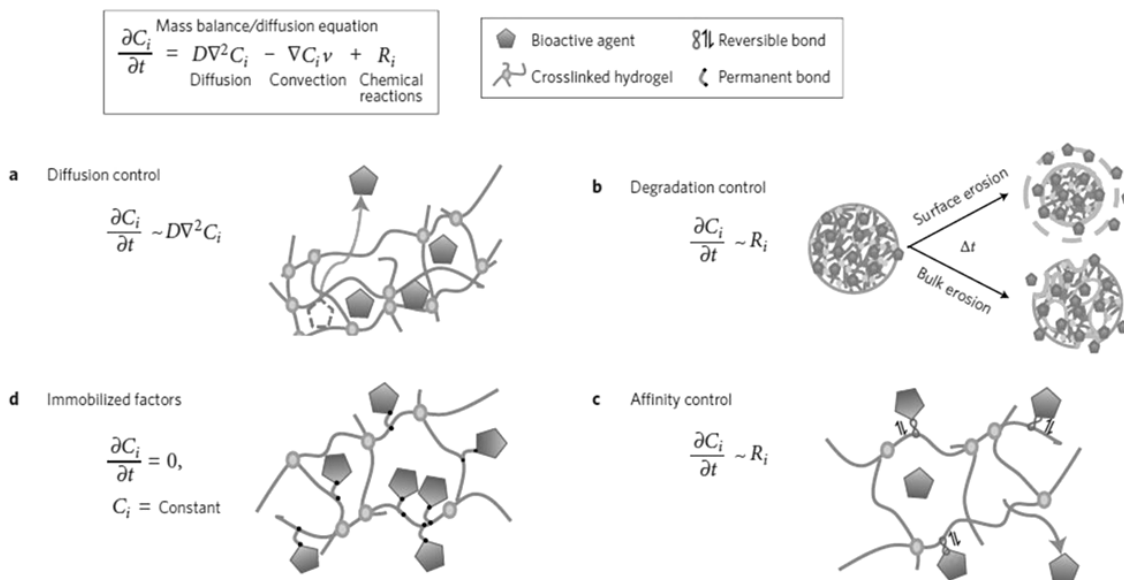


**Figure 2.10: Mathematical modeling of different methods of controlled drug release, adapted from [79]**

As an example, alginate-based polymers are known to display reduced solubility and shrinkage at low pH, forming a skin of alginic acid that can protect compounds encapsulated in it, while they become freely soluble in the slightly alkaline intestine, allowing the release and absorption to the blood stream of the carried drug [80]. Also polymers usually regarded as "non-smart" can display a specific, triggered release

behavior, if used for carefully chosen applications. For instance, PLGA microspheres were used to target intracellularly macrophages and deliver nucleic acids for gene therapy. The release of the compound is triggered by the polymer degradation by the acidic phagosomal environment after internalization of the carrier [81].

The type of biological target addressed by the drug-carrier complex also depends on the size of the biomaterial device, which can range from a few nanometers to several centimeters. Controlled delivery devices can be roughly classified into macroscale devices or particulate devices, the latter including micro- and nano-sized carriers [76]. Size clearly affects not only the target tissue/cell but also the route of delivery of the device, with nanosized carriers being suitable for parenteral injection and most macroscale product needing surgical implantation. Of course, drug-loaded devices can be successfully implemented also in tissue engineering and cell delivery strategies, for instance, macroscale devices can also be loaded with cells and be easily thought as medicated scaffolds for tissue engineering [79].

Besides the need to control *when* a drug is released, advanced carriers should be able to target *where* the delivery has to occur. Furthermore, smart carriers can be endowed with functionalities able to recognize or specifically interact with their target in order to enhance specifically bind to it, or to enhance the biological activity of the drug. This is especially important for the production of drug carriers able to overcome biological barriers, which are usually impermeable to many drugs (such as the skin, blood-brain barrier, cancer cell membranes, and intestinal capillaries). This objective can be achieved taking advantage of the properties of the same materials used to fabricate the device, such as surface chemistry and charge, or by modifying it with active molecules able to conceal the material to the immune system (such as PEG chains), to perform specific biological activities (such as enzymes), to bind ligands in the target (i.e. lectins or antibodies), or to be accepted by cancer cells, for instance covering the material carrier surface with transferrin or folic acid, metabolic compounds highly required by tumors [82].

## 2.4 Polymeric biomaterials for scaffolds and delivery devices

Several methods to fabricate 3D scaffolds and therapeutic agent carriers exist, and differ according to the nature of the chosen material. As mentioned in the previous paragraph, material choice is the first step in biomaterial-based devices design. In this field, polymeric materials are among the most promising due to their huge versatility, since they can be easily processed into virtually any shape and into a variety of physical forms such as sponges, fibers meshes, hydrogels and particles. Polymers can also be prepared from a wide assortment of natural or synthetic origin materials, and, according to their composition, can display very diverse mechanical and physic-chemical properties. Synthetic polymers are easily obtained in highly reproducible way, allowing accurate control over their purity, degree of crystallinity and molecular weight. This advantage makes that the final product can be well defined and its exact composition is well known, which makes easier the generation of medical-grade materials and their eventual approval by regulatory

sources. Additionally, biocompatible synthetic polymers may not induce uncontrolled immunological reactions once implanted in the body. These features signed the success of several classes of polymers that are currently well-accepted in the medical practice and in biomaterials research, such as poly(α-hydroxyesters), polyurethanes, polyanhydrides, and polyphosphazenes [14]. Poly(α-hydroxyesters) are thermoplastic polymers with hydrolytically labile aliphatic ester linkages in their backbone. They can be obtained from a variety of monomers via ring opening polymerization (ROP), and a few examples are polyglycolide (PGA), polylactide (PLA), polydioxanone, polycaprolactone (PCL), poly(trimethylene carbonate) (PTMC). Additionaly, some of these polymers, such as polyhydroxybutyrate (PHB) can be generated by certain bacterial bio-process synthetic routes. Among these polymers, the most extensively investigated materials are poly(α-hydroxy acids), that include PLA, PGA, and their copolymers (PLGA), which are FDA-approved in several biomedical devices [83]. An example of the PLA synthesis is depicted in Figure 2.11, while Figure 2.12 shows some bioresorbable medical products made of this polymer. The monomers that build these macromolecules are lactic acid and glycolic acid, two compounds that can be obtained by natural sources like corn starch, and are common metabolic compounds in the cell cycle. Lactic acid has one chiral carbon, and therefore can be either in the form of L-lactic acid or D-lactic acid. Polymers composed only by one stereoisomer (either D or L) tend to be partially crystalline, as the polymeric chains can reorganize without excessive steric hindrance, whereas copolymers or mixtures of the D and L isomers tend to be amorphous. Thermal and mechanical properties of these polymers are listed in Table 2.2.
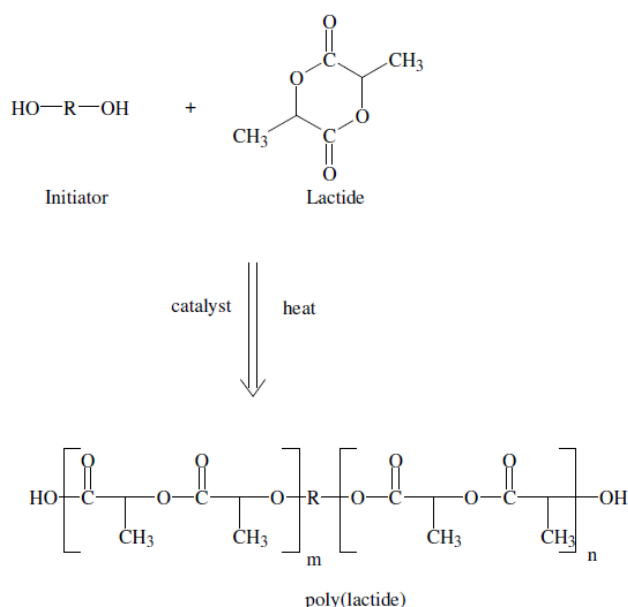


**Figure 2.11 Example of a possible ROP synthetic route for PLA.**
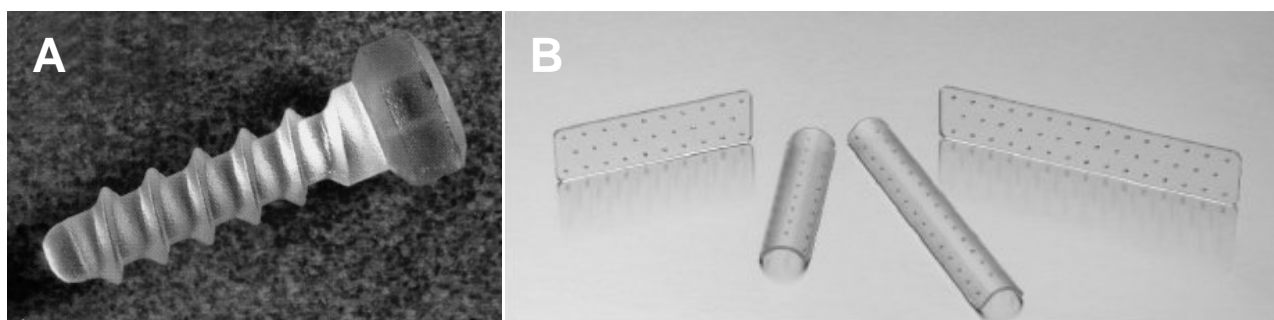
**Figure 2.12: Biodegradable orthopedics fixation devices made of PLA, (A) screw and (B) plates.**

**Table 2.2: Properties of bulk PLA and PGA, adapted from [14].**

| Polymer | Crystallinity | Young modulus [GPa] | Glass transition [°C] | Melting point [°C] | Degradation time [months] |
|---------|---------------|---------------------|-----------------------|---------------------|---------------------------|
| PLLA | 37% | 4.8 | 60-65 | 175 | 48-96 |
| PDLLA | - | 1.9 | 55-60 | 170 | 12-16 |
| PGA | 45.55% | 7.1 | 35-40 | >200 | 6-12 |
| PLGA (50-50) | - | 2.0 | 44-55 | 180 | 1-2 |

The degradation of these polymers occurs by bulk hydrolytic erosion, and the degradation kinetics can be easily tuned by copolymerizing PLA and PGA, adjusting the molecular weight of the polymers and the lactic-to-glycolic acid ratio.

While PLA has a long history in medicine, it also posseses some drawbacks that may limit its application for advanced therapies and regenerative medicine. A versatile and common way to process polymers is working from dissolution into solvents. However, PLA is only soluble in toxic organic compounds, such as chloroform, which has to be carefully removed in order to ensure the biocompatibility of the final device and its regulatory approval. Furthermore, PLA is a hydrophobic material lacking of chemical function that can be instructive for cell-behavior, and the only usable groups for chemical modifications are the pending OH and COOH at the end of the chain. As PLA *per se* has no smart or cell-instructive capability, the development of strategies to functionalize the polymer or to exploit the physical properties that can be introduced during the fabrication and shaping of the device in order to stimulate specific biological targets, is a necessary step. This can be done by a combination of mechanical, physical and biochemical signals introduced on the final, PLA-based device. In this perspective, it could be said that PLA is an *old*, well-known polymer that can be used as a platform to fabricated biomedical devices with *new* and *advanced* functionalities, able to interact with the biological milieu in ways that enhance regenerative therapies and controlled release approaches. Therefore, successful PLA engineering and modification would allow to produce novel, biologically active devices that can benefit from the favorable regulatory status of this polymer.

Besides synthetic materials, natural-origin polymers are attracting increasing interest for their potential biomedical applications. These polymers are usually extracted or derived from animal, fungi or plant tissues or bio-processes, and often consist in polysaccharides and proteins. They display several advantages as they are obtained from biological sources (often wastes of the food industry), and they resemble structural components of native ECM (proteins, glycosaminoglycans and proteoglycans) that can be easily recognized by cells and used for chemical modification as well [84]. Additionally, most of these materials are very hydrophilic, and can be obtained to generate hydrogels, structures that swell, but do not dissolve in water, that can simulate well the highly hydrated environment of living tissues. However, these materials also carry several limitations. The purification of the polymer retrieved from natural sources is difficult, and undesired impurities may remain in the material, bringing risk of contamination. Additionally, large batch-to-batch variations are experienced (in terms of composition and molecular weight distribution), due to the intrinsic inter-individual variability. A solution to this drawback can be the fabrication of these macromolecules by means of recombinant nucleic acid technology [85]. The similarity of such polymers to ECM components also means that they may provoke undesired immune responses. High water contents usually mean low mechanical properties, unsuitable to match those of load-bearing tissues; moreover, they often need to undergo crosslinking to improve their stability to degradation [84]. A non-exhaustive list of natural origin polymers is reported in Table 2.3.

**Table 2.3: List of some natural origin polymers having biomedical applications.**

| Polymer | Type | Natural source |
|---|---|---|
| Collagen | Protein | Animal connective tissues (bovine, porcine, fish origin) |
| Elastin | Protein | Animal connective tissues |
| Fibrinogen | Protein | Blood |
| Gelatin | Protein | Denatured collagen |
| Silk fibroin | Protein | Coocon of *bombyx mori* / produced by spiders |
| Chitosan and Chitin | Polysaccharide | Crustacean exoskeleton |
| Alginate | Polysaccharide | Brown algae |
| Gellan Gum | Polysaccharide | Bacterial synthesis |
| Dextran | Polysaccharide | Bacterial synthesis |

Among the large number of biopolymers that belong to this category, in this work we provide further details of a protein and a carbohydrate polymer, gelatin and gellan gum (Figure 2.13), that were used in the experimental part of the Thesis.
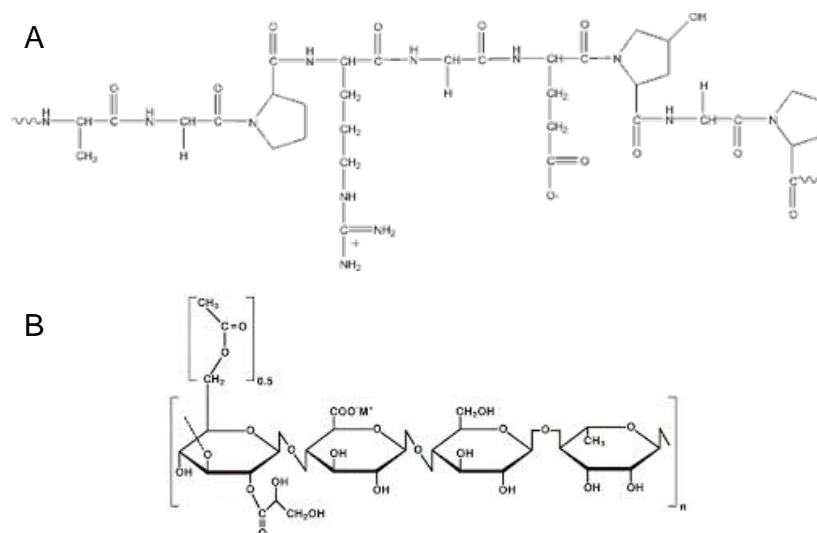
**Figure 2.13: Chemical formula of A) a section of a gelatin chain, and B) gellan gum repetitive unit.**

Gelatin is a protein obtained from the denaturation of collagen (usually from bovine or porcine skin), that have a wide range of application as scaffolds and carrier devices. Similarly to its progenitor protein, it preserves in its primary structure a large amount of glycine, proline and hydroxyproline residues. Being a product of alkaline or acidic hydrolysis, gelatin chains are generally shorter than collagen ones, characterized by a wide molecular weight distribution and mantaines a left-handed proline helix conformation, although the native triple helical organization, typical of collagen I, is preserved only in certain regions of the chain; this phenomenon generates a material with poorer mechanical properties [86]. However, due to the degradation treatment gelatin has relatively low antigenicity, and according to the alkaline or acidic-processing can display an isolectric point of about 9.0 or 5.0. The possibility to generate gelatin with different charges, permits flexibility to enable the formation of biomaterials devices via polyelectrolytes complexation of gelatin chains with oppositely charged macromolecules (i.e. via layer-by-layer deposition, LBL) [87]. Moreover, like its parent protein, gelatin is rich in binding domains for chemokines and cell-recognition sites, such as the RGD (arginine-glycine-aspartic acid) peptide, a sequence well known to mediate integrin-binding and cell adhesion [87]. Gelatin is also a water-soluble macromolecule that forms hydrogels at low temperatures, but displays a poor stability at 37 °C, for this reason chemical modification and/or crosslinking reaction are necessary to guarantee its stability in the body. These modification can also be used to obtain gelatin-derivatives with stimuli-responsive behavior or capable of crosslinking only when exposed to certain stimulations such as UV radiation [88].

Gellan gum is a high molecular weight microbial exopolysaccharide, synthesized by certain bacteria strains. It is a linear anionic polysaccharide composed of the tetrasaccharide (1→4)-L-rhamnose-α(1→3)-D-glucose-β(1→4)-D-glucuronic acid-β(1→4)-D-glucose as a repeating unit [89]. Soluble in water at high temperatures (>50°C) It can form heat- and acid-resistant hydrogels, that are soft, elastic, flexible and transparent even at polymer concentrations as low as 1% w/v. Thermal gelation appears on cooling due to a conformational change of the polymer in solution, where randomly distruibuted chains, reorganize into pairs of

macromolecules in the form of double helices. Single chains can be involved in the formation of more than one helix, provoking inter-molecular junctions that stabilize the gel. The gelation also occurs in presence of mono- and divalent cations in solution. Known for its use in food industry and thanks to its biocompatibility and good mechanical properties, gellan gum raised interest for the fabrication drug delivery devices, and tissue engineering and cell encapsulation matrices [89].

## 2.5 Injectable biomaterial systems

Advanced biomedical devices face the continuous challenge for the translation from the research to the clinical use. Many common strategies involve the implantation of preformed devices into the patient through an invasive surgical procedure, with open problematics related to possible complications, to patient compliance, to the handling of the material, and its colonization from seeded or recruited cells (if applicable). Furthermore, if the material has to fill a tissue defect, as it happens in the case of scaffolds for tissue engineering, it should be ideally custom-made to perfectly match the geometry of the defect, or better able to fit defects not-having standardized shapes [90].

Injectable biomaterial devices are a class of materials that hold the promise to solve most of the aforementioned problems. They can be administrated topically as a low viscosity solution or suspensions and can easily fill defects with irregular geometries. Moreover, they can encapsulate cells and bioactive molecules, that will be distributed homoegenously in the device matrix, thus sensibly reducing the problematics due to the low efficiency of cell seeding on preformed scaffolds, as well as lowering systemic side effects of loaded drugs [91].

The concept of injectability, adopted from pharmaceutical sciences, is a key-product performance parameter of any parenteral dosage form. The expression refers to the performance of the material formulation during injection, in terms pressure or force required for the delivery, evenness of the flow, and freedom from clogging (i.e., no blockage of the syringe needle) [92]. Injectable biomaterials systems can be either in the form of *in situ* gelating/solidifying materials [93] or suspensions of  micro-  and nanoparticles (MPs and NPs).

### 2.5.1 In situ forming polymeric matrices and hydrogels

Solidification or gelation of polymeric solution can be achieved with different methods including precipitation and chemical or physical crosslinking (Table 2.4). As all these methods require the injection of the scaffold in a sol state, a preliminary and restrictive requirement is the use of biocompatible solvents, thus imposing limitations also on the type of material. Water and saline solutions are obviously the preferred choices, anyway a few solvents, such as tetraglycol (FDA approved for pharmaceutical injectable

preparations), may be suitable choices, as they are deemed as safe under a certain ratio over the body weight [103].

**Table 2.4: Examples of in *situ* forming polymeric scaffolds for tissue engineering.**

| Material | Physical form | Forming Method | Type of study | Reference |
|---|---|---|---|---|
| PLGA | Porous scaffold | Injected PLGA solution in Tetraglycol with porogens. *In situ* hardening after solvent displacement | *In vitro* MC3T3-E1 cells seeding for bone regeneration. *In vivo* injection of the scaffold without cells. | [90] |
| PEGdA | Hydrogel, with laminin adhesive sequences | UV photocrosslinking, Initiated with Irgacure 184 | Murine preadipocytes encapsulation of adipose tissue engineering. Hydrogels modified with peptides and biodegradable sequences support cell proliferation. | [94] |
| OPF | Composite with gelatin microparticles | Crosslinking with PEGdA, initiated with APS/TEMED | Injected with chondrocytes. Cell proliferation and GAG production has been tested. | [95] |
| PPF | Composite with PLGA/PEG microparticles encapsulating an ostegenic peptide | Crosslink with PPFDA, initiate by BP and DMT | Implanted *in vivo* in rabbit radial segmental defect. Bone growth related to release profile of osteogenic peptides. | [96] |
| Peptide amphipile | Nanofibrous gels | Self assembly due to hydrophobic interaction | *In vitro* differentiation of MSC into chondrocytes. *In vivo* repair of rabbit full-thickness chondral defect | [97] |
| PLGA-PEG-PLGA | Hydrogel | Inverse thermogelation | *In vitro* epithelial cells encapsulation. *In vivo* bandage of a rabbit corneal wound | [98] |
| Hydroxy butyl Chitosan | Hydrogel | Inverse thermogelation | *In vitro* hMSC suspension in the hydrogel. Evaluate viability as a potential treatment for intervertebral disk degeneration | [99] |
| PEG-Hyaluronic acid | Hydrogel | Enzymatic crosslinking | *In vitro* mesenchymal progenitors encapsulation and cartilage deposition for IVD repair. *In vivo* immune response evaluation | [100] |
| Alginate dialdehyde-Gelatin | Hydrogel | Aldehyde groups linked by borax buffer, then Schiff reaction to bind gelatin | *In vitro* chondrocytes encapsulation. Toxicity and GAGs deposition evaluation | [101] |
| Thiolated gellan gum | Hydrogel | Thermal gelation + disulfide bond formation | *In vitro* cytotoxicty assays, injectability | [102] |

Using this approach, Krebs and co-workers injected solutions of PLGA and different porogens (ammonium bicarbonate, sodium bicarbonate or sucrose) in tetraglycol in an immunodeficient mouse. Porous scaffolds were obtained due to precipitation of the polymer after the removal of tetraglycol by effect of biological fluids, and the procedure showed no significant cytotoxicity (Figure 2.14) [90].
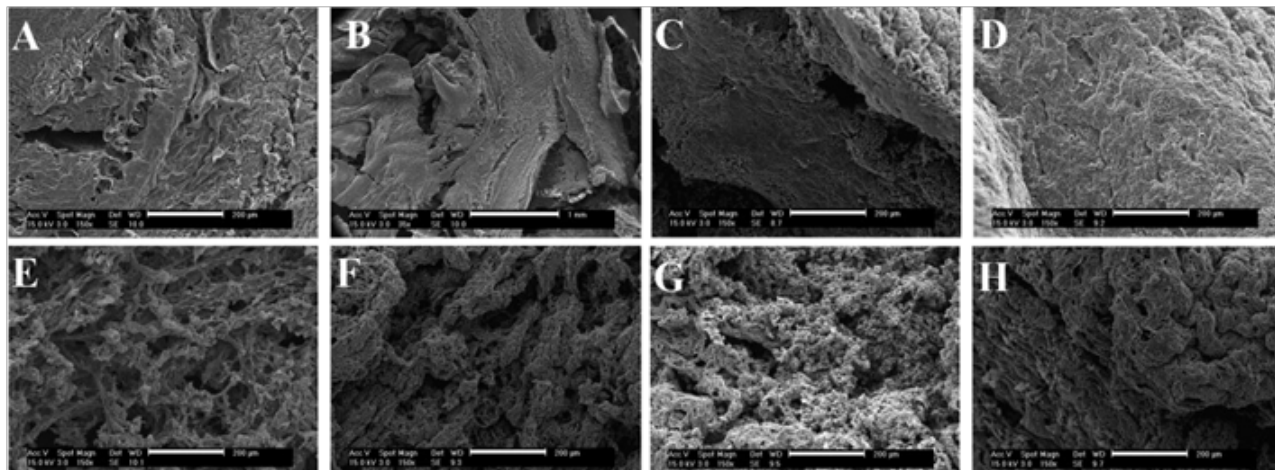


**Figure 2.14: SEM photomicrographs of 50:50 PLGA scaffolds depicting interior and surface microarchitecture. (A and B) PLGA only; (C and D) PLGA + sucrose; (E and F) PLGA + sucrose + diH2O; (G and H) PLGA + diH2O. (C, E and G) Scaffold inner morphology; (A, B, D, F and H) scaffold surface. All scale bars represent 200 μm except in (B), where it represents 1 mm. Adapted from [90].**

Despite this result, water based systems are currently the most common choices in the field of injectable biomaterials, which employ water-soluble monomers or macromers that form 3D matrices either via chemical or physical crosslinking.

Chemical crosslinking often needs initiators capable of creating free radicals that react with functional groups, often unsaturated bonds, to propagate the crosslinking reaction. Crosslinking enhances certain mechanical properties of the scaffold, such as stiffnes, usually at the cost of resilience. A challenge in this area is controlling the solidification time, which must be clinically relevant in order to avoid tissue necrosis around the injected material. Not only, any exothermic reaction that takes place should not reach temperatures capable of causing thermal necrosis of the tissues, a renowned issue with commercially available polymeric bone cements [91]. When a source of energy is required to activate the initiator, it can be provided by light or temperature, for instance. Photopolymerization has the potential to be triggered by the surgeon with, for example, an UV lamp or optical guide, and may be preferred to thermally-induced crosslinking for tissues were light transmission is still easily permitted (e.g. derma, subcutaneous adipose tissue). Overviews of cytocompatibility of different photoinitiating systems are provided in literature [104]. Acrylic derivatives of poly(ethylene glycol) (PEG), like poly(ethylene glycol) diacrylate (PEGdA), are extensively studied in tissue engineering and drug release due to their biocompatibility and as they can form covalent hydrogels whose mechanical properties can be tuned to resemble those of soft tissues.

Patel et al. synthesized PEGdA 6000 Da hydrogels (Figure 2.15) modified with biodegradable and cell adhesive peptide sequences (a collagenase-sensitive sequence and a laminin domain) that could form after 5 minutes of UV treatment. The system was proven to be suitable for preadipocytes proliferation, thus having a potential as in situ forming scaffold for adipose tissue engineering [94]. Similarly Witte and Kao studied the UV gelation kinetics of an interpenetrated network of PEGdA and gelatin, optimizing the UV time exposure, distance from the radiation source and quantity of photoiniziator [105].
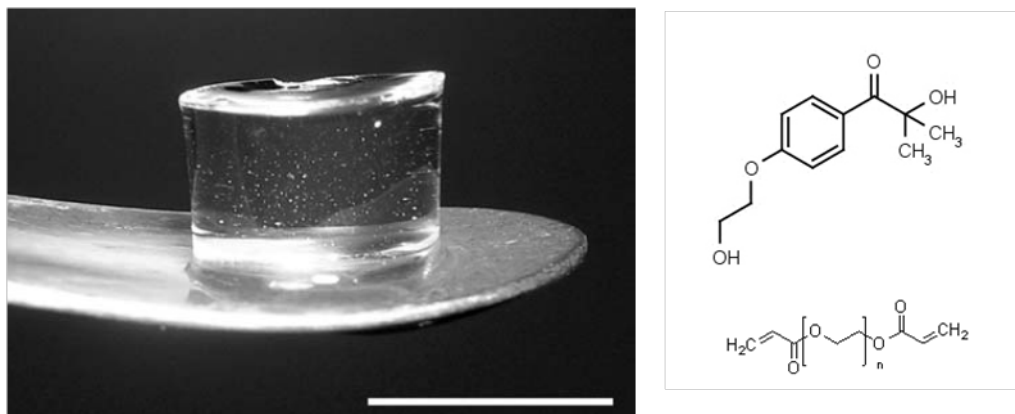


**Figure 2.15: PEGdA 6000 Da hydrogel, scale bar 5 mm (*left*), PEGdA and Irgacure 184 chemical structure (*right*) [94].**

However, several tissues are not easily reached by external light sources, and thus in many cases thermally-activated crosslinking agents are preferred. Ammonium persulfate/N,N,N',N' –tetramethylethylenediamine (APS/TEMED) is a well known water soluble and cytocompatible thermal radical initiator. Parks and co-workers recently used this system to obtain solid scaffolds from oligo or poly(propylene fumarate) (OPF or PPF) [95]. Solidification at 37 °C was achieved in 10 minutes and the scaffold supported chondrocytes delivery and biosynthetic activity. Inner porosity was achieved forming composites with gelatin or PLGA drug-loaded microspheres. PPF is a widely studied polymer for in situ radical polymerization and therefore was also studied in combination with other crosslinkers, such as the system benzoyl peroxide (BP) and N,N-dimethyl-p-toluidine (DMT) [96]. Other biocompatible ways to achieve chemical crosslinking include biologically inspired bonds such as biotin-avidin [106] and thrombin-factor XIII coupling [107]. Anyway, their application on a large-scale production presents several challenges.

More recently a great interest around physically crosslinkable systems has been grown. Biomaterials whose solidification can be triggered in situ by self-assembly or by environmental cues (pH, temperature, ionic concentration) are desiderable as they can be set in mild physiological conditions and avoid the used of initiator, whose concentration and choice is strictly limited by cytoxicity issues, as briefly mentioned above.

Physical crosslinking is generally driven by reversible interactions that form either strong (e.g. ionic) or weak bonds (most commonly hydrophobic interactions). A first group of physical hydrogels utilizes ionic crosslinking to trigger gel formation. The most famous polymers exhibiting this gelation are alginates, polyanionic saccaridhes derived from certain algae or mushrooms, that can be crosslinked by divalent cations such as $Ca^{2+}$. These cations bind between the guluronic acid that forms alginate chains, forming interchains bridges. Alginate hydrogels have been commonly used as extracellular matrix analogues, as they provide the advantage of biocompatibility, and recent research has focused on optimizing their gelation kinetics, homogeneity, mechanical properties and bioactive behavior [108]. Apart from ionic concentration, body temperature is one of the most appealing stimuli to drive sol-gel/solid transitions and in the last years several polymers that show a reverse sol-gel transition around 37 °C have been synthesized. They are generally amphiphilic polymers that are soluble in water at temperatures below the Low Critical Solution Temperature (LCST). Above LCST and in a proper range of concentration, hydrophobic interactions between the polymeric chains prevail, causing coacervation, micellization and partial crystallization of the macromolecules that induce the precipitation of a hydrogel. For example, PLGA-PEG-PLGA copolymers can be designed to exhibit a LCST between 20 and 35°C (Figure 2.16).
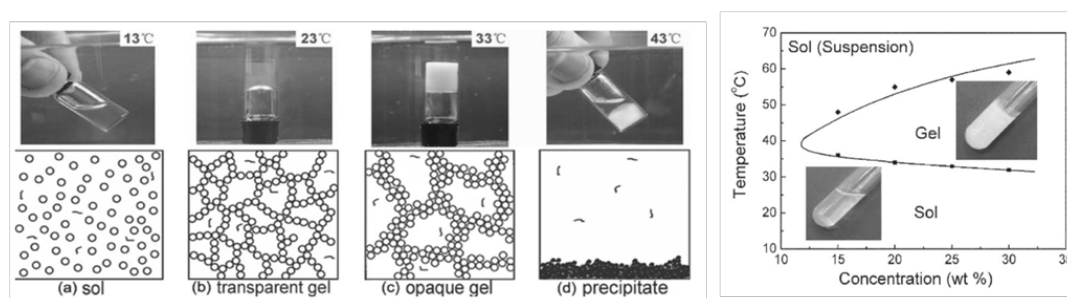


**Figure 2.16: Mechanism of gelation in a PLGA-PEG-PLGA thermoreversible hydrogel. Adapted from [93].**

The forerunners of these types of polymers are Pluronic (BASF) and Poloxamer (ICI), which are not biodegradable. A wide variety of synthetic and natural biodegradable polymers with thermally responsive characteristic have afterwards been synthesized or identified, so that their sol-gel transition can take place in the range of physiological temperatures (fig. 2.17). Several synthetic routes have been explored to obtain block or graft copolymers of hydrophobic and hydrophilic chains (Figure 2.18), to chemically modify natural-origin biopolymers, or to obtain amphiphilic polypeptides either through solid-phase synthesis or recombinant technology [109].
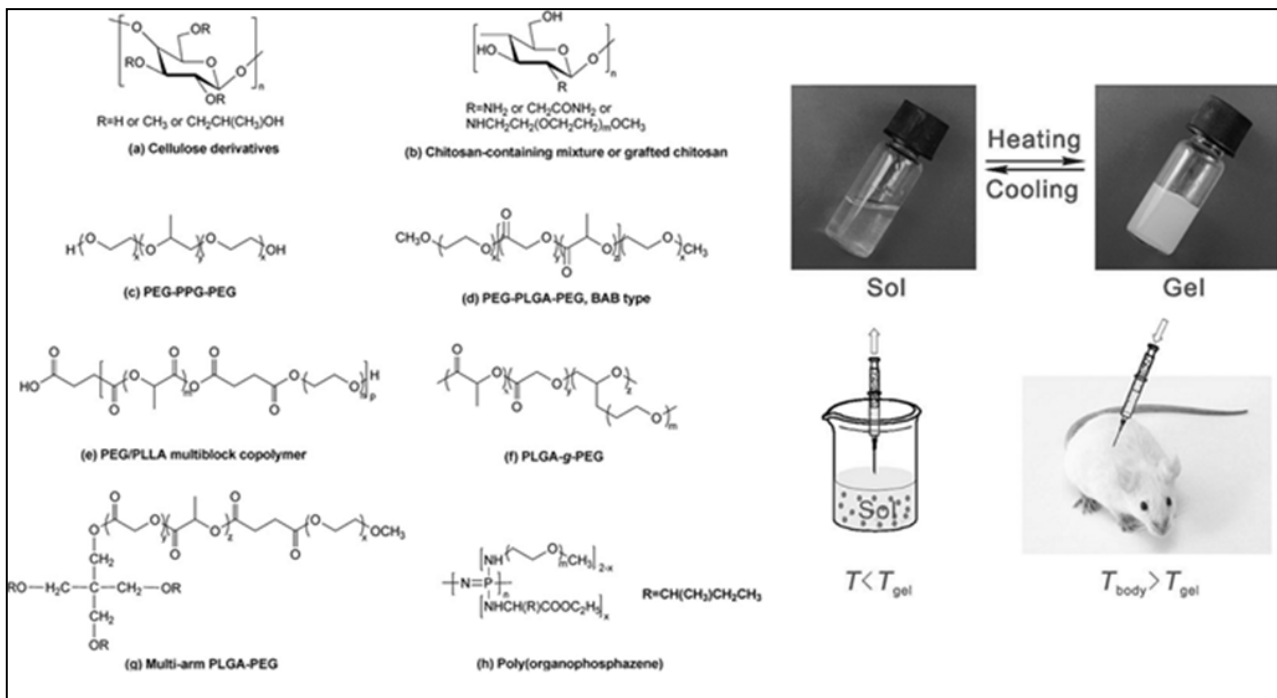
**Figure 2.17: Chemical formulae of some inverse thermosensitive hydrogels and schematic of their gelation process. Adapted from [93].**
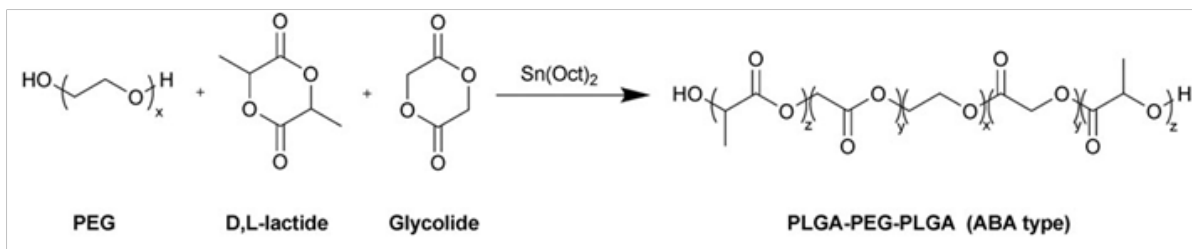


**Figure 2.18: Example of synthesis of PLGA-PEG-PLGA triblock copolymer.**

Many of these systems have also been evaluated specifically for applications in tissue engineering, elucidating many parameters that affect both their thermosensitive nature and the release kinetics of encapsulated drug and cells. For instance, ephitelial cells viability and potential to repair corneal wounds was assessed for a PLGA-PEG-PLGA formulation [98], while the mechanical suitability of a thermosensitive chitosan derivative to act as a scaffold in intervertebral disk injuries was evaluated, together with the cytocompatibility with MSCs [99].

However, despite of the interesting properties of physical hydrogels, there are several key-points that should be taken into account when choosing these systems as injectable biomaterials. Physical crosslinking and self-assembly often lack the mechanical strength that can be achieved using the conventional methods of chemical crosslinking, potentially rendering these systems inappropriate for load bearing tissues such as

tendon, bone, cartilage. Not only, the degree of physical crossliking cannot be finely tuned, thus making more difficult to control the drug release profile.

*2.5.2 Bioprinting and injectable biomaterials*

Injectability, together with the ability of a biomaterial to solidify or maintain a determined shape imposed after the injection step, is a very versatile property. The concept of injectability of biomaterials followed by shape-retention can be associated with extrudability under conditions and parameters (injection stresses, temperature, material and solvent composition) that are compatible with labile, biological matter, including cells. In polymer engineering, extrusion is a well-established processing method, and can be followed, for instance by molding or fiber spinning. Fibers obtained in this way can be also used as building units for the bottom-up production of novel biomaterial devices, for instance, using additive manufacturing techniques. This concept is the foundation of *Biofabrication*, which consist in the replication of complex 3D living tissues, via a computer-controlled fabrication process that involved the deposition, patterning and assembly of both living and non-living matter with a pre-designed 3D organization [110]. Biofabrication methods include 3D printing of *bioinks*, hydrogel-based materials encapsulating living cells, which can be also called *bioprinting* [111].
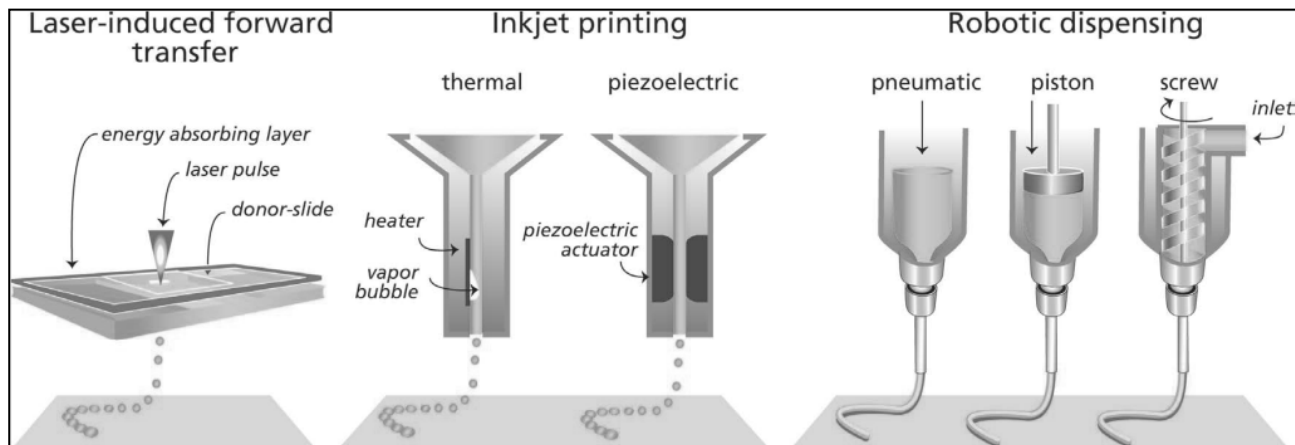


**Figure 2.19: Examples of different bioprinting approaches. Hydrogels fulfiling the extrudability requirement can be used in robotic dispensing systems as bioinks. Adapted from [111].**

The bioprinting process starts from a blueprint of the tissue to be fabricated in Computer Aided Design (CAD) softwares. This allows designing and generating custom-made devices such as patient-specific implants, as the computerized model can also be acquired from tomographic images. Subsequently, a Computer Aided Manufacturing (CAM) software instructs the hardware of the bioprinting apparatus. An example of different experimental set-ups for bioprinting is depicted in figure 2.19. In the case of robotic dispensing of bioink fibers, a dispensing tool head navigates in the x, y, z direction, depositing the gel fibers

in a layer-by-layer fashion [112]. Figure 2.20 shows some anatomically-shaped structures produced using a bioprinting technology. This relatively new, still under development, area of technology has the great potential to revolutionize many fields of bio-based industries. As for biomedical engineernig, biofabricated constructs can be obtained combining several materials and cell types, thus allowing to recapitulate complex, multilayered or multicomponent tissues, such as articular cartilage [113], or recreate tissue-like grafts with *ex vivo* pre-generated vascular networks [114]. Potential biomedical applications include, but are not limited to, fabrication of i) tissue and organs for transplantation and regenerative medicine, ii) living, 3D tissue models of human disease, and iii) platforms for drug toxicity and drug discovery research.
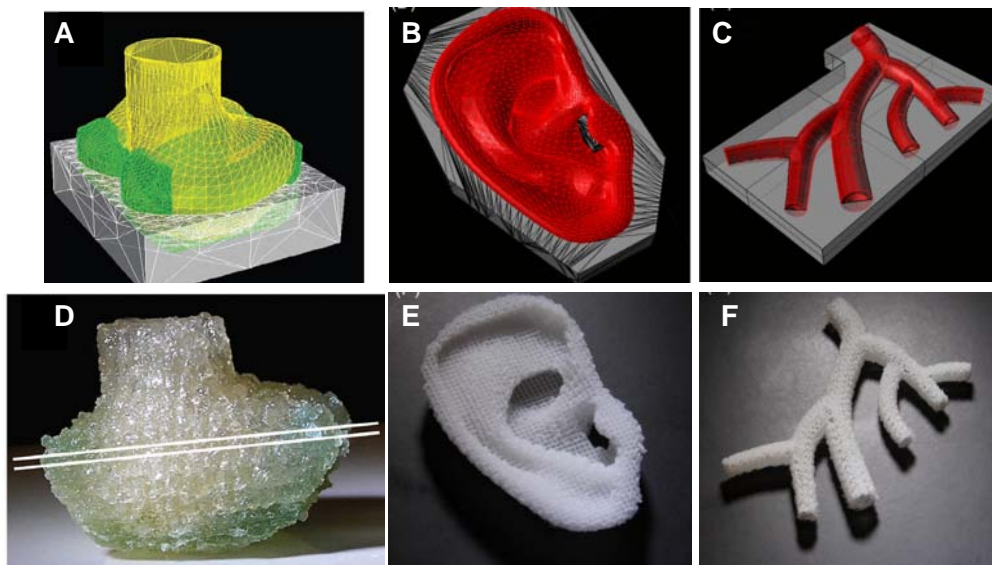


**Figure 2.20: (A, B, C) CAD designs of 3D printed tissue models. (D) Distal femur made with a gelatin-methacrylamide bioink. (E) and (F) ear and vascular network made with a thermoplastic polymer; the structure fabricated via additive manufacturing can be then colonized with cells, allowing also "classical" tissue engineering approaches. Adapted from [112].**

Most of the hydrogel systems that can be extruded and quickly set to maintain the geometry imposed during the bioprinting process are potential candidates as bioinks. Gelation and long-term shape stabilization can be also induced exploiting certain hydrogels physical crosslinking capability as well as crosslinking methods, as described in the previous paragraph for injectable gels. Moreover, bioinks must not only be designed in order to achieve high printing fidelity, but also to offer a matrix to guide encapsulated cell behavior, allow migration and neo-tissue deposition. The implication of bioink design in biofabrication and the delicate balance between fabrication and cell culture necessity has been extensively reviewed elsewhere [111], and this knowledge has brought to the application of many hydrogel-forming materials for bioprinting, including alginate, gelatin and its derivatives, gellan gum, agarose, fibrin, collagen, hyaluronic acid, and PEG [111]. Hydrogels tend to be unsuitable to withstand high mechanical stresses, therefore strategies to reinforce the printed constructs have to be devised, when aiming to generate load bearing constructs, as for bone or cartilage tissue engineering, for instance [115, 116].

Controlling the 3D distribution of multiple (artificial or natural) ECM components, cell population and growth factor, although representing a great innovation, it is still not enough to reproduce ideal grafts for *ex vivo* tissue fabrication or for the generation of implantable device that can fully regenerate native tissues. A strong understanding of the biological mechanism underlying tissue homeostasis and regeneration, stem cell biology, and the development of biomaterials and molecules inspired by this knowledge that can trigger and guide cell bioactivity are essential. For this reason, strategies that can provide the inclusion of cell-instructive, physic-chemicals cues into the bioink matrix are still sought to achieve *ex vivo* tissue regeneration [117]. Furthermore, as for all cell-based tissue fabrication approaches, techniques that are compliant with GMP to obtain high amount of regenerative-competent cells, are also necessary, in order to allow scaling-up of the production [118].

## 2.6 Microcarriers and Nanocarriers

### 2.6.1 Micro and Nanocarriers in biomedical technology

In the field of injectable biomaterials, apart from macroscale devices, particulate systems can be used as carriers of therapeutic agents. Particles suspension in physiological solutions can share some properties with *in situ* forming devices, namely injectability, capability of filling defects with irregular geometries and encapsulate and delivery labile compounds, depending on their dimension and shape. Additionally, particles display a great versatility for biomedical applications. They can be either presented in the form of nano- (NPs) or microparticles (MPs). It should be noted that, especially in the pharmacology literature, the terms nanoparticle is (mis)used for particles ranging from hundreds of nanometers to a few micrometers. For the sake of clarity, and to facilitate the distinction between the materials prepared in this experimental work, particles sizes up to a few hundreds of nanometers will be termed nanoparticles. Size is the main parameter affecting the type of application these biomaterials are designed for, as drug delivery systems, carriers for cell therapy, or components for tissue engineering (Figure 2.21). Injectability is mainly dependent on particles size and concentration in the suspension; according to these two parameters, the needle gauge for the injection should be chosen in order to minimize the strength necessary to administrate the particles and therefore the pain for the patient.
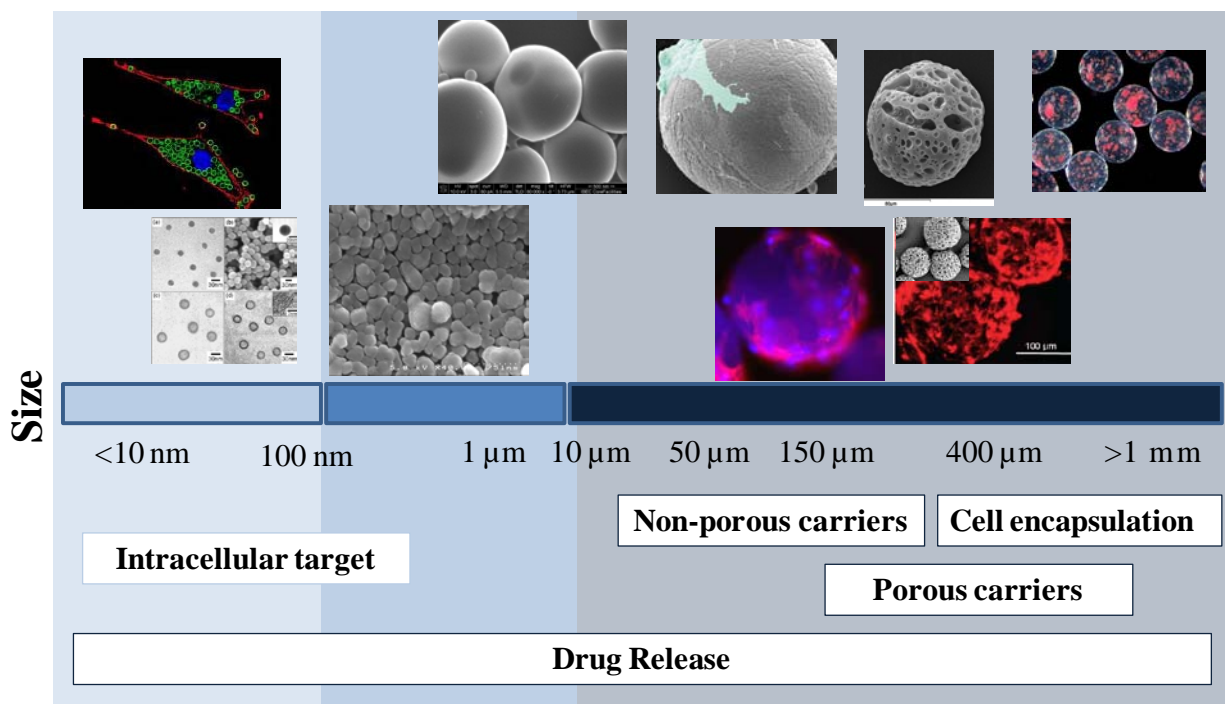


**Figure 2.21: Example of typical applications of micro- and nanocarriers according to the size.**

While NPs are more suitable for drug delivery and intracellular targeted release of bioactive compounds (particles whose dimension is less than 5 µm are readily subject to endocytosis by macrophages), MPs can be also manufactured with dimensions that are adequate for cell adhesion and spreading, as cell culture and expansion platforms, either alone or in combination with 3D scaffolds to form composites [119]. MPs are

extensively studied and already in use in pharmaceutical practice for biomolecules encapsulation and controlled drug release, thus a broad range of up-to-date studies related to MPs production, modification and applications is presented in literature, constituting a valid base for the development of particle-based biomaterials.

MPs are also advantageous regarding in vitro culture of anchorage-dependent cells, as they offer a high surface-volume ratio, suitable for cell homing. Other important properties of nano- and microparticles are their shape (spherical, cylindrical, laminates, needle-like) and degree of inner porosity (Figure 2.22), which determine *where* in the carrier the therapeutic agent will be located (encapsulated in the matrix, confined in inner porous compartment, or even adhering at the particle surface, the latter being more common for living cells, rather than drugs).



capsules (core-shell)　Porous　Open, interconnected porosity　Dense particles
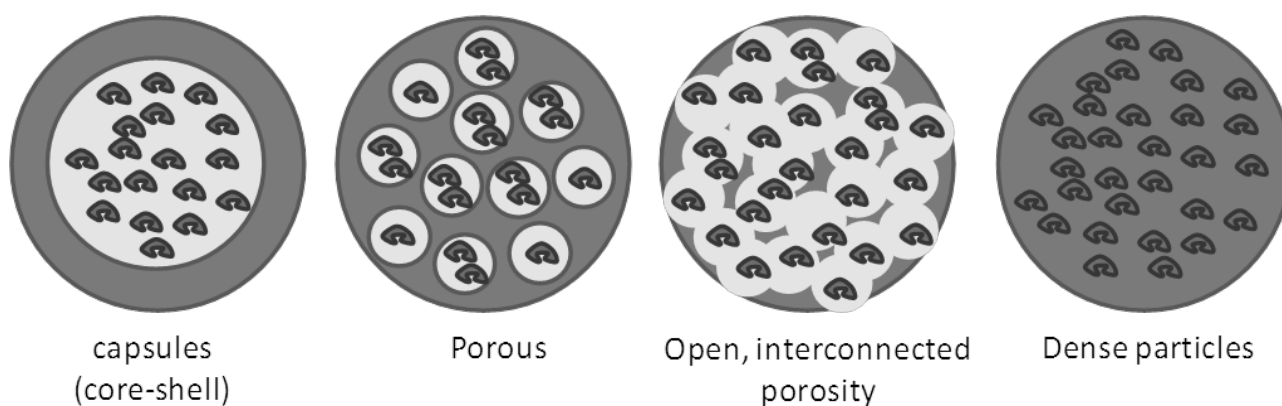
**Figure 2.22: Examples of possible inner morphology of particles, with a schematic representation of the distribution of bioactive compounds.**

Looking into the field of regenerative medicine, MPs can be applied not only as pharmaceutical devices, but also as active components in tissue engineering and cell delivery strategies. Tissue regeneration through cell therapy with pluripotent or stem cells have recently achieved interesting results even in repairing tissues with low self-renewal capability, such as cartilage, or composed by post-mitotic cells, such as neuronal tissue [120]. However, free-cell transplantation faces many problems related to cell survival, as only a small percentage of the implanted cells survives or remains in the area of the tissue defect. Instead, cell delivery on MPs has several biological and practical advantages, if compared with delivery without carriers. In fact, cells can easily aggregate on MP surface forming complexes that promote cell-cell interaction, while, once injected, the cell-MP complexes are less likely to be dispersed by biological fluids than free cells. Not only, during their fabrication process, MPs can be loaded with drugs and growth factors capable to support tissue regeneration. MPs diameter for adequate cell adhesion should be at least around 50 µm, as smaller particles could be easily eliminate by the organism, or induce undesired inflammatory responses [120].

Many different materials have been processed to obtain microparticles. Natural polymers such as chitosan, alginate, gelatin and pectin are mostly used in combination with cell suspension, in order to achieve cell encapsulation [121], even though dextran microparticles, in commercial formulation known as Cytodex®,

have been utilized also to carry cells on their surface, together with other materials [122]. Anyway, biocompatible and biodegradable synthetic polymers, such as PLA, PGA and their copolymers are the most studied and used in pharmaceutical practice as well as in tissue engineering, due to their ease, reproducible and standard manufacturing.

## 2.6.2 Fabrication Methods

Although it is possible to produce particulate materials in a *top-down* fashion, starting from a macroscale material and reducing it to particles, for instance by grinding, these approaches allow little to no control over the particles shape, size, as well as surface and inner morphology. Therefore, the most investigated particles fabrication methods require the generation of liquid droplets of polymer solutions and their subsequent solidification into particles (Table 2.5). The way the first step is performed is fundamental in determining the type of particle produced and its size, from the nano- to the microscale.

**Table 2.5: Overview of particle fabrication methods**

| Droplet generation process | Particles size | Polymers | Advantages | Disadvantages |
|---|---|---|---|---|
| Emulsion (turbulent mixing) | 10 nm to mm scale | All types | Size dependent of emulsification method. Control over porosity. | High polydispersity |
| Membrane emulsification | 1-100 µm | PLA, PGA, PLG, PCL, PEG-PLA | High control over size and porosity. | Low production rate |
| Emulsion (microfluidics) | 1-300 µm | All types | Monodisperse particles, low mechanical stresses | Low production rate |
| Flow focusing | 10-300 µm | All types | Low stresses, monodisperse particles | Only works at specific ranges of flow ratios |
| Electrohydrodynamic jetting | 0.1 to 30 µm | All types | Type of electrospray. Control over particle size and shape | Small diameter |
| Ultrasound atomization | > 40 µm | All types | Reproducible, scalable, fast | Polymer solution must have low viscosity |
| Spray drying and electrospray | 10 nm to 100 µm | All types | Fast and scalable | High polydispersity |
| Supercritical fluid atomization methods | 10 nm to 100 µm | PLA, PGA, PLG, PCL, PEG-PLA | Limited use of toxic chemicals | High polydispersity |
| Nanoprecipitation | 50-400 nm | All types | Fast. Monodisperse particles | Size depends on solvent/non-solvent pair |

*2.6.2.1 Emulsion-based techniques*

Emulsions rely on the mixing of two (or more) immiscible liquid phases. A general representation of an emulsion-based fabrication method is depicted in Figure 2.23. At least an "oil" phase (which can be typically an organic solvent with a polymer dissolved in it) and a water phase are needed, and one as to act as a dispersed phase and the other as a continuous phase. The two phases are mixed and droplets of the oil phase are formed, whose diameter is highly dependent on the type of emulsion (nature solvent used, multiple, double or single emulsion) and on the shear stress applied to the suspension (the higher, the smaller the mean dimension but with broader size distribution; therefore use of homogenizer or magnetic stirrers strongly affects the result). In this step, if the emulsification is performed using high-speed homogenizers or sonication devices, small, nanosized drops can also be produced [123]. The addition of amphiphilic surfactants to the water-phase is helpful to stabilize the boundaries between the oil and the water phase, thus also controlling shape and diameter of the droplets [124].

Single emulsions are mainly used for particle production which may be coupled with encapsulation of biomolecules that are soluble in the phase used to dissolve the polymer (typically the oil phase), while double emulsions are mainly used to encapsulate drugs that are not soluble in the solvent for the polymer (e.g. water soluble proteins encapsulated into PLGA spheres). When organic, volatile solvents are used, droplet solidification into particles occurs over time, with solvent evaporation. Nano- and microparticles are formed as the solvent is transported out from the initial droplet, diffused into the continuous phase and evaporated through the emulsion-air interface [125]. Right after the emulsification, the water is saturated with the solvent; once the evaporation initiates, the droplets near by the interface will start to solidify. As the polymer precipitates, the remaining solvent inside the droplets is expulsed and the microparticle generates. A slow solvent evaporation rate induce particle volumetric shrinkage and thus produces smaller particles (but also can eliminate part of the encapsulated drug). Faster evaporation rates avoid shrinkage and may retain more drug, but the droplet is soon covered by a thin hard surface layer with a less dense core that may induce either the collapse of the sphere or to the formation of hollow capsules, as the polymer accumulates only on the surface (in this conformation, burst release of the drug is more intense, as part of the drug is pushed and trapped to the polymeric shell). Parameters such as polymer concentration, type of surfactants and water flows induced by osmotic imbalance may cause the formation of random porosity on the surface (more similar to cracks in the polymeric outer shell of the particle). Addition of porogens as well as the use of double emulsion methods can introduce a certain extent of porosity which can be desiderable for cell delivery, and must be carefully controlled in drug delivery applications in order to limit the burst diffusion of the drug [126].
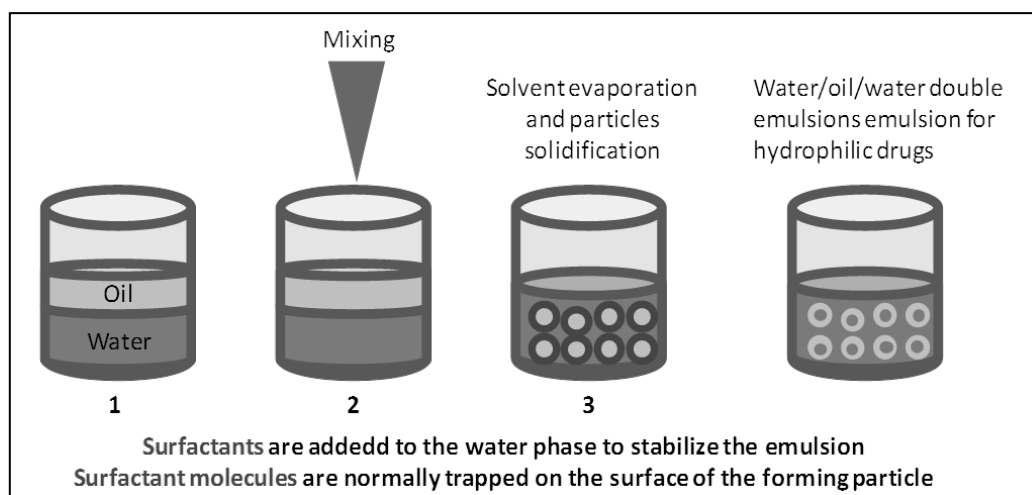
**Figure 2.23: General scheme of an emulsion/solvent evaporation procedure.**

Emulsification by turbulent mixing of the oil and water phases, generate a population of droplets with a very high dispersion in diameter distribution. Polydispersed particles will display a dishomogenoeus behavior, for instance, in terms of degradation patterns (i.e. smaller particles have higher surface area and degrade faster), which can be detrimental to accurately control the release profile of encapsulated drugs [127]. In order to solve this problem, modifications of the emulsion system have been explored, such as membrane emulsification [128] and emulsification in microfluidic systems [129]. Once the emulsion is established, apart from solvent evaporation, particles can also be obtained by other phase separation techniques, such as non-solvent or thermally induced phase separation [130, 131], or in the case of some hydrogel forming materials, by triggering gelation (i.e. immersion in $Ca^{2+}$ rich solutions for sodium alginate droplets) [132].

### 2.6.2.2 Nozzle- or injection based methods

Dripping of a liquid medium at an orifice is a common phenomenon that produces drops and can be observed in our daily life, for instance, when considering water dripping from a faucet. A liquid coming from an orifice, if the flow rate is high enough, can also assume the form of a jet, that can be defined as a stream of matter having a more or less columnar shape [133]. Jets with a laminar flow are usually thinner than the nozzle they are coming from, and present an inherent fluid dynamic instability (Rayleigh instability) that can lead to their eventual break-up, provoking the atomization of the liquid (Figure 2.24) [133]. Addition of external stresses such as high injection pressures, mechanical perturbations, electrical fields or coflowing fluids can tune a jet diameter, as well as the way a jet breaks and generate droplets of controlled size.
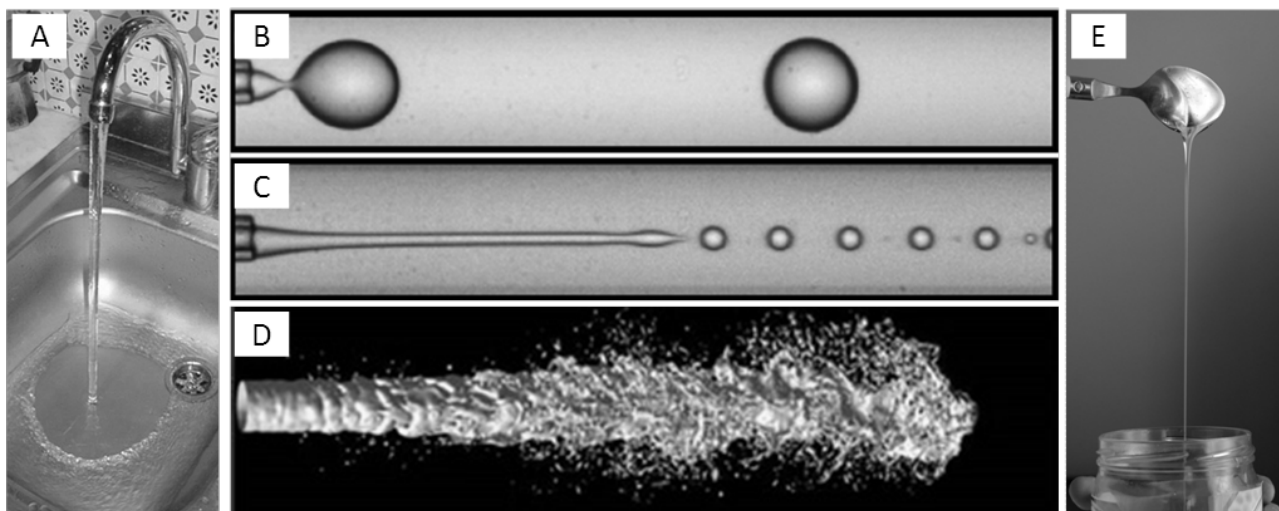
**Figure 2.24: (A)** Liquid jets are experienced every day, for instance, as water flowing from a faucet. Fluids at a nozzle tip can generate **(B)** large drops by dripping or stretch into laminar jets that will eventually break-up **(C)** into a train of similarly-sized droplets. **(D)** Turbulent flows, for instance those generated by high pressures, can break into a spray of polydispersed droplets. Jet stability and break-up also depend of the flow speed, external stresses and fluid viscosity, with high viscosities acting as a protective factor for jet stability - **(E)** shows a viscous honey jet stretching without breaking -. Adapted from [133].

These principles are the bases of many droplets-generation techniques, which, tuning the flow parameters and the intensity of the external applied stress, can also be used to produce filaments of the polymer, as well as particles with complex shapes (discs, needles). The combination of fluid flows, viscosity and external stress determines the final size of the fabricated particles. Flow Focusing technology, for instance exploits the interaction between an inner fluid pulled by a coflowing, immiscible fluid. The higher the flow rate of the outer fluid, the small the droplets; while the higher the flow rate of the inner fluid, the larger the produced droplets. The main advantage of this method is that only mild, hydrodynamic forces are involved in the drop generation, allowing to operate the system in conditions suitable for the encapsulation of labile compounds (i.e. proteins) or even cells [134]. If the outer fluid is a gas, drops can be either dried before reaching a collector plate, or be collected in a liquid bath to be solidified with other methods. Once the drops are formed following jet break-up, they can be readily solidified by rapid solvent evaporation, thermal or non-solvent induced phase separation, drying or through chemical reaction (i.e. for polymer crosslinking and hydrogel formation). Moreover, methods based on laminar jets are extremely useful to obtain highly monodisperse particles [135]. Droplets generated in this way can also be dispersed in a continous immiscible liquid phase to obtain an emulsion, which can be processed as described in the previous paragraph [136].

Solution atomization using ultrasound pulses generators, as well as electrical fieldsapplied to the dispensing nozzle, have also been successfully used in cell [137] and drug encapsulation applications [138]. Electrohydrodynamic jetting is a technique described by Bashakar and co-workers [139, 140], this method exploits a typical electrospinning apparatus, whose parameters have been tuned to obtain spherical particles instead of fibers. By tuning polymer concentration, distance of the collector and solvent systems, the authors have been able to produce particles with discoid and rod-like conformation, with characteristic dimensions in

the order of 3-5 µm. In the range of polymer solution concentration studied (1.3 to 4.3% w/v), the final shape of the particles resulted from a combination of the solvent evaporation behavior related to the jet conformation imposed by the flow rate and the voltage applied to the system. An interesting feature of this work was the possibility of co-jetting 2 or more solutions of different polymers (dissolved with compatible or possibly with the same type of solvent) from two spinnerets in order to obtain bicompartimental particles with spatially controlled chemical composition. This configuration was applied to selectively functionalize only one compartment of the particle, with targeted reactions. The procedure was also used to obtain bicompartimental nanofibers.

Atomization of a polymer solution flowing from a nozzle can also be obtained with stresses inducing a turbulent break-up, however at the cost of renouncing to the monodispersity of the generated particles. A typical example of this approach is the case of spray drying, a solution is injected applying a high pressure through a nozzle, and at the nozzle tip it atomizes due to the pressure drop [141]. This process is exploited also in many supercritical fluids based technology. Any substance whose pressure and temperature are above the critical point is called supercritical fluid (SCF). Supercritical fluids possess the solvent power of liquids and the diffusivity of gases, and their properties vary extremely by tuning their density with small changes of parameters such as pressure. There are used as solvent systems, reaction media or in the processing of materials to obtain foams, fibers and particles. According to the solubility of the material to be processed, they may be used either as solvents or antisolvent for precipitation of the polymer. The most studied supercritical fluid is carbon dioxide, as it is non-toxic, non-inflammable and has a critical point close to environmental conditions (304 K and 7.28 atm). Several biodegradable polymers, including polylactide and its copolymers have been processed in the form of micro and nanoparticles (with or without drugs) through different methods involving supercritical $CO_2$. Among this techniques the most relevant are:

- Rapid expansion of supercritical solutions (RESS): the polymer is dissolved in the supercritical fluid and the high pressure solution is rapidly depressurized by spraying through a noozle. The pressure induced phase separation leads to the formation of the particles. PLLA solutions in supercritical carbon dioxide have been obtained by addition of co-solvents such as acetone and ethanol.

- Supercritical antisolvent (SAS) and solution enhanced dispersion by supercritical fluids (SEDS) processes: A solution of the polymer in an organic solvent is sprayed in a chamber saturated with the supercritical fluid that acts as an non-solvent and forces the particles to precipitate (SAS), or the SCF and the polymer solution are sprayed together from a coaxial nozzle (SEDS). In the last case, the SCF acts as an antisolvent and a dispersion medium at the same time. PLA have been processed in this way after dissolution in methylene chloride, using carbon dioxide as an antisolvent.

The most interesting feature of these methods is the possibility to target the size of the particles and obtain even submicron diameters in a relatively easy, fast way, which can be also suitable for scaling up the production. Several studies have demonstrated that, even though process parameters may affect the shape of the particles, their actual morphology is mainly dependent on the material properties. Semicrystalline

polymers (including PLLA) tend to form almost perfectly spherical particles, but as the crystallinity increases, polymers are more likely to produce fibrous or spherulite-resembling structures.

Drug encapsulation in the particles has been proven to be either possible during particle formation (obtaining a drug-polymer blend) or by inducing SCF-mediated polymerization in presence of the bioactive molecule [124, 142].

*2.6.2.3 Nanoprecipitation*

Nanoprecipitation is best known for being a quick, single-step technique preparation of nanoparticles that can encapsulatate high yields of water-insoluble drugs [143]. Due to its ease of application is currently one of the most applied methods to produce nanoparticles between 100 and 300 nm for drug encapsulation [144].This method consist in the precipitation of the polymer in a semi-diluted solution following the displacement of the solvent into a water-based bath, assumed that the organic solvent is miscible with this bath (Figure 2.25). A typical system is PLGA dissolved in acetone, dispensed in a water bath.
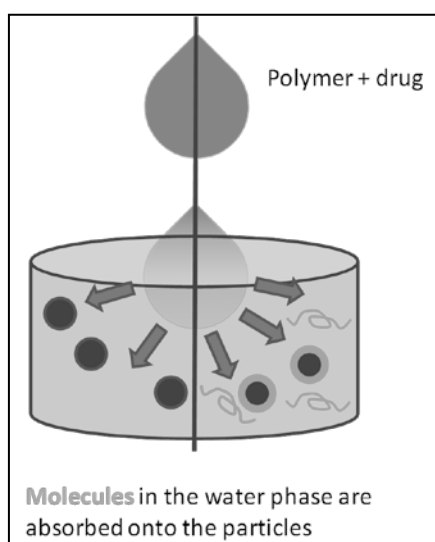


**Figure 2.25: Schematic representation of the nanoprecipitation principle with** *(right)* **or without** *(left)* **NPs functionalization by adsorption of molecules dissolved in the coagulation bath.**

The polymer solution is added dropwise (e.g. syringe pump) into a coagulating bath, while parameters such as pH of the water solution, addition of active substances or other polymers to the organic phase and polymer concentration affect the drug incorporation efficiency (depending on the properties of the drug an alkaline or acid bath may be preferred) and the particle shape. As soon as the (large) polymer droplet enters the bath it is broken into a multitude of nanoparticles by the turbulent flows driven by the gradient of surface tension between the two liquid (Marangoni effect) [145]. The nanoparticles can then be collected via ultracentrifugation, for instance. Large amounts of toxic solvent may be avoided with this method. This method is widely used for manufacturing nanoparticles that are generally smaller than those obtained with emulsion methods [146]. The aqueous phase may also be charged with additives that will be partially

entrapped on the surface of the polymeric particle (e.g. magnetic compounds, charged macromolecules or inorganic ions), and this fact can be exploited to functionalize the device surface. Alternative coagulating solvent may be chosen according to the organic solvent employed; studies reported in literature describe, for example, the use of ethanol and methanol and their influence on particle size [146]. The lack of a stabilizer in the water bath may frequently lead to agglomeration of the particles; therefore the use of small amounts of surfactants may still be necessary. Finally, NPs produced as hollow capsules or solid, filled spheres can be obtained, using or not template materials (such as oils mixed with the polymer phase), that can be removed at the end of the fabrication procedure.

## *2.6.3 Drug delivery with functionalized active carriers*

Micro- and nanocarriers, especially the latter, are of great interest in the field of drug delivery devices. Polyesters like PCL, PLA and PLGA are widespread choices as biocompatible vehicles whose physic-chemical properties can be tuned selecting the polymer molecular weight and copolymerization degree [147]. Indeed, functionalization strategies can be applied in order to endow polyester-based carriers with *smart* behaviors, since they are materials that, *per se*, are unable to elicit specific responses from, or to interact actively with the biological milieu. Functionalization of nano- (or micro-) particles for drug delivery can have multiple purposes, but in general aims to improve the efficiency of drug delivery, either by enhancing passive targeting or allowing active interactions with certain ligand presented on cells or tissue components (such as ECM molecules) [148]. As seen in paragraph 2.5.2, several methods of preparation, including emulsions and nanoprecipitation, allow the modification of the NPs during the same fabrication procedure by means of incorporation of active molecules. Moreover, functionalization can be achieved choosing-synthesizing polymers to produce NPs that are already endowed with particular properties, or by chemical modification (i.e. covalent grafting or physisorption of biomolecules) on the already generated NPs.

Passive targeting of cells or diseased tissues consists in improving the chances of a NPs device to localize into a given target, in an unspecific way. For instance, coating NPs with PEO, pluronic or other non-fouling molecules, increase the NPs circulation time in the bloodstream, increasing the number of carriers able to accumulate in their target without being eliminated by phagocytic cells or by renal clearance [149]. Pluronic coatings have also been proven effective in increasing drugs and NPs ability to cross the blood brain barrier, underlining the importance of these polymers in improving the efficacy of the drug delivery process [150]. Modification of the surface charge (Z-potential) of nanocarriers, for instance grafting anionic or cationic polymer (e.g. alginate and chitosan, respectively), is also a method to promote interaction with certain tissues, although in an unspecific way [151]. Controlled drug release with functionalized NPs is also a fundamental area of research for the treatment of tumors. Nanomedicine strategies to target cancer cells involve both active target recognition methods, as well as approaches that could be classified as "in between" passive and active delivery. As for active delivery techniques, NPs can be functionalized with antibodies or

lectins, that are capable to bind specific ligands on the cell membrane and thus locally release high amounts of chemiotherapeutic drugs in the proximity (or even inside) cancerous cells. For instance, PLGA-based NPs have been surface grafted with anti HER-2, Anti Fas, and against antigen rich MCF7 cells antibodies, to successfully bind ovarian [152], breast and colorectal [153] cancers. While it is possible to graft such molecules with high efficacy on NPs, identifying univocal cell surface markers for cancerous cells is a major challenge, due to the continuous adaptation and mutation of these cell types. For this reason, NPs for cancer therapy is often performed developing *smart* passive targeting. Cancer cells are known to have higher metabolic activity, compared to healthy cells, and thus tend to incorporate more nutrients. Functionalization of NPs with metabolic compounds that these cells require in higher amounts, such as folic acid [154] and transferrin [155], have been proven as successful methods to deliver nucleic acids for gene therapy and chemotherapy compounds preferentially to cancer cells, in the lung and in the ovary. Furthermore, active strategies that aim to overcome the hurdle of drug resistance from cancer cells, have also been devised. P-glycoprotein inhibitors-modified PLGA NPs, that can disable one of the mechanism of defense of these cells, have been successfully experimented *in vitro* and *in vivo*, for delivery to adenocarcinoma cells resistant to the drug Taxol [156]. As it can be seen by these few examples, there is a wide amount of molecules to guide NPs localization and improved their spatial distribution and thus drug delivery. A more detailed description of these molecules and their application falls out of the scope of this Thesis. An extensive review of the topic can be found in the literature [157].

Persistent bacterial infections and established biofilms infections are among the pathologies that may be treated using drug loaded-NPs. In biofilms (Figure 2.26), bacteria group together on a surface and start producing their own ECM, mostly made of polysaccharides and extracellular DNA [158]. Sessile bacterial cells are phenotypically different from their planktonic counterpart, are less metabolically active, which make them less susceptible to drugs, and are able to communicate with other cells in the biofilm, develop resistance to antibiotics and respond cooperatively to environmental stresses and threats [159]. Biofilms act as a biological barrier that can protect the encapsulated bacteria and render most antibiotic treatments useless. The degradation of β-lactam antibiotics by β-lactamase, the binding of aminoglycosides antibiotics to the matrix in *P. aeruginosa* biofilms and the inhibition of the activity of tobramycin by lung mucus in cystic fibrosis patients are good examples of unwanted interactions of the antimicrobial agent with the biofilm or tissues of the patient [160]. Nanomedicine treatments using liposomes and polymeric nanoparticles have been proposed to overcome these limitations. Functionalized nanocarriers that are able to bring drugs within the biofilm matrix, thus increasing local antibiotic concentration in the proximity of bacterial cells, and, at the same time, are able to establish interactions with the bacterial ECM thus overcoming its defense, will be discussed more extensively in Chapter 4.
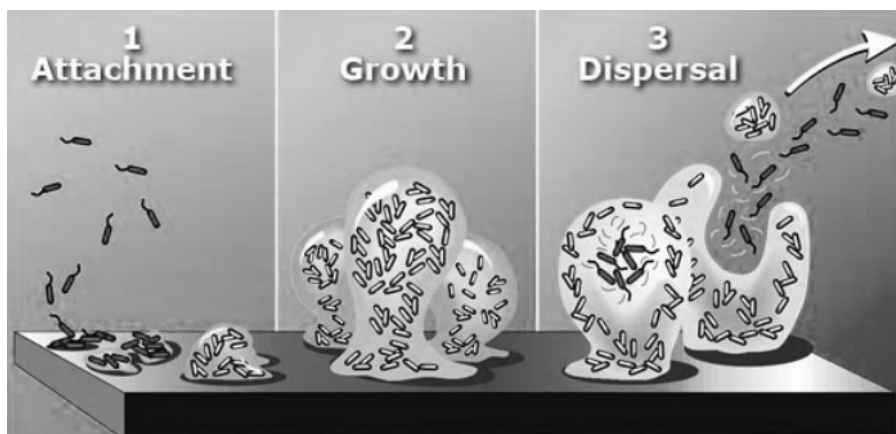
**Figure 2.26: Stages of biofilm formation and maturation. (1) Planktonic cells adhesion on the surface, (2) bacterial ECM synthesis and biofilm growth and (3) dispersion of biofiLm parts or planktonic bacteria can cause the propagation of the infection.**


*2.6.4 Microcarrier culture technology*

MPs with size above 40-50 µm are large enough to home cells growing as monolayers on their surface. Larger particles, with diameter above 100-150 µm, can also display an open porous morphology, with pores large enough to allow cell ingrowth and colonization of the inside of the particle. These types of MPs are usually addressed as microcarriers (MCs). Additionally, large particle made of hydrogel materials (from 150 µm up to a few millimeters), can also be used as microcapsules, whose core may be made of the same hydrogel or be hollow and filled with liquid medium compatible with cells, to enclose cells inside.

The use of microparticles to culture mammalian cells can be traced back to the early 1950-1960s [161], and the first microcarriers were initially derived from spherical chromatographic beads, such as diethylaminoethyl (DEAE)-Sephadex, and the growth of anchorage-dependent cells on microcarriers was a main breakthrough for the culture of virus-infected cells and mass production of vaccine agents [162]. Since then, MC technology has evolved together with the increasing knowledge in cell biology and biomaterials science. A wide variety of materials, geometries and chemical compositions have been exploited to produce MCs. Furthermore, MC technology has received increasing attention for its implications in mammalian cells expansion, especially for cell therapy and tissue engineering purposes. The first, great advantage of MC culture is that MCs can display high surface area for reduced volumes, thus allowing the expansion of cells to great numbers, without requiring the large amount of materials, disposable and space that standard 2D tissue culture techniques would need (Figure 2.27) [163]. Additionally, it is feasible to scale up MCs culture under Good Manufacturing Practice (GMP), for instance using stirred tanks bioreactors [164]. This advantage made MCs culture a fundamental tool in the past decades for recombinant proteins and vaccine fabrication, and has nowadays the potential to allow the production of the high cell amounts need in regenerative therapies, and that are otherwise impossible to retrieve by tissue biopsies.
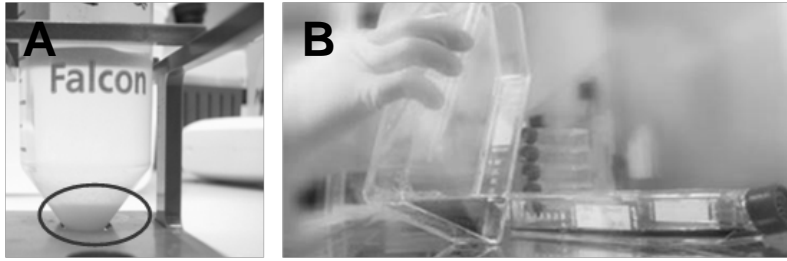
**Figure 2.27: A visual representation of an advantage of microcarrier culture over standard T-flasks. MCs have high specific surface area, so that a minute volume such as that of a pellet of MCs fabricated in this Thesis work (A), offers the same surface for cell growth as that of two standard T175 flasks (B).**

MCs culture in stirred tanks bioreactors is also suitable for medium sampling for continuous monitoring of the cell culture parameters (pH, oxygen tension) and cell metabolites (glucose) consumption and catabolite secretion (lactate and ammonia) which are fundamental for large scale and GMP-compliant processing [165]. MCs exist in many commercially available formulations (Table 2.6) and are used to culture cell lines, primary differentiated cells and stem cell types, including MSCs, ESCs and iPSCs. Most of these cell types respond to mechanical forces and mechanical properties of the substrate (mechanosensing), as well as morphological, topographical and biochemical cues. For this reason, the design and control of MCs shape, surface and material properties and chemical composition plays a fundamental role in modulating cell shape, organization, proliferation and phenotype expression. As a consequence, several research groups have generated MCs of different materials (PLA, PCL, PLGA, gelatin, chitosan, alginate, pectin among others) as cell-instructive biomaterials [166-173]. Moreover, as it can be seen in table 2.5, most of these commercial MCs are not biodegradable, thus they are mainly designed for cell culture rather than as injectable devices for regenerative therapies.

**Table 2.6: List of commercially available microcarriers (adapted from [174])**

| MC type | Manufacturer | Material | Charged | Diameter [μm] | Surface area [cm²/g] | Pore size | Coating |
|---------|--------------|----------|---------|---------------|----------------------|-----------|---------|
| Biosilon | Nunc | Polystyrene | No | 160-300 | 255 | Solid | None |
| Collagen | SoloHill | Polystyrene | No | 90-150 | 480 | Solid | Collagen I |
| CultiSpher-S | Percell-Biolytica | Gelatin | No | 130-380 | 7500 | 20 μm | None |
| Cytopore 2 | GE Health Care | DEAE-Cellulose | + | 200-280 | 11000 | 30 μm | None |
| Cytodex-3 | GE Health Care | Dextran-based | No | 141-211 | 2700 | Solid | Gelatin |
| Cytodex-1 | GE Health Care | Dextran-based | + | 190 ± 58 | 4400 | Solid | None |
| DE-53 | Whatman | Cellulose-DEAE | + | 35-40 | 6800 | Solid | None |
| DE-52 | Whatman | Cellulose-DEAE | + | 35-40 | 6800 | Solid | None |
| FACT III | SoloHill | Polystirene | + | 90-150 | 480 | Solid | Collagen I |
| Fibra-Cel | New Brunswick | PET-PP disks | n/a | 6000 | 120 | Porous | None |
| Hillex II | SoloHill | Polystirene-based | + | 160-200 | 515 | Solid | None |
| Glass | SoloHill | Polystyrene | No | 125-212 | 360 | Solid | Si glass |
| MicroHex | Nunc | Polystyrene | n/a | 125-212 | 360 | Solid | None |
| Plastic | SoloHill | Polystyrene | n/a | 90-150 | 480 | Solid | None |
| Pronectin F-COATED | SoloHill | Polystyrene | + | 90-150 | 480 | Solid | Protein with RGD |
| RapidCell | MP Biomedical | Glass | No | 150-210 | 325 | Solid | None |
| Synthemax II | Corning | Polystyrene | n/a | 125-212 | 360 | Solid | Vitronectin peptide |
| Tosoh 65 PR | Tosoh Bioscience | OH-methacrylate | n/a | 65 | 4200 | Solid | Protamine sulfate |
| Tosoh 10 PR | Tosoh Bioscience | OH-methacrylate | n/a | 10 | 90000 | Solid | Protamine sulfate |

### 2.6.5 MC properties to control cell adhesion, proliferation and fate

The characterization of commercial and custom-, lab-scale made MCs is generally incomplete, as it is also the establishment of an exact correlation between MCs biochemical, topographical and mechanical properties on cell fate. It is generally acknowledged that surface charge plays a key role in regulating protein adsorption, especially ECM molecules (i.e. collagens, fibronetinc, laminin, vitronectin) from biological fluids, such as serum. Positively charged MCs are thought to enhance ECM coatings like laminin and collagen IV [175], although the cationic Cytodex 1 MCs, have been shown to preferentially bind bovine serum albumin (BSA) and only a minor fraction of fibronectin [176]. $NH_2$-rich MCs promoted fibronectin and vitronectin adsorption, which resulted in MSCs spreading, and therefore higher tendency to differentiate towards osteoblasts [178], whereas on COOH-rich MCs, these cells adopted a rounded morphology and a marked commitment towards chondrogenic lineages [179]. Gelatinous carriers like CultiSpher, have high affinity for fibronectin [180], but showed limited attachment of other ECM proteins.

Anyhow, ideal MCs should be able to display improved cell adhesion also in absence of ECM molecules in the culture media, as serum-free culture is more compliant with GMP requirements for cell production. [181]. Functionalization of MCs with pro-adhesive molecules (full proteins and peptides) thus becomes an important strategy to tune cell response. Controlling the density of coatings of RGD peptides on MCs was shown to improve cell proliferation and its implications will be further deepened in Chapter 5. Biomolecules coatings are known to modulate the degree of cell spreading and proliferation mostly via integrin signaling [182]. For instance, the density of RGD peptides on MCs surface was positively correlated to an increment in MSCs proliferation; furthermore, if the cells were induced to differentiate towards osteoblasts or chondrocytes, expression of lineage markers was higher for higher RGD densities [183]. The surface topography and MCs overall geometry are other important parameters to be taken into account. For instance, while the overall curvature of the MCs has an impact on cell viability, as higher curvature expose seeded cells to higher shear stresses during dynamic culture, microscale curvature of the surface, provided by grooved and rough surfaces has been shown to promote osteogenesis over adipogenesis in MSCs [184].

Mechanical properties, such as material stiffness [185] and storage modulus [186] have also an impact on cell behavior and differentiation, via modification of cell and cytoskeleton and shape mechanosensing pathways. However, their exact role is even more difficult to be discerned on MCs, that, due to their shape and size, are hard to be tested via conventional deformation systems, and a more detailed biomechanical characterization of MCs is required [174]. A proposed mechanism for multi- and pluripotent cells differentiation via cell shape regulation on MCs involves RhoA/ROCK signaling (Figure 2.28), whose activation stimulated osteogenesis at the expense of adipogenesis (and its downregulation provoked the opposite outcome) [187]. Alteration of cytoskeletal tensions in 3D MC culture was also reported to induce spontaneous osteogenesis of MSCs [188]. MCs have also great potential in ESC and iPSC cell expansion, however, the clinical application of these cells is still limited. Due to their potential health risk, these cells should be induced to differentiate before implantation, and effective protocols to remove undifferentiated cells should be carefully set (i.e magnetic sorting or FACS) [189].
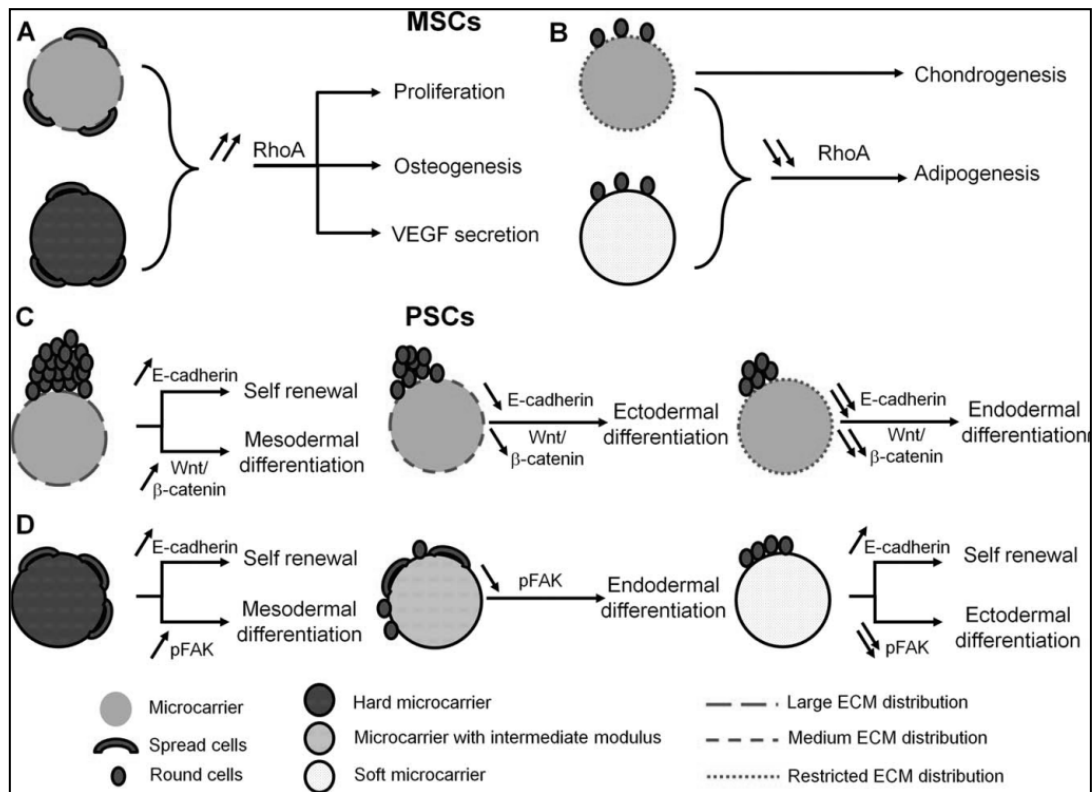
**Figure 2.28: Possible mechanisms by which MCs properties modulate (A,B) MSCs and (C,D) PSCs (ESCs and iPSCs) fate. Adapated from [174]**

*2.6.6 MCs for cell therapy*

After cells have been expanded on MCs, they can potentially be then retrieved and used as injectable living drugs with no biomaterial. MCs culture, in fact, can be successfully used to achieve cell proliferation, while preserving the culture cell specific, differentiated phenotype or multipotency, increasing their biological activity and therapeutic potential, compared to cells cultured in T-flasks. For instance, Malda et al. showed that chondrocytes cultured in gelatin CultiSpher G MCs retain their chondrogenic phenotype and, once retrieved from the MCs and seeded on a 3D synthetic scaffold had enhanced proteoglycan deposition compared to cells cultured in 2D [190]. Analogously, Goh et al. have demonstrated that MSCs after culture on MCs have higher potential for calcium deposition and bone formation both *in vitro* (seeded on polyester 3D scaffolds) and *in vivo*, respect to their counterpart expanded with conventional methods [191]. Cell retrieval can also be simplified, without involving any enzymatic treatment, if MCs made of thermosensitive materials are used [192].

More importantly, cells clustered on MCs made of biodegradable and biocompatible materials can be injected directly together with their carrier, as long as the size of the cell-MCs complex permits the injection and the implantation at the desired site. This type of approach shows considerable advantages, as the MCs can provide cell homing, and possibly prevent the massive cell death and dispersion that typically occurs after delivery of cells *in vivo* with no biomaterial support. A variety of applications for cell-laden MCs are being considered (Table 2.7).

**Table 2.7: List of relevant studies involving MCs as cell delivery systems.**

| Application | Cell type | MCs | Type of study | Reference |
|---|---|---|---|---|
| Myocardial infarction | Human AFSCs | PLGA porous beads 246.3 ± 17.7 µm | Injection of cell-MCs complexes into rat heart, improvement of scar remodeling and heart functions | [193] |
| Myocardial infarction | Rat MSCs | Alginate- PLL-alginate 10, 200 or 400 µm | Injection into rat myocardium of cells encapsulated into the MCs. Larger MCs improved cell survival. Identification of a cell amount threshold to improve heart function. | [194] |
| Myocardial infarction | Rat MSCs | FN-coated PLGA loaded with VEGF 60 µm | *In vitro* cell survival and proliferation is improved under hypoxic conditions. | [195] |
| Parkinson disease | Rat MIAMI cells | Laminin-PLGA loaded with neurothropin 3 60 µm | Injection in a dopaminergic-deafferent rat striatum. Improvement of injected cell survival, secretion of chemokines and protection/repair of nigrostriatal pathway | [196] |
| Parkinson disease | Rat ACCs | Cytodex beads | Cells on MCs injected in hemiparkinsonian rat striatum. Improved behavioral score up to 12 months post transplantation. | [197] |
| Parkinson disease | Human RPE | Gelatin MCs (Spheramine) 60 µm | Randomized, double-blind clinical trial, cell-seeded MCs implanted into human striatum. No significant difference vs. sham surgery | [198] |
| Degenerative retinal and macular disease | Human RPE cell-line | PLLA-PLGA blends 30-120 µm | *In vitro* cell culture. Characterization of cell viability, proliferation and phenotype retention. Proof-of-concept study of potential use of cell-MCs for intraocular delivery | [199] |
| Articular cartilage repair | Human MSCs | FN-coated PLGA TGF-β3 loaded 60 µm | Co-release of growth factor and cells. Improved *in vitro* chondrogenic differentiation. Injected in SCID mice cartilage, formation of neo-cartilage. | [200] |
| Diabetes | Allogenic Langherans islets | Alginate microcapsules 400 µm | Clinical trial. Intraperitoneal implantation of encapsulated cells in non-immunosuppressed patients. No relevant immunological response, transient reduction of insulin-dependence | [201] |

Since MSCs can be induced to differentiate into cardiomyocites, and have been found in ischemic heart [202], this cell type is widely studied for heart cell therapy. While many reports focus on the use of hydrogels to implant these cells [203], a few promising works involve MCs as cell delivery devices. PLGA porous MCs were used to culture MSCs derived from the amniotic fluid in a spinner flask bioreactor and obtain cell-MCs complexes enriched with neo-deposited ECM. These systems sustained MSCs survival, homing and bioactivity, while permitting cell migration from the carriers, as tested *in vitro*, and thus allowing *in vivo* scar tissue remodeling and an interesting recovery of the left ventricle ejection fraction [193]. In order to enhance MSCs engraftment into the heart, cells should be able to withstand the mechanical stress imposed by the cardiac muscle upon intramyocardial injection. MCs can be used as means to mechanically (and biochemically) protect cells, when cells are encapsulated inside hydrogel matrices (i.e. alginates) or hidden in the polymer porous network, and the size of microcapsules appears to be a key parameter in preserving cell viability [194]. As mentioned earlier in this Thesis, the main therapeutic mechanism of action of MSCs upon transplantation is the secretion of trophic factors, rather than direct differentiation. For this reason MCs for cell therapy should enhance -or at least preserve- MSCs paracrine secretion, a result that can be achieved, for instance, thanks to the improved cell-cell and cell-ECM contact in MSC-MCs complexes [193]. Such a property is also especially important for therapies targeting the central nervous system. In fact, less than 1% of the successfully implanted MSCs into the brain have been found to undergo neurogenic commitment, and the almost totality of the positive effect observed *in vivo* are attributed to the synthesis of neurotrophic and immunomodulating molecules, that allow surviving native neural cells to compensate the lost, impaired or damaged tissue [204, 205]. This mechanism has been observed in cell therapy for Parkinson disease [205], and MSCs beneficial secretory activity can be improved transplanting these cells with Pharmacologically Active MCs (PAM). These are microdevices that home cells on their surface and are loaded internally with growth factors, which are gradually released. For instance, MIAMI cells (a subset of MSCs) cultured on PAM encapsulating neurothropin 3 displayed higher bioactive molecules secretion, improving the otherwise impaired dopamine related pathways in a rat animal model [196]. Other cell type, such as those from Retinal Pigment Epitelium (RPE), have been shown to exert therapeutic and neuroprotective activity, which may be enhanced with MC-based transplantation. However, it should be pointed out that Spheramine, which, to date, is the only RPE-MCs device tested in a clinical trial, showed no significant therapeutic activity against Parkinson disease in humans, despite of the encouraging pre-clinical results [198].

The applicability and efficacy of MC-based cell delivery is also strongly affected by MCs diameter in relationship with the site of transplantation, as the size of the device may trigger undesired immunological responses. PLGA MCs implantation into the brain induced no specific astrocytic reaction, and although macrophages and microglia cells were showed to be present after biomaterial injection, they disappeared after the first days, indicating only acute inflammation [9]. Inflammation intensity was shown to be dependent on MPs size and geometry. Particles with diameter between 1 and 30 µm were correlated with higher production of TNFα, IL-6 and IL-10 from macrophages, while larger particles induced mild response

and no phagocytosis (in rat striatum). Given this observation and the necessity to reduce needle size to deliver the therapy to the brain, particles with size around 60-80µm are usually regarded as appropriate for brain cell therapy, while MCs can be generally larger for transplantation in other tissues [120].

While most MC-based delivery devices are characterized for their ability to sustain cell viability and proliferation, only a limited amount of studies focus on how to achieve control cell release in terms of spatial and temporal distribution [74]. The understanding of how cells on biomaterial carriers sense and respond to the multitude of signals to which they are subject *in vivo* (i.e. chemokines that regulate repair/disease pathways), is a necessary step in order to prevent cell dispersion or unspecific delivery. Moreover, knowing how to control these responses with biomaterials properties will be beneficial to design advanced cell therapies.

Another highly promising application of MCs for cell therapies is related to microencapsulation technology, consisting in the fabrication of hydrogel-based MCs that enclose cells in their core. This capsules act as a barrier that prevents the penetration of large molecules like immunoglobulins, while allowing secretion of chemokines or other small cellular products towards the host organism, and have great potential for allo- or even xenogenic cell therapy. The cut-off molecular weight of these membranes depends on the polymer molecular weight, concentration and degree of crosslinking. Transplantation of microencapsulated cells has been studied, for instance to support or partially replace hepatic [206], renal [207] and pancreatic function [208]. Devices for the allotransplantation of microenscapsulated Langherans islets into alginate beads, for instance, are already being tested in clinical trials for the treatment of insulin-dependent diabetes, and have been demonstrated to induce a degree of improvement in patients, while successfully concealing the donor cells from the host immune system [201]. The establishment of effective purification protocols to obtain clinical grade devices (in case that natural origin polymers are used as raw materials), as well as the development of accurate control over cell/MC ratio, MC size and permeability, identification of optimal implantation sites and surgery are among the main open challenges in this field [209].

*2.6.7 MCs in Tissue Engineering*

Cells cultured on MCs, that are retained and proliferate on Mc surface, can be used as components for tissue engineering strategies (Table 2.8). In this perspective, MCs can be thought as "discrete" scaffold units, which can be injected after being colonized with cells. Injection of these cell-MCs complexes is the most straightforward application of MCs, and has been studied for engineering a wide variety of tissues.

**Table 2.8: MCs and their application in Tissue Engineering strategies**

| Target | Cell type | MCs | Type of study | Ref. |
|---|---|---|---|---|
| Adipose tissue | 3T3-L1 preadipocytes | Porous PLGA 50 µm | Cell culture on MCs, partial MC aggregation and injection of cell-MCs complexes in mices. Formation of neo-adipose tissue. | [210] |
| Adipose tissue | Human ASCs | Decellularized adipose tissue bead foams 1-2 mm | Improved in vitro *ASCs* differentiation. *In vivo* implantation in Wistar rats showed strong angiogenesis and adipose tissue regeneration. Complete resorption in 12 weeks. | [211] |
| Cartilage | Rabbit chondrocytes | Nanofibrous star-shaped PLLA 20-70 µm | Porous MCs, with fibrous nanostructure improved cartilage repair *in vivo*. Higher quality tissue compared to ACI. | [212] |
| Cartilage | Bovine articular chondrocytes | Porous PLGA 175 µm | Culture in spinner flask on MCs with interconnected porosity. $NH_2$-modified MCs increase *in vitro* cell proliferation and COL II and GAGs expression | [213] |
| Cartilage | Mouse MSCs | Fibrin microbeads 105-180 µm | *In vitro* improved cartilage regeneration | [214] |
| Bone | - | β-TCP/PLA 177.6 ± 33 µm | *In vivo* transplantation into rabbit bone defect. Enhanced repair compared to MCs without β-TCP | [215] |
| Bone | Rat MSCs | CultiSphere S | Enhanced bone regeneration in rat calvaria defect | [216] |
| Bone | MC3T3-E1 preosteoblats | Pectin 300-500 µm | Microencapsulation. Improved mineralization and bone deposition *in vitro* | [217] |
| Heart | Human MSCs | Alginate-RGD 100-300 µm | Microencapsulated cells. *In vivo* reduction of infarcted area an improved left ventricle function | [218] |
| Smooth muscle | Porcine aortic SMCs | Porous PLGA (TIPS) 200 ± 50 µm | *In vitro* cell colonization of the MCs and matrix deposition. Improved cell migration and SMCs markers. Preserved viability upon injection *in vivo* | [219] |
| Skin | Human keratinocytes | Cytodex 3 | *In vitro* expansion in spinner flasks and *in vivo* transplantation in nude mice. Reconstitution of multilayered and keratinized epithelium | [220] |
| Skin | Bovine fibroblasts | CultiSpher G 130-380 µm | *In vitro* formation of microtissue aggregates of cells, MCs and neo-synthesized ECM. *In vitro* assembly into large skin tissue precursors. | [221] |

Injectable cell- laden MCs usually tend to cluster into multiparticles aggregates, depending on the culture condition (Figure 2.29). In this case, the size of the cell-material unit is increased, at the expense of ease of injectability, but at the same time such aggregates can display interesting bioactivity, due to higher cell-cell communication and ECM matrix deposition [221], that resulted in improved regenerative potential for adipose, cartilagineous, bone and skin tissues [212, 213, 216, 221]. MCs composition is always among the most important parameters to promote cell differentiation and tissue regeneration. For instance, MCs made of decellularized adipose tissue have been shown to already possess a complex combination of signals necessary to push seeded ASCs to sustain *in vivo* angiogenesis and regeneration of native-like adipose tissue [218]. MCs based on synthetic polymers like PLGA, which bear no specific signal to guide cell fate, can instead benefit from modification with bioactive compounds, such as ion-release ceramic/glass particles for bone tissue engineering [215].
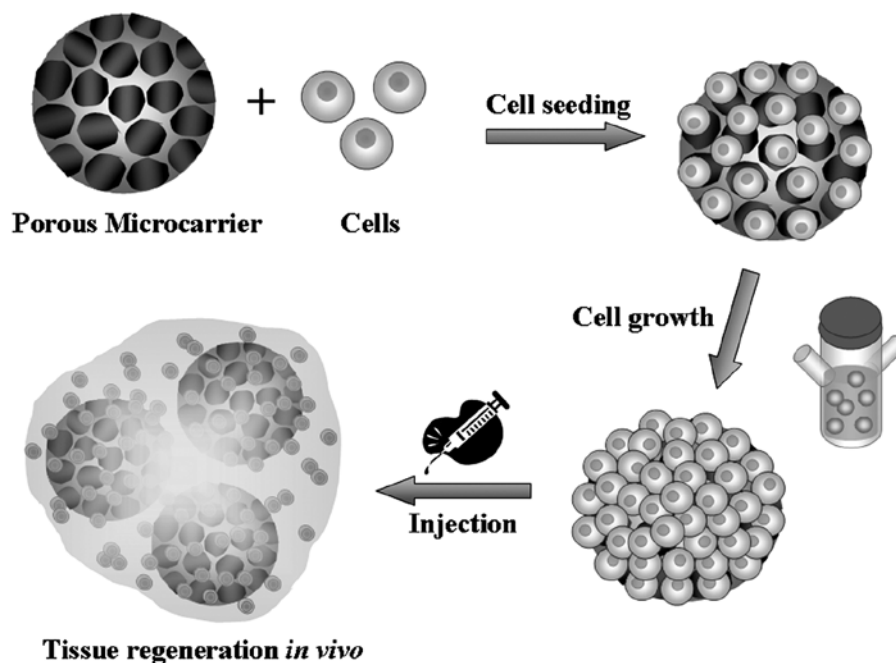


**Figure 2.29: Scheme of the procedure for Tissue regeneration using cell-laden MCs and injectable devices. Adapted from [210].**

MCs can be designed with open porosity or as solid particles. The main advantage of open porosity consists in increasing the surface area available for cell growth and promoting the establishment of cell-cell contacts in a limited volume. Also, the structure of the polymer skeleton in the MCs can be controlled during the fabrication step to add a degree of control over cell behavior through topographical cues. For instance, Liu et al. were able to shape the polymer structure of their MCs into a nanofibrous mesh, to better mimick the conformation of the native collagenous ECM of cartilage, an thus improve regeneration in an articular cartilage defect [212]. Solid sphere MCs, on the other hand, can be easily used to encapsulate and deliver over time drugs that can provide biochemical stimuli to guide cell regeneration [196, 200].

Due to their high versatility, MCs are often used in combination with other materials. MCs without cells can be encapsulated into the matrix of "classical" macroscale scaffolds. Ruhé et al. incorporated fast degrading PLGA MCs in order to increase the porosity of cement scaffold for bone TE implanted *in vivo* [222]. Also, Kaplan and co-workers have produced silk sponges incorporating silk microparticles, to increase the elastic stiffness of the device, which improved for higher MCs loadings, and, at the same time affected the differentiation of MSCs towards osteogenic lineage [223]. MCs can be promisingly incorporated into hydrogels to generate composite materials. A typical purpose for including MCs in gel matrix is to improve the stiffness of these soft materials, as shown by Hu and coworkers, which generated chitosan gels reinforced with stiff PLGA MCs [224]. Additionally, since most hydrogels can be used as injectable devices and can gelate under mild cell-friendly conditions, cell-MCs complexes can be encapsulated as well. In this way, MCs can be introduced in a continuous matrix that can solidify upon injection *in situ* and prevent MCs undesired movements [225]. At the same time, MCs can provide cues to modulate cell viability and fate, through their surface topography, mechanical and chemical properties as described in Section 2.5.5. This is especially important when considering, cells in hydrogels are mostly confined in a rounded morphology [226], and such condition is even more evident when using non-functionalized anti-fouling gels (such as PEG, PVA, agarose).
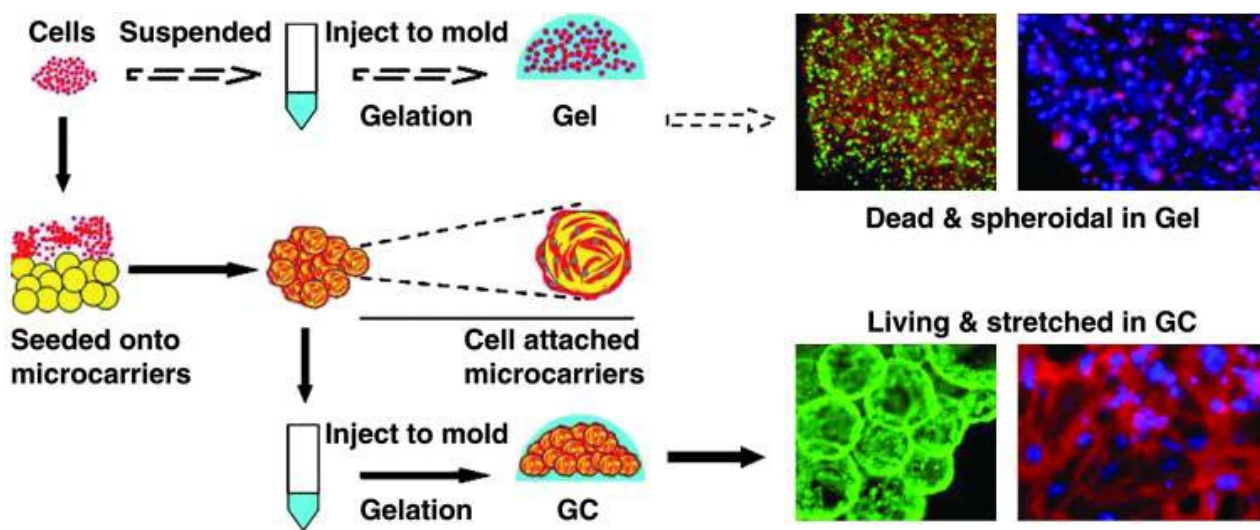


**Figure 2.30: Experimental design of two modes of tissue engineering using cells suspended in a hydrogel as free cells or as cell-laden MCs. Adapted from [227].**

For instance, Wang et al. have shown that osteblastic cell viability and bone matrix synthesis upon suspension in an agarose matrix can be dramatically increased if cells are encapsulated as complexes on TriG (gelatin-grafted-gellan) MCs (Figure 2.30) [227].

*2.6.8 MCs in bottom-up TE and biofabrication*

MCs can also be thought as building blocks in bottom-up tissue engineering strategies. Before seeding cells, MCs can be assembled together to build-up macroscale porours scaffold, whose porosity is dependent on MCs size and due to the hindrance between neighboring particles (Figure 2.31). Recently, using a MCs fabrication method derived from the work presented in this Thesis, Salerno et al. have shown how to combine a microfluidics system and a sintering approach to produce PLA MCs assembled into large scaffolds. The porosity of such systems can be controlled mixing particles of different sizes, and MSC were shown to proliferate on these matrices [131]. MCs-assembled scaffolds with controlled geometry and porosity at the micro- and macroscale can also be obtained by means of rapid prototyping/sintering technique [228].
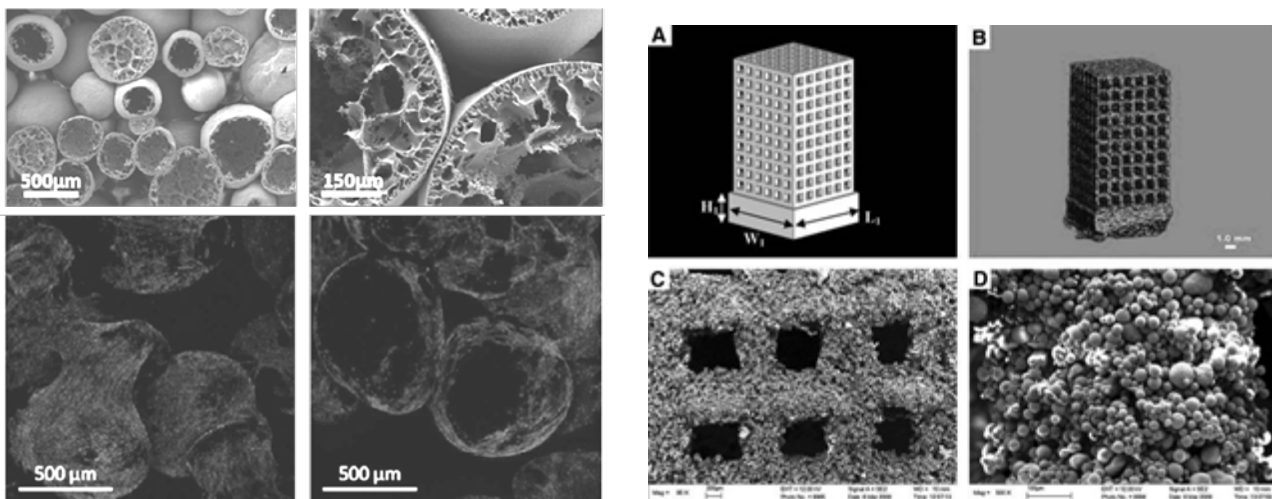


**Figure 2.31: (*Left*) Scaffold made with a microfluidic-PLA MCs sintering combined approach (adapted from [131]). (*Right*) Rapid prototyping scaffold made of sintered CaP/PHBV MCs. (A) CAD design, (B) µCT, (C, D) SEM micrographs [229].**

Thanks the ability of cells to self-assemble, another interesting bottom-up fabrication approach consist in exploiting the tendency of cell-MCs complexes to coalesce, and then use these aggregates as living building blocks. Palmiero et al. have described a process to culture fibroblasts on gelatin MCs, let them self-assemble in a preliminary culture step, producing microtissue precursos rich in cell and ECM proteins, and collect these units in a perfusion bioreactor to facilitate their assembly into larger tissue engineered construct. This approach was proven advantageous to generate skin grafts whose ECM composition resembles that of the native tissue [221]. If hydrogel microcapsules are used for this class of biofabrication approaches, it can be possible to generate constructs having multiple compartments to home different cell types. Recently, collagen gels were used to host two different cell lines (one encapsulated and the other on the MCs surface), and then induce cell-MCs complexes self-assembly in a PDMS mold (Figure 2.32) [230]. Although the

researchers used 3T3 and HepG2 cell lines, this approach promises to allow the generation of constructs with virtually any desired shape and cell composition.
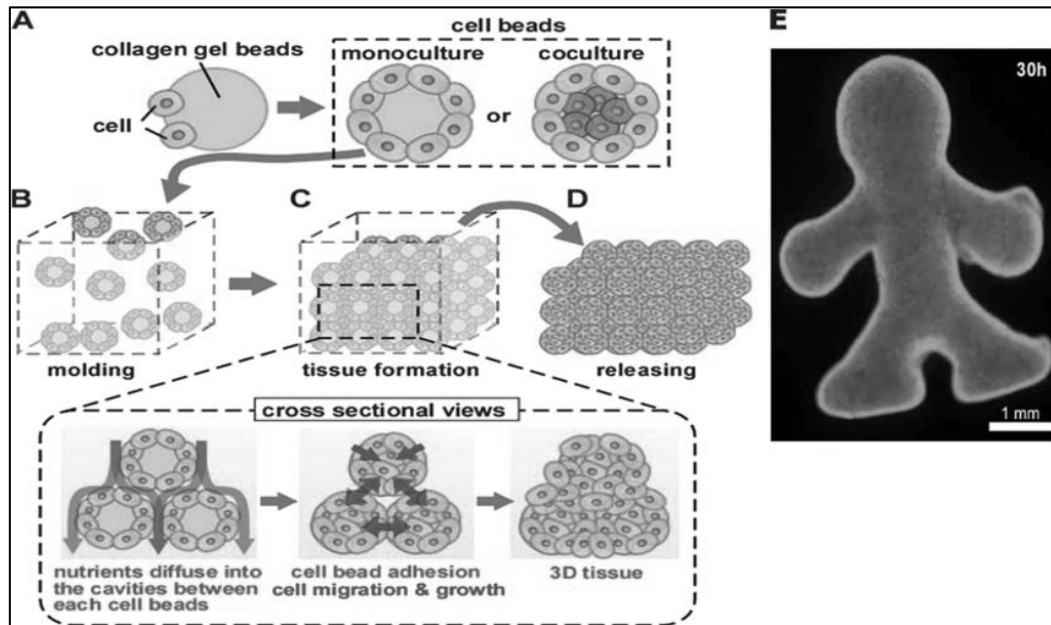


**Figure 2.32: (A to E) Procedure of a bottom-up cell-mediated assembly of MCs into a 3D tissue. MCs aggregates can be shaped into any desired form, and in this proof-of-concept a doll-like figure is generated. Adapted from [230].**

As novel frontiers for MCs based biofabrication, considering the examples reported so far and the possibility to form hydrogels-MCs composites, injectable, cell-laden MCs could be used as components in bioinks to fabricate novel, bioprinted grafts (as described with more detail in Chapter 6).Similarly to many TE product, these devices have great potential applications for regenerative medicine, as *in vitro* disease models and drug testing platforms.

## 2.7 References

[1] Ratner BD, Hoffman AS, Schoen FJ, Lemons JE. Biomaterials Science: An Introduction to Materials in Medicine. Academic Press (1996).

[2] Ratner BD, Bryant SJ. Biomaterials: where we have been and where are we going. Annu Rev Biomed Eng. 6 (2004) 41-75.

[3] Hench LL, Wilson J. Surface active biomaterials. Science 226 (1984) 630-636.

[4] Hofmann GO. Biodegradable implants in orthopaedic surgery--a review on the state-of-the-art. Clin Mater. 10(1-2) (1992)75-80.

[5] Williams DF. Definitions in Biomaterials. Proceedings of a Consensus Conference of the European Society for Biomaterials, Chester, England, March 3-5 1986, Vol. 4, Elsevier, New York.

[6] Hench LL, Polak JM. Third-generation biomedical materials. Science. 295 (2002) 1014-7.

[7] Williams DF. On the nature of biomaterials. Biomaterials 30 (2009) 5897–909.

[8] Holzapfel BM, Reichert JC, Schantz JT, Gbureck U, Rackwitz L, Noth U, et al. How smart do biomaterials need to be? A translational science and clinical point of view. Adv Drug Deliv Rev. 65 (2013) 581-603.

[9] Jeronimidis G. Structural biological materials, design and structure-property relationships (pp. 3-29). Amsterdam: Pergamon (2000).

[10] Fratzl P, Weinkamer R. Nature's hierarchical material. Progress in Materials Science 52 (2007) 1263–1334.

[11] Richter C, Reinhardt M, Giselbrecht S, Leisen D, Trouillet V, Truckenmüller R, et al. Spatially controlled cell adhesion on three-dimensional substrates. Biomed Microdevices. 12(5) (2010) 787-95.

[12] Melchels FP, Tonnarelli B, Olivares AL, Martin I, Lacroix D, Feijen J, et al. The influence of the scaffold design on the distribution of adhering cells after perfusion cell seeding. Biomaterials. 32(11) (2011) 2878-84.

[13] Yang J, Yamato M, Shimizu T, Sekine H, Ohashi K, Kanzaki M, et al. Reconstruction of functional tissues with cell sheet engineering. Biomaterials. 28(34) (2007) 5033-43.

[14] Nair SL, Laurencin CT. Biodegradable polymers as biomaterials. Progress in Polymer Science 32 (2007) 762-98.

[15] 2005 Satellite Consensus Conference of the European Society of Biomaterials (ESB), Sorrento, Italy.

[16] Gomillion CT, Burg KJL. Review: Stem cells and adipose tissue engineering. Biomaterials 27 (2006) 6052-63.

[17] Silleart F, Findlay M, Palmer J, Idrizi R, Cheang S, Messina A, et al. Host rather than graft origin Matrigel-induced adipose tissue in murine tissue-engineering chamber. Tissue Engineering B Rev 14(2) (2008) 199-215.

[18] Tanzi MC, Farè S. Adipose Tissue Engineering: state of the art, recent advances and innovative approaches. Expert Rev. Med. Devices 6(5) (2009) 533-551.

[19]  Nichol JW, Khademhosseini A. Modular Tissue Engineering: Engineering Biological Tissues from the Bottom Up. Soft Matter 5(7) (2009) 533-551.

[20]  Place ES, Evans ND, Stevens MM. Complexity in biomaterials for tissue engineering. Nat Mater. 2009 8(6):457-70.

[21]  Chwalek K, Bray LJ, Werner C. Tissue-engineered 3D tumor angiogenesis models: Potential technologies for anti-cancer drug discovery. Adv Drug Deliv Rev  (2014) doi: 10.1016/j.addr.2014.05.006.

[22]  Thibaudeau L, Taubenberger AV, Holzapfel BM, Quent VM, Fuehrmann T, Hesami P, et al. A tissue-engineered humanized xenograft model of human breast cancer metastasis to bone. Dis Model Mech 7(2) (2014) 299-309.

[23]  Handschel J, Wiesmann HP, Depprich R, Kübler NR, Meyer U. Cell-based bone reconstruction therapies--cell sources. Int J Oral Maxillofac Implants. 21(6) (2006) 890-8.

[24]  Koh CJ, Atala A. Tissue engineering, stem cells, and cloning: opportunities for regenerative medicine.J Am Soc Nephrol.15(5) (2004) 1113-25.

[25]  Zandstra PW, Nagy A. Stem cell bioengineering. Annu Rev Biomed Eng. 3 (2001) 275-305.

[26]  Heath JK, Smith AG. Regulatory factors of embryonic stem cells. J Cell Sci Suppl. 10 (1988) 257-66.

[27]  Aznar J, Gómez I. Possible clinical usefulness of embryonic stem cells. Rev Clin Esp. 212(8) (2012) 403-6.

[28]  Young HE, Duplaa C, Romero-Ramos M, Chesselet MF, Vourc'h P, Yost MJ, et al. Adult reserve stem cells and their potential for tissue engineering. Cell Biochem Biophys. 40(1) (2004) 1-80.

[29]  Kopper L, Hajdú M. Tumor stem cells. Pathol Oncol Res. 10(2) (2004) 69-73.

[30]  Pontikoglou C, Delorme B, Charbord P. Human bone marrow native mesenchymal stem cells. Regen Med.3(5) (2008) 731-41.

[31]  Horwitz EM, Le Blanc K, Dominici M, Mueller I, Slaper-Cortenbach I, Marini FC, et al. Clarification of the nomenclature for MSC: The International Society for Cellular Therapy position statement. Cytotherapy. 7(5) (2005) 393-5.

[32]  Dominici M, Le Blanc K, Mueller I, Slaper-Cortenbach I, Marini F, Krause D, et al. Minimal criteria for defining multipotent mesenchymal stromal cells. The International Society for Cellular Therapy position statement. Cytotherapy. 8(4) (2006) 315-7.

[33]  Yang B, Zheng JH, Zhang YY. Myogenic differentiation of mesenchymal stem cells for muscle regeneration in urinary tract. Chin Med J (Engl). 126(15) (2013) 2952-9.

[34]  Krabbe C, Zimmer J, Meyer M. Neural transdifferentiation of mesenchymal stem cells--a critical review. APMIS. 113(11-12) (2005) 831-44.

[35]  Caplan AI, Bruder SP. Mesenchymal stem cells: building blocks for molecular medicine in the 21st century. Trends Mol Med 7(6) (2001) 259-64.

[36]  Strem BM, Heidrick MH. The growing importance of fat in regenerative medicine. Trends Biotechnol. 23(2) (2005) 64-6.

[37]  Zhu Y, Liu T, Song K, Fan X, Ma X, Cui Z. Adipose-derived stem cell: a better stem cell than BMSC. Cell. Biochem Funct. 26(6) (2008) 664-75.

[38]  Takahashi K, Yamanaka S. Induction of pluripotent stem cells from mouse embryonic and adult fibroblast cultures by defined factors. Cell. 126(4) (2006) 663-76.

[39]  Gieseck RL, Colquhoun J, Hannan NR. Disease modeling using human induced pluripotent stem cells: Lessons from the liver. Biochim Biophys Acta. (2014) doi: 10.1016/j.bbalip.2014.05.010.

[40]  Brownlee C. Role of the extracellular matrix in cell-cell signalling: paracrine paradigms. Curr Opin Plant Biol.5(5) (2002) 396-401.

[41]  Peter SJ, Miller MJ, Yasko AW, Yaszemski MJ, Mikos AG. Polymer concepts in tissue engineering. J Biomed Mater Res. 43(4) (1998) 422-7.

[42]  Bacáková L, Filová E, Rypácek F, Svorcík V, Starý V. Cell adhesion on artificial materials for tissue engineering. Physiol Res. 53 (2004) S35-45.

[43]  Almeida CR, Serra T, Oliveira MI, Planell JA, Barbosa MA, Navarro M. Impact of 3-D printed PLA- and chitosan-based scaffolds on human monocyte/macrophage responses: unraveling the effect of 3-D structures on inflammation. Acta Biomater 10(2) (2014) 613-22.

[44]  Wendt D, Riboldi SA, Cioffi M, Martin I. Potential and bottlenecks of bioreactors in 3D cell culture and tissue manufacturing. Adv Mater 21(32-33) (2009) 3352-67.

[45]  Macchiarini P, Jungebluth P, Go T, Asnaghi MA, Rees LE, Cogan TA, et al. Clinical transplantation of a tissue-engineered airway. Lancet 372 (2008)2023-30.

[46]  Candiani G, Riboldi SA, Sadr N, Lorenzoni S, Neuenschwander P, Montevecchi FM, Mantero S. Cyclic mechanical stimulation favors myosin heavy chain accumulation in engineered skeletal muscle constructs. J Appl Biomater Biomech. 8(2) (2010) 68-75.

[47]  Olivares AL, Marsal E, Planell JA, Lacroix D. Finite element study of scaffold architecture design and culture conditions for tissue engineering. Biomaterials 30(30) (2009) 6142-9.

[48]  Fassina L, Visai L, Asti L, Benazzo F, Speziale P, Tanzi MC, Magenes G. Calcified matrix production by SAOS-2 cells inside a polyurethane porous scaffold, using a perfusion bioreactor. Tissue Eng 11(5-6) (2005) 685-700.

[49]  Tandon N, Taubman A, Cimetta E, Saccenti L, Vunjak-Novakovic G. Portable bioreactor for perfusion and electrical stimulation of engineered cardiac tissue. Conf Proc IEEE Eng Med Biol Soc (2013) 6219-23.

[50]  Hansmann J, Groeber F, Kahlig A, Kleinhans C, Walles H. Bioreactors in tissue engineering - principles, applications and commercial constraints. Biotechnol J 8(3) (2013) 298-307.

[51]  Tandon N, Taubman A, Cimetta E, Saccenti L, Vunjak-Novakovic G.Portable bioreactor for perfusion and electrical stimulation of engineered cardiac tissue. Conf Proc IEEE Eng Med Biol Soc. (2013) 6219-23.

[52] Abousleiman RI, Sikavitsas VI. Bioreactors for tissues of the musculoskeletal system. Adv Exp Med Biol. 585 (2006) 243-59.

[53] Santos MI, Reis RL. Vascularization in bone tissue engineering: physiology, current strategies, major hurdles and future challenges. Macromol Biosci. 10(1) (2010) 12-27.

[54] Cohen-Haguenauer O. A Comprehensive Resource on EU Regulatory Information for Investigators in Gene Therapy Clinical Research and Advanced Therapy Medicinal Products. Human Gene Therapy 24 (2013) 12–18.

[55] Atala A, Bauer SB, Soker S, Yoo JJ, Retik AB. Tissue-engineered autologous bladders for patients needing cystoplasty. Lancet 367(9518) (2006) 1241-6.

[56] Martin I, Baldomero H, Tyndall-Bocelli C, Emmert MY, Hoerstrup SP, Ireland H, et al. The Survaey on Cellular and Engineered Tissue Therapies in Europe 2011. Tissue Eng Part A 20 (2014) 842-50.

[57] Kanate AS, Pasquini MC, Hari PN, Hamadani M. Allogeneic hematopoietic cell transplant for acute myeloid leukemia: Current state in 2013 and future directions. World J Stem Cells. 6(2) (2014) 69-81.

[58] Ducheyne P, Mauck RL, Smith DH. Biomaterials in the repair of sports injuries. Nat Mater. 11(8) (2012) 652-4.

[59] Foldager CB. Advances in autologous chondrocyte implantation and related techniques for cartilage repair. Dan Med J 60(4) (2014) B4600.

[60] Murray IR, West CC, Hardy WR, James AW, Park TS, Nguyen A, et al. Natural history of mesenchymal stem cells, from vessel walls to culture vessels. Cell Mol Life Sci 71 (2014) 1353-74.

[61] Dai W, Hale SL, Martin BJ, Kuang JQ, Dow JS, Wold LE, Kloner RA. Allogenic mesenchymal stem cells transplanttion in post-infarcted myocardium: short- and long-term effects. Circulation 112(2) (2005) 214-23.

[62] Lotfinegad P, Shamsasenjan K, Movassaghpour A, Majidi J, Baradaran B. Immunomodulatory nature and site specific affinity of mesenchymal stem cells: a hope in cell therapy. Adv Pharm Bull. 4(1) (2014) 5-13.

[63] Bensidhoum M, Chapel A, Francois S, Demarquay C, Mazurier C, Fouillard L, et al. Homing of in vitro expanded Stro-1- or Stro-1+ human mesenchymal stem cells into the NOD/SCID mouse and their role in supporting human CD34 cell engraftment. Blood. 103(9) (2004) 3313-9.

[64] Shi S, Gronthos S. Perivascular niche of postnatal mesenchymal stem cells in human bone marrow and dental pulp. J Bone Miner Res. 18(4) (2003) 696-704.

[65] Bianco P, Riminucci M, Gronthos S, Robey PG. Bone marrow stromal stem cells: nature, biology, and potential applications. Stem Cells. 19(3) (2001) 180-92.

[66] Xu F, Shi J, Yu B, Ni W, Wu X, Gu Z. Chemokines mediate mesenchymal stem cell migration toward gliomas in vitro. Oncol Rep. 23(6) (2010) 1561-7.

[67] Menon LG, Pratt J, Yang HW, Black PM, Sorensen GA, Carroll RS. Imaging of human mesenchymal stromal cells: homing to human brain tumors. J Neurooncol. 107(2) (2012) 257-67.

[68]    Bexell D, Gunnarsson S, Tormin A, Darabi A, Gisselsson D, Roybon L, et al. Bone marrow multipotent mesenchymal stroma cells act as pericyte-like migratory vehicles in experimental gliomas. Mol Ther, 7(1) (2009) 183-90.

[69]    Alieva M, Bagó JR, Aguilar E, Soler-Botija C, Vila OF, Molet J, et al. Glioblastoma therapy with cytotoxic mesenchymal stromal cells optimized by bioluminescence imaging of tumor and therapeutic cell response. PLoS One. 7(4) (2012) e35148.

[70]    Devine SM, Bartholomew AM, Mahmud N, Nelson M, Patil S, Hardy W, et al. Exp Hematol. 29(2) (2001) 244-55. Mesenchymal stem cells are capable of homing to the bone marrow of non-human primates following systemic infusion.

[71]    Jones E, McGonagle D. Human bone marrow mesenchymal stem cells in vivo. Rheumatology.47(2) (2008) 126-31.

[72]    Muraglia A, Cancedda R, Quarto R. Clonal mesenchymal progenitors from human bone marrow differentiate in vitro according to a hierarchical model. J Cell Sci. 113 (2000) 1161-6.

[73]    Wiehe JM, Kaya Z, Homann JM, Wöhrle J, Vogt K, Nguyen T, et al. GMP-adapted overexpression of CXCR4 in human mesenchymal stem cells for cardiac repair. Int J Cardiol. 167(5) (2013) 2073-81.

[74]    Vacharathit V, Silva EA, Mooney DJ. Viability and functionality of cells delivered from peptide conjugated scaffolds. Biomaterials. 32 (2011) 3721-8.

[75]    Rossi F, Santoro M, Perale G. Polymeric scaffolds as stem cell carriers in bone repair. J Tissue Eng Regen Med. (2013) doi: 10.1002/term.1827.

[76]    Hoffman AS. The origins and evolution of "controlled" drug delivery systems. J Control Release 132 (2008) 153-163.

[77]    Bern H, Langer R. Polymer-based drug delivery to the brain. Sci Med 3 (1996) 52-61.

[78]    Laurencin CT, Gerhart T, Witschger P, Satcher R, Domb A, Rosenberg AE, et al. Bioerodible polyanhydrides for antibiotic drug delivery: in vivo osteomyelitis treatment in a rat model system. J Orthop Res. 11(2) (1993) 256-62.

[79]    Kearney CJ, Mooney DJ. Macroscale delivery systems for molecular and cellular payloads. Nat Mater 12 (2013) 1004-1017.

[80]    Chen SC, Wu YC, Mi FL, Lin YH, Yu LC, Sung HW. A novel pH-sensitive hydrogel composed of N,O-carboxymethyl chitosan andalginate cross-linked by genipin for protein drug delivery. J Control Release 96(2) (2004) 285-300.

[81]    Walter E, Dreher D, Kok M, Thiele L, Kiama SG, Gehr P, Merkle HP. Hydrophilic poly(DL-lactide-co-glycolide) microspheres for the delivery of DNA to human-derived macrophages and dendritic cells. J Control Release 76(1-2) (2001) 149-68.

[82]    Zhong Y, Meng F, Deng C, Zhong Z. Ligand-directed active tumor-targeting polymeric nanoparticles for cancer chemotherapy. Biomacromolecules. 15(6) (2014) 1955-69.

[83]    Simamora P, Chern W. Poly-L-lactic acid: an overview. J Drugs Dermatol. 5(5) (2006) 436-40.

[84] Silva SS, Mano JF, Reis RL. Potential applications of natural origin polymer-based systems in soft tissue regeneration. Crit Rev Biotechnol. 30(3) (2010) 200-21.

[85] Báez J, Olsen D, Polarek JW. Recombinant microbial systems for the production of human collagen and gelatin. Appl Microbiol Biotechnol. 69(3) (2005) 245-52.

[86] Veis A. The physical chemistry of gelatin. Int Rev Connect Tissue Res. 3 (1965) 113-200.

[87] Singh SS, Siddhanta AK, Meena R, Prasad K, Bandyopadhyay S, Bohidar HB. Intermolecular complexation and phase separation in aqueous solutions of oppositely charged biopolymers. Int J Biol Macromol. 41(2) (2007) 185-92.

[88] Benton JA, DeForest CA, Vivekanandan V, Anseth KS. Photocrosslinking of gelatin macromers to synthesize porous hydrogels that promote valvular interstitial cell function. Tissue Eng Part A. 15(11) (2009) 3221-30.

[89] Prajapati VD, Jani GK, Zala BS, Khutliwala TA. An insight into the emerging exopolysaccharide gellan gum as a novel polymer. Carbohydr Polym. 93(2) (2014) 670-8.

[90] Krebs MD, Sutter KA, Lin ASP, Guldberg RE, Alsberg E. Injectable poly(lactic-co-glycolic) acid scaffolds with in situ pore formation for tissue engineering. Acta Biomater 5 (2009) 2847-59.

[91] Kretlow JD, Klouda L, Mikos AG. Injectable matrices and scaffolds for drug delivery in tissue engineering. Adv Drug Delivery Rev 59 (2007) 263-73.

[92] Cilurzo F, Selmin F, Minghetti P, Adami M, Bertoni E, Lauria S, Montanari L. Injectability Evaluation: An Open Issue. AAPS PharmSciTech. 12(2) (2011) 604–9.

[93] Yu L, Ding J. Injectable hydrogels as unique biomedical materials. Chem Soc Rev 37 (2008) 1473-81.

[94] Patel PN, Gobin AS, West JI, Patrik CW. Poly(ethylene glycol) Hydrogel System Supports Preadipocyte Viability, Adhesion and Proliferation. Tissue Eng 11 (2005) 1498-505.

[95] Parks H, Temenoff JS, Holland HA, Tabata Y, Mikos AG. Delivery of TGF-beta and chondrocytes via injectable, biodegradable hydrogels for cartilage tissue engineering applications. Biomaterials 26 (2005) 7095-103.

[96] Hedberg EL, Kroese-Deutman HC, Shih CK, Crowther RS, Carney DH, Mikos AG, Jansen JA. Effect of varied release kinetics of the osteogenic thrombin peptide TP508 from biodegradable, polymeric scaffolds on bone formation in vivo. J Biomed Mater Res A 72 (2005) 343-53.

[97] Shah RN, Shah NA, Del Rosario Lim MM, Hsieh C, Nuber G, Stupp SI. Supramolecular design of self-assembling nanofibers for cartilage regeneration. PNAS. 10.1073/pnas.0906501107.

[98] Pratoomsoot C, Tanioka H, Hori K, Kawasaki S, Kinoshita S, Tighe PJ, Dua H, Shakesheff KM, Rose FRAJ. A thermoreversible hydrogel as a biosynthetic bandage for corneal wound repair. Biomaterials 29 (2008) 272-81.

[99] Dang JM, Sun DDN, Shin-Ya Y, Sieber AN, Kostuik JP, Leong KW. Temperature-responsive hydroxybutil chitosan for the culture of intervertebral disk cells. Biomaterials 27 (2006) 406-18.

[100] Frith JE, Cameron AR, Menzies DJ, Ghosh P, Whitehead DL, Gronthos S, et al. An injectable hydrogel incorporating mesenchymal precursor cells and pentosan polysulphate for intervertebral disc regeneration. Biomaterials. 34(37) (2013) 9430-40.

[101] Balakrishnan B, Joshi N, Jayakrishnan A, Banerjee R. Self-crosslinked oxidized alginate/gelatin hydrogel as injectable, adhesive biomimetic scaffolds for cartilage regeneration. Acta Biomater (2014). doi: 10.1016/j.actbio.2014.04.031.

[102] Du H, Hamilton P, Reilly M, Ravi N. Injectable in situ physically and chemically crosslinkable gellan hydrogel. Macromol Biosci 12(7) (2012) 952-61.

[103] Budden R, Kuhl UG, Bahlsen J. Experiments on the toxic, sedative and muscle relaxant potency of various drug solvent in mice. Pharmacol Ther 5 (1979) 467.

[104] Williams CG, Malik AN, Kim TK, Manson PN, Elisseeff JH. Variable cytocompatibility of six cell lines with photoinitiators used for polymerizing hydrogels and cell encapsulation. Biomaterials 26(11) (2006) 1211-8.

[105] Witte RP, Kao WJ. Keratinocyte-fibroblast paracrine interaction: the effects of substrate and culture condition. Biomaterials 26 (2005) 3673-82.

[106] Salem AK, Rose FRJA, Oreffo ROC, Yang X, Davies MC; Mitchell JR, Roberts CJ, Stolnki-Trenkic S, Tendler SJB, Williams PM, Shakesheff KM. Porous polymer and cell composites that self-assemble in situ. Adv Mater 15 (1979) 210-13.

[107] Sanborn TJ, Messersmith PB, Barron AE Barron. In situ crosslinking of a biomimetic peptide-PEG hydrogel via thermally triggered activation of factor XIII. Biomaterials 23 (2002) 2703-10.

[108] Rowley JA, Madlambayan G, Mooney DJ. Alginate hydrogels as synthetic extracellular matrix materials. Biomaterials 20 (1999) 45-53.

[109] Costa RR, Custódio CA, Testera AM, Arias FJ, Rodríguez-Cabello JC, Alves NM, Mano JF. Stimuli-Responsive Thin Coatings Using Elastin-Like Polymers for Biomedical Applications. Adv Funct Mater 19 (2009) 3210-8.

[110] Mironov V, Trusk T, Kasyanov V, Little S, Swaja R, Markwald R. Biofabrication: a 21st century manufacturing paradigm. Biofabrication 1(2) (2009) 022001.

[111] Malda J, Visser J, Melchels FP, Jüngst T, Hennink WE, Dhert WJ, Groll J, Hutmacher DW. 25th anniversary article: Engineering hydrogels for biofabrication. Adv Mater 25(36) (2013) 5011-28.

[112] Visser J, Peters B, Burger TJ, Boomstra J, Dhert WJ, Melchels FP, Malda J. Biofabrication of multi-material anatomically shaped tissue constructs. Biofabrication 5(3) (2013) 035007.

[113] Klein TJ, Rizzi SC, Reichert JC, Georgi N, Malda J, Schuurman W, Crawford RW, Hutmacher DW. Strategies for Zonal Cartilage Repair using Hydrogels. Macromol Biosci 9 (2009) 1049-58

[114] Miller SJ, Stevens KR, Yang MT, Baker BM, Nguyen DHT, Cohen DM, Toro E, Chen AA, Galie PA, Yu X, Chaturvedi R, Bhatia SN, Chen CS. Rapid casting of patterned vascular networks for perfusable engineered three-dimensional tissues. Nat Mater 11 (2013) 768-74

[115] Schuurman W, Levett PA, Pot MW, van Weeren PR, Dhert WJA, Hutmacher DW, Melchels FPW, Klein TJ, Malda J. Gelatin-Methacrylamide Hydrogels as Potential Biomaterials for

[116] Xu T, Binder KW, Albanna MZ, Dice D, Zhao W, Yoo JJ, Atala A. Hybrid printing of mechanically and biologically improved constructs for cartilage tissue engineering applications. Biofabrication 5(1) (2013) 015001.

[117] Ahearne M. Introduction to cell-hydrogel mechanosensing. Interface Focus 4(2) (2014) 20130038.

[118] Mironov V, Kasyanow V, Markwald RR. Organ printing: from bioprinter to organ biofabrication line. Curr Opin Biotechnol 22(5) (2011) 667-73.

[119] Chau DYS, Agashi K, Shakesheff KM. Microparticles as tissue engineering scaffolds: manufacture, modification and manipulation. Mat Sci Technol. 24(9) (2008) 1031-44.

[120] Delcroix GJR, Schiller PC, Benoit JP, Montero-Menei CN. Adult cell therapy for brain neuronal damages and the role of tissue engineering. Biomaterials 31 (2010) 2105-20.

[121] Munarin F, Petrini P, Farè S, Tanzi MC. Structural properties of polysaccharide-based microcapsules for soft tissue re generation. J Mater Sci Mater Med. 21 (2010) 365-375.

[122] Malda J, Frondoza CG. Microcarriers in the engineering of cartilage and bone. Trends Biotechnol. 24(7) (2006) 299-30.

[123] Burapapadh K, Takeuchi H, Sriamornsak P. Novel pectin-based nanoparticles prepared from nanoemulsion templates for improving in vitro dissolution and in vivo absorption of poorly water-soluble drug. Eur J Pharm Biopharm. 82(2) (2012) 250-61.

[124] Wischke C, Schwendeman SP. Principles of encapsulating hydrophobic drugs in PLA/PLGA microparticles. Int J Pharm. 364 (2008) 298-327.

[125] Sahoo SK, Panda AK, Labhasetwai V. Characterization of Porous PLGA/PLA Microparticles as a Scaffold fot Three Dimensional Growth of Breast Cancer Cells. Biomacromolecules. 6 (2005)1132-8.

[126] Rosca ID, Watari F, Uo M. Microparticle formation and its mechanism in single and double emulsion solvent evaporation. J Control Release. 99 (2004) 271-80.

[127] Tran VT, Benoît JP, Venier-Julienne MC. Why and how to prepare biodegradable, monodispersed, polymeric microparticles in the field of pharmacy? Int J Pharm. 407(1-2) (2011) 1-11.

[128] Sun G, Qi F, Wu J, Ma G, Ngai T. Preparation of Uniform Particle-Stabilized Emulsions Using SPG Membrane Emulsification. Langmuir. 30(24) (2014) 7052-6.

[129] Romanowsky MB, Abate AR, Rotem A, Holtze C, Weitz DA. High throughput production of single core double emulsions in a parallelized microfluidic device. Lab Chip. 12(4) (2012) 802-7.

[130] Blaker JJ, Knowles JC, Day RM. Novel fabrication techniques to produce microspheres by thermally induced phase separation for tissue engineering and drug delivery. Acta Biomater. 4(2) (2008) 264-72.

[131] Salerno A, Levato R, Mateos-Timoneda MA, Engel E, Netti PA, Planell JA. Modular polylactic acid microparticle-based scaffolds prepared via microfluidic emulsion/solvent displacement process:

fabrication, characterization, and in vitro mesenchymal stem cells interaction study. J Biomed Mater Res A. 101(3) (2013) 720-32.

[132] Martinez CJ, Kim JW, Ye C, Ortiz I, Rowat AC, Marquez M, Weitz D. A microfluidic approach to encapsulate living cells in uniform alginate hydrogel microparticles. Macromol Biosci. 12(7) (2012) 946-51.

[133] Eggers J, Villermaux E. Physics of liquid jets. Rep. Prog. Phys. 71 (2008) 036601.

[134] Martín-Banderas L, Flores-Mosquera M, Riesco-Chueca P, Rodríguez-Gil A, Cebolla A, Chávez S, Gañán-Calvo AM. Flow Focusing: a versatile technology to produce size-controlled and specific-morphology microparticles. Small. 1(7) (2005) 688-92.

[135] Holgado MA, Arias JL, Cózar MJ, Alvarez-Fuentes J, Gañán-Calvo AM, Fernández-Arévalo M. Synthesis of lidocaine-loaded PLGA microparticles by flow focusing. Effects on drug loading and release properties. Int J Pharm. 358(1-2) (2008) 27-35.

[136] Xu Q, Hashimoto M, Dang TT, Hoare T, Kohane DS, Whitesides GM, Langer R, Anderson DG. Preparation of monodisperse biodegradable polymer microparticles using a microfluidic flow-focusing device for controlled drug delivery. Small. 5(13) (2009) 1575-81.

[137] Hallé JP, Leblond FA, Pariseau JF, Jutras P, Brabant MJ, Lepage Y. Studies on small (&lt; 300 microns) microcapsules: II--Parameters governing the production of alginate beads by high voltage electrostatic pulses. Cell Transplant. 3(5) (1994) 365-72.

[138] Felder ChB, Blanco-Príeto MJ, Heizmann J, Merkle HP, Gander B. Ultrasonic atomization and subsequent polymer desolvation for peptide and protein microencapsulation into biodegradable polyesters. J Microencapsul. 20(5) (2003) 553-67.

[139] Bashakar S, Roh KH, Jiang X, Baker GL, Lahann J. Spatioselective Modification of Bicompartimental Polymer Particles and Fibers via Huisgen 1,3-Dipolar Cycloaddition. Macromol Rapid Communications. 29 (2008)1655-60.

[140] Bashakar S, Pollock M, Yoshida M, Lahann J. Towards Designer Microparticles: Simultaneous Control of Anisotropy, Shape and Size. Small. 6(3) (2010) 404-11.

[141] Patel BB, Patel JK, Chakraborty S. Review of patents and application of spray drying in pharmaceutical, food and flavor industry. Recent Pat Drug Deliv Formul. 8(1) (2014) 63-78.

[142] Yeo SD, Kiran E. Formation of polymer particles with supercritical fluids: a review. J Supercritical Fluids 34 (2005) 287-308.

[143] Fessi H, Puisieux F, Devissaguet JP, Ammoury N, Benita S. Nanocapsule formation by interfacial polymer deposition following solvent displacemen, J Pharm, 55 (1989) R1-R4.

[144] Chidambaram M, Krishnasamy K. Modifications to the conventional nanoprecipitation technique: an approach to fabricate narrow sized polymeric nanoparticles. Adv Pharm Bull.4(2) (2014) 205-8.

[145] Beck-Broichsitter M1, Rytting E, Lebhardt T, Wang X, Kissel T. Preparation of nanoparticles by solvent displacement for drug delivery: a shift in the "ouzo region" upon drug loading. Eur J Pharm Sci. 41(2) (2010) 244-53.

[146]	Lasalle V, Ferreira MJ. PLA Nano- and microparticles for drug delivery: an overview of the methods of preparation. Macromol Biosci 7 (2007) 767-83.

[147]	Mohamed F, van der Walle CF. Engineering biodegradable polyester particles with specific drug targeting and drug release properties. J Pharm Sci. 97(1) (2008)71-87.

[148]	Grandhi TS, Rege K. Design, synthesis, and functionalization of nanomaterials for therapeutic drug delivery. Adv Exp Med Biol. 811 (2014)157-82.

[149]	Ren J, Hong HY, Ren TB, Teng XR.Preparation and characterization of magnetic PLA-PEG composite nanoparticles for drug targeting. React Funct Polym. 66 (2006) 944–951.

[150]	Gelperina S, Maksimenko O, Khalansky A, Vanchugova L, Shipulo E, Abbasova K, et al. Drug delivery to the brain using surfactant-coated poly(lactide-co-glycolide) nanoparticles: influence of the formulation parameters. Eur J Pharm Biopharm. 74(2) (2010)157-63.

[151]	Erdogar N, Iskit AB, Eroglu H, Sargon MF, Mungan NA, Bilensoy E. Cationic core-shell nanoparticles for intravesical chemotherapy in tumor-induced rat model: Safety and efficacy. Int J Pharm. 471(1-2) (2014) 1-9.

[152]	Cirstoiu-Hapca A, Buchegger F, Bossy L, Kosinski M, Gurny R, Delie F. Nanomedicines for active targeting: physico-chemical characterization of paclitaxel-loaded anti-HER2 immunonanoparticles and in vitro functional studies on target cells.Eur J Pharm Sci. 38(3) (2009) 230-7.

[153]	Kocbek P, Obermajer N, Cegnar M, Kos J, Kristl J. Targeting cancer cells using PLGA nanoparticles surface modified with monoclonal antibody. J Control Release. 120(1-2) (200/ 18-26.

[154]	Saeed AO, Magnusson JP, Moradi E, Soliman M, Wang W, Stolnik S, et al. Modular construction of multifunctional bioresponsive cell-targeted nanoparticles for gene delivery. Bioconjug Chem.22(2) (2011) 156-68.

[155]	Zheng Y, Yu B, Weecharangsan W, Piao L, Darby M, Mao Y, et al. Transferrin-conjugated lipid-coated PLGA nanoparticles for targeted delivery of aromatase inhibitor 7alpha-APTADD to breast cancer cells. Int J Pharm. 390(2) (2010) 234-41.

[156]	Xu L, Li H, Wang Y, Dong F, Wang H, Zhang S. Enhanced activity of doxorubicin in drug resistant A549 tumor cells by encapsulation of P-glycoprotein inhibitor in PLGA-based nanovectors. Oncol Lett. 7(2) (2014) 387-92.

[157]	Nicolas J, Mura S, Brambilla D, Mackiewicz N, Couvreur P. Design, functionalization strategies and biomedical applications of targeted biodegradable/biocompatible polymer-based nanocarriers for drug delivery.Chem Soc Rev. 42(3) (2013) 1147-235.

[158]	Stoodley P, Sauer K, Davies DG, Costerton JW. Biofilms as complex differentiated communities.Annu Rev Microbiol. 56 (2002) 187-209.

[159]	Bassler BL. How bacteria talk to each other: regulation of gene expression by quorum sensing. Curr Opin Microbiol. 2(6) (1999) 582-7.

[160] Forier K, Raemdonck K, De Smedt SC, Demeester J, Coenye T, Braeckmans K. Lipid and polymer nanoparticles for drug delivery to bacterial biofilms. J Control Release. (2014) doi: 10.1016/j.jconrel.2014.03.055.

[161] van Wezel AL. Growth of cell-strains and primary cells on micro-carriers in homogeneous culture. Nature.216(5110) (1967) 64-5.

[162] van Wezel AL, van Herwaarden JA, van de Heuvel-de Rijk EW. Large-scale concentration and purification of virus suspension from microcarrier culture for the preparation of inactivated virus vaccines. Dev Biol Stand.42 (1979) 65-9.

[163] van der Velden-de Groot CA. Microcarrier technology, present status and perspective. Cytotechnology. 18(1-2) (1995) 51-6.

[164] Lecina M, Ting S, Choo A, Reuveny S, Oh S. Scalable platform for human embryonic stem cell differentiation to cardiomyocytes in suspended microcarrier cultures. Tissue Eng Part C Methods. 16(6) (2010) 1609-19.

[165] Schop D, Janssen FW, Borgart E, de Bruijn JD, van Dijkhuizen-Radersma R. Expansion of mesenchymal stem cells using a microcarrier-based cultivation system: growth and metabolism. J Tissue Eng Regen Med. 2(2-3) (2008) 126-35.

[166] Botchwey EA, Pollack SR, Levine EM, Laurencin CT. Bone tissue engineering in a rotating bioreactor using a microcarrier matrix system. J Biomed Mater Res. 55(2) (2001) 242-53.

[167] Chun KW, Yoo HS, Yoon JJ, Park TG. Biodegradable PLGA microcarriers for injectable delivery of chondrocytes: effect of surface modification on cell attachment and function. Biotechnol Prog. 20(6) (2004) 1797-801.

[168] Thomson HA, Treharne AJ, Backholer LS, Cuda F, Grossel MC, Lotery AJ. Biodegradable poly(α-hydroxy ester) blended microspheres as suitable carriers for retinal pigment epithelium cell transplantation. J Biomed Mater Res A. 95(4) (2010) 1233-43.

[169] Bao TQ, Franco RA, Lee BT. Preparation and characterization of novel poly(ε-caprolactone)/biphasic calcium phosphate hybrid composite microspheres. J Biomed Mater Res B Appl Biomater. 98(2) (2011) 272-9.

[170] Kodali A, Lim TC, Leong DT, Tong YW. Cell-Microsphere Constructs Formed with Human Adipose-Derived Stem Cells and Gelatin Microspheres Promotes Stemness, Differentiation, and Controlled Pro-Angiogenic Potential. Macromol Biosci. (2014) . doi: 10.1002/mabi.201400094.

[171] Fang J, Zhang Y, Yan S, Liu Z, He S, Cui L, Yin J. Poly(L-glutamic acid)/chitosan polyelectrolyte complex porous microspheres as cell microcarriers for cartilage regeneration. Acta Biomater. 10(1) (2014) 276-88.

[172] Kwon YJ, Peng CA. Calcium-alginate gel bead cross-linked with gelatin as microcarrier for anchorage-dependent cell culture. Biotechniques. 33(1) (202) 212-4.

[173] Munarin F, Petrini P, Farè S, Tanzi MC. Structural properties of polysaccharide-based microcapsules for soft tissue regeneration. J Mater Sci Mater Med. 21(1) (2010) 365-75.

[174]  Sart S, Agathos SN, Li Y. Engineering Ste Cell Fate with Biochemical and Biomechanical Properties of Microcarriers. Biotechnol Prog. 29(6) (2013) 1354-66.

[175]  Chen AK, Chen X, Choo AB, Reuveny S, Oh SK.Critical microcarrier properties affecting the expansion of undifferentiated human embryonic stem cells. Stem Cell Res. 7(2) (2011) 97-111.

[176]  Mukhopadhyay A, Mukhopadhyay SN, Talwar GP. Influence of serum proteins on the kinetics of attachment of Vero cells to cytodex microcarriers. J Chem Technol Biotechnol. 56(4) (1993) 369-74.

[178]  Keselowsky BG, Collard DM, García AJ. Integrin binding specificity regulates biomaterial surface chemistry effects on cell differentiation. Proc Natl Acad Sci U S A. 102(17) (2005) 5953-7.

[179]  Curran JM, Chen R, Hunt JA. Controlling the phenotype and function of mesenchymal stem cells in vitro by adhesion to silane-modified clean glass surfaces. Biomaterials. 26(34) (2005) 7057-67.

[180]  Brew S, Ingram K. Purification of human plasma fibronectin. J Tissu Culture Methods. 16 (1994) 197-9.

[181]  Santos FD, Andrade PZ, Abecasis MM, Gimble JM, Chase LG, Campbell AM, et al. Toward a clinical-grade expansion of mesenchymal stem cells from human sources: a microcarrier-based culture system under xeno-free conditions.Tissue Eng Part C Methods. 17(12) (2011) 1201-10.

[182]  Gronthos S, Simmons PJ, Graves SE, Robey PG. Integrin-mediated interactions between human bone marrow stromal precursor cells and the extracellular matrix.Bone. 28(2) (2001) 174-81.

[183]  Schmidt JJ, Jeong J, Kong H. The interplay between cell adhesion cues and curvature of cell adherent alginate microgels in multipotent stem cell culture. Tissue Eng Part A. 17(21-22) (2011) 2687-94.

[184]  Kilian KA, Bugarija B, Lahn BT, Mrksich M. Geometric cues for directing the differentiation of mesenchymal stem cells. Proc Natl Acad Sci U S A. 107(11) (2010)4872-7.

[185]  Engler AJ, Sen S, Sweeney HL, Discher DE. Matrix elasticity directs stem cell lineage specification. Cell. 126(4) (2006) 677-89.

[186]  Trappmann B, Gautrot JE, Connelly JT, Strange DG, Li Y, Oyen ML, et al. Extracellular-matrix tethering regulates stem-cell fate. Nat Mater. 11(7) (2012) 642-9.

[187]  Eyckmans J, Lin GL, Chen CS. Adhesive and mechanical regulation of mesenchymal stem cell differentiation in human bone marrow and periosteum-derived progenitor cells. Biol Open. 1(11) (2012) 1058-68.

[188]  Tseng PC, Young TH, Wang TM, Peng HW, Hou SM, Yen ML. Spontaneous osteogenesis of MSCs cultured on 3D microcarriers through alteration of cytoskeletal tension. Biomaterials 33(2) (2012) 556-64.

[189]  Schaedlich K, Knelangen JM, Navarrete Santos A, Fischer B, Navarrete Santos A. A simple method to sort ESC-derived adipocytes. Cytometry A. 77(10) (2010) 990-5.

[190]  Malda J, Kreijveld E, Temenoff JS, van Blitterswijk CA, Riesle J. Expansion of human nasal chondrocytes on macroporous microcarriers enhances redifferentiation. Biomaterials. 24(28) (2003) 5153-61.

[191] Goh TKP, Zhang ZY, Chen AKL, Reuveny S, Choolani M, Chan JKY, Oh SKW 2013 Microcarrier Culture for Efficient Expansion and Osteogenic Differentiation of Human Fetal Mesenchymal Stem Cells. BioRes Open Access. 2(2) (2013) 84-96.

[192] Yang HS, Jeon O, Bhang SH, Lee SH, Kim BS. Suspension culture of mammalian cells using thermosensitive microcarrier that allows cell detachment without proteolytic enzyme treatment. Cell Transplant. 19(9) (2010) 1123-32.

[193] Huang CC, Wei HJ, Yeh YC, Wang JJ, Lin WW, Lee TY, et al. Injectable PLGA porous beads cellularized by hAFSCs for cellular cardiomyoplasty. Biomaterials. 33(16) (2012) 4069-77.

[194] Kindi AH, Asenjo JF, Ge Y, Chen GY, Bhathena J, Chiu RC, Prakash S, Shum-Tim D. Microencapsulation to reduce mechanical loss of microspheres: implications in myocardial cell therapy. Eur J Cardiothorac Surg. 39(2) (2011) 241-7.

[195] Penna C, Perrelli MG, Karam JP, Angotti C, Muscari C, Montero-Menei CN, Pagliaro P. Pharmacologically active microcarriers influence VEGF-A effects on mesenchymal stem cell survival. J Cell Mol Med. 17(1) (2013) 192-204.

[196] Delcroix GJ, Garbayo E, Sindji L, Thomas O, Vanpouille-Box C, Schiller PC, Montero-Menei CN. The therapeutic potential of human multipotent mesenchymal stromal cells combined with pharmacologically active microcarriers transplanted in hemi-parkinsonian rats.Biomaterials. 32(6) (2011) 1560-73.

[197] Borlongan CV, Saporta S, Sanberg PR. Intrastriatal transplantation of rat adrenal chromaffin cells seeded on microcarrier beads promote long-term functional recovery in hemiparkinsonian rats. Exp Neurol. 151(2) (1998) 203-14.

[198] Gross RE, Watts RL, Hauser RA, Bakay RA, Reichmann H, von Kummer R, et al. Intrastriatal transplantation of microcarrier-bound human retinal pigment epithelial cells versus sham surgery in patients with advanced Parkinson's disease: a double-blind, randomised, controlled trial. Lancet Neurol. 10(6) (2011) 509-19.

[199] Thomson HA, Treharne AJ, Backholer LS, Cuda F, Grossel MC, Lotery AJ. Biodegradable poly(α-hydroxy ester) blended microspheres as suitable carriers for retinal pigment epithelium cell transplantation. J Biomed Mater Res A. 95(4) (2010) 1233-43.

[200] Bouffi C, Thomas O, Bony C, Giteau A, Venier-Julienne MC, Jorgensen C, Montero-Menei C, Noël D. The role of pharmacologically active microcarriers releasing TGF-beta3 in cartilage formation in vivo by mesenchymal stem cells. Biomaterials. 31(25) (2010) 6485-93.

[201] Calafiore R, Basta G, Luca G, Lemmi A, Montanucci MP, Calabrese G, et al. Microencapsulated pancreatic islet allografts into nonimmunosuppressed patients with type 1 diabetes: first two cases. Diabetes Care. 29(1) (2006) 137-8.

[202] Wu Y, Zhao RC. The role of chemokines in mesenchymal stem cell homing to myocardium. Stem Cell Rev. 8(1) (2012) 243-50.

[203] Johnson TD, Christman KL. Injectable hydrogel therapies and their delivery strategies for treating myocardial infarction. Expert Opin Drug Deliv. Jan;10(1) (2013)59-72.

[204] Kim SS, Yoo SW, Park TS, Ahn SC, Jeong HS, Kim JW, et al. Neural induction with neurogenin1 increases the therapeutic effects of mesenchymal stem cells in the ischemic brain. Stem Cells. 26(9) (2008) 2217-28.

[205] Paul G, Anisimov SV. The secretome of mesenchymal stem cells: potential implications for neuroregeneration. Biochimie. 95(12) (2013) 2246-56.

[206] Zhang Y, Chen XM, Sun DL. Effects of coencapsulation of hepatocytes with adipose-derived stem cells in the treatment of rats with acute-on-chronic liver failure. Int J Artif Organs. 37(2) (2014) 133-41.

[207] Nikolovski J, Gulari E, Humes HD. Design engineering of a bioartificial renal tubule cell therapy device. Cell Transplant. 8(4) (1999) 351-64.

[208] Basta G, Montanucci P, Luca G, Boselli C, Noya G, Barbaro B, et al. Long-term metabolic and immunological follow-up of nonimmunosuppressed patients with type 1 diabetes treated with microencapsulated islet allografts: four cases. Diabetes Care. 34(11) (2011) 2406-9.

[209] Calafiore R, Basta G. Clinical application of microencapsulated islets: actual prospectives on progress and challenges. Adv Drug Deliv Rev. 67-68 (2014) 84-92.

[210] Chung HJ, Park TG. Injectable cellular aggregates prepared from biodegradable porous microspheres for adipose tissue engineering. Tissue Eng Part A. 15(6) (2009) 1391-400.

[211] Yu C, Bianco J, Brown C, Fuetterer L, Watkins JF, Samani A, Flynn LE. Porous decellularized adipose tissue foams for soft tissue regeneration. Biomaterials. 34(13) (2013) 3290-302.

[212] Liu X, Jin X, Ma PX. Nanofibrous hollow microspheres self-assembled from star-shaped polymers as injectable cell carriers for knee repair. Nat Mater. 10(5) (2011) 398-406.

[213] Chung HJ, Kim IK, Kim TG, Park TG. Highly open porous biodegradable microcarriers: in vitro cultivation of chondrocytes for injectable delivery. Tissue Eng Part A. 14(5) (2008) 607-15.

[214] Gorodetsky R. The use of fibrin based matrices and fibrin microbeads (FMB) for cell based tissue regeneration. Expert Opin Biol Ther. 8(12) (2008) 1831-46.

[215] Lin FH, Chen TM, Lin CP, Lee CJ. The merit of sintered PDLLA/TCP composites in management of bone fracture internal fixation. Artif Organs. 23(2) (1999)186-94.

[216] Yang Y, Hallgrimsson B, Putnins EE. Craniofacial defect regeneration using engineered bone marrow mesenchymal stromal cells. J Biomed Mater Res A. 99(1) (2011) 74-85.

[217] Munarin F, Guerreiro SG, Grellier MA, Tanzi MC, Barbosa MA, Petrini P, Granja PL. Pectin-based injectable biomaterials for bone tissue engineering. Biomacromolecules. 12(3) (2011) 568-77.

[218] Yu J, Du KT, Fang Q, Gu Y, Mihardja SS, Sievers RE, Wu JC, Lee RJ. The use of human mesenchymal stem cells encapsulated in RGD modified alginate microspheres in the repair of myocardial infarction in the rat. Biomaterials. 31(27) (2010) 7012-20.

[219]  Ahmadi R, Mordan N, Forbes A, Day RM. Enhanced attachment, growth and migration of smooth muscle cells on microcarriers produced using thermally induced phase separation. Acta Biomater. 7(4) (2011) 1542-9.

[220]  Voigt M, Schauer M, Schaefer DJ, Andree C, Horch R, Stark GB. Cultured epidermal keratinocytes on a microspherical transport system are feasible to reconstitute the epidermis in full-thickness wounds. Tissue Eng. 5(6) (1999) 563-72.

[221]  Palmiero C, Imparato G, Urciuolo F, Netti P. Engineered dermal equivalent tissue in vitro by assembly of microtissue precursors. Acta Biomater. 6(7) (2010) 2548-53.

[222]  Ruhé´ PQ, Hedberg-Dirk EL, Padron NT, Spauwen PHM, Jansen JA, Mikos AG. Porous poly(D,L-lactic-co-glycolic acid)/calcium phosphate cement composite for reconstruction of bone defects. Tissue Eng. 12 (2006) 789–800.

[223]  Rockwood DN, Gil ES, Park SH, Kluge JA, Grayson W, Bhumiratana S, Rajkhowa R, Wang X, Kim SJ, Vunjak-Novakovic G, Kaplan DL. Ingrowth of human mesenchymal stem cells into porous silk particle reinforced silk composite scaffolds: an in vitro study. Acta Biomater. 7 (2010) 144–51.

[224]  Hu X, Zhou J, Zhng N, Tan H, Gao C. Preparation and properties of an injectable scaffolds of poly(lactic-co-glycolic acid) microparticles/chitosan hydrogel. J Mech Behav Biomed Mater I. 1 (2008) 352–59.

[225]  Hong Y, Gong Y, Gao C, Shen J. Collagen-coated polylactide microcarriers/chitosan hydrogel composite: injectable scaffold for cartilage regeneration. J Biomed Mater Res A. 85(3) (2008) 628-37.

[226]  Toh WS, Lim TC, Kurisawa M, Spector M. Modulation of mesenchymal stem cell chondrogenesis in a tunable hyaluronic acid hydrogel microenvironment. Biomaterials. 33(15) (2012) 3835-45.

[227]  Wang C, Gong Y, Zhong Y, Yao Y, Sui K, Wang DA. The control of anchorage-dependent cell behavior within a hydrogel/microcarrier system in an osteogenic model. Biomaterials 30 (2009) 2259-69.

[228]  Duan B, Wang M, Zhou WY, Cheung WL, Li ZY,and Lu, W.W. Three-dimensional nanocomposite scaffolds fabricated via selective laser sintering for bone tissue engineering. Acta Biomater. 6(12) (2010) 4495-505.

[229]  Wang H, Leeuwenburgh SC, Li Y, Jansen JA. The use of micro- and nanospheres as functional components for bone tissue regeneration. Tissue Eng Part B Rev. 18(1) (2012) 24-39.

[230]  Selimović Š, Khademhosseini A. Research highlights. Cell beads for building macroscopic tissues. Lab Chip. 11(16) (2011) 2651-2.

# Chapter 3

# Green-inspired fabrication of polylactic acid MCs with controlled size

*In this chapter, a new method to fabricate polylactic acid microcarriers is described and characterized. This method involves no harmful chemicals and is the first report of a processing method to obtain PLA devices involving the green solvent ethyl lactate. Particles generation is obtained by i) generating a polymer solution jet and its subsequent break-up into droplets by means of aero- and hydrodynamic forces, and ii) the solidification of these droplets in a coagulation bath. Experimental parameters to control particles size in the range suitable for drug and cell delivery applications are also characterized, paying particular attention to particle size, polidispersity and morphology. The adaptability of such fabrication method to encapsulate drugs is also assessed in a proof-of-concept assay using a model, fluorescent compound.*

**3.1 Introduction**

MCs can be fabricated with different types of biomaterials, each possessing appealing physico-chemical properties for specific devices and offering different approaches to drug and cell release applications. For instance, several synthetic (*e.g.* polyethylene glycol derivatives) and natural polymers (alginates, chitosans, pectins), can be processed under cell-friendly conditions (such as photocrosslinking and ionotropic gelation) to form hydrogel spheres suitable for direct encapsulation of cells into the core of the carrier [1]. On the other hand, synthetic biodegradable polyesters, including polylactide (PLA), polyglicolide (PGA) and their copolymers (PLGA), are mainly used to produce microcarriers to deliver cells cultured on their surface. Besides, these carriers can be easily loaded with bioactive molecules as support for the cell therapy [2]. Biodegradable polyesters, especially PLA/PLGA, are widely used as they degrade through hydrolysis, a process whose kinetics can be tailored varying the polymer molecular weight, crystallinity and lactide/glycolide ratio. These features have led to an increasing number of commercial drug delivery matrices based on polylactic acid and its copolymers [3]. However, the use of these polymers for drug delivery and cell therapy applications still deals with several challenges. Besides their hydrophobic nature and the lack of bioactive functional groups, the processing of polylactide often requires the usage of toxic solvents, whose residues must be carefully removed from the final device, for patient safety and regulatory approval of the device [4]. This aspect becomes fundamental with particular respect to those PLA-based products designed to interact with biological milieu. Thus, a PLA processing route that minimize or eliminate hazardous compounds will lead to environmentally and regulatory- safe procedures and products.

Ethyl lactate (EtLac) is a green, water-miscible, biodegradable solvent and Food and Drug Administration (FDA) approved aroma in food industry, which does not show any potential health risks [5]. EtLac is not teratogenic and it readily undergoes hydrolysis to ethanol and lactic acid, this last compound being a natural metabolite in humans. In addition, its ecotoxocity is very low, it is a non-ozone depleting fluid, it can be produced from renewable resources with cost-effective technologies, and it has already been studied in pharmaceutical applications [6, 7]. Recently, a description of the liquid-liquid equilibrium of PLA and ethyl lactate, which present partial miscibility was reported [8]. Considering these features, it is evident that a new, well defined PLA MCs preparation process involving ethyl lactate can offer appealing advantages for many biomedical applications in terms of biocompatibility and waste disposal, in contrast to methods based on traditional organic solvents.

Among all the described fabrication methods for PLA-based MCs preparation, the emulsion/solvent evaporation method is the most used. This process usually requires the use of toxic chlorinated solvents and has limited control over certain important MCs parameters, such as size distribution [9]. Another family of methods for the fabrication of MCs relies on the preliminary formation of liquid droplets, such as spray drying [10], solution dripping [11], ultrasonic and electrohydrodynamic atomization [12, 13], and flow focusing [14]. Among these methods, the last three consist of the generation of a liquid jet from a stable meniscus at the dispensing tip due to external applied forces and subsequent rupture of the jet into a monodisperse train of droplets.

In the present study, an alternative ethyl lactate-based manufacturing technique to obtain PLA MCs with potential application as cell and drug carriers has been developed. A simple solution extrusion strategy coupled with a coaxial flow of gaseous nitrogen was adopted, providing the necessary conditions to induce meniscus formation, stretching and break up into droplets. MCs were fabricated through dissolution of PLA in ethyl lactate, atomization of the solution into liquid droplets and their subsequent precipitation in a hydroalcoholic coagulation bath. Upon immersion into the bath, ethyl lactate was removed and particles were formed due to non-solvent induced phase separation (NIPS). MCs size could be controlled by simply tuning the gas and solution flow parameters or varying the solution concentration. A complete characterization of the MCs morphology, their inner structure and a preliminary assessment of drug encapsulation using a fluorescent model compound are also described. This method constitutes a proof of principle for the use of EtLac as a processing agent of PLA. The obtained MCs might be used as cell delivery systems with potential applications in the field of tissue engineering and drug delivery.

## 3.2 Materials and Methods

### 3.2.1 Materials

Polylactic acid (Purasorb PLDL 7038, inherent viscosity midpoint 3.8 dl g-1, Mw≈ 850000 Da) was purchased from Purac. (-)Ethyl L-lactate (photoresist grade; purity≥ 99.0%) was obtained from Fluka and used without further purification. Poly(vinyl alcohol) (PVA, 30-70 kDa, 88% hydrolyzed) and all the other reagents were from Sigma-Aldrich.

### 3.2.2 Differential scanning calorimetry

A thermal characterization of the material processed from ethyl lactate was performed by Differential Scanning Calorimetry (DSC, 2029 TA). PLA films (200 µm thick) were prepared by solvent casting. Two solutions of PLA 2.5 % w/v in EtLac and in chloroform were prepared, cast into petri dishes and left to evaporate under a fume hood for three days. The films were then collected, rinsed thoroughly with distilled water and air dried. For each DSC test, about 5 mg of material were loaded in the furnace of the instrument and were heated from room temperature up to 220 °C (1st run, heating rate 10 °C/min), then rapidly cooled down to room temperature and heated up to 200 °C again (2nd run, rate 10 °C/min).

### 3.2.3 Viscosity of EtLac-PLA solution

PLA was dissolved in EtLac at 50°C under stirring to obtain solutions of different concentrations in the range between 1 and 4.5 % w/v. The viscosity of 10 ml samples from each solution was measured at room temperature (25 ± 2 °C) through a vibration viscosimeter (SV-10, A&D Company Ldt, Japan). For solutions 3.5 and 4.0 % w/v, viscosity measurements were also taken at different temperatures (up to 50°C).

### 3.2.4 MCs preparation

The polymer solution was loaded into a syringe pump and dispensed at a constant rate through the inner bore (30G) of a dual concentric nozzle (NNC-DN-2230, NanoNC, South Korea), while the outer coaxial bore (22G) was fed with $N_2$ (feeding pressure P = 0.5 bar). The inner needle protruded from the external conduct for 1 mm. The coagulation bath, composed by a hydroalcoholic solution (70% EtOH in water with 0.3% PVA) under stirring at 100 rpm, was placed 8 cm below the dispensing tip. The solution concentration and dispensing rate were varied between 3.5 and 4.0 % w/v and from 10 to 50 mL h-1, respectively. MCs were allowed to harden into the coagulation bath for 1 hour before being collected by centrifugation. Following extensively rinsing with deionized water, MCs were flash frozen in liquid nitrogen and lyophilized for 48 hours. MCs batches were coded as XXDNYY to indicate their preparation parameters, where XX stands for the polymer concentration, DN stands for dual nozzle and YY is the dispensing rate expressed in mL h-1. Particles 35DN10 were prepared varying also the dispensing tip-bath distance from 8 to 18 cm and lowering the bath temperature from 18°C to 9°C.

### 3.2.5 MCs size distribution determination

MPs images were taken with an optical microscope (Leica E600 Upright Microscope) and analyzed with *ImageJ* software to determine particle size [15]. For each MCs batch more than 100 measurements were taken and the average diameter, standard deviation, dispersion index and geometric standard deviation were calculated. A stereomicroscope (Leica MZ16F Fluorescence Stereomicroscope) was used to qualitatively describe the overall geometry and shape of the MCs.

### 3.2.6 MCs morphology

Morphological analysis of the MCs surface was carried out using a Scanning Electron Microscope (SEM Quanta Q200, FEI Company). Before the analysis, samples were mounted on a sample holder and sputtered with gold. Surface wrinkles patterns were analyzed from SEM micrographs. Wrinkle wavelength λ, defined as the peak-to-peak distance between two neighboring wrinkles, was measured directly from high magnification SEM pictures for several MCs in different diameter ranges, using *ImageJ* software. The inner morphology of 35DN10 MCs prepared under different experimental conditions was investigated. To obtain MCs cross sections, the samples were dispersed at room temperature in Cryo M-Bed embedding medium (Bright), with 5% v/v EtOH to facilitate solution penetration into the MCs, thus preserving the inner microstructure during the slicing procedure. The MCs suspension was subsequently frozen at -21°C and cut into slices (20 µm thick) with a cryostat (Leica CM 1900), and collected on glass slides. Once defrosted, the embedding compound was removed by gently washing the slides with water. Samples were air dried, prior to metallization and SEM analysis.

*3.2.7 Encapsulation of rhodamine*

Rhodamine B (Sigma-Aldrich, $\lambda_{excitation}$ = 540 nm, $\lambda_{emission}$ = 625 nm) was dissolved in the polymeric solution at a 1% w/wPLA concentration or added to the coagulation bath (0.2% w/v bath solution). In both cases, MCs were prepared setting the polymer concentration and the dispensing rate at 3.5% w/v and 10 mL h-1, respectively. Rhodamine-loaded MCs were collected on a glass slide, dispersed with mineral oil, and their fluorescence distribution was then analyzed with a confocal laser scanning microscope (CLSM, Leica TCS-SP1).

## 3.3 Results

*3.3.1 PLA-EtLac solution characterization*

Differential Scanning Calorimetry (DSC) analysis showed no difference in the glass transition temperatures ($T_g$) between PLA samples obtained from solution in chloroform and ethyl lactate (Tg of 57.22 and 57.16 °C in the first heating run, and 57.63 and 57.41 °C in the second run). The absence of endothermic peaks in the thermogram (*i.e.* the absence of a melting event of crystalline domains) confirmed the amorphous nature of the materials in all the tested samples.

Together with the thermal properties, viscosity is a key parameter in polymer solution processing [16,17]. The variation of viscosity of the EtLac-PLA solution as a function of polymer concentration and temperature is shown in Figure 3.1.

Two linear regions in the viscosity-concentration curve can be identified (Figure 3.1a). The viscosity is slightly affected by the increase of PLA concentration up to 3.0%. In contrast, a dramatic rise in viscosity is found for higher polymer concentrations. Two PLA solution concentrations in this range, 3.5 and 4.0 % w/v, were chosen in this work to produce MCs. The temperature dependent behavior of the solution viscosity at these concentrations was analyzed. As shown in Figure 3.1b the viscosity values decreased from 77.1 and 158 cP at 25 °C, to 29.9 and 75.6 cP at 50 °C, respectively.
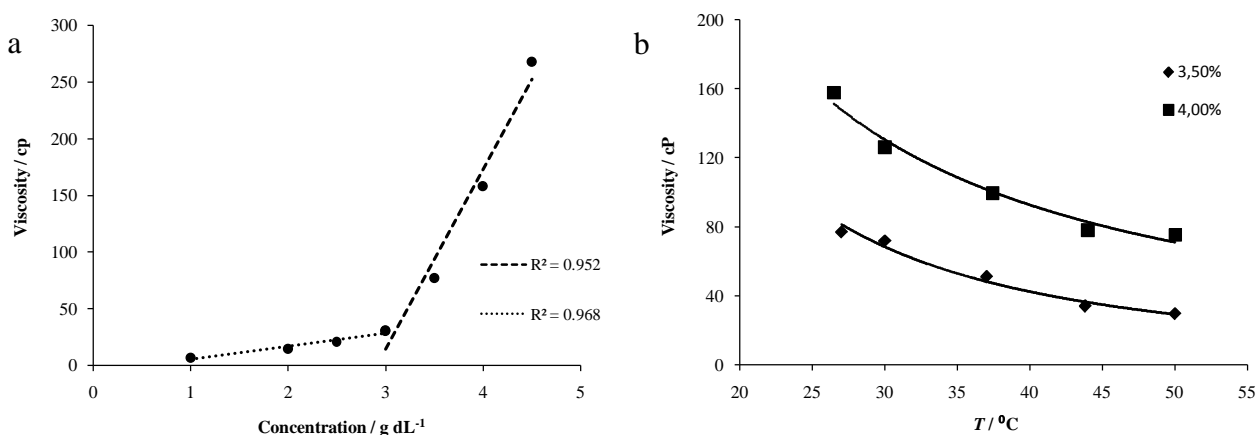


**Figure 3.1. Viscosity of PLA-EtLac solutions as function of (a) polymer concentration and (b) temperature.**

*3.3.2 MCs preparation and size determination*

A simple and streamlined apparatus for MCs preparation was set (Figure 3).
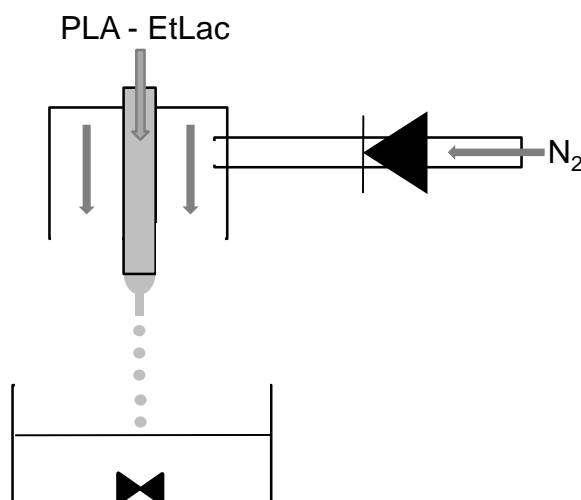


**Figure 3.2. Schematic representation of the MCs preparation set up.**

Several water-based and hydroalcoholic solutions were tested as coagulation baths, with or without addition of surfactants to lower bath surface tension, as summarized in Table 3.1.

Surprisingly, not all the bath compositions evaluated in this study were suitable for MCs formation. Upon dropping PLA-EtLac solution into water, only formation of aggregates was detected. In the case of water-only baths provided with surfactants like polyvinyl alcohol (PVA) or Tween (1% w/v), the formation of polymer aggregates was observed, whereas the addition of Triton X-100 (1% w/v) allowed for particles formation. However, increasing the ratio of ethanol in water above 55% v/v led to the formation of spherical particles, regardless of surfactants addition. According to these experimental observations, only those baths whose surface tension was lower than that of ethyl lactate showed the formation of spherical MCs, regardless of their chemical composition. Eventually, for all the MCs characterized in this study, the bath composition was set to 70% EtOH in water with 0.3% w/v PVA.

**Table 3.1. Composition of the evaluated coagulation baths.**

| Solution composition | Surfactant | $\gamma$ / dynes cm$^{-1}$ at RT | Spherical Particles |
|---|---|---|---|
| **Water** | 1% PVA | 52.21 [18a] | No |
| **Water** | 1% Triton X-100 | 30.00 [18b] | Yes |
| **Water** | 1% Tween 20 | 33.90 [18c] | No |
| **Ethanol** | - | 21.81 [18d] | Yes |
| **Water : EtOH (70 : 30)** | - | 33.53 [18d] | No |
| **Water : EtOH (30 : 70)** | - | 25.01 [18d] | Yes |
| **Water : EtOH (30 : 70)** | 0.3% PVA | - [18e] | Yes |
| **Water : EtOH (45 : 55)** | 0.3% PVA | - [18e] | Yes |
| **Ethyl Lactate** | **-** | **31.30** [5] | **-** |

Under these conditions, the highest number of spherical particles was obtained, with an overall particle formation yield over 95%. Once the proper coagulation bath was designed, MCs with tailored size could be obtained directly from generating spherical drops of PLA-EtLac solution.

With the experimental set-up used in this study, a wide range of MCs sizes could be achieved by simply tuning the polymer concentration and fluid flow parameters at the dispensing stage, as it is shown by optical and stereomicroscopy analysis results (Figures 3.3, 3.4 and Table 3.2).
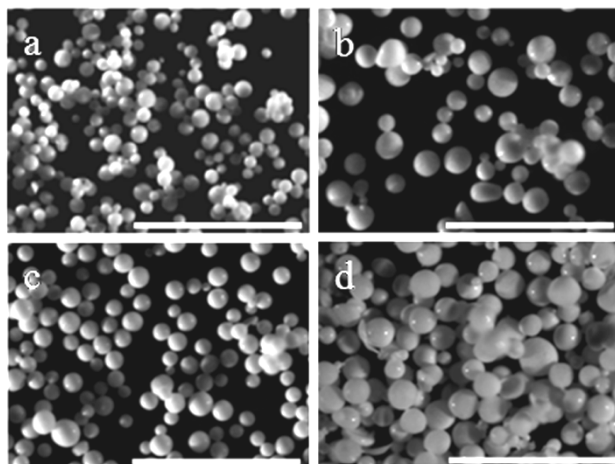


**Figure 3.3. Stereo microscopy images of 35DN10 (a), 35DN50 (b), 40DN10 (c) and 40DN50 (d) MCs. All pictures are taken at the same magnification (white bar = 1 mm).**
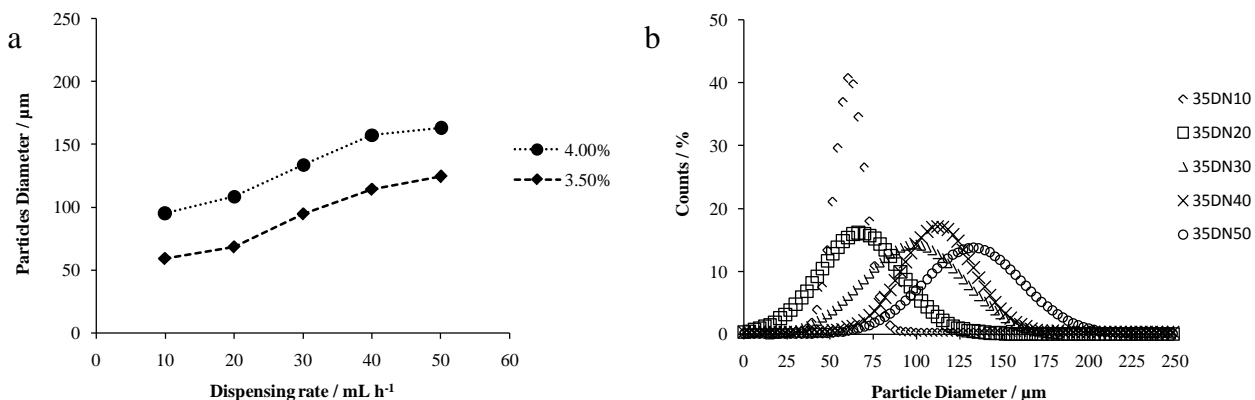


**Figure 3.4. MCs diameter as function of polymer concentration and dispensing rate (a) and size distribution of MCs prepared with 3.5% EtLac-PLA solution (b).**

**Table 3.2. MCs size and diameter distribution parameters.**

| Sample | Mean / µm | SD | DI | GSD |
|--------|-----------|------|-------|------|
| **35DN10** | 59.57 | 12.14 | 20.38 | 1.22 |
| **35DN20** | 71.68 | 21.20 | 29.58 | 1.33 |
| **35DN30** | 95.11 | 26.05 | 27.39 | 1.32 |
| **35DN40** | 114.46 | 28.88 | 25.23 | 1.27 |
| **35DN50** | 124.53 | 29.26 | 23.50 | 1.29 |
| **40DN10** | 95.23 | 23.79 | 24.98 | 1.29 |
| **40DN20** | 108.77 | 25.41 | 23.36 | 1.27 |
| **40DN30** | 133.95 | 26.11 | 19.49 | 1.32 |
| **40DN40** | 157.62 | 37.44 | 23.75 | 1.29 |
| **40DN50** | 163.14 | 47.54 | 29.14 | 1.41 |

The particles diameter and geometric standard deviation varied from 60 to 180 µm and 1.22 to 1.41, for 35DN10 and 40DN50 MCs respectively. MCs size increased with the dispensing rate of the solution, for a given polymer concentration, as shown in Figure 3.4. For example, for a 3.5% solution, a particle average diameter of ~60 µm was obtained for a dispensing rate of 10 mL h$^{-1}$, while increasing the dispensing rate to 50 mL h$^{-1}$ led to particles with average diameter of ~125 µm.

*3.3.3 MCs morphology, inner porosity and Janus wrinkle pattern*

The MCs morphology was qualitatively analyzed from SEM micrographs, revealing that PLA MCs possessed an overall spherical shape (Figure 3.5).
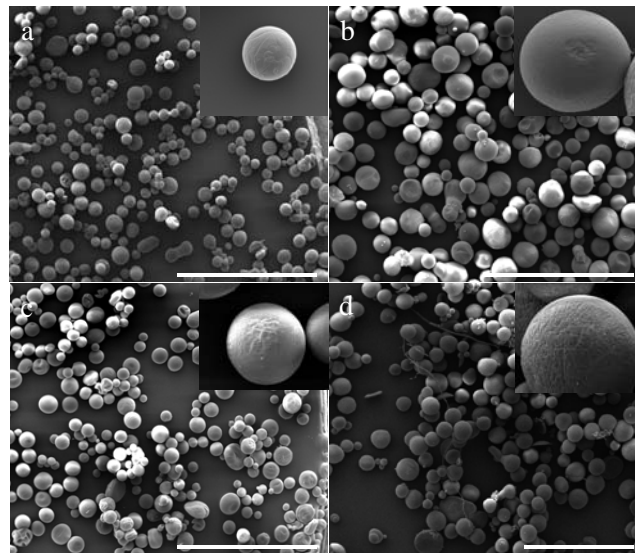


**Figure 3.5. SEM images of MCs 35DN10 (a), 35DN50 (b), 40DN10 (c), 40DN50 (d). Scale bar = 1 mm.**

The particles surface, showed a Janus topography, with two different hemispheres: one with a smoother surface and the other displaying a wrinkled-labyrinthine pattern. This asymmetric morphology is present in

all the MCs formulations prepared, regardless of the adopted experimental parameters. In order to provide a characterization of the obtained patterns, wrinkle wavelength λ was measured (Figure 3.6).
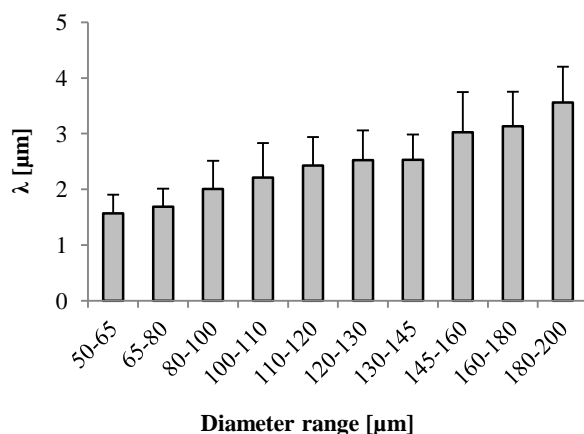


**Figure 3.6. Values of λ, wrinkles wavelength, as calculated for MCs falling in different ranges of size.**

Values of λ ranges from 1.5 to 3.5 μm for MCs with diameters from 50 to 200 μm. In batches prepared at higher polymer concentration and under faster dispensing flow conditions, such as 40DN50, a limited quantity of non-spherical particles, sometimes possessing drop-like morphology, were observed.

The analysis of the cross-section of 35DN10 samples revealed that the MCs possessed a thin, dense outer polymeric shell, enclosing a microporous layer. This interior layer is thicker underneath the smoother surface hemisphere of the MCs while is thinner, presenting larger pores, in correspondence to the rougher one (Figure 3.7). In the radial direction, towards the center of the sphere, the MCs are characterized by the presence of macrovoids or by a single macropore, whose dimension is higher in larger MCs, forming an empty core surrounded by the polymer shell. As consequence of this heterogeneity, the MCs inner microstructure may appear different according to whether the cross-section is taken closer or farther from the equatorial plane of the particle.
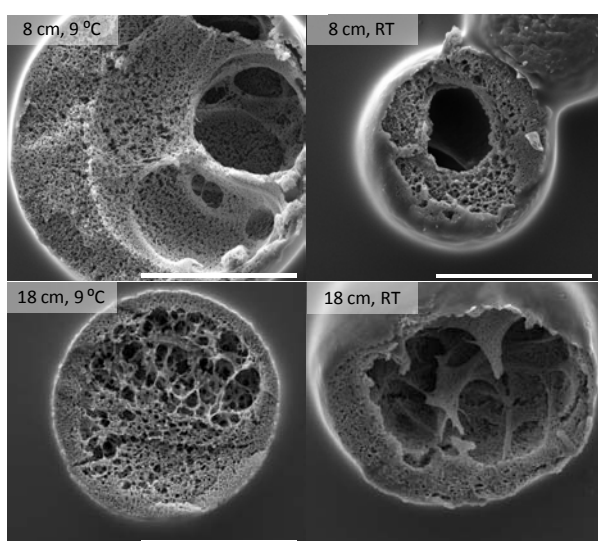


**Figure 3.7. SEM micrographs of 35DN10 MCs prepared varying needle-to-bath distance and coagulation bath temperature. Scale bar = 50 μm.**

Finally, diameter and morphological analysis from batches of particles prepared cooling the coagulation bath from room temperature to 9°C or increasing tip-to-bath distance from 8 to 18 cm were not significantly different from those reported above, suggesting no influence of these parameters on the particle size and morphology.

*3.3.4 Drug encapsulation*

To assess the possibility to encapsulate bioactive molecules and to qualitatively evaluate their distribution into the MCs, Rhodamine B was chosen as model fluorescent compound. Rhodamine B is soluble in EtLac, water and ethanol, thus suitable to assess designed system both for encapsulating compounds dispersed in the polymeric phase as well as for uptaking solutes from the coagulation bath. Confocal Laser Scanning Microscopy (CLSM) analysis allowed for visualization of rhodamine encapsulation and distribution inside the MCs (Figure 3.8).
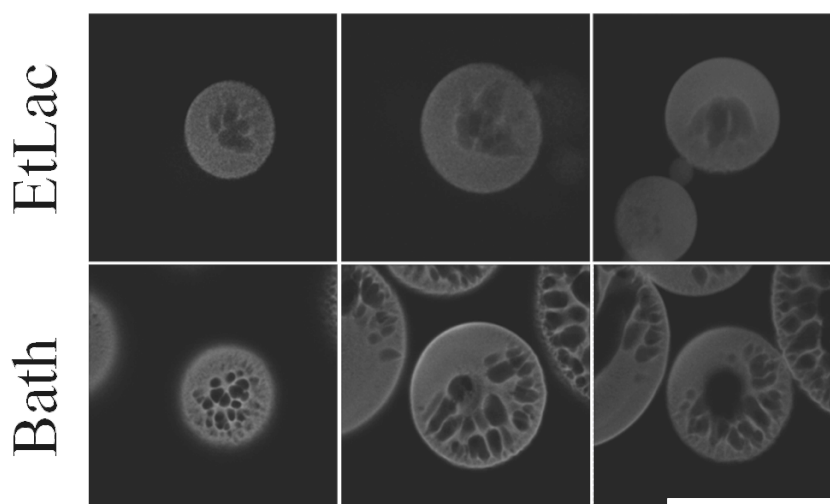


**Figure 3.8. CLSM images of cross-sections of 35DN10 MCs prepared dissolving rhodamine into the polymer solution (*top*) and the coagulation bath (*bottom*). Each set of images depicts different cross-sections/MPs in order to underline the variability in the fluorescence distribution profile due to the exact position of a given cross-section. Pictures are taken at the same magnification (scale bar = 50 μm).**

Fluorescence was clearly detected not only when rhodamine was blended directly into the polymeric solution but also when it was dissolved in the coagulation bath. In both cases, the fluorophore appeared to be concentrated in the outer shell of the MCs and in the inner ramified polymeric structures. Moving towards equatorials cross sections, it was possible to appreciate a reduction of the fluorescent areas, paired to the increment of porosity.

## 3.4 Discussion

In this study, a novel method to prepare microparticles made of PLA, using non-toxic solvents has been set and characterized.Before the preparation of the MCs is carried out, it is important to study the effect of the dissolution in EtLac on the structure of PLA. For this purpose, the thermal properties of PLA processed from EtLac solutions were evaluated and compared to those of the same polymer treated from dissolution in chloroform, a chlorinated solvent commonly used in PLA processing. As expected, the polymer processing with this green solvent does not modify the bulk thermal properties of the material.

Viscosimetric characterization shows the transition from a lower to a higher viscosity region, around the PLA concentration of 3.0% w/v. The first region may correspond to the condition in which the polymer is present as isolated coils in a diluted solution, whereas the second can be related to stronger polymer-polymer interactions and the transition to a semi-concentrated solution; the latter being a condition required for nearly all technical applications of polymer solutions [17]. This is especially important for the herein proposed strategy for MCs preparation, which consisted in two steps. The first step is the generation of liquid droplets of a polymer dissolved in a water-ethanol miscible solvent, and the second one is the solidification of these droplets in the coagulation bath via solvent displacement. This phenomenon is driven by mixing of the solvent and non-solvent phase, due to turbulent liquid flows generated by differences in surface tension. On one hand, if the drops are made of a diluted solution, with little polymer chain-to-chain interactions, this harsh mixing will simply break the drop into a multitude of submicron particles. Such a procedure is exploited to generate polymeric nanoparticles, and is a variant of the nanoprecipitation method, proposed by Fessi et al. [19], also described in Chapter 4 of this Thesis. On the other hand, viscous PLA solutions that show enough cohesion between the polymeric chains, can allow the preservation of the spherical droplet shape, upon immersion in a non-solvent with specific physical characteristics (i.e. surface tension).

The PLA-EtLac solution was extruded through a 30G needle (internal diameter 150 µm) in a coaxial flow of gaseous nitrogen. In the air gap outside the dispensing needle, the perturbation given by the gas flow stretches the forming solution meniscus. At the relatively high flow rate set in this study, solution jetting mode dispensing occurs, followed by break-up into liquid droplets induced by the same nitrogen flow. These drops are eventually collected into a coagulation bath under stirring, and solidified into MCs.

EtLac is a very low volatile compound, and particles precipitation occurs due to NIPS inside the bath rather than solvent evaporation in the air gap. For this reason, the composition of the coagulation bath was investigated, in order to identify a suitable formulation for particles formation and hardening. The proposed MCs formation technique involves a ternary system (polymer, solvent and non-solvent), and its outcome is strictly dependent on their compatibility/incompatibility, therefore, the non-solvent choice is a key design issue. Regarding PLA, several solvent/non-solvent systems have been studied, including chloroform/methanol, dioxane/methanol, dioxane/water and N-methylpyrrolidone/water, among others [20,21]. The EtLac miscibility profile oriented the choice towards a non-solvent (*i.e.* coagulation bath) based on water, ethanol and their binary mixtures. Even though solvent displacement and particle solidification are relatively fast processes that do not strictly require surfactant presence to stabilize the hardening drop, a

small amount of PVA was added to the precipitation mixture in order to avoid particles aggregation and reduce the surface tension of the bath. Only baths formulations whose surface tension was lower than that of EtLac were able to generate spherical particles. This effect might be due to an interplay between the ease of overcoming a bath surface layer possessing lower tension and the stabilizing effect on the droplet shape given by surface tension gradient driven motions [22].

Analogously to flow focusing [14], the proposed method is only driven by aero- and hydrodynamic forces, thus it is possible to tailor droplets (and MCs) size by simply adjusting the fluid flow velocity. Setting a given polymer concentration and outer fluid feeding pressure and tuning the dispensing rate of the polymer solution, allowed to control the particle dimension; a relation known and described in several gas-liquid or liquid-liquid co-flowing experiments [23].

The polydispersity of the particles is not dependent on their size. For all the cases, dispersion index (DI, standard deviation over average percent ratio) and the geometric standard deviation (GSD) are in the range of 19 to 29%, and 1.22 to 1.41, respectively. These values are determined by the fact that under the flowing conditions used (nitrogen feeding pressure of 0.5 bar and solution dispensing rate between 10 and 50 mL h$^{-1}$), jet break-up is not axysimmetric due to the geometry and design of the system. GSD values give an estimation of extent of polydispersity. Ideally, GSD should be close to 1, and up to 1.3 generally indicate monodisperse populations [24]. Apart from batch 40DN50, which clearly exceeds the threshold of polydispersity, almost all the MCs formulation are characterized by GSD values ranging between 1.22 and 1.33, suggesting a moderate diameter distribution dispersion.

It should be noticed that methods like emulsion/solvent evaporation and spray drying in their standard procedure, intrinsically produce highly polydisperse MCs (23 % < DI < 48%), prior to post-processing sieving steps [25,26], The fabrication of MCs with very low size polydispersity has been reported using microfluidic devices (DI < 5%) [34], or flow focusing droplet generation methods (DI < 15%) [25].

These droplet generation methods could be used in combination with our proposed strategy using EtLac, thus allowing further improvement of the MCs dispersity.

Another parameter affecting MCs size is the initial PLA concentration. A similar trend for the particles size with the dispensing rate variation was observed for both solution concentrations tested, with an increment in particles size by slightly increasing the polymer concentration from 3.5 to 4.0 %. Besides this limited difference in polymer content, the 4.0% formulation corresponds to a sensibly higher value for solution viscosity, which appears to affect particle formation step.

In general, opposite theoretical results are reported in literature for coflowing fluid atomization processes characterized by axysimmetric jet break up. In these cases, solution viscosity had no effect on drop size [27]; especially regarding Flow Focusing (FF) devices, in which the droplet dimension has been related to flow parameters independently from viscosity through the equation:

$$ \overline{\quad\quad} \quad \overline{\quad} \quad \overline{\ } \tag{1} $$

Where $d$ is drop diameter,     solution density,     gas pressure difference at the orifice and $Q_l$ fluid flow velocity [28, 29]. Nevertheless, FF experiments for the preparation of polystyrene microspheres, reported by Martín-Banderas et al. [14]  showed that increasing polymer concentration from 4 to 8% w/v caused an increment in the droplets size (10 to 20 µm approximately), despite of the theoretical background.

Here, for the non-axysmmetric droplet generation procedure described, the variation of the solution concentration and thus the viscosity, allowed to control MCs dimension.

While the particles size is mainly affected by the droplet generation conditions, the MCs morphology and inner microstructure might be governed by solvent removal rate into the coagulation bath and the mechanism of diffusion and interaction between the polymer, solvent and non-solvent. As previously discussed, EtLac is miscible in all proportions in both ethanol and water, while PLA is markedly incompatible with these non-solvents. The MCs configuration displaying a dense, thin toplayer enclosing an open porous structure with macrovoids is caused by the kinetic of liquid-liquid demixing and phase separation.

This peculiar morphology can be explained by the mechanism responsible of the microstructure found in NIPS membranes, and proposed by Smolders and co-workers [30]. The groundwork of this theory is the kinetics of growth of polymer-lean phases and the exchange rate of solvent/non-solvent [31]. In our case, once the polymeric drop enters the coagulation bath, a thin polymeric shell at the drop-non-solvent interface rapidly precipitates (Figure 3.9). Under this PLA solid layer, solution composition changes as ethyl lactate is being extracted to the external bath while the coagulation mixture diffuses within the droplet. This condition provokes instantaneous liquid-liquid demixing inside the drop, forming in the solution a polymer-rich phase and nuclei of polymer-lean (solvent rich) phase. In the inner shells of the drop, farther from the bath-drop interface, precipitation is locally delayed, giving the possibility to the polymer-poor nuclei to grow and even coalesce, towards the center of the droplet.

Eventually, the increased uptake of non-solvent and loss of solvent will cause precipitation, with the PLA rich regions giving rise to an inner polymer solid structure, while polymer-lean areas will leave space to pores and macrovoids, as shown in Figure 3.7. The fact that the extent of porosity and surface roughness appears to be higher in larger MCs suggests an additional delay of precipitation due to longer non-solvent diffusion distances along the sphere radius.
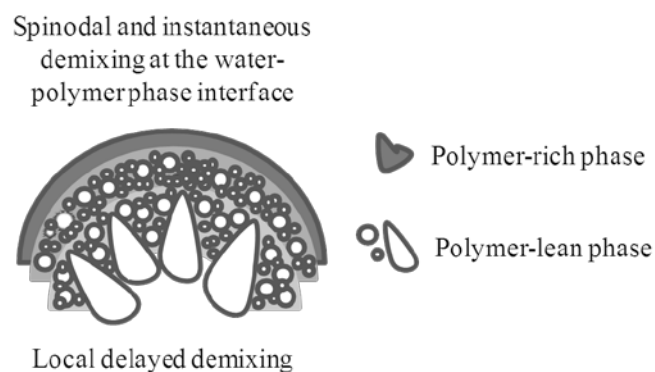


**Figure 3.9: Scheme of the phase separation process, representing the degree of solution demixing and polymer phase separation occurring before the precipitation and solidification of the PLA.**

A similar behavior with formation of macroporous inner structures was observed in PLA 2D membranes obtained from EtLac solutions by NIPS after immersion in the same coagulation bath used for the MCs fabrication (observed by SEM micrographs of cross-sections, data not shown), in accordance with the proposed mechanism.

The hemisphere with rough outer surface finally forms during the hardening of the particle, in correspondence to the high porous layers underneath. The origin of the more homogeneous porosity on the opposite hemisphere, instead, is unclear, but may be related to partial solvent evaporation and precipitation in the air gap between the dispensing tip and the bath.

The Janus morphology is an interesting morphological feature of the formed MCs displaying a smoother hemisphere opposed to another presenting labyrinthine wrinkling patterns.

Janus particles, so named after the Roman God depicted with two heads facing opposites directions, likewise possess two sides with distinct compositions or surface structures. Such particles have attracted increasing interest because of their unique properties and potential applications in a number of fields including optical biosensors and functional surfactants [32]. Not only, several studies have been reported focusing on the generation and characterization of wrinkled surfaces [33,34], and wrinkle microparticles [35]. For instance, Janus wrinkled topographies were obtained on elastomeric MCs by selective UV irradiation of a single hemisphere of already prepared MCs [32].

In our case, we report the spontaneous generation of Janus wrinkles in a one step procedure, directly during MCs solidification and drying. Wrinkle wavelength shows a tendency to increase in larger particles, and this finding is in agreement with previous studies on microparticles with wrinkled surfaces [32, 37]. During the lyophilization of the microparticles, as the water trapped into the pores is removed, the part of the polymer shell on the top of the macroporous inner layer undergoes partial collapse and wrinkles, while the surface at the opposite hemisphere, having an inner, more stable layer, remains smoother. To explain such behavior we propose the following scenario. When the polymer drop is solidifying into the coagulation bath, the precipitating polymer structure it is found in a swollen, stretched state due to the solvent presence. Gradually, EtLac is replaced by the water/EtOH mixture, which, during the washing steps, is replaced by water only. The surface dense thin PLA skin is stiffer than the underlying core on which it lays, because of the high porosity of the inner layer, rich in macrovoids. Eventually, during water removal by lyophilization the prestrain in which the polymer is found may be relieved through the buckling of the stiffer surface shell. Instead, when water is removed faster with simple air drying, the MCs present a more marked, irregular wrinkle formation (data not shown), with even partial collapsing of the spherical structure, thus suggesting that the water extraction condition provokes the buckling and plays a role on the stress applied to the MCs layers. This solidification-induced deformation scenario is similar to the buckling of a stiff thin elastic film on a compliant soft substrate which has been recently reported to happen also during phase inversion preparation of polymeric membranes [38]. At the smoother hemisphere, instead, the presence of a thicker, less porous, and more stable layer under the polymeric shell, as depicted in Figure 3.7, can prevent buckling and surface wrinkles formation.

Finally, the peculiar solidification process and the exchange between solvent and non-solvent described above suggest that the proposed manufacturing route could be adequate to load compounds present both in the polymer solution and in the coagulation bath into the forming MCs.

Due to the localization of rhodamine inside precipitated PLA, CLSM allowed for a 3D scan of the inner morphology from the poles towards the equatorial plane of the MCs, thus supporting the solidification mechanism explained above. Moreover, this finding suggests that the precipitation of the polymer is fast enough to trap the fluorophore, and penetration of non-solvent into the drop allows for uptaking of solutes. On the other hand, the first procedure may be efficient mainly regarding hydrophobic drugs, since hydrophilic molecules may suffer a great leakage towards the hydroalcoholic bath.

## 3.5 Conclusion

In the present work, a novel manufacturing method to produce PLA MCs using non toxic chemicals was developed. MCs were generated from EtLac solution droplets obtained by break-up of the polymeric solution due to coflowing gaseous nitrogen. In such a configuration, tuning solution dispensing rate and polymer concentration were found to be effective in modifying and controlling the size of the produced particles. The proposed method is versatile enough to be adapted to other droplet generation dispensing methods in order to achieve different ranges of particles size and monodispersity. The obtained MCs display a macroporous inner structure and a compact surface, due to non-solvent penetration into the drop, liquid-liquid demixing, nucleation and growth of the polymer lean phase. By this method, MCs with Janus surface with a smoother and wrinkle-patterned hemisphere were obtained. As a consequence of the polymer precipitation mechanism, the MCs produced from EtLac solution and NIPS can be suitable for encapsulation of bioactive compounds that, according to their solubility, degree of hydrophobicity and solvent compatibility profiles, may be loaded from different components of the precipitation strategy. With the proposed method, we were able to obtain PLA MCs with potential applications in cell and drug delivery. Finally, this method gives a proof-of-concept of the possibility to process PLA with ethyl lactate, which may be of more general interest to manufacture the polymer for other types of application, such as membranes for separation technology and films for packaging purposes.

## 3.6 References

[1]     Malafaya PB, Silva GA, Reis RL. Natural-origin polymers as carriers and scaffolds for biomolecules and cell delivery in tissue engineering applications. Adv Drug Deliv Rev. 259(4-5) (2007) 207-33.

[2]     Hernández RM, Orive G, Murua A, Pedraz JL. Microcapsules and microcarriers for in situ cell delivery. Adv. Drug Delivery Rev. 2010, 62, 711-30.

[3]     Mohamed F, van der Walle CF. Engineering biodegradable polyester particles with specific drug targeting and drug release properties. J Pharm Sci. 97 (2008) 71-87.

[4]     Wischke C, Schwendeman SP. Principles of encapsulating hydrophobic drugs in PLA/PLGA microparticles. Int J Pharm.364(2) (2008) 298-327.

[5]     Clary JJ, Feron VJ, van Velthuijsen JA. Safety assessment of lactate esters. Regul Toxicol Pharmacol. 27(2) (1998) 88-97.

[6]     Mottu F, Laurent A, Rufenacht DA, Doelker E. Organic solvents for pharmaceutical parenterals and embolic liquids: a review of toxicity data. PDA J Pharm Sci Technol. 54(6) (2000) 456-69.

[7]     Aparicio S, Alcalde R. The green solvent ethyl lactate: an experimental and theoretical characterization. Green Chem. 11 (2009) 65-78.

[8]     Ferreira R, Pedrosa N, Marrucho IM, Rebelo LPN. Biodegradable polymer-phase behavior: Liquid-liquid equilibrium of ethyl lactate and poly(lactic acid). J Chem Eng Data. 53 (2008) 588-90.

[9]     Liu W, Yang XL, Ho WS.  Preparation of uniform-sized multiple emulsions and micro/nano particulates for drug delivery by membrane emulsification. J Pharm Sci. 100(1) (2011) 75-93.

[10]    Chaw CS, Tan CW, Yang YY, Wang L, Moochhala S. Design of physostigmine-loaded polymeric microparticles for pretreatment against exposure to organophosphate agents. Biomaterials. 24(7) (2003) 1271-7.

[11]    Munarin F, Petrini P, Farè S, Tanzi MC. Structural properties of polysaccharide-based microcapsules for soft tissue regeneration. J Mater Sci Mater Med. 21(1) (2010) 365-75.

[12]    Berkland C, Kim K, Pack DW. Fabrication of PLG microspheres with precisely controlled and monodisperse size distributions. J Control Release. 73(1) (2001) 59-74.

[13]    Bhaskar S, Pollock KM, Yoshida M, Lahann J. Towards designer microparticles: simultaneous control of anisotropy, shape, and size. Small. 6(3) (2010) 404-11.

[14]    Martín-Banderas L, Rodríguez-Gil A, Cebolla A, Chavez S, Berdún-Álvarez T, Garcia JMF, Flores-Mosquera M, Gañán-Calvo AM. Towards high-throughput production of uniformly encoded microparticles. Adv Mater. 18 (2006) 559-64.

[15]    W. S. Rasband, ImageJ, U. S. National Institutes of Health, Bethesda, Maryland, USA, http://imagej.nih.gov/ij/, 1997-2011.

[16]    Clarke N, O'Connor K, Ramtoola Z. Influence of formulation variables on the morphology of biodegradable microparticles prepared by spray drying. Drug Dev Ind Pharm. 24(2) (1998) 169-74.

[17]    W. M. Kulicke, C. Clasen, in *Viscosimetry of Polymers and Polyelectrolytes*, Springer Laboratory, Germany, 2004, Ch.7.

[18]  a)  Bhattacharya A, Ray P. Studies on Surface Tension of Poly(Vinyl Alcohol): Effect of Concentration, Temperature, and Addition of Chaotropic Agents.  J App Polym Sci. 93 (2004) 122-30.

b) Dai NWJ, Micale FJ. Dynamic Surface Tension Measurement with a Dynamic Wilhelmy Plate Technique. J Colloid Interface Sci. 215 (1999) 258-69.

c) Niño MRR, Patino JMR. Surface Tension of Bovine Serum Albumin and Tween 20 at the Air–Aqueous Interface.  J Am Oil Chem Soc 75 (1998) 1241-8.

d) Vázquez G, Alvarez E, Navaza JM. Surface Tension of Alcohol + Water from 20 to 50°C. J Chem Eng Data. 40 (1995) 611-4.

e) Exact surface tension values are not exactly known due to the addition of PVA. The values for the hydroalcoholic mixture only are reported in reference 28d, and they are however lower than the corresponding value found for ethyl lactate.

[19]  Fessi H, Puisieux F, Devissaguet JP, Ammoury N, Benita S. Nanocapsule formation by interfacial polymer deposition following solvent displacement. J Pharm. 55 (1989) R1-R4.

[20]   van de Witte P, Dijkstra PJ, van der Berg JWA, Feijen J. Phase behavior of polylactides in solvent–nonsolvent mixtures. J Polym Sci B Polym Phys. 34 (1996) 2553-68.

[21]  van de Witte P, Esselbrugge H, Dijkstra PJ, van der Berg JWA, Feijen J. A morphological study of membranes obtained from the systems polylactide-dioxane-methanol, polylactide-dioxane-water, and polylactide-n-methyl pyrrolidone-water. J Polym Sci B Polym Phys. 34 (1996) 2569-78.

[22]  Blanchette F, Messio L, Bush JWM. The influence of surface tension gradients on drop coalescence. Phys Fluid, 21 (2009) 072107.

[23]  Eggers J, Villermaux E. Physics of liquid jets. Rep Prog Phys. 71 (2008) 036601.

[24]  Luque A, Perdigones F, Estevé J, Montserrat J, Gañán-Calvo A, Quero JM. Reduction of droplet-size dispersion in parallel flow-focusing microdevices using a passive method . J. Micromech Microeng. 19 (2009) 045029.

[25]  Holgado MA, Arias JL, Cózar MJ, Alvarez-Fuentes J, Gañán-Calvo AM, Fernández-Arévalo M. Synthesis of lidocaine-loaded PLGA microparticles by flow focusing. Effects on drug loading and release properties. Int J Pharm. 358(1-2) (2008) 27-35.

[26]  Schwach G, Oudry N, Delhomme S, Lück M, Lindner H, Gurny R. Biodegradable microparticles for sustained release of a new GnRH antagonist--part I: Screening commercial PLGA and formulation technologies. Eur J Pharm Biopharm. 56(3) (2003) 327-36.

[27]  Choi SW, Cheong IW, Kim JH, Xia Y. Preparation of uniform microspheres using a simple fluidic device and their crystallization into close-packed lattices. Small. 5(4) (2009) 454-9.

[28]  Cramer C, Fischer P, Windhab EJ. Drop formation in a co-flowing ambient fluid. Chem Eng Sci. 59 (2004) 3045-58.

[29]  Gañán-Calvo AM. Generation of steady liquid microthreads and micron-sized monodisperse sprays in gas streams. Phys Rev Lett. 80 (1998) 285.

[30] Smolders CA, Reuvers AJ, Boom RM, Wienk IM. Microstructures in phase-inversion membranes. Part 1. Formation of macrovoids. J Memb Sci. 73 (1992) 259-75.

[31] Zhang Q, Liu J,Wang X, Li M, Yang J. Controlling internal nanostructures of porous microspheres prepared via electrospraying. Colloid Polym. Sci. 288 (2010) 1385-91.

[32] Trindade AC, Canejo JP, Pinto LFV, Patrício P, Brogueira P, Teixeira PIC, Godinho MH. Wrinkling Labyrinth Patterns on Elastomeric Janus Particles. *Macromolecules, 44* (2011) 2220-8.

[33] Chung JY, Nolte AJ, Stafford CM. Surface wrinkling: a versatile platform for measuring thin-film properties. Adv Mater. 23(3) (2011) 349-68.

[34] Genzer J, Groenewold J. Soft matter with hard skin: From skin wrinkles to templating and material characterization. Soft Matter, 2 (2006) 310-23.

[35] Zhao T, Qiu D. One-pot synthesis of highly folded microparticles by suspension polymerization. Langmuir. 27(21) (2011) 12771-4.

[36] Cao G, Chen X. Self-Assembled Triangular and Labyrinth Buckling Patterns of Thin Films on Spherical Substrates. Phys Rev Lett. 100 (2008) 036102.

[37] Yin J, Coutris N, Huang Y. Groove Formation Modeling in Fabricating Hollow Fiber Membrane for Nerve Regeneration. J Appl Mech. 78 (2011) 011017.

# Chapter 4

# Preparation of PLGA nanoparticles functionalized with DNase I to target biofilm extracellular matrix  for advanced antibiotic delivery

*In this chapter, nanoparticles made with biodegradable poly(lactic-co-glycolic acid) were produced, using a technique derived from the green solvent-based processing approach explored in the previous chapter. The nanoparticles were studied as drug delivery devices for the treatment of bacterial biofilm infections. For this reason, the antibiotic drug ciprofloxacin was encapsulated, and the nanoparticles tested against P. aeruginosa. In order to endow the NPs with advanced functionality to enhance their antibiofilm potential, a surface coating with DNase I was applied and evaluated.*

*This work was developed in collaboration with the "Bacterial infections: antimicrobial therapies" group (Institute for Bioengineering of Catalonia, Spain) lead by Dr. Eduard Torrents.*

## 4.1 Introduction

Micro- and nanocarriers, such as polymeric particles [1], liposomes [2], and hydrogels [3], including polymeric biodegradable nanoparticles (NPs) made of PLGA, have been studied to treat bacterial infections due to their potential to encapsulate and deliver therapeutic compounds in a sustained fashion. A wide array of methods to fabricate such NPs is available, and most of them are easy to scale-up [4], and allow the encapsulation of several compounds having different chemical and physical properties. PLGA has tunable degradation profile which allows controlling the release kinetics of loaded drugs [5]. Additionally, PLGA has already been FDA approved for several biomedical devices. All these features are especially important, in order to make easier the translation of drug-loaded PLGA NPs to the clinical practice, as both regulatory and technical limitations at scaling-up are major bottlenecks in the traslation from the bench to the bedside [6]. Persistent bacterial infections are becoming a major burden to the healthcarte system. The use of PLGA NPs which display a controlled releae of the antimicrobial drug may help to treat these infections.

*P. aeruginosa* is the major cause of nosocomial infections in humans and is frequently associated with chronic pulmonary infections. It is also one of the main actors in chronic obstructive pulmonary disease (COPD) and cystic fibrosis (CF), where it is the principal cause of morbidity and mortality for patients [9]. The establishment of chronic *Pseudomonas* infections correlates with the formation of a biofilm, a structure with clusters of cells encapsulated in an extracellular polymeric matrix. In such an environment, bacteria are more likely to resist to antibiotic treatments, as most drugs do not freely diffuse into the biofilm and thus do not reach optimal therapeutic concentrations [10]. Additionally, bacteria in biofilms display a different physiology compared to planktonic cells –such as a diminished metabolic rate, as well as improved cell to cell communication-, which makes antibiotics less effective and increases the chance of development of resistances [11]. Moreover, the emergence and increasing prevalence of bacterial strains that are resistant to available antibiotics demand the discovery of new therapeutic approaches [12].

PLGA NPs can be properly designed in terms of size to penetrate airway mucus, avoid steric inhibition by the dense mucin fiber meshes, and can hide chemical properties of the encapsulated drug (e.g., charge, degree of lipophilicity) in order to reduce its unspecific interactions with the biofilm surrounding the target bacteria [13]. Therefore, NPs can provide a temporal control on release kinetics and enhanced efficacy of loaded compounds [14]. Although these properties make antibiotic-loaded PLGA NPs suitable devices to treat bacterial infections, advanced delivery strategies are necessary to achieve biofilm infections eradication. Besides the bacterial cells, the biofilm matrix itself can be an additional target for anti-biofilm treatments. In fact, unlike the bacterial cells, the extracellular substance is highly exposed to the environment and often has a porous structure [15-17]. Biofilm matrix is mainly composed by proteins, polysaccharides chains, and extracellular DNA (eDNA). Recent studies have pointed out how the latter is a key factor in biofilm formation, structural stabilization, and pathogenicity, acting as a matrix crosslinker and chelator of cataionic antimicrobial agents and participates in the events that can trigger the insurgence of antibiotic resistance [17]. These findings lead to the development of treatments of cystic fibrosis patients with lytic enzymes like deoxyribonuclease (DNase), in the form of aresols, which have been proven successful at reducing mucus

secretion viscoelasticity and thus their clearance [18]. Fabrication of smart drug delivery devices, capable not only to control antibiotic release, but also to interact with and harm directly the biofilm extracellular matrix, and particularly its DNA component, can constitute a fundamental advance in treating persistent infections such as those associated with cystic fibrosis. Co-treatment with antimicrobial agents and DNase, may in fact enhance biofilm removal and, at the same time, improve the diffusional rates of antibiotic into biofilm, thus increasing the elimination of colonized bacterial cells.

The aim of this study is to assess the potential of functionalized and drug loaded PLGA NPs in the treatment of *P. aeruginosa* infections. PLGA-NPs were obtained and loaded with the fluorquinone antibiotic ciprofloxacin (CPX) through a fabrication method involving non-toxic chemicals. Different surface coatings were applied to the NP, to modify the material and to tune the interaction with biofilm matrices. In this way, negatively charged NPs and poly-L-lisine coated NPs were produced, in order to study the effect on the antimicrobial activity of released ciprofloxacin of their passive (via surface charge) interactions with planktonic bacteria and biofilm. Novel NPs functionalized with DNase I were investigated in order to combine controlled drug release with an active ability of inducing direct degradation of the biofilm matrix.

## 4.2 Material and methods

### 4.2.1 Preparation of nanoparticles

Poly(lactic-co-glycolic) acid (Purasorb PDLG 5010, Purac, the Netherlands) nanoparticles were prepared using a novel, non-toxic chemicals-based methodology, derived from the nanoprecipitation technique [19]. PLGA was dissolved in (–)-Ethyl-L-lactate (photoresist grade; purity = 99.0%; Sigma-Aldrich, Spain), to form a 1.5 % w/v solution. The solution was loaded into a syringe, mounted on a syringe pump and dispensed dropwise (50 mL h$^{-1}$) into a water bath, provided with 0.3 % w/v of poly(vinyl alcohol) (80% hydrolyzed, $M_w$ = 9000 – 10000 Da, Sigma-Aldrich, Spain), under moderate stirring. The nanoparticles were left to stir for 1h at room temperature, and then recollected by three cycles of ultracentrifugation (11500 rpm, 15 minutes, 4°C) and resuspension in MilliQ water. Eventually, the nanoparticles suspension was flash frozen in liquid nitrogen, freeze-dried and stored at -20°C until used. Several compounds were added to the polymer phase and the water phase in order to obtain NPs with different properties, as described in Table 4.1.

**Table 4.1: Composition, encapsulation efficiency and overall properties of drug loaded nanoparticles.**

| | Coating | DNase activity [µg DNA/mg NPs/1h] | CPX content [w/w %] | Size [nm] | Size PDI | Z-potential [mV] |
|---|---|---|---|---|---|---|
| **PLGA-CPX** | - | - | 0.26 | 213.6 | 0.085 | -12.9 ±11.20 |
| **PLGA-PL-CPX** | PL | - | 0.24 | 272.5 | 0.101 | +33.5 ± 5.99 |
| **PLGA-PL-CPX-DNase** | PL DNase I | 26.2 | 0.17 | 251.9 | 0.122 | +28.9 ± 1.43 |

To load ciprofloxacin (CPX, ciprofloxacin base, Sigma-Aldrich, Spain) into the nanoparticles, 700 µg mL$^{-1}$ were added to the polymer phase and the water bath was saturated with 50 µg mL$^{-1}$ of antibiotic. Poly(L-lysine) coated nanoparticles were obtained by addition to the water phase of 70 µg mL$^{-1}$ poly(L-lysine) (PL, $M_w$ = 70000 – 150000 Da, Sigma-Aldrich, Spain). Finally, PL-coated nanoparticles, were modified by covalently grafting deoxyribonuclease I from bovine pancreas (DNAse I) (Sigma-Aldrich, Spain) to the ε-aminogroups of the PL adsorbed onto the nanoparticles surface. Immediately after the nanoparticles formation, ethyl(dimethylaminopropyl) carbodiimide (Acros Organics, Belgium) and N-hydroxysuccinimide (Sigma-Aldrich, Spain) (EDC/NHS) were added to the water bath to obtain a 0.1/0.2 M solution. Subsequently, 100 µg mL$^{-1}$ DNAse I were added to the nanoparticles suspension and were stirred for 30 minutes. Cycles of ultracentrifugation and washing steps were performed in order to remove the unreacted chemicals and water-soluble by products. NPs yield was quantified by measuring the weight of the dry particles mass after lyophilization and normalized against the mass of PLGA dissolved into ethyl lactate at the beginning of the fabrication process.

### 4.2.2 Nanoparticles characterization

Lyophilized NPs were reconstituted in MilliQ water by sonication and their size and surface charge were measured using a ZetaSizer NanoZS (Malvern Instruments, UK). Nanoparticles suspension were loaded in a standard quartz cuvette to be analyzed by Dynamic Light Scattering (DLS) for size determination or in a flow cell cuvette for Laser Doppler Velocimetry (LDV) assays, used to measure the zeta potential of the particles (n=5). A morphological characterization of the nanoparticles was carried out using Field Emission-Scanning Electron Microscopy (FE-SEM, Hitachi S-4100, Japan). To prepare the sample for the analysis, a drop of a concentrated nanoparticles suspension was deposited on clean glass coverslip, mounted on a metal stub and water was left evaporate. The dried particles were then coated with carbon.

### 4.2.3 Drug encapsulation and in vitro release

To quantify the amount of antibiotic encapsulated, 5 mg of dried ciprofloxacin-loaded nanoparticles were fully degraded into 0.5 M NaOH, in order to hydrolyze the PLGA. The resulting solution was analyzed with UV-vis spectroscopy to detect ciprofloxacin absorbance peak at 280 nm.

*In vitro* release kinetics of ciprofloxacin was assessed using a High Performance Liquid Chromatography (HPLC, Waters e2695, USA). A known amount of nanoparticles was suspended in PBS and loaded into a Slide-A-Lyzer Dyalisis Cassette, MWCO 2000 Da (Thermo Scientific, Spain). The cassette was immersed in 30 mL PBS and left at 37°C. 500 µL aliquots of PBS were taken at any given time point, and stored at 4°C until HPLC analysis. After every time point, 500 µL of fresh PBS was added to maintain the sinking volume. Samples (n=3) were run through a C18 stationary phase (Sunfire C18 5µm column, Ireland), and the mobile phase consisted of a mixture of 900 mL 0.5% v/v acetic acid in milliQ water, 50 mL of acetonitrile and 50 mL of methanol. The elution peak was detected with a photodiode array system (Waters 2998, USA), monitoring ciprofloxacin absorbance peak at 280 nm. Antibiotic quantification was then carried out using a

proper standard curve and calculating the area below the elution peak, using the Origin 8.0 software (OriginLab Corporation, USA).

### 4.2.4 Quantification of DNase I activity containing NP

50 µg of DNase I-containing NPs were added to a 400 ng DNA plasmid pGEM-T (Promega, Spain) in water. A control consisting of DNA alone (400 ng in water) and NPs with no DNase (50 µg in water) were also tested. After incubation 30 minutes at 37 °C the mixtures were loaded onto a 0.8 % TAE agarose gel, stained in ethidium bromide and visualized under UV light (Gel DocTM XR+, Bio-Rad Laboratories, Spain). DNase I activity was calculated by quantification of DNA degradation using Quantity One software package (Bio-Rad Laboratories).

### 4.2.5 Bacterial Strain and growth conditions

Wild-type Pseudomonas aeruginosa PAO1 strain CECT 4122 (ATCC 15692) was obtained from the Spanish Type Culture Collection (CECT). The strain were stored at−80°C as glycerol stocks. To obtain inocula for examination, the strain was cultured overnight on LB (Pronadisa, Spain) medium for P. aeruginosa at 37°C. Cells were then harvested by centrifugation ($8,000 \times g$ for 10 min). Bacterial growth was measured by reading absorbance measurements ($OD_{550}$).

### 4.2.6 Minimal inhibitory concentration (MIC) assays

MICs were determined by a microtiter broth dilution method as described by Cole et al. [20] and modified by Beckloff et al. [21]. In brief, 100 µL of bacteria at a density of $5 \times 10^5$ CFU mL$^{-1}$ in Mueller-Hinton broth (BD Biosciences) were inoculated into the wells of 96-well assay plates (tissue culture-treated polystyrene; Costar 3595, Corning Inc., Corning, NY). Different concentrations of nanoparticles were added to each well, in order to achieve an equivalent amount of encapsulated CPX of 0.0078, 0.0156, 0.03125, 0.0625, 0.125, 0.25, 0.5, or 1 µg mL$^{-1}$. The microplates were incubated at 37°C at 150 rpm for 12 h in an Infinite 200 Pro microplate reader (Tecan) and every 15 minutes an absorbance measurement at $OD_{550}$ was performed.

### 4.2.7 NPs activity against P. aeruginosa biofilm

The minimum biofilm eradication concentration (MBEC) physiology and genetic assay (MBEC BioProducts Inc., Edmonton, Alberta, Canada) was previously described by Ceri et al. [22]. In brief, *P. aeruginosa* suspension (200 µL, $5 \times 10^5$ CFU mL$^{-1}$) was inoculated into the wells of an MBEC device, together with increasing concentrations of NPs or free soluble CPX. The peg lids were then inserted into the microplates containing the inocula (Figure 4.1). Microplates were incubated at 37ºC for 24 h. The peg lids with biofilm were rinsed twice with PBS (by placing the lid in a microplate containing 200 µL of PBS in each well) to remove loosely adherent planktonic cells, and cells forming biofilms were recovered by centrifugation. Serial dilutions of recovered cells were plated in LB or TSB agar plates and colony-forming units were counted.

To evaluate the effect of NPs functionalized with DNase I against already established biofilms, the same procedure explained above was followed, apart that the bacteria inoculum was cultivated in absence of NPs. After this step, the peg lids with biofilm were then transferred to 96-well assay plates (tissue culture-treated polystyrene; Costar 3595) containing 200 μl of Mueller-Hinton broth (BD Biosciences) supplemented with different concentrations of positively charged NPs, or free soluble CPX and DNase I as a control (to make up for an equivalent concentration of CPX of 0.0078, 0.0156, 0.03125, 0.0625, 0.125, 0.25, 0.5, or 1 μg mL$^{-1}$). These plates were incubated at 37°C for another 12 h. Subsequently, the peg lids were rinsed twice with 0.9% saline, and cells forming biofilms were recovered by centrifugation. Serial dilutions of recovered cells were plated in LB or TSB agar plates and colony-forming units were counted.

To assess the capability of NPs to eradicate established biofilms after repeated administration of the treatment, the biofilm assay was also repeated. Biofilms were let mature for two days. After that, the culture period was extended up to 3 days, and every 24 hours the culture medium was removed and refreshed with medium supplemented with a dose of NP-CPX formulation. Every day, samples were analyzed as explained above, to quantify the number of biofilm forming cells.
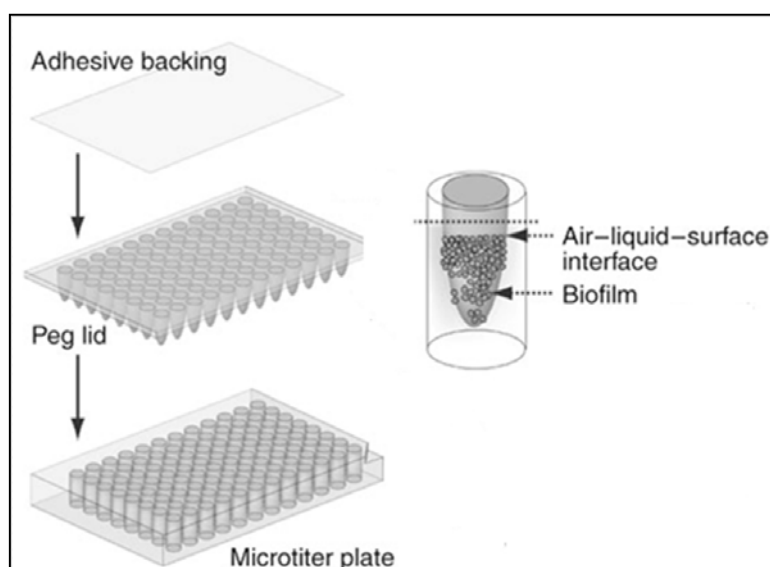


**Figure 4.1: Scheme of the experimental set up for biofilm formation on the peg lid.**

*4.2.8 NPs cytotoxicity*

Macrophage cells (murine cell line J774, ATCC) were seeded into 96-well tissue culture plates (6x10$^4$ per well) in culture medium without antibiotics, supplemented with different concentration of nanoparticles, or left untreated. Cell viability was assessed by using a 3-(4,5-dimethylthiazol-2-yl)-2,5-diphenyltetrazolium bromide (MTT) colorimetric assay (Sigma-Aldrich, Spain). After, 24 and 48 hours of exposure to the different compounds, culture supernatants were removed and 10% of MTT in complete medium was added to each well and incubated for 3 hours at 37ºC. Then, water-insoluble formazan salt was dissolved by adding acidic isopropanol. Absorbance was measured at 550 nm (Infinite M200 Microplate Reader, Tecan).

## 4.2.9 Statistical Analysis

Values are expressed as mean ± Standard Error of the Mean (SEM) or median of three to five replicates (n=3 to 5). Statistical analyses were performed using GraphPad Prism 4.00 (GraphPad Software, San Diego, CA, USA) software package. Single comparisons were performed by unpaired Mann-Whitney test. Correlation analyses were performed using non-parametric correlation Spearman test. A value of $p<0.05$ was considered as statistically significant.

## 4.3 Results

### 4.3.1 Preparation of nanoparticles and drug encapsulation

NPs with spherical shape (as shown in Figure 4.2) were fabricated using a modification of the nanoprecipitation method, and their physical characteristics are listed in Table 4.1. The NPs final yield was $96.3 \pm 1.7\%$ of the total polymer mass at the beginning of the fabrication protocol. The average diameter ranged between 200 and 300 nm, with a narrow, monodisperse, size distribution (PDI values between 0.085 and 0.122). The Z-potential of the NPs varied accordingly to the type of surface coating applied. When PVA was the only additive in the coagulation bath, negatively charged NPs were obtained (approx. -13 mV), whereas addition of PL generated positively charged particles (+30 mV). Functionalization with DNase, had no significant effect on the overall surface charge. For all NPs formulation, CPX encapsulation efficiency was low, and the average drug content in the carriers varied between 1.7 (for PLGA-PL-DNase-CPX) and 2.6 µg mg$^{-1}$ of NPs (for PLGA-CPX). DNase I grafted on PL coated NPs retained its DNase activity, as quantified by gel electrophoresis, with 1 mg of functionalized NPs being able to degrade 26.2 µg of DNA in 1 hour (Figure 4.3).

### 4.3.2 In vitro release of ciprofloxacin

Negatively and positively charged (both PL and PL-DNase coating) NPs presented a burst release in the first hour, upon suspension in PBS, when between 40 and 50% of the total CPX load is released (Figure 4.2). After this period, the drug release is slower, and negatively charged NPs end up depleting their drug amount within 12 hours. Positively charged NPs showed a steady release of the remaining antibiotic, and after 12 hours PL and PL-DNase coated NPs delivered respectively about 60 and 80% of the loaded ciprofloxacin.
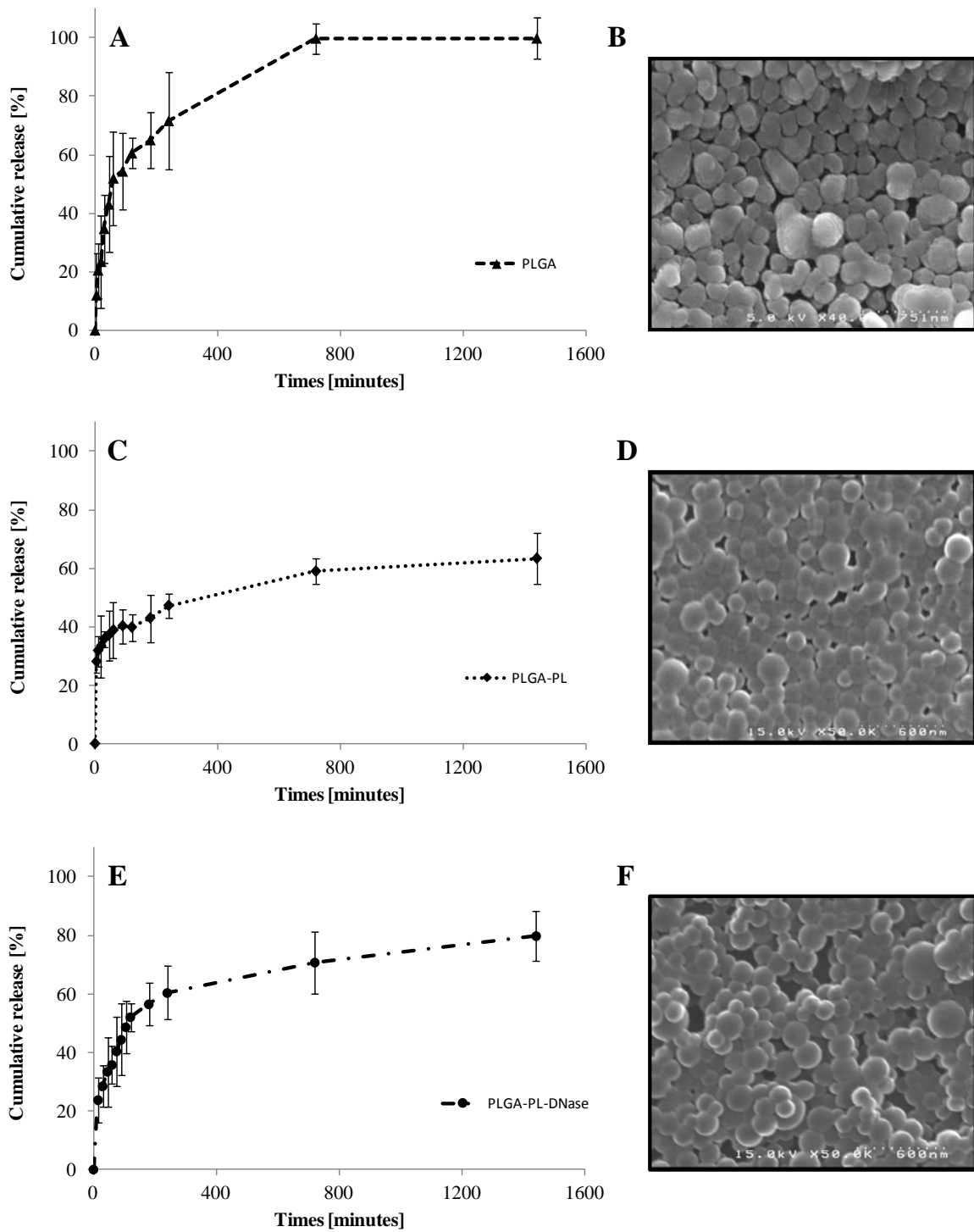
**Figure 4.2: CPX release profile and SEM micrographs of (A, B) uncoated, (C, D) PL-coated and (E, F) PL-DNase I functionalized NPs.**
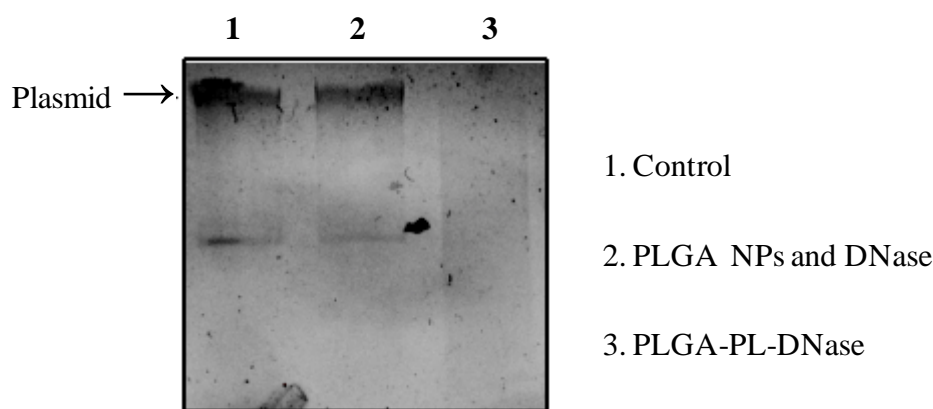
Figure 4.3: Degradation of a DNA plasmid by DNAse and PLGA-PL-DNase NPs.

*4.3.3 Minimum inhibitory concentrations (MICs)*

The MICs of different ciprofloxacin formulations (alone and encapsulated) are given in Table 4.2. Negatively charged PLGA-CPX worked better against *P. aeruginosa*, when compared to free-soluble CPX. The MIC was 0.39 µg mL$^{-1}$ for soluble CPX, 0.0625 µg mL$^{-1}$ for PLGA-CPX, 0.5 µg mL$^{-1}$ for PLGA-PL-CPX and 0.5 µg mL$^{-1}$ for PLGA-PL-CPX-DNase (equivalent total dose of CPX). Considering the drug release kinetics, at the end of the MIC assay (12 h), only a portion of encapsulated drug has been effectively released in the bacteria culture media. The effective MICs for the NPs, as corrected considering the release profiles are 0.0625 µg mL$^{-1}$ for PLGA-CPX, 0.29 µg mL$^{-1}$ for PLGA-PL-CPX, and 0.35 µg mL$^{-1}$ PLGA-PL-CPX-DNase I. NPs with no drug encapsulated showed no antimicrobial effect.

Table 4.2: Minimal inhibitory concentrations of soluble and encapsulated ciprofloxacin.

| *P. aeruginosa* PAO1 ATCC 4122 | MIC (ciprofloxacin- µg mL$^{-1}$) | | | |
|---|---|---|---|---|
| | CPX | PLGA-CPX | PLGA-PL-CPX | PLGA-PL-CPX-DNase I |
| **CPX total equivalent dose** | 0.39 | 0.0625 | 0.50 | 0.50 |
| **CPX release at 12h** | 0.39 | 0.0625 | 0.29 | 0.35 |

*4.3.4 Antibiofilm activity of CPX loaded NP*

All formulations, including free-soluble CPX resulted effective to reduce biofilm formation, starting from the lower drug concentration (0.0078 µg mL$^{-1}$) (a reduction between 80 and 90% of the cell content in the biofilm, compared to the untreated control), and complete prevention of biofilm formation was achieved with higher concentrations of drug and NPs (between 0.125 and 0.5 µg mL$^{-1}$) (Figure 4.4).
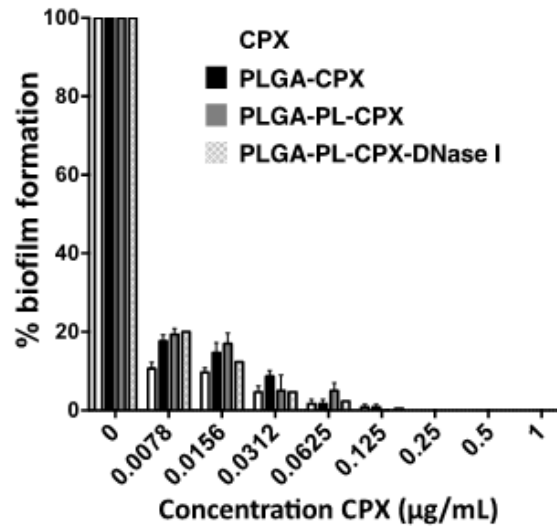
**Figure 4.4: Degree of biofilm formation for different NPs formulations.**

Treatment with DNase and CPX was found to be effective against already formed biofilms (Figure 4.5). The samples with no DNase, PLGA-CPX and PLGA-PL-CPX NPs, were less effective on biofilms, being able to reduce bacterial cells respectively by 10 to 50 and 30 to 55%, in a concentration-dependent fashion. The combination of DNase and CPX lead to a decrease between 85 and 95% (comparable for free soluble molecules, and PLGA-PL-DNAse NPs without CPX, but mixed with PLGA-PL-CPX NPs). PLGA-PL-CPX-DNase I NPs that carry both the antibiotic and the enzyme showed the best results, reducing bacterial cells by 95% at the lower concentration and by more than 99% at the highest.
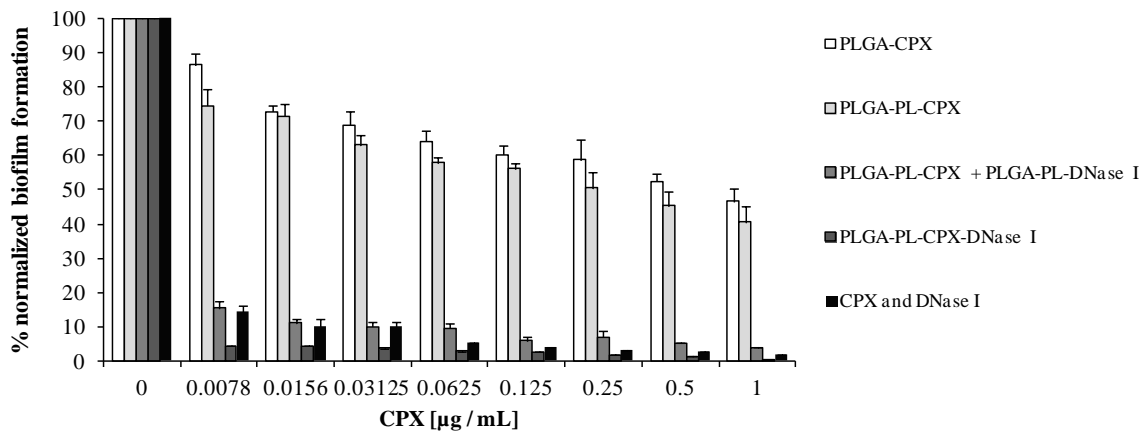


**Figure 4.5: Effect of DNase and DNase-functionalized NPs on already established biofilms.**

Multiple administrations of NPs (one dose/day, up to three days) were also tested against established biofilms (Figure 4.6). PLGA-CPX were effective starting from 0.03125 µg mL$^{-1}$ of equivalent concentration of encapsulated CP. At the highest concentration and at the end of the three days treatment a 90% reduction of the bacterial cells was observed. PLGA-PL-CPX worked better against *P. aeruginosa* biofilms, eliminating between about 80 and 96% (for the lowest and the highest drug concentration respectively) of the

bacterial cells at the end of the 3 day treatment. NPs with DNase I gave the best results, eliminating by the third day from 90 to 99.9% of the bacteria forming the biofilm.
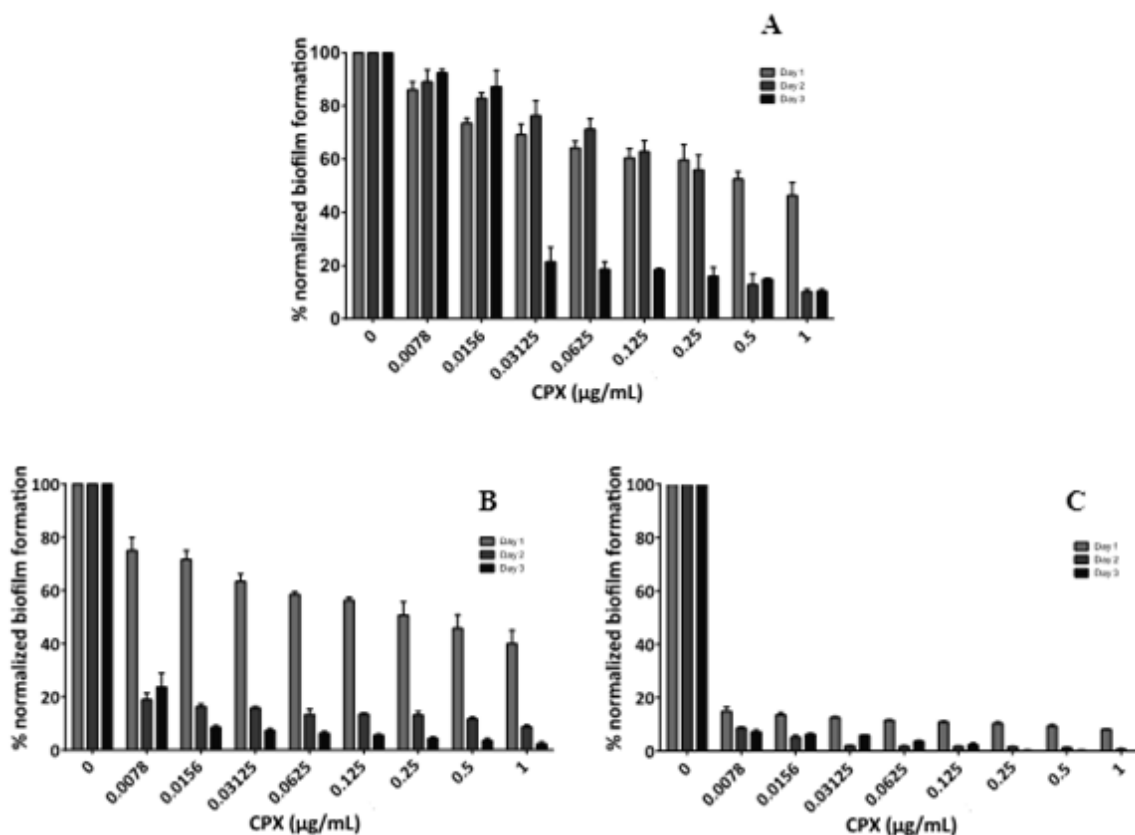


**Figure 4.6: NPs 3-days treatment on established biofilms. (A) PLGA-CPX, (B) PLGA-PL-CPX, and (C) PLGA-PL-CPX-DNase I.**

*4.3.5 Cytotoxicity*

Cytotoxicity was evaluated for PLGA-CPX, PLGA-PL-CPX and PLGA-PL-CPX-DNase I nanoparticles (Figure 4.7). No relevant cytotoxic effect was observed, although some NPs formulations showed a slight reduction in macrophages metabolic activity. Compared to macrophages cultured with no NPs, metabolic levels measured in presence of NPs after 24 hours were slightly lower (between 70% for PLGA-PL-CPX-DNase and 85% for PLGA-PL-CPX). At 48 hours, in all the experimental groups an increment in the metabolic activity could be observed, possibly indicating cell proliferation. Furthermore, samples conditioned with NPs showed a significant improvement in metabolic activity, which became more similar to that of the NPs-free controls (between 76% for PLGA-PL-CPX-DNase and 90% for PLGA-CPX and PLGA-PL-CPX).
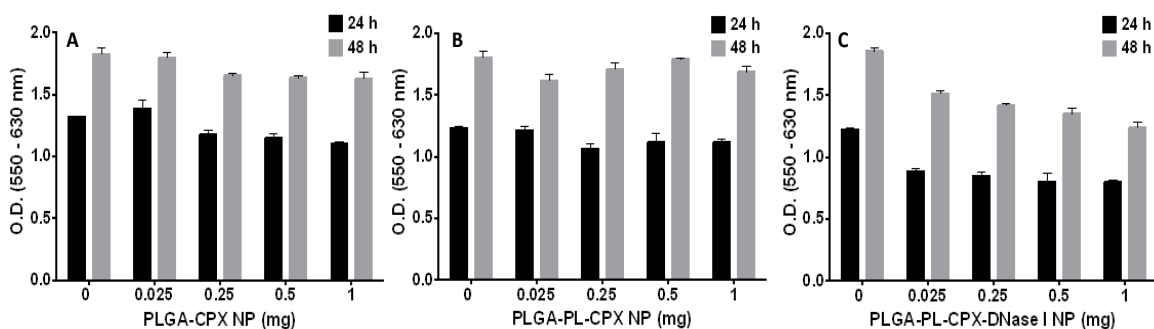
**Figure 4.7: Cytoxicity assessment of CPX loaded (A) PLGA, (B) PLGA-PL and (C) PLGA-PL-DNase I NPs (MTT assay).**

## 4.4 Discussion

In this work, PLGA NPs encapsulating the antibiotic ciprofloxacin have been prepared using a green solvent-based method. The size of the obtained particles falls in the typical range to diffuse in the mucus pores in chronically infected lungs (between 200 and 500 nm) [23]. Untreated, polylysine, and polylysine-DNase I coated NPs were produced, characterized and tested *in vitro* for their capability to treat established biofilm of *P. aeruginosa*.

The polymeric nanoparticles were fabricated using a modification of the nanoprecipitation method, starting from a PLGA-ethyl lactate semi-diluted solution. As the polymeric solution drops enter the water medium, they are quickly broken by eddies generated surface tension gradient between the solvent and the non-solvent, and nanoparticles are immediately formed by solvent displacement and interfacial deposition of the PLGA [24]. Typically, NPs with monodisperse size distribution can be obtained with such method, as it is confirmed by the DLS measurements. As a downside, it is best suitable to encapsulate hydrophobic compounds (with very high efficiencies [25]), since hydrophilic molecules are easily dispersed into the water phase during the particle formation, and even though approaches to improve the encapsulation of hydrophilic drugs have been studied, they lead to limited improvement of encapsulation efficiencies [26]. This is confirmed by our results, showing a quite low CPX loading, despite of working at neutral pH, where CPX displays its minimum solubility in water [27], and are consistent with what has already been reported in literature in relation to encapsulation of fluoroquinone antibiotics [28]. Addition of hydrophilic moieties to the NPs formulations, such as lechitin or pluronic, has also been suggested to improve efficiency [13], but preliminary tests performed in our case did not improve the amount of encapsulated drug (data not shown). A consequence of low loading of hydrophilic molecules is their tendency to accumulate at the NPs surface. As a consequence, this mode of entrapment usually leads to a burst release of the drug in the first hours, due to the compound being washed off the particle [29], as also seen in the CPX release profiles described in this study (Figure 4.2). A fast burst release, followed by a sustained release is preferred, in the case of antibiotics in biofilms, since this can help preventing the insurgence of antibiotic tolerance of the surviving biofilm [28,

117

30]. However, PLGA-CPX NPs quickly depleted their antibiotic load, unlike PL-and PL-DNase I coated NPs. In the two positively charged NP types, the polycationic PL may have helped to stabilized the NPs and interact ionically with the antibiotic, reducing its rate of removal from the NPs [31]. These differences in the release kinetics may have an implication in the determination of the MICs for encapsulated CPX against *P.Aeruginosa*. Encapsulated antibiotic tend to have a higher efficacy against planktonic cells compared to free drug, especially negatively charged PLGA-CPX NPs, although no appreciable difference is shown regarding the capability of preventing biofilm formation. NPs advantage consists in treating established biofilms, such as those in persistent lung infections [32,33,34], where properly designed NPs can penetrate the biofilm porous matrix and provide high local concentrations of antibiotics in the proximity of bacterial cells. Ideally, NPs should be able to diffuse homogenously through the target biofilm, and their ability to penetrate the biofilm matrix depends on their size and surface chemistry. Forier et al., have demonstrated on model polystirene NPs systems that both positively and negatively charged NPs bind into biofilms, and suffer an equal reduction in diffusion velocity [35]. Positively charged NPs were found to be bound to wire-like components, possibly biofilm polymers and eDNA, while negatively charged NPs, were bound in the proximity of bacterial cells, probably due to hydrophobic interactions. Although some researchers have proposed non-fouling, PEG-coated particles in streategies to enhance carriers mobility [36], NPs functionalized with mucolytic agents hold the promise to improve the distribution of antibiotics into biofilms, while increasing biofilm eradication. In the work developed in this thesis, combination of CPX and DNase I on PLGA NPs was shown to be an effective strategy to target established *P. areuginosa* biofilms. While PLGA-CPX and PLGA-PL-CPX NPs alone showed a good extent of biofilm eradication, antibacterial activity of CPX was greatly improved in presence of DNase I (Figures 4.5 and 4.6). Free-soluble and CPX and DNase I showed comparable activity to PLGA-PL-CPX NPs combined with PLGA-PL-DNase I with no drug encapsulated NPs. This is due to an improved mobility of NPs, as the enzyme is actively degrading the eDNA of the biofilm matrix, as also indicated by Messiaen et al., who have found 10-times improved diffusional rates of charged polymeric NPs in biofilm, in presence of DNase [37]. Moreover, greater results were obtained when NPs bearing both CPX and DNase I at the same time were used (PLGA-PL-CPX-DNase I), even at lowest CPX concentrations and with a single application, suggesting that drug delivery-ECM degrading NPs may penetrate better into the bacterial colony, and better harness its integrity. This result is even more important when considering a longer treatment of the infection, as repeated administration of this NPs formulation up to 3 day, bacteria reduction was steadily improved with no sign of tolerace arising. Moreove, at the higher concentrations, PLGA-PL-CPX-DNase I NPs were even able to eradicate the established biofilm. Cytoxicity of the NPs at the used doses was very low, and although slightly higher for PLGA-PL-CPX-DNase I, for all NPs formulation, macrophage cells had their metabolic activity increased during the second day of culture, indicating they were proliferating, which is an indicator of cells health [38]. This data, together with other reassuring results regarding PLGA NPs cytocompatibility [39, 40], supports the feasibility of the proposed drug delivery approach.

## 4.5 Conclusions and future perspectives

In this work, CPX-loaded PLGA NPs were successfully prepared using a method involving no harmful chemicals. These NPs have adequate size for antibiotic drug delivery to biofilms located in the airways, and also display a profitable drug release profile for this specific application. However, CPX loading was quite low, and further refinement of the fabrication parameters would be required to improve encapsulation efficiency. The proposed NPs could be employed as a platform for chemical modification and to test the efficacy of functionalization with active DNase I. Coating the NPs with polylysine enriched the carriers with chemically reactive groups, enabling a simple way to functionalize them. Enzyme-linked NPs, able to degrade *P. aeruginosa* biofilm ECM, were successful at improving antibacterial potential of the encapsulated drug and to achieve biofilm eradication. These results allow obtain novel, antibiofilm-active drug delivery devices and to apply the proposed approach to more type of carriers and antimicrobial compounds combination, to treat persistent bacterial infections.

## 4.6 References

[1]     Kalluru R, Fenaroli F, Westmoreland D, Ulanova L Maleki A, Roos N, et al. Poly(lactide-co-glycolide)-rifampicin nanoparticles efficiently clear Mycobacterium bovis BCG infection in macrophages and remain membrane-bound in phago-lysosomes. J Cell Sci, 126 (2013) 3043-54.

[2]     Khameneh B, Iranshahy M, Ghandadi M, Ghoochi Atashbeyk D, Fazly Bazzaz BS, Iranshahi M. Investigation of the antibacterial activity and efflux pump inhibitory effect of co-loaded piperine and gentamicin nanoliposomes in methicillin-resistant Staphylococcus aureus. Drug Dev Ind Pharm. 20 (2014) 1-6.

[3]     Zhao Y, Zhang X, Wang Y, Wu Z, An J, Lu Z, Mei L,Li C. In situ cross-linked polysaccharide hydrogel as extracellular matrix mimics for antibiotics delivery. Carbohydr Polym. 105 (2014) 63-9.

[4]     Tran VT, Benoit JP, Venier-Julienne MC. Why and how to prepare biodegradable, monodispersed, polymeric microparticles in the field of pharmacy? Int J Pharm. 407 (2011) 1-11.

[5]     Mohamed F, van der Walle CF. Engineering biodegradable polyester particles with specific drug targeting and drug release properties. J Pharm Sci. 97 (2008) 71-87.

[8]     Duncan R, Gaspar R. Nanomedicine(s) under the microscope. Mol Pharm. 8 (2011) 2101-2141.

[9]     Mulcahy LR, Isabella VM, Lewis K. Pseudomonas aeruginosa Biofilms in Disease. Microb Ecol. 68(1) (2014) 1-12.

[10]    Costerton JW, Stewart PS, Greenberg EP. Bacterial biofilms: a common cause of persistent infections. Science. 284 (1999) 1318-22.

[11]     Stewart PS, Franklin MJ. Physiological heterogeneity in biofilms. Nat Rev Microbiol. 6 (2008) 199-210.

[12]     Spellberg B, Guidos R, Gilbert D, Bradley J, Boucher HW, Scheld WM, Bartlett JG, Edwards J. The epidemic of antibiotic-resistant infections: a call to action for the medical community from the Infectious Diseases Society of America. Clin Infect Dis. 46 (2008) 155-64.

[13]     Ungaro F, d'Angelo I, Coletta C, d'Emmanuele di Villa Bianca R, Sorrentino R, Perfetto B, Tufano MA, Miro A, La Rotonda MI, Quaglia F. Dry powders based on PLGA nanoparticles for pulmonary delivery of antibiotics: modulation of encapsulation efficiency, release rate and lung deposition pattern by hydrophilic polymers, J Control Release. 157 (2012) 149-59.

[14]     Zweers ML, Grijpma DW, Engbers GH, Feijen J. The preparation of monodisperse biodegradable polyester nanoparticles with a controlled size, J Biomed Mat Res B. 66 (2003) 559-66.

[15]     Gloag ES, Turnbull L, Huang A, Vallotton P, Wang H, Nolan LM, et al. Self-organization of bacterial biofilms is facilitated by extracellular DNA, Proceedings of the National Academy of Sciences of the United States of America, 110 (2013) 11541-6.

[16]     Peterson BW, van der Mei HC, Sjollema J, Busscher HJ, Sharma PK. A distinguishable role of eDNA in the viscoelastic relaxation of biofilms. mBio. 4 (2013) e00497-00413.

[17]     Okshevsky M, Meyer RL. The role of extracellular DNA in the establishment, maintenance and perpetuation of bacterial biofilms. Crit Rev Microbio (2013) doi:10.3109/1040841X.2013.841639.

[18]     Shah PI, Bush A, Canny GJ, Colin AA, Fuchs HJ, Geddes DM, et al. Recombinant human DNase I in cystic fibrosis patients with severe pulmonary disease: a short-term, double-blind study followed by six months open-label treatment. Eur Respir J. 8 (1995) 954-8.

[19]     Fessi H, Puisieux F, Devissaguet JP, Ammoury N, Benita S. Nanocapsule formation by interfacial polymer deposition following solvent displacement. J Pharm. 55 (1989) R1-R4.

[20]     Cole AM, Weis P, Diamond G. Isolation and characterization of pleurocidin, an antimicrobial peptide in the skin secretions of winter flounder. J Biol Chem, 272 (1997) 12008-13.

[21]     Beckloff N, Laube D, Castro T, Furgang D, Park S, Perlin D, et al. Activity of an antimicrobial peptide mimetic against planktonic and biofilm cultures of oral pathogens. Antimicrob Agents Chemother. 51 (2007) 4125-32.

[22]     Ceri H, Olson M, Morck D, Storey D, Read R, Buret A, Olson B. The MBEC Assay System: multiple equivalent biofilms for antibiotic and biocide susceptibility testing. Methods Enzymol. 337 (2001) 377-85.

[23]     Suk JS, Lai SK, Wang YY, Ensign LM, Zeitlin PL, Boyle MP, Hanes J. The penetration of fresh undiluted sputum expectorated by cystic fibrosis patients by non-adhesive polymer nanoparticles. Biomaterials. 2009 30(13) (2009) 2591-7.

[24]     Morales-Cruz M, Flores-Fernández GM, Morales-Cruz M, Orellano EA, Rodriguez-Martinez JA, Ruiz M, Griebenow K. Two-step nanoprecipitation for the production of protein-loaded PLGA nanospheres. Results Pharma Sci. 2:79 (2012) 85.

[25]  Barichello JM, Morishita M, Takayama K, Nagai T. Encapsulation of hydrophilic and lipophilic drugs in PLGA nanoparticles by the nanoprecipitation method. Drug Dev Ind Pharm. 25(4) (1999) 471-6.

[26]  Bilati U, Allémann E, Doelker E. Development of a nanoprecipitation method intended for the entrapment of hydrophilic drugs into nanoparticles. Eur J Pharm Sci. 24(1) (2005) 67-75.

[27]  Caço AI, Varanda F, Pratas de Melo MJ, Dias AMA , Dohrn R, Marrucho IM. Solubility of Antibiotics in Different Solvents. Part II. Non-Hydrochloride Forms of Tetracycline and Ciprofloxacin. Ind. Eng. Chem. Res. 47(21) (2008) 8083–9.

[28]  Cheow WS, Chang MW, Hadinoto K. Antibacterial efficacy of inhalable levofloxacin-loaded polymeric nanoparticles against E. coli biofilm cells: the effect of antibiotic release profile. Pharm Res. 27(8) (2010) 1597-609.

[29]  Enayati M, Stride E, Edirisinghe M, Bonfield W. Modification of the release characteristics of estradiol encapsulated in PLGA particles via surface coating. Ther Deliv. 3(2) (2012) 209-26.

[30]  Forier K, Raemdonck K, De Smedt S, Demeester J, Coenye T, Braeckmans K. Lipid and polymeric nanoparticles for drug delivery to bacterial biofilms. J Control Release. (2014) doi: 10.1016/j.jconrel.2014.03.055.

[31]  Cheow WS, Hadinoto K. Green preparation of antibiotic nanoparticle complex as potential anti-biofilm therapeutics via self-assembly amphiphile-polyelectrolyte complexation with dextran sulfate. Colloids Surf B Biointerfaces. 1 (2012) 92:55-63.

[32]  Henning A, Schneider M, Nafee N, Muijs L, Rytting E, Wang X, Kissel T, Grafahrend D, Klee D, Lehr CM. Influence of particle size and material properties on mucociliary clearance from the airways. J Aerosol Med Pulm Drug Deliv. 23(4) (2010) 233-41.

[33]  Nafee N, Husari A, Maurer CK, Lu C, de Rossi C, Steinbach A, Hartmann RW, Lehr CM, Schneider M. Antibiotic-free nanotherapeutics: Ultra-small, mucus-penetrating solid lipid nanoparticles enhance the pulmonary delivery and anti-virulence efficacy of novel quorum sensing inhibitors. J Control Release. (2014) doi: 10.1016/j.jconrel.2014.06.055.

[34]  Jørgensen KM, Wassermann T, Jensen PØ, Hengzuang W, Molin S, Høiby N, Ciofu O. Sublethal ciprofloxacin treatment leads to rapid development of high-level ciprofloxacin resistance during long-term experimental evolution of Pseudomonas aeruginosa. Antimicrob Agents Chemother. 57(9) (2013) 4215-21.

[35]  Forier K, Messiaen AS, Raemdonck K, Deschout H, Rejman J, De Baets F, Nelis H, De Smedt SC, Demeester J, Coenye T, Braeckmans K. Transport of nanoparticles in cystic fibrosis sputum and bacterial biofilms by single-particle tracking microscopy. Nanomedicine (Lond). 8(6) (2013) 935-49.

[36]  Miller JK, Neubig R, Clemons CB, Kreider KL, Wilber JP, Young GW, Ditto AJ, Yun YH, Milsted A, Badawy HT, Panzner MJ, Youngs WJ, Cannon CL. Nanoparticle deposition onto biofilms. Ann Biomed Eng. 41(1) (2013) 53-67.

[37]    Messiaen AS, Forier K, Nelis H, Braeckmans K, Coenye T. Transport of nanoparticles and tobramycin-loaded liposomes in Burkholderia cepacia complex biofilms. PLoS One. 8(11) (2013) e79220.

[38]    Xiang K, Dou Z, Li Y, Xu Y, Zhu J, Yang S, Sun H, Liu Y. Cytotoxicity and TNF-alpha secretion in RAW264.7 macrophages exposed to different fullerene derivatives. J Nanosci Nanotechnol. 12(3) (2012) 2169-78.

[39]    Xiong S, George S, Yu H, Damoiseaux R, France B, Ng KW, Loo JS. Size influences the cytotoxicity of poly (lactic-co-glycolic acid) (PLGA) and titanium dioxide (TiO(2)) nanoparticles. Arch Toxicol. 87(6) (2013) 1075-86.

[40]    Coowanitwong I, Arya V, Kulvanich P, Hochhaus G. Slow release formulations of inhaled rifampin. AAPS J. 2008 Jun;10(2) (2008) 342-8.

# Chapter 5

# Cell delivery from functionalized polylactic acid microcarriers tuning MSCs migratory behavior in response to chemokine stimulation

*In this chapter, microcarriers produced following the fabrication method described in chapter 3 are characterized as cell carriers for mesenchymal stromal cell therapy. The surface of the microcarreries is modified with different approaches to introduce bioactive coatings, and the effect of these coatings over cell homing, adhesion, proliferation, expression of CXCR4 -a receptor involved in chemokine-dependent migratory pathways-  and cell migration in response to SDF-1α stimulation are studied.*

## 5.1 Introduction

One of the most challenging limitations in cell therapy is poor cell survival upon transplantation, since more than 90% of the therapeutic cell population dies in the first days after intravenous or direct injection [1]. Moreover, the limited amount of surviving cells suffers of poor tissue localization, because biological fluids can easily disperse them from the desired site [2]. This massive cell death can occur for mechanical damage during the injection, but also for the environmental stress imposed by the target tissue, since injected cells are usually required to attach, home and survive in injuried tissues, that can be ischemic, highly inflamed and even necrotic [3]. The use of biomaterial carriers can dramatically increase anchorage-dependent cells viability and engraftment in host tissues, by providing mechanical support, homing and pro-survival cues. As reviewed in Chapter 2, several injectable biomaterials, such as in situ-forming hydrogels [4] or microcarriers [5] have been proposed to deliver differentiated and progenitor cells, including Mesenchymal Stromal Cells (MSCs) [6]. However, cell survival and engraftment alone may not be sufficient for clinical applications, since cells are often required to migrate and localize at specific sites throughout the target tissues, in order to express their therapeutic activity.

The use of MSCs for cell therapies has received a lot of attention due to the ability of these cells to differentiate towards several phenotypes, exert immunomodulatory activity and secrete paracrine factors [7]. Furthermore, MSCs can migrate towards damaged tissues in a specific manner, and thus can act as vehicles to deliver therapeutic agents to organs whose surgical treatment is not always possible. For example, MSCs transplanted to treat myocardial infarction, can localize to the ischemic heart, and improve its function via bystander effects [8]. Moreover, MSCs have been used to target tumoral cells in aggressive gliomas. It has been shown that, in the brain, MSCs are recruited to the forming tumor vascular network, and then spread into the main tumor mass. At the same time, they can also track satellite glioma cells in process of invasion, and associate with them with great accuracy [9]. To exploit this capability, MSCs have been engineered to deliver tumor-killing agents, able to effectively reduce glioma mass in an animal model [10].

This MSCs specific migration occurs in response to chemokines expressed by the pathological tissue. Among these signals, a major role is played by Stromal cell-Derived Factor 1α (SDF-1α, or CXCL12), which is a potent chemotactic agent for MSCs, and is also secreted by ischemic and tumoral tissues [8, 11]. Additionally, the recognition of SDF-1α by its receptor, CXCR4, triggers a cascade of pro-survival and homing responses [12], and MSCs (as well as immature osteoblasts) continuously secrete SDF-1α, presumably to keep themselves in their niche [13]. CXCR4 and SFD-1α are fundamental in physiological tissues, and their knock outs are lethal, resulting in severe bone marrow failure and abnormal development of the heart and brain [14, 15]. In this context, the SDF-1α/CXCR4 axis became a promising target for regenerative medicine approaches aiming cardiac, nervous and osteochondral tissue repair [16]. A variety of studies have been conducted to fabricate SDF-1α controlled delivery devices able to induce progenitor cells recruiting for tissue engineering [17, 18], as well to improve CXCR4 expression in MSCs, in order to increase viability, migration and regenerative potential, e.g. for cardiac cell therapy [19] and angiogenesis

[13]. Along with these strategies, biomaterials are still deemed necessary for cell delivery. Therefore, it is important to design biomaterial carriers not only to retain seeded cells, but also to act as reservoirs from which cells can migrate, possibly in a temporally-controlled manner. Even though the study of cell-materials interactions is a fundamental aspect of tissue engineering, it is still unclear how to tune biomaterials properties to control cell responsiveness to cytokines stimulation. Furthermore, there is no report about how common biomaterials engineering strategies, such as surface modification, can influence key cell migratory pathways. A deeper understanding of such relationship would provide fundamental hints to improve cell delivery devices design.

The aim of this work is to characterize polylactic acid microcarriers as vehicles for cell homing and delivery, and to evaluate their effect on MSCs migratory potential. Polylactic acid Microcarriers (MCs) design was studied to discern how to target SDF-1a/CXCR4 axis via surface functionalization strategies, and thus exert a control over cell release. Herein, the effect of several MCs functionalization approaches on MSCs viability, release and migration in relation to SDF-1α/CXCR4 axis were studied in vitro. Collagen and RGD peptide-modified MCs were compared to evaluate coatings having different nature -long extracellular matrix (ECM) protein vs. short functional sequence-. The biomolecules were introduced either via covalent grafting or simple physisoprtion, in order to assess also the role of the stability of the coating on cell delivery potential.

## 5.2 Materials & Methods

### 5.2.1 Materials

Poly(lactic acid) (Purasorb PLDL 7038, inherent viscosity midpoint 3.8 dL / g-1, Mw ≈ 850 000 Da) was purchased from Purac. (-)-Ethyl L-lactate (purity > 99.0%) was obtained from Fluka and used without further purification. Glass microcarriers beads, poly(vinyl alcohol) (PVA, 30–70 kDa, 88% hydrolyzed) and all the other reagents were from Sigma-Aldrich, unless specified otherwise.

### 5.2.2 MCs fabrication

PLA MCs were prepared following a previously described in Chapter 3. Briefly, a 3.5 % w/v PLA solution in Ethyl Lactate was dispensed at 10 mL h$^{-1}$, and the formed droplets were collected into a coagulation bath, composed by 0.3% w/v PVA in 70 vol% ethanol. MCs were rinsed with deionized water, frozen in liquid nitrogen and lyophilized for 48 h. MCs were visualized with Scanning Electron Microscopy (SEM, Quanta Q200, FEI company) and their size, polydispersity and surface area were measured via electrical sensing zone technique (Coulter Counter Multisizer IIe, Beckman Coulter).

### 5.2.3 MCs functionalization

Surface modification of the MCs was carried out using a three step procedure [27]. First, MCs were immersed into a 50 mM NaOH solution for 10 minutes to induce hydrolysis of the PLA backbone and thus

enrich the MCs surface with carboxyl groups. After that, exposed COOH terminals were activated with a ethyl(dimethylaminopropyl) carbodiimide / N-hydroxysuccinimide 100 mM / 200 mM (EDC/NHS) solution in 70 vol% ethanol for 2 hours. Finally, biomolecules coatings were covalently attached to the MCs surface through amide bonds between the activated carboxyles and the amino groups from the target protein or peptide. For this purpose, human recombinant Collagen type I (FibroGen Inc., USA) or custom-made GGGGGGRGDS peptides (RGD, GenScript Inc., USA) were dissolved in PBS at a concentration of 100 µg mL$^{-1}$ and incubated with the MCs for 24 hours. Functionalization via physisorption was carried out by simply immersing untreated PLA MCs into a 100 µg mL$^{-1}$ solution of the desired biomolecule for 24 hours. Bicinchoninic acid assay (BCA assay, Thermo Scientific) allowed for the quantification of the grafted protein, following the protocol described by the manufacturer. The different experimental groups are summarized in Table 5.1.

**Table 5.1: MCs modified with the different functionalization strategies analyzed in this study.**

| Sample | Biomolecule | Type of coating |
|--------|-------------|-----------------|
| PLA | none | none |
| CC | collagen | covalent |
| CP | collagen | physisorbed |
| RC | RGD peptide | covalent |
| RP | RGD peptide | physisorbed |

*5.2.4 Isolation of mesenchymal stromal cells*

Mesenchymal Stromal Cells (MSCs) where isolated from long bones of 2-4 weeks old Lewis rats according to a previously decribed protocol [28]. Briefly, rats were anesthetized using 5% isoflurane and the sacrifice was performed through $CO_2$ saturated atmosphere. Bone-marrow was obtained by flushing control medium (M199 supplemented with 20% Fetal Bovine Serum –FBS-, 1% Pyr, 1% Pen/Strep, 1% L-glu and 22 µg mL$^{-1}$ heparin) through the bone. The cell fraction was resuspended in control medium and plated in Petri dishes for 24 h. The adherent cell population was cultured in Advanced DMEM supplemented with 15% FBS, 1% Pen/Strep and 1% L-glu until reaching sub-confluence, and expanded into a T75 Nunclon$^{TM}$ flask until passage 2. The acquired population of cells was highly enriched in Stro-1$^+$, CD105$^+$, CD44$^+$, CD34$^-$ and CD45$^-$ MSCs. For all the experiments described in this study, cells between passage 4 and 6 were used. All the protocols concerning the animal care were previously approved by Committee on the Ethics and Animal Experiments of the Scientific Park of Barcelona (Permit number: 0006S/13393/2011). Cell expansion and experiments were carried out culturing MSCs in proliferation medium, consisting of Advanced DMEM, provided with 15% FBS, 1% Pen/Strep and 1% L-glu.

*5.2.5 Cell culture assays*

Biological assays were carried out to describe the effect of surface modifications on cell adhesion, proliferation and migratory potential in response to specific chemoattractant stimulation.

*5.2.5.1 MSCs adhesion assay*

3 mg of the different MCs, previously disinfected by immersion in a 70 vol% EtOH solution, were placed into a well of an anti-adhering 24-well plate (Costar® Ultra Low-Attachment Cluster Plate, Corning Inc, USA) and let equilibrate for 2 hours in serum-free medium. $9 \times 10^4$ cells suspended in serum-free medium were seeded under static conditions in each well and placed in an incubator at 37 °C, 95 % relative humidity and 5 % $CO_2$ partial pressure. Tissue Culture Polystyrene (TCPS) was used as control. In the first hour, every ten minutes the plate was gently shaken in order to facilitate an even distribution of the cells on the MCs. After 4 hours, the medium was removed and the MCs were washed with PBS to remove unattached cells. Number of adhered and metabolically active cells was quantified using the alamarBlue® (Life Technologies) assay (n=4), following the instructions of the manufacturer. Briefly, the samples were incubated for 2h with adhesion medium provided with 10% v/v alamarBlue®. After this period, the reduction of resazurin to the fluorescent compound resorufin, due to cell metabolic activity, was analyzed ($\lambda_{ex} = 560$ nm, $\lambda_{em} = 590$ nm).

The degree of cell adhesion on the MCs was studied by means of immunofluorescence (n = 3). 4 hours after seeding, cell-laden MCs were collected, washed with PBS, fixed with paraformaldehyde (PFA) and permeabilized with Triton X-100. MC-MSCs complexes were incubated in a 3% w/v bovine serum albumin (BSA) in PBS-Gly as a blocking solution for 30 minutes. Nuclei were stained with 4',6-diamidino-2-phenylindole (DAPI), Actin cytoskeleton with phalloidin-rhodamine (Life Technologies). Vinculin was stained using a mouse anti-rat vinculin primary antibody (Life Technilogies) and with a goat anti-mouse secondary antibody conjugated to AlexaFluor 488 dye (Life Technologies). Images were taken with a confocal laser scanning microscope (Leica TCS SP5, Leica Microsystems).

*5.2.5.2 MSCs proliferation assay*

MCs preparation and seeding were performed as described for the adhesion assays; except that PLA untreated MCs were equilibrated in proliferation medium (supplemented with serum). For all the samples (n = 4), cell seeding was also performed suspending cells in proliferation medium. MSCs proliferation on the MCs was estimated using the alamarBlue® assay after 1, 3, 5, 7 and 14 days of static culture. Medium was replaced every 2 days. Cell quantification was carried out using a standard curve, referring to known amounts of cells seeded on TCPS. Immunofluorescence was used to qualitatively describe cell colonization of the MCs surface during the assay. MCs samples taken at day 1, 7 and 14 of culture were stained with DAPI and phalloidin-ActiStain 488 (Cytoskeleton Inc.).

*5.2.6 CXCR4 expression analysis*

*5.2.6.1 Immunofluorescence*

CXCR4 expression by MSCs was revealed by immunofluorescence in cell cultured on 2D surfaces (TCPS) and in 3D on MCs, both untreated and functionalized. MSCs were cultured in proliferation medium for 24 hours and then fixed with PFA and permeabilized with Triton X-100. BSA was used as a blocking agent. Rabbit anti-rat CXCR4 (Abcam) was used as a primary antibody, while the secondary antibody was a goat anti-rabbit conjugated with AlexaFluor 488 (Life Technologies).

*5.2.6.2 Flow cytometry*

MSCs pool expressing CXCR4 was determined with flow cytometry. Cells were cultured for 24 hours or 4 days on the MCs (untreated PLA, functionalized and glass beads) and on 2D surfaces (TCPS, PLA films and collagen-coated PLA films) and then dissociated with 0.25 % trypsin-EDTA for 3 minutes at 37 °C. MSCs were also cultured for 24h on CC MCs and then retrieved and subcultured on 2D TCPS for 3 additional days. MSCs where collected and washed with a flow cytometry buffer (PBS, 1% bovine serum albumin and 1 mM EDTA). Staining of surface CXCR4 was performed using rabbit anti-rat CXCR4 as a primary antibody at 4 °C in the dark for 30 minutes. The secondary antibody, a goat anti-rabbit conjugated with AlexaFluor 488, was applied for additional 30 minutes at 4 °C in the dark. Background staining was assessed by incubation of cells with rabbit isotypematched immunoglobulins (isotype controls). Flow cytometric analysis of MSCs was performed with a Gallios flow cytometer (Beckman Coulter). Signals from subcellular debris were eliminated during data acquisition by gating. The Summit v4.3 software package was used to process the data. Moreover, MCs without cells were filtered with a 90 µm sieve and analyzed. These MCs underwent the immunostaining procedure detailed above and were analyzed with the flow cytometer, in order to exclude false-positive signals.

*5.2.7 Migratory response of MSC to SDF-1α*

MSCs capability to migrate from the MCs upon chemotactic stimulation was assessed using a modified Boyden chamber assay (Figure 5.1). $3x10^4$ cells were seeded on 1 mg of microcarriers and let adhere for 12 hours. Cell-loaded MCs were moved to a 24-well Millicell®, hanging cell culture insert (Millipore) with a porous membrane (pore size 8 µm), already placed in a 24-well culture plate. In order to simulate a tissue-like 3D environment, the MCs were embedded in 100 µL of Matrigel (Growth Factor Reduced, phenol-red free, BD Biosciences) solution 1:1 in culture medium, and put in the incubator at 37 °C for 30 minutes to allow for Matrigel gelification. The lower well of the Boyden chamber was loaded with low-serum medium (LS) consisting of ADMEM with 0.5% FBS, L-glutamine and 1% penicillin-streptomicin, supplemented or not with 50 ng mL$^{-1}$ of either Stromal cell-Derived Factor 1α (SDF-1α, rat recombinant, Peprotech) or Vascular Endothelial Growth Factor (VEGF, rat recombinant, Peprotech). MSCs were allowed to migrate for 12 hours. After this time, the cells were fixed with PFA, the content of the upper side of the insert (Matrigel,

cells and MCs) was accurately removed using a cotton swab, and the cells nuclei stained with DAPI. The number of cells that migrated through the membrane was counted from 5 randomly chosen fields using a fluorescence inverted microscope with a 10x magnification objective. The number of cells that crossed the membrane was normalized against the actual number of adhered cells on the MCs at the beginning of the assay, determined with an alamarBlue assay. Cell migration was expressed through a Migration Index, defined as the ratio between the normalized numbers of migrated cells for a given sample and for the untreated PLA MCs under basal condition (low serum medium without chemoattractants). The experiment was performed also with cells seeded directly on the insert membrane and embedded in Matrigel. Furthermore, in order to evaluate MSCs capability to migrate towards gradients of SDF-1α, a standard boyden chamber assay was performed, using increasing concentrations of this chemokine and VEGF as a positive control.
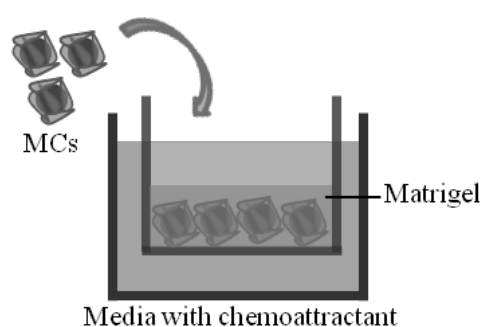


**Figure 5.1: Schematic representation of the modified Boyden chamber assay.**

*5.2.8 Statistical analysis*

Each experiment was performed in three to five replicates (n=3 to 5). Data are presented as mean and standard deviation of the replicates. Statistical significance was assessed performing Student's t-test using Origin 8.0 Software (OriginLab, USA).

**5.3 Results**

*5.3.1 MCs characterization and surface coating*

PLA MCs with an average diameter of $67.68 \pm 21.80$ µm were prepared, with a measured specific surface area of $2.31 \pm 0.28$ cm$^2$ mg$^{-1}$. The density of collagen coating on the MCs surfaces was quantified as $2.57 \pm 0.17$ and $0.71 \pm 0.04$ µg cm$^{-2}$ for covalent and physisorption functionalization approaches, respectively.

*5.3.2 Cell response in terms of adhesion and proliferation*

All MCs types, independently of their surface treatment, allowed cell attachment (Figure 5.2). Untreated PLA and physisorbed RGD samples showed the lowest number of adhering cells after 4 hours in serum-free medium, with about 60% of adhered cells, compared to the control. Collagen coatings, both covalent and physisorbed gave the best result, with more than 90% of adhering cells. These MCs also promoted the

highest degree of adhesion and spreading (Figure 5.3). Particularly, CC MCs were the only carriers to show positive vinculin staining, a marker for the formation of focal adhesion points. Cells on RC MCs (>80% cells adhered) appeared to be non-spread but with already developed filopodia stretching on the particles surface, indicating an early phase of attachment. MSCs seeded on RP and PLA MCs were rounded and poorly attached to the surface.
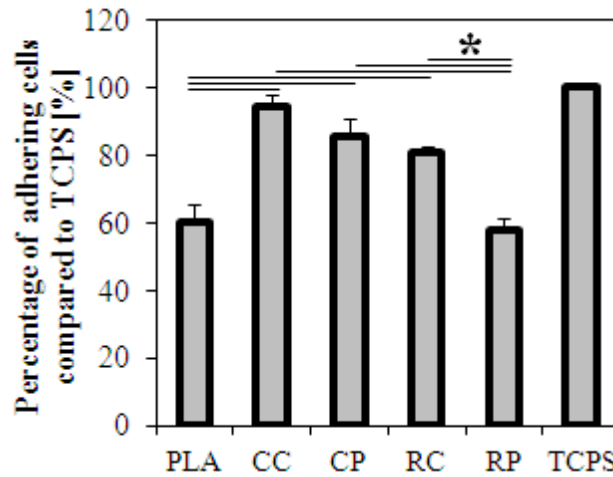


**Figure 5.2: Quantification of adhering cells after 4 hours. Results are expressed as percentage of adhering MSCs on a TCPS control surface. Lines show statistically significant differences (p<0.05).**
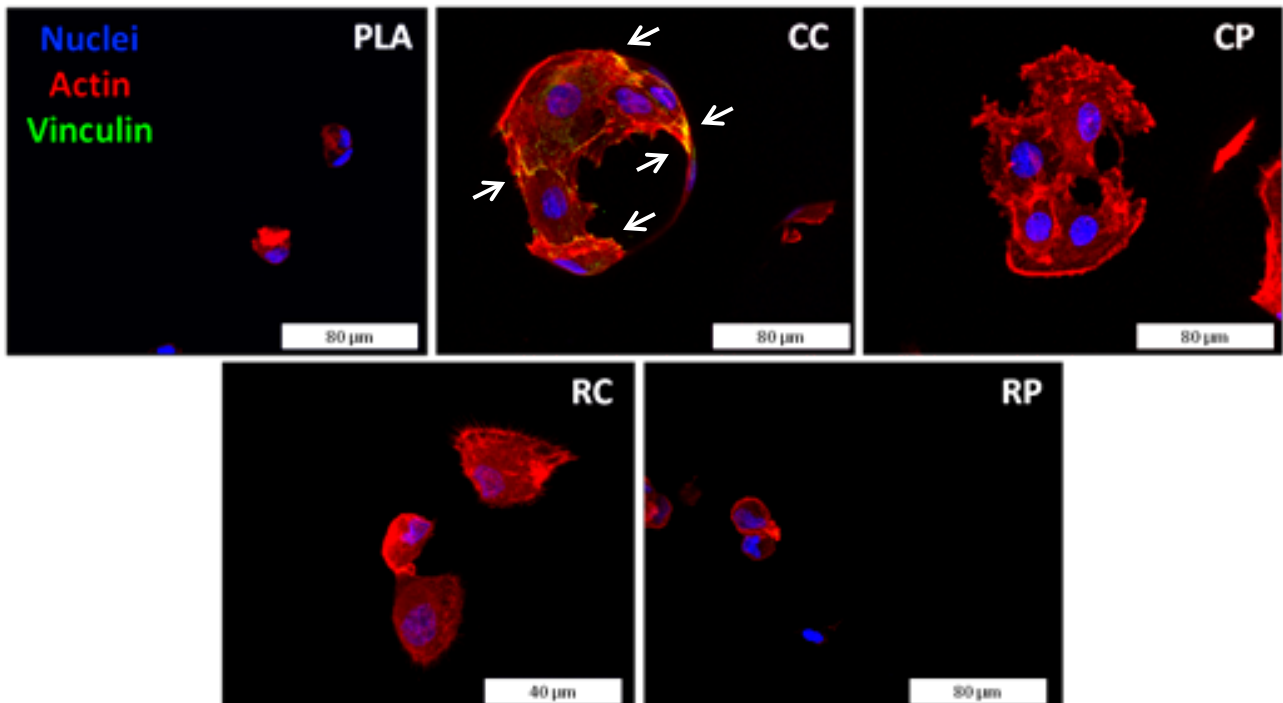


**Figure 5.3: Immunofluorescence of MSCs adhesión on different MCs after 4 hours. Arrows indicate the formation of focal adhesion points.**

In longer cell culture assays with complete medium (supplemented with FBS), MSCs proliferation could be observed (Figure 5.4). All MCs formulations allowed cell homing and cell number increased steadily until reaching confluence after 5 days of culture. Afterwards, cell population started to decrease for all non-covalently coated samples. Instead, CC and RC MCs were able to maintain their cell pool constant. Furthermore, CC MCs showed a significantly higher MSCs number than RC samples. Cell proliferation was also observed by immunofluorescence staining (Figure 5.5). In all samples, MSCs started colonizing individual or small groups of MCs. As the static culture time increased, MSCs started connecting neighboring particles and formed larger MC-MSCs complexes. At day 14, all MCs in the culture wells were clustered in a macroaggregate, and no qualitative difference could be appreciated between the experimental groups.
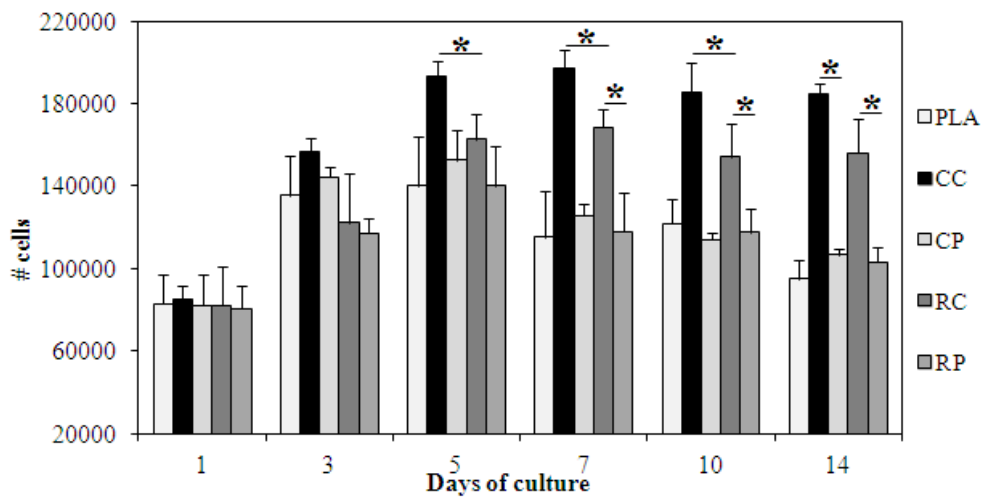


Figure 5.4: Proliferation of MSC on MCs. Stars indicates statistically significant differences (p<0.05).
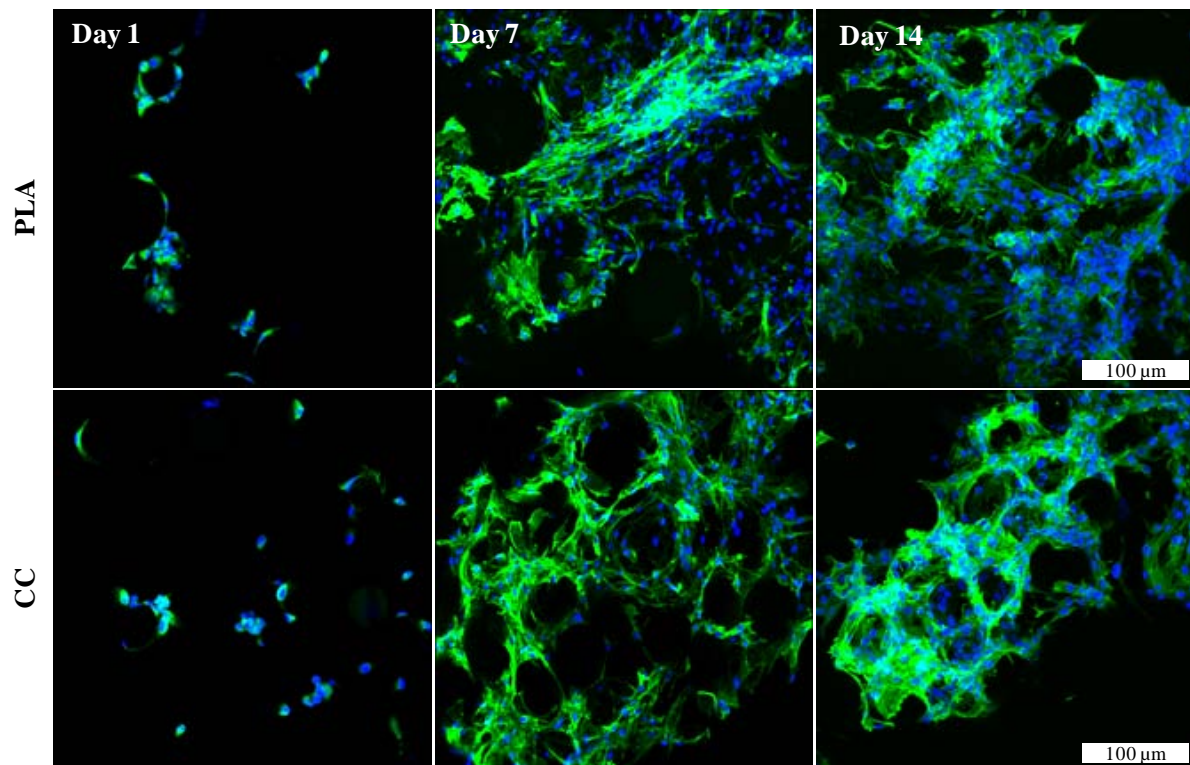
**Figure 5.5: Immunofluorescence of proliferating MSC on PLA and CC MCs.**

*5.3.3 Evaluation of migratory potential in response to SDF-1α*

*5.3.3.1 CXCR4 expression*

MSCs cultured on 2D TCPS were positive for CXCR4 staining, and this expression was preserved in cells homing to 3D MCs (Figure 5.6). The receptor was found in the cytoplasm, both at the perinuclear space, and in the cell periphery, in presence of, but not co-localized with, developed actin fibers. The distribution of the receptor in 3D MC culture was comparable to that observed for 2D TCPS. No difference could be appreciated between the MCs experimental groups, regardless of their surface coatings.
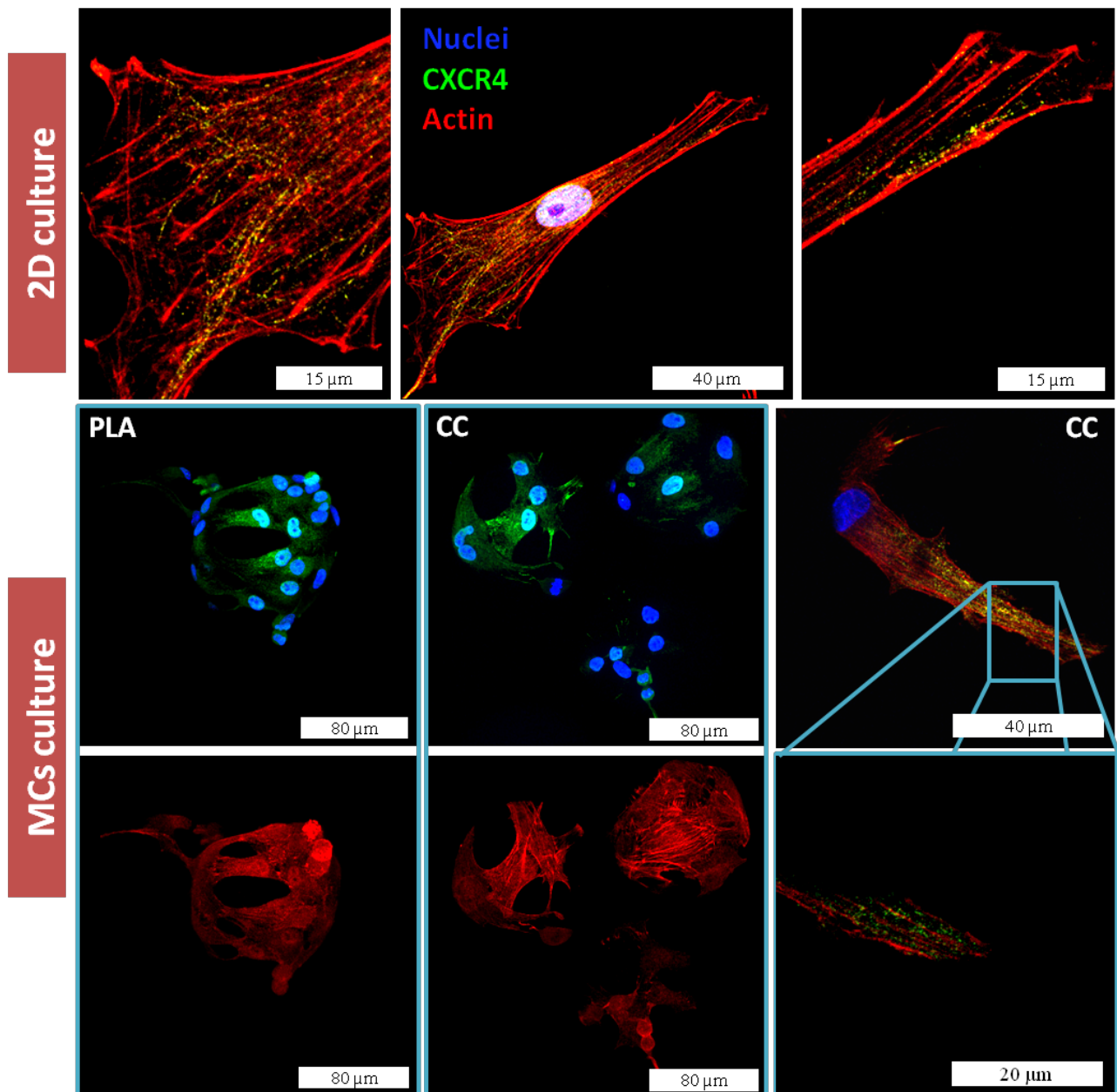
**Figure 5.6: CXCR4 expression and localization in MSCs cultured on 2D TCPS surfaces and in 3D, on two representative experimental groups of MCs.**

Flow cytometry (Figure 5.7) confirmed CXCR4 intracellular expression, with $97.18 \pm 1.83\%$ of the whole MSCs population showing positive staining (Figure 5.8). However, only a small pool of cells (less than 4%), expressed the receptor at the cell membrane, where it can be functional for SDF-1α sensing. Similar results were found for 2D culture on different materials, namely PLA films coated or not with collagen. 3D cell culture on MCs, instead, promoted functional expression of CXCR4 as a surface receptor, as showed in Figures 5.9, and 5.10. Among MSCs seeded on MCs, the population of positively stained cells for CXCR4 at the cell membrane increased significantly, compared to 2D culture. Most notably, collagen coated MCs (both covalent and physisorbed), induced a 5-fold increment (up to 25-30% of the overall cell population). About 15% of the cells cultured on PLA, RC and RP samples expressed CXCR4 at the membrane. This effect on

CXCR4 expression is reversible and dependent on the culture condition, as shown in Figure 5.11. The cell pool expressing the receptor at the surface quickly returned at values lower than 4%, when MSCs were retrieved from collagen coated MCs, and subsequently plated on TCPS.
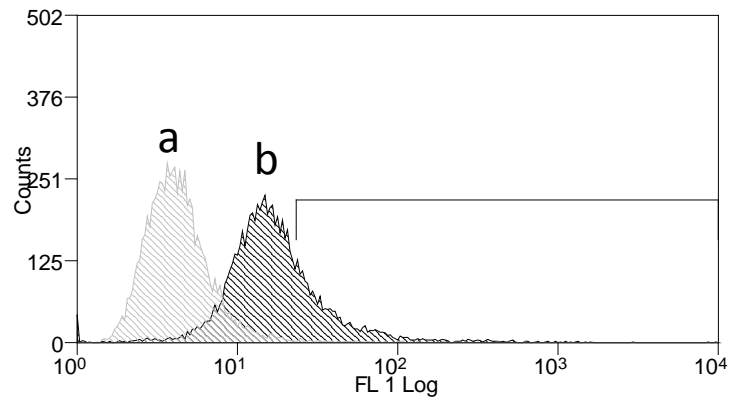


**Figure 5.7: Example of surface CXCR4 expression flow cytometry results for (a) isotype control (b) cells cultured on CC MCs.**
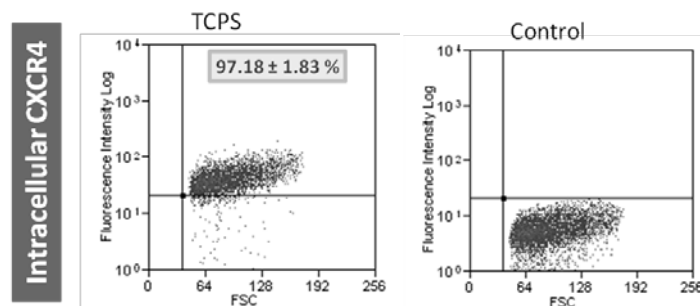


**Figure 5.8: Intracellular expression of CXCR4 in MSCs (cultured on TCPS and isotype control are shown).**
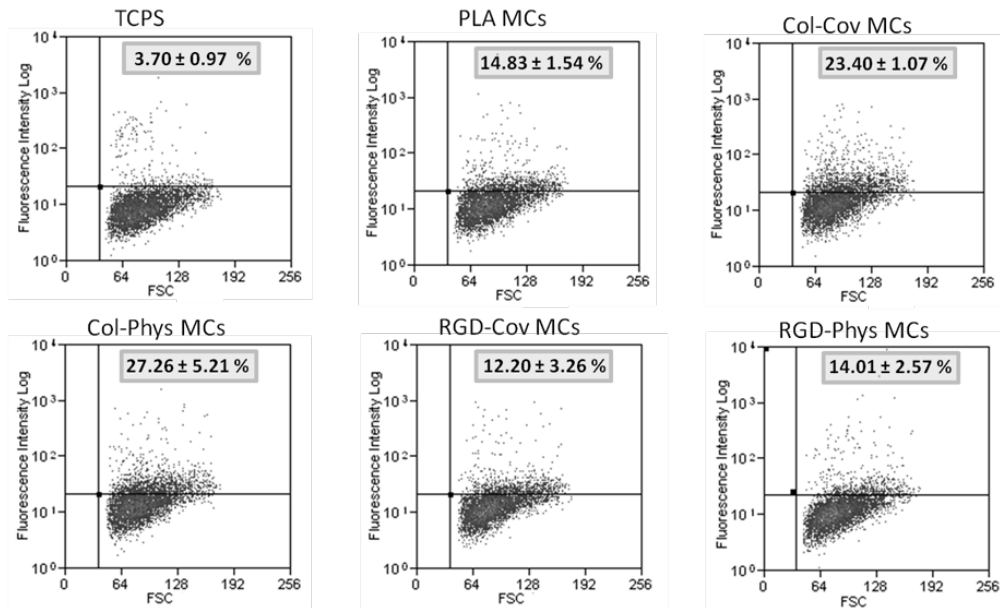
**Figure 5.9: Surface CXCR4 expression for MSCs cultured on different substrates.**
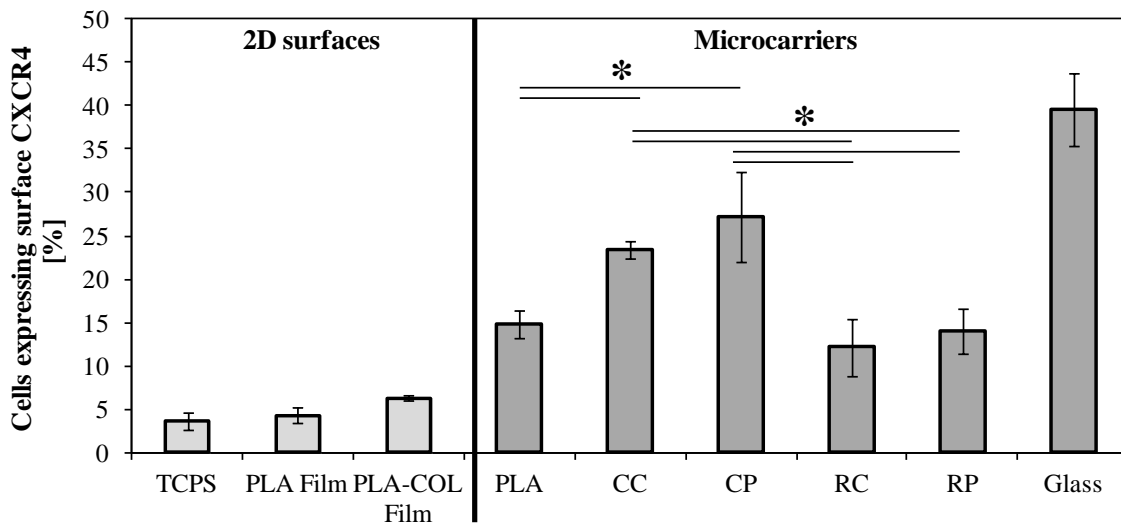


**Figure 5.10: Pool of MSCs expressing CXCR4 at the cell membrane as obtained analyzing flow cytometry data. Lines indicate statistically significant differences ($p < 0.05$).**
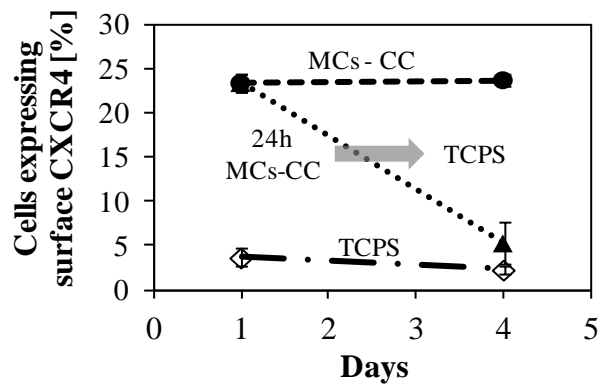


**Figure 5.11: Adaptive beahvior of MSCs expression of CXCR4 to the culture condition.**

*5.3.3.2 Migratory response of MSC to SDF-1α*

MSCs were able to migrate towards gradients of SDF-1α in a concentration dependent manner, reaching migration index values between 3 and 4 at the highest chemoattactant concentration. MSCs responded to SDF and VEGF gradients also when encapsulated in Matrigel, although showing a migration index of 3, a slightly lower value compared to when seeded directly on the membrane of the boyden chamber insert (Fig. 5.12).
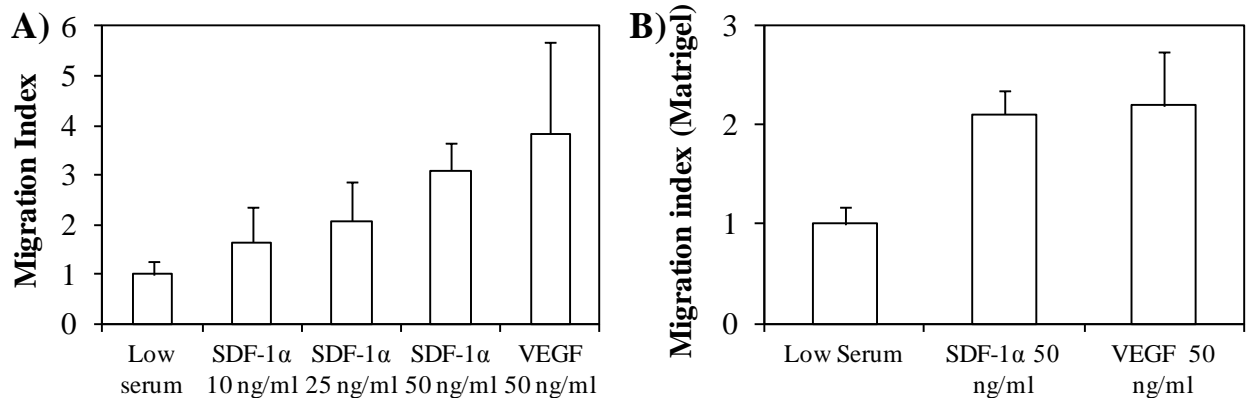


**Figure 5.12: Standard (A) and Matrigel-modified (B) Boyden chamber assay with SDF-1α gradients.**

MSCs cultured on MCs were able to migrate from the carriers in response to SDF and VEGF gradients (Figure 5.13). For all the experimental groups, in presence of the Matrigel, the migration index of MSCs increased 2-fold after chemokines stimulation, compared to the basal condition (low serum medium). Cells homing on PLA MCs and physisorptive coatings showed a migration index between 2 and 2.5, whereas the index was halved on surfaces modified with stable, covalent coatings –both collagen and RGD-. Furthermore, the number of migrating cells was comparable for the two covalent coatings, on one side and for the untreated and physically modified MCs on the other.
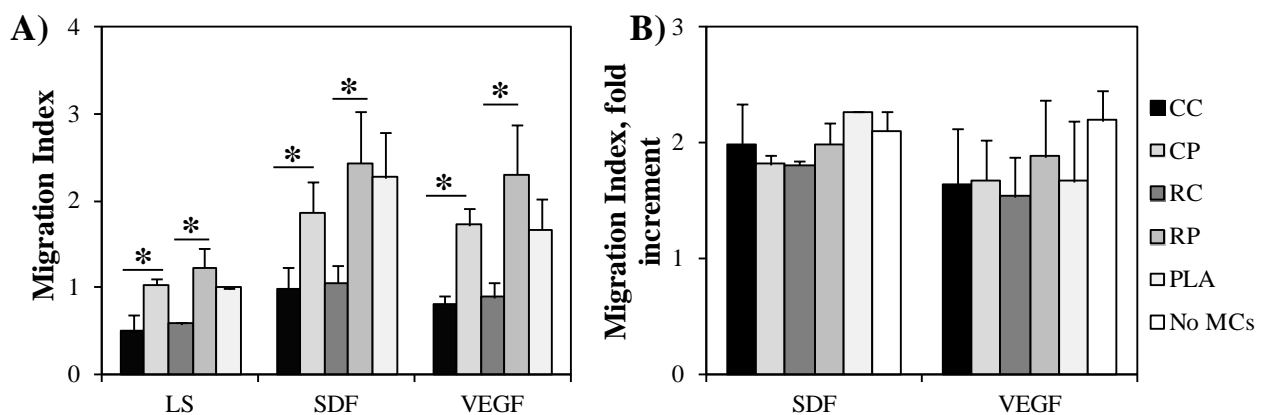


**Figure 5.13: Migration index for cells cultured on MCs, normalized against the value for PLA untreated MCs (A), and increment of migratory index respect to basal conditions after chemokines stimulation (B). MSCs-MCs complexes were encapsulated in Matrigel. Lines highlight the statistically significant differences between samples (p<0.05).**

## 5.4 Discussion

The development of injectable delivery devices is required for cell therapy, in order to improve the otherwise poor survival of adherent-dependent cells upon transplantation. A common strategy to enhance cell attachment and viability is surface modification of biomaterials with bioactive molecules. However, the interplay between materials surface properties, functionalization, cell migration and release is still not understood. This is especially important, as in the body, injected cells are influenced by several chemokines, that are crucial to recruit therapeutic cells and trigger tissue repair.

In this study, PLA MCs were designed to promote MSCs i) survival and proliferation, and ii) controlled release. The combination of physical and chemical factors provided by the carrier morphology and functionalized surfaces, was used to act on SDF-1α/CXCR4 axis, a key target in chemotactic and regenerative processes.

Since PLA lacks of chemical groups to trigger specific cell response, PLA MCs were modified with two molecules: collagen, or a short peptide, bearing the cell-adhesive sequence RGD.

Collagen is a large ECM protein rich in: i) functional groups that allow for chemical reactions (i.e. crosslinking), ii) cell-adhesive motifs, and iii) domains able to bind growth factors and other signaling molecules [29]. On the other hand, the short RGD peptide is a simplified construct, bearing a single, but specific signal to promote cell adhesion [30]. Such molecules were introduced on PLA surfaces either via covalent or physisorbed mode of coupling. Unlike physisorption, covalent grafting induced higher collagen densities, since it forms a stable and durable coating, more resistant to being degraded, displaced or masked by competitor proteins found in biological fluids. Additionally, covalently bound macromolecules can present multiple grafting points to the surface, that limit the degree the coating can be stretched by cells, therefore affecting mechanosensing and cell behavior [27, 31]. Thus, these coatings provide the MCs with different physic-chemical properties that induce a broad spectrum of responses on MSCs, in terms of adhesion, proliferation, migration and targeting CXCR4/SDF-1α axis, as summarized in Table 2.

**Table 5.2: Effect of the functionalized MCs on MSC behavior. Plus and minuses indicate improvement and reduction, respectively.**

|      | Adhesion | Proliferation | CXCR4 expression | Migration |
|------|----------|---------------|------------------|-----------|
| PLA  | -        | -             | +                | ++        |
| CC   | +++      | +++           | ++               | -         |
| CP   | ++       | -             | ++               | ++        |
| RC   | +        | +++           | +                | -         |
| RP   | -        | -             | +                | ++        |

All the biomolecules introduced on PLA carriers are well-known promoters of cell adhesion and proliferation, which are indicators of cell health. However, physisorption of RGD short peptides appeared to be an unsuitable procedure to improve MSCs response to PLA, and thus to produce optimal MCs for cell delivery. In fact, for all the analyzed parameters (adhesion, proliferation, migratory potential), RP samples showed no significant difference with untreated MCs. This is most likely because physical interactions

between the short peptide and the surface are too weak to allow an efficient engraftment, and such surfaces may not be enriched with enough RGD domains that can influence cell adhesion. On the other hand, functionalization with collagen showed the best results, both in terms of number of attached cells and degree of spreading after 4 hours, indicating a rapid adhesion process. This is especially remarkable for CC MCs on which MSCs expressed clusters of vinculin, an indicator of focal adhesion complexes [32]. RC modification was suitable to enhance cell adhesion on PLA, although less efficiently than collagen-coated surfaces, both qualitatively and quantitatively.

MSCs proliferated on all the MCs, and for all samples confluence was reached between day 5 and 7 of culture. After this point only cell populations cultured on covalently coated surfaces maintained their pool, whereas all the other samples experienced a decrease in cell number, possibly due to detachment of cells aggregates. This result suggests that stable coatings, particularly collagen ones, might be suitable for long-term cell culture and expansion, which is necessary to achieve relevant amounts of MSCs for clinical applications. Furthermore, covalently modified MCs are able to preserve the pool of therapeutic cells for a longer period of time, thus presenting an advantage as cell delivery vehicles. The formation of large cell-MCs aggregates observed in this static culture assay can be avoided using a dynamic culture system, such as a spinner flask bioreactor [33]. Cell proliferation on individual or small groups of carriers is preferable, as it would make easier to administrate the therapy with direct injections. Implications of this culture technology in different aspects of regenerative medicine, as well as the injectability/extrudability of MCs suspensions are discussed Chapter 6.

Besides sustaining cell attachment and proliferation, the different functionalized surfaces had an impact on cell migratory capability. [12]. MSCs have been shown to migrate towards gradients of SDF-1α, which activates its cognate receptor on the cell membrane, CXCR4. This pathway plays a major role in MSCs recruitment, homing and specific localization in damaged, tumoral and ischemic tissues [12]. Although such migratory behavior was observed both *in vitro* and *in vivo* [34], harvested MSCs that are expanded with conventional techniques in T-flasks are known to quickly lose the functional expression of CXCR4 at the cell membrane [35]. Our results for MSCs cultured on 2D TCPS confirm this tendency: almost the totality of the cell population expressed the receptor intracellularly, but only a small pool (3-5%) retained surface CXCR4. To explain this, in previous studies it was postulated that MSCs undergo a certain degree of differentiation during *in vitro* expansion [36]. However, the stimuli provided by 3D culture on MCs determined a sensible increment of surface CXCR4 positive cells. This change in the receptor expression is reversible, as MSCs can resume expressing CXCR4 only intracellularly if retrieved from the MCs and plated again on TCPS. Therefore, such behavior appears to be due to an adaptation of MSCs to the culture condition, rather than a differentiation or ageing process. A comparable result was observed by Potapova *et al.,* when culturing MSCs as spheroids, and may be attributed to cytoskeleton reorganization or improved cell-cell communication in MSCs aggregates in spheroids and MCs [13].

In the search for improved recruitment and engraftment into damaged tissues, enhancing functional CXCR4 expression of *in vitro* cultured MSCs is a promising target for cell therapy. For instance, Wiehe *et al.*

successfully transfected MSCs expanded on standard TCPS to highly overexpress surface CXCR4 (> 90% of the cells) [19]. Culture and subsequent transplantation of MSC-laden MCs can be a powerful method to perform MSCs expansion with improved CXCR4 expression and localization, without the need of genetic modification. The modulation of such expression can be controlled by MCs design. In fact, CXCR4 expression also greatly depends on an accurate choice of the chemistry of the biomaterial substrate, varying widely between untreated particles, collagen coating or even glass-coated polystyrene MCs. The mechanism behind this effect is not clear yet, although it has been suggested that CXCR4 can be a part of complexes assembled at the point of focal adhesions [13]. Furthermore, SDF-1α was found to activate focal adhesion kinase in hematopoietic cells and to induce cytoskeleton rearrengements [37]. Thus, it can be hypothesized that MSCs tuning of CXCR4 expression and localization may be related to integrin-mediated pathways dependent on the material chemistry, MSCs cytoskeletal reorganization on 3D, spherical MCs, and possibly improved cell-cell contacts, typical in MCs culture [38].

The only parameter affecting cell delivery potential after SDF-1α stimulation was the mode of coating attachment. Given a mode of functionalization, comparable migration indexes were found for both RGD and collagen coatings, even though with the latter MSCs had improved CXCR4 surface expression. CXCR4 overexpression, although beneficial for *in vivo* homing [39], was found ineffective to enhance the already high MSCs tendency to migrate *in vitro* [19]. Covalent functionalizations reduced cell migration from MCs, whereas physisorbed coatings and untreated PLA MCs were associated with higher migration indexes. Cell migration had been previously related to the method of coupling of ECM ligands, in studies involving 2D biomaterials surfaces. HUVECs cultured on covalent fibronectin coatings grew as monolayers and were unable to properly migrate, whereas they were able to migrate and associate into capillaries if seeded on coatings weakly bound to the biomaterial [40]. This behavior was related to ECM sensing and reorganization mediated by specific integrins [40, 41]. A similar mechanism might play a role in tuning MSCs adhesion and migration from MCs. Mechanosensing of stiffer covalent coatings, which influences stem cells differentiation [31], could also guide cells fate in terms of migration, inducing retention on MCs surface, rather than release. MCs functionalization affected the non-specific basal migration of the MSCs, in absence of SDF-1α and VEGF gradients, rather than their response to chemoattractants. In fact, for all the samples, including MSCs cultured without MCs, the efficacy of chemokines stimulation was comparable, and induced a 2-fold migration index increment, compared to the basal condition. Switching between physisorptive and covalent functionalization methods could be used to exert a control over cell delivery. On one hand, covalent coatings should be preferred when retention of MSCs on the biomaterial carrier is needed (i.e. several tissue engineering strategies), but also when it is necessary to prevent unspecific cell dispersion, towards tissues that are not secreting SDF-1α. On the other hand, MCs with physisorbed coatings could be beneficial when quick release of higher amounts of cells is desired.

**5.5 Conclusions**

PLA MCs are promising devices for cell therapy. MCs modified covalently with collagen enhance MSCs adhesion and proliferation, thus offering a suitable environment for cell survival, homing and expansion. Surface functionalization allows acting on MSCs migratory behavior in response to chemokines, and directly affects SDF1-α/CXCR4 axis. In fact, MCs culture, combined with the mode of binding and the nature of the coating, permits to tune CXCR4 expression during in vitro cell expansion. Higher CXCR4 functional localization on collagen-modified surfaces, regardless of the mode of coating, suggests such modification can be profitable to use MCs to improve cell grafting after transplantation. Simplified constructs such as RGD short peptides, although successful in promoting cell attachment, cannot trigger the mechanical or chemical pathways that improve the expression of the receptor. Physisorptive and covalent modifications respectively maintain and reduce the basal level of MSCs migration from the MCs, while not affecting the efficacy of SDF-1α at mobilizing cells. This knowledge can be useful to apply MCs to exploit or limit untriggered cell release, and balance SDF-1α mediated MSCs recruitment towards specific target tissues. Furthermore, these are key findings to aid the design of new biomaterials devices for efficient and controllable cell delivery.

**5.6 References**

[1]     Vacharathit V, Silva EA, Mooney DJ. Viability and functionality of cells delivered from peptide conjugated scaffolds. Biomaterials. 32(15) (2011) 3721-8.

[2]     Hofmann M, Wollert KC, Meyer GP, Menke A, Arseniev L, Hertenstein B, et al. Monitoring of bone marrow cell homing into the infarcted human myocardium. Circulation. 111 (2005) 2198-202.

[3]     Zhiqiang L, Haibin W, Yan W, Qiuxia L, Anning Y, Feng C et al. The influence of chitosan hydrogel on stem cell engraftment, survival and homing in the ischemic myocardial microenvironment. Biomaterials. 33 (2012) 3093-106.

[4]     Reis LA, Chiu LL, Liang Y, Hyunh K, Momen A, Radisic M. A peptide-modified chitosan-collagen hydrogel for cardiac cell culture and delivery. Acta Biomater. 8(3) (2012) 1022-36.

[5]     Hernández RM, Orive G, Murua A, Pedraz JL. Microcapsules and microcarriers for in situ cell delivery. ADV Drug Deliv Rev. 62(1-8) (2010) 711-30.

[6]     Mooney DJ, Vandenburgh H. Cell delivery mechanisms for tissue repair. Cell Stem Cell. 2(3) (2008) 205-13.

[7]     Das M, Sundell IB, Koka PS. Adult mesenchymal stem cells and their potency in the cell-based therapy. J Stem Cells. 8(1) (2013) 1-16.

[8]     Zhang M, Mal N, Kiedrowski M, Chacko M, Askari AT, Popovic ZB, Koc ON, Penn MS. SDF-1 expression by mesenchymal stem cells results in trophic support of cardiac myocytes after myocardial infarction. FASEB J. 21(12) (2007) 3197-207.

[9]     Bexell D, Gunnarsson S, Tormin A, Darabi A, Gisselsson D, Roybon L, et al. Bone marrow multipotent mesenchymal stroma cells act as pericyte-like migratory vehicles in experimental gliomas. Mol Ther. 17(1) (2009) 183-90.

[10]    Alieva M, Bagó JR, Aguilar E, Soler-Botija C, Vila OF, Molet J, et al. Glioblastoma therapy with cytotoxic mesenchymal stromal cells optimized by bioluminescence imaging of tumor and therapeutic cell response. PLos One. 7(4) (2012) e35148.

[11]    Xu F, Shi J, Yu B, Ni W, Wu X, Gu Z. Chemokines mediate mesenchymal stem cell migration toward gliomas in vitro. Oncol Rep. 23(6) (2010) 1561-7.

[12]    Liu X, Duan B, Cheng Z, Jia X, Mao L, Fu H, et al. SDF-1/CXCR4 axis modulates bone marrow mesenchymal stem cell apoptosis, migration and cytokine secretion. Protein Cell. 2(10) (2011) 845-54.

[13]    Potapova IA, Brink PR, Cohen IS, Doronin SV. Culturing of human mesenchymal stem cells as three-dimensional aggregates induces functional expression of CXCR4 that regulates adhesion to endothelial cells. J Biol Chem. 283(19) (2008) 13100-7.

[14]    Nagasawa T, Hirota S, Tachibana K, Takakura N, Nishikawa S, Kitamura Y, et al. Defects of B-cell lymphopoiesis and bone-marrow myelopoiesis in mice lacking the CXC chemokine PBSF/SDF-1. Nature. 382 (1996) 635-8.

[15]    Zou YR, Kottmann AH, Kuroda M, Taniuchi I, Littman DR. Function of the chemokine receptor CXCR4 in haematopoiesis and in cerebellar development. Nature. 393 (1998) 595-9.

[16]    Lau TT, Wang DA. Stromal cell-derived factor-1 (SDF-1): homing factor for engineered regenerative medicine. Expert Opin Biol Ther. 11(2) (2011) 189-97.

[17]    Gonçalves RM, Antunes JC, Barbosa MA. Mesenchymal stem cell recruitment by stromal derived factor-1-delivery systems based on chitosan/poly(γ-glutamic acid) polyelectrolyte complexes. Eur Cell Mater. 23 (2012) 249-60.

[18]    Huang YC, Liu TJ. Mobilization of mesenchymal stem cells by stromal cell-derived factor-1 released from chitosan/tripolyphosphate/fucoidan nanoparticles. Acta Biomater. 8(3) (2012) 1048-56.

[19] Wiehe JM, Kaya Z, Homann JM, Wöhrle J, Vogt K, Nguyen T, et al. GMP-adapted overexpression of CXCR4 in human mesenchymal stem cells for cardiac repair. Int J Cardiol. 167(5) (2013) 2073-81.

[27] Puñet X, Machauffé R, Giannotti MI, Rodríguez-Cabello JC, Sanz F, Engel E, Mateos-Timoneda MA, Planell JA. Enhanced cell-material interactions through the biofunctionalization of polymeric surfaces with engineered peptides. Biomacromolecules. 14(8) (2013) 2690-702.

[28] Gonzalez-Vazquez AG, Planell JA, Engel E. Extracellular calcium and CaSR drive osteoinduction in mesenchymal stromal cells. Acta Biomater. (2014) doi:10.1016/j.actbio.2014.02.004.

[29] Ferreira AM, Gentile P, Chiono V, Ciardelli G. Collagen for bone tissue regeneration. Acta Biomater. 8(9) (2012) 3191-200.

[30] Hersel U, Dahmen C, Kessler H. RGD modified polymers: biomaterials for stimulated cell adhesion and beyond. Biomaterials. 24 (2003) 4385-415.

[31] Trappmann B, Gautrot JE, Connelly JT, Strange DG, Li Y, Oyen ML, et al. Extracellular-matrix tethering regulates stem-cell fate. Nat Mater. 11(7) (2012) 642-9.

[32] Filová E, Brynda E, Riedel T, Chlupáč J, Vandrovcová M, Svindrych Z, et al. Improved adhesion and differentiation of endothelial cells on surface-attached fibrin structures containing extracellular matrix proteins. J Biomed Mater Res A. 102(3) (2014) 698-712.

[33] Rafiq QA, Brosnan KM, Coopman K, Nienow AW, Hewitt CJ. Culture of human mesenchymal stem cells on microcarriers in a 5 l stirred-tank bioreactor. Biotechnol Lett. 35(8) (2013) 1233-45.

[34] Egea V, von Baumgarten L, Schichor C, Berninger B, Popp T, Neth P, et al. TNF-α respecifies human mesenchymal stem cells to a neural fate and promotes migration toward experimental glioma. Cell Death Differ. 18(5) (2011) 853-63.

[35] Wynn RF, Hart CA, Corradi-Perini C, O'Neill L, Evans CA, Wraith JE, et al. A small proportion of mesenchymal stem cells strongly expresses functionally active CXCR4 receptor capable of promoting migration to bone marrow. Blood. 104(9) (2004) 2643-5.

[36] Honczarenko M, Le Y, Swierkowski M, Ghiran I, Glodek AM, Silberstein LE. Human bone marrow stromal cells express a distinct set of biologically functional chemokine receptors. Stem Cells. 24(4) (2006) 1030-41.

[37] Glodek AM, Le Y, Dykxhoorn DM, Park SY, Mostoslavsky G, Mulligan R, et al. Focal adhesion kinase is required for CXCL12-induced chemotactic and pro-adhesive responses in hematopoietic precursor cells. Leukemia. 21(8) (2007) 1723-32.

[38] Sart S, Errachid A, Schneider YJ, Agathos SN. Modulation of mesenchymal stem cell actin organization on conventional microcarriers for proliferation and differentiation in stirred bioreactors. J Tissue Eng Regen Med. 7(7) (2013) 537-51.

[39] Chen W, Li M, Cheng H, Yan Z, Cao J, Pan B, et al. Overexpression of the mesenchymal stem cell Cxcr4 gene in irradiated mice increases the homing capacity of these cells. Cell Biochem Biophys. 67(3) (2013) 1181-91.

[40]    Herklotz M, Werner C, Pompe T. The impact of primary and secondary ligand coupling on extracellular matrix characteristics and formation of endothelial capillaries. Biomaterials. 30(1) (2009) 35-44.

[41]    Pompe T, Markowski M, Werner C. Modulated fibronectin anchorage at polymer substrates controls angiogenesis. Tissue Eng. 10(5-6) (2004) 841-8.

# CHAPTER 6

# Cell-laden microcarriers as building elements for tissue constructs via 3D bioprinting

*In this chapter, polylactic acid microcarriers developed according to the method described in Chapter 3 are used as components to generate 3D living tissue constructs, by means of a bioprinting technology. The microcarriers are colonized by MSCs and characterized for their ability to support osteogenic differentiation. Cell-laden microcarriers are mixed with a gelatin-methacrylamide/gellan gum hydrogel to form a composite bioink. The suitabiltiy of this mixture for bioprinting is characterized, together with its effect on hydrogel mechanical properties, cell viability and bone formation in vitro, and eventually constructs are biofabricated, via an additive manufacturing process. With such technique, osteochondral models, consisting of bone and a cartilage-mimicking layers, printed using the composite bioink and the gelatin-based hydrogel alone, are produced to show the potential of the proposed approach.*

*This work was developed in collaboration with the Department of Orthopaedics of the University Medical Center Utrecht (UMC Utrecht, The Netherlands). Part of the experimental work was performed during a research stay at UMC Utrecht, under the supervision of Dr. Jos Malda.*

## 6.1 Introduction

Tissue engineering can yield three-dimensional (3D) tissue-like constructs that can serve as experimental platforms for biological studies and drug screening [1], and as implants for clinical application. Recapitulating the complexity of living tissues, with regards to the variations in cell types, matrix components and organization, remains however a major challenge. Bioprinting is an innovative technology that allows for the generation of organized 3D tissue constructs via a layer-by-layer deposition process of cells and biomaterials [2, 3]. In this way, hydrogel matrices with embedded viable cells have already been produced, such as functional vascular-like networks with enhanced transfer of nutrients [4, 5]. In this fashion, bioprinting can potentially address the zonal organization of cartilage and osteochondrondral constructs [6-8].

The building materials in biofabrication are generally cell-laden hydrogels - also known as bioinks. Bioinks are critical components in biofabrication, as they should possess the right rheological parameters required for the printing process and, simultaneously, offer an optimal environment for cell survival, proliferation, migration and biosynthetic activity [9, 10]. Among them, thermo- and photoresponsive gelatin methacrylamide (GelMA) has been proven as a versatile and promising platform for cartilage tissue engineering [11]. At the same time, by blending GelMA with viscosity enhancers, such as hyaluronic acid [12] or gellan gum [6, 13], it displays improved properties for printing of geometrically complex structures.

There are several challenges in the fabrication of hydrogel-based tissue constructs. For example, hydrogels provide a highly hydrophilic microenvironment in which suspended cells are constrained to a round shape, regardless their native morphology [14]. Therefore, inclusion of cues to guide cell fate would be desired. Second, printing of large, clinically-relevant grafts requires the encapsulation of high amounts of cells, which are difficult to obtain from biopsies [15]. For this reason, time-consuming 2D expansion steps are required, which reduces the therapeutic potential of the cultured cells by affecting their phenotype (e.g. dedifferentiation, loss of pluripotency) [16]. Moreover, hydrogels are too soft for application in load-bearing locations in the body [8]. Consequently, strategies to enhance biological and mechanical properties of bioinks, and the high numbers of regenerative cells which will have to be incorporated or attracted once implanted in the host in order to obtain functional tissue constructs.

A potential solution would be to produce composite printable materials by suspending particles with bioactive potential into the hydrogel matrix. Among particulate materials, microcarriers (MCs) are especially interesting, due to their versatility and wide array of applications. Injectable MCs designed to promote attachment, homing and survival of adherent-dependent cells [17, 18], and suitable for cell expansion in stirred bioreactors, allow for the generation of high cell amounts and cell-MCs complexes. These aggregates are rich in cell contacts and extracellular matrix (ECM), that resemble the *in vivo* microenvironment, resulting in improved biological activity of cells [19]. Fo instance, many cell types cultured on MCs, including chondrocytes [20], osteoblasts [20], keratinocytes [21] and tenocytes [22] have been found to better retain their phenotype and display greater potential to regenerate the tissue of their competence

compared to 2D culture. Mesenchymal Stromal Cells (MSCs) from different sources (i.e. bone marrow, adipose tissue, placenta-derived) can be cultured on MCs to either preserve their pluripotency or to improve their differentiation [17, 23]. Moreover, MCs can be loaded with bioactive molecules as a cue to guide the differentiation of cells [24, 25]. Cultured MCs can be easily embedded in hydrogel matrices, and their encapsulation increases the mechanical strength of the gel, and offers a high cell-anchoring and spreading surface [26, 27, 28]. In addition, osteoblastic cells have been shown to induce superior formation in a synthetic hydrogel when incorporated as complexes with MCs compared to suspended cells. This indicates that MC-loaded hydrogels are promising composite materials for bone regeneration [14]. Thus, MCs are potential candidates to perform cell expansion, improve hydrogels mechanical properties and introduce cues to guide cell behavior.

The aim of this work is to generate living tissues constructs of clinically relevant sizes, by combining bioprinting and MC culture technologies. GelMA-based hydrogels were used as bioinks, and the effect of the incorporation of custom designed polylactic acid MCs was evaluated for the mechanical and printing properties. In addition, morphology and osteogenic potential of cells in MC-laden bioinks was assessed. Several methods were explored to obtain MC-enriched bioinks, including culture of MSCs on MCs in a spinner flask bioreactor, prior to biofabrication. To provide a proof of application of such an approach, biphasic scaffolds consisting of an osteogenic layer with MC-laden bioink, and a cartilage region composed by MC-free bioink were fabricated.

## 6.2 Materials and Methods

### 6.2.1 Materials

Polylactic acid (PLA, Purasorb PLDL 7038, IV midpoint 3.8 dL g$^{-1}$, Mw $\approx$ 850000 Da) was purchased from Purac (The Netherlands). (–)-Ethyl-L-lactate (purity = 99.0%) and polyvinyl alcohol (PVA, 30–70 kDa, 88% hydrolyzed) were obtained from Sigma-Aldrich (Spain). PLA MCs were fabricated with the method described in Chapter 4. MCs with a mean diameter of 120 µm, and a surface area of 2 cm$^2$ mg$^{-1}$ were used. GelMA was synthesized from gelatin derived from porcine skin (Sigma-Aldrich) as described elsewhere [8]. GelMA hydrogels were obtained by dissolving GelMA (10% w/v) in deionized water supplemented with 5.4% w/v D-mannose (Sigma-Aldrich) and 0.1% w/v of Irgacure 2959 (Ciba, BASF, Germany) under magnetic stirring for 20 minutes at 90°C. In order to optimize GelMA as a bioink for 3D printing, 1% w/v gellan gum (Gelzan$^{tm}$ CM, Sigma-Aldrich) was added. Cells and cell-laden MCs were mixed in the GelMA solutions. The other reagents where purchased from Sigma-Aldrich, unless specified otherwise.

### 6.2.2 Microcarrier surface modification

PLA MCs were functionalized with human recombinant collagen type I (FibroGen, USA), in order to improve cell response to the material, according to the protocol described in Chapter 5 [29]. Briefly, MC

surface was enriched in carboxyl group by controlled hydrolysis in 50 mM NaOH for 10 minutes. The generated groups were activated with ethyl(dimethylaminopropyl) carbodiimide (Acros Organics, Belgium) and N-hydroxysuccinimide. This allowed for the covalent binding between the free amines of the collagen and the activated COOH, after soaking the samples in a collagen type I solution (100 µg mL$^{-1}$, 24 hours). All reactions byproducts were water soluble and eliminated by washing the samples in Phosphate Buffered Saline (PBS).

### 6.2.3 Cells and culture conditions

MSCs were isolated from the long bones of 2-4 weeks old Lewis rats according to a previously published protocol and as already described in Chapter 5 [30]. The protocols concerning the animal care were previously approved by Committee on the Ethics and Animal Experiments of the Scientific Park of Barcelona (Permit number: 0006S/13393/2011). Cell expansion and experiments were carried out by culturing MSCs in proliferation medium, consisting of Advanced DMEM, supplemented with 10% FBS, 1% Pen/Strep and 1% L-glu.

### 6.2.4 Microcarrier culture

MCs were prepared for cell culture by soaking them in 70% v/v ethanol, repeated washing with PBS under sterile conditions, and incubation in serum-free tissue culture medium. MSCs were cultured on PLA MCs both under static and dynamic conditions. For static culture, 3 mg of MCs were placed into an ultra-low attachment multiwell plate (Costar, Corning Inc., USA). The MSC suspension was seeded directly onto the particles, at a density between $1 \cdot 10^5 - 3 \cdot 10^5$ cells/well. For dynamic culture, a 250 mL spinner flask device was used (BellCo, USA). The bioreactor was filled with 100 mL of culture medium and 2 g L$^{-1}$ of MCs. The inoculum consisted of $2 \cdot 10^5$ cells mL$^{-1}$. An intermittent stirring regime was maintained for the first 6 hours of culture (30 rpm for 1 minute every 30 minutes). After this seeding period, the suspension was stirred continuously at 30-35 rpm. 2 mL samples were taken from the MCs suspension to estimate the number of cells in culture. The MC-MSCs complexes were lysed with M-PER solution (Thermo Scientific, Spain). The cell amount was calculated from a standard curve, by measuring lactate dehydrogenase (LDH) activity in the supernatant using the Cytotoxicity Detection Kit$^{PLUS}$ (Roche, Switzerland).

### 6.2.5 Cell viability in MC-laden bioinks

30 mg mL$^{-1}$ of MCs where either preseeded with MSCs and then suspended into GelMA-Gellan Gum solutions, or directly co-suspended with the cells into the hydrogels. The mixtures were then manually dispensed through a 20G conical needle (inner diameter = 0.61 mm, Nordson EFD, USA) into a multiwell plate and exposed to UV irradiation (intensity of 4 mWcm$^{-2}$, $\lambda$ = 365 nm for 15 minutes) to induce an irreversible crosslinking of the hydrogel. At day 1 and 3 of culture, MSC viability was evaluated from microscopy images using a LIVE/DEAD Assay (calcein AM/ethidium homodimer, Life Sciences, USA). 5 random fields for each sample (n=3) were used to count living cells. A control group was prepared by

dispensing MSC-laden MCs suspended in PBS and not exposed to UV light. To evaluate cell localization on MCs and into the hydrogel, samples were cultured for 4 hours, fixed in buffered paraformaldehyde, permeabilized with 0.5% v/v Triton X-100 and stained with phalloidin-FITC (Life Sciences, USA) and 4',6-diamidino-2-phenylindole (DAPI).

*6.2.6 Mechanical properties of MC-laden bioink*

The effect of MC concentration on the compressive modulus of GelMA-Gellan Gum hydrogels was assessed in an unconfined uniaxial compression test, using a dynamic mechanical analyzer (TA 2980 DMA, TA Instruments, USA). UV-crosslinked hydrogels samples measuring 4x4x2 mm, containing increasing amounts of MCs (0, 30, 40 and 50 mg/mL) were subjected to a force ramp of 1 N/min up to 4 N and the related stress-strain curve was obtained. The slope of the curve in the elastic region was used as a representative value for the compression modulus. 5 replicates for each sample were tested. The assay was performed at room temperature.

*6.2.7 Osteogenic differentiation*

The role of MCs in the differentiation of MSCs towards the osteogenic lineage was investigated. First, MC culture was compared to standard culture on 2D polystyrene surfaces. After that, the differentiation capability of the cells encapsulated in GelMA based hydrogels was evaluated. To this end, 30 µL of hydrogel mixture was placed into a poly(dimethyl siloxane) mold and UV-crosslinked. A preliminary test evaluating the effect of different MCs concentrations on osteogenic differentiation was also performed. Since no consistent differences were found, we kept the concentration of MCs at 30 mg/mL for the differentiation assay. The volume of the gels samples used (30 uL), the cells densities and MCs amount where chosen so that all the experimental group had approx. the same number of cells. The experimental groups are summarized in Table 6.1.

**Table 6.2: Experimental groups analyzed in the osteogenic differentiation assay.**

| Experimental group | Description | MSCs density |
|---|---|---|
| TCPS | Culture on 2D tissue culture polystyrene surfaces | $10^5\,cm^{-2}$ |
| MCs | Static culture on MCs | $10^5\,cm^{-2}$ |
| GelMA | Cells encapsulated in GelMA | $8 \cdot 10^6\,mL^{-1}$ |
| GelMA-GG | Cells encapsulated in GelMA-Gellan Gum | $8 \cdot 10^6\,mL^{-1}$ |
| GelMA-GG MC-MSCs | Preseeding on 30 mg mL$^{-1}$ MCs overnight and encapsulation in GelMA-Gellan Gum hydrogels | $8 \cdot 10^6\,mL^{-1}$ |
| GelMA-GG MCs and MSCs | 30 mg mL$^{-1}$ MCs and the cell suspension are mixed together in GelMA-Gellan Gum hydrogels, with no preseeding | $8 \cdot 10^6\,mL^{-1}$ |

All samples were cultured for 21 days either in medium with or without supplemented osteogenic factors ($10^{-8}$ M dexamethasone, 50 µg mL$^{-1}$ ascorbic acid, 10 mM β-glycerol phosphate). Differentiation was studied by quantifying alkaline phosphatase (ALP) activity at day 7, 14 and 21 of culture; osteocalcin (OCN) secretion at day 14 and 21, and by alizarin red staining on cryostat sections at day 21 to assess the deposition of mineralized matrix. For ALP analysis, samples were washed with sterile PBS and the hydrogels were grinded using a pestle. Protein extracts were obtained inducing cell lysis with M-PER solution, followed by centrifugation for 15 minutes at 2500 rpm, to remove debris from cells, gels and MCs. ALP activity was measured using Sensolyte® pNPP Alkaline Phosphatase Assay Kit (AnaSpec, Inc., USA). OCN quantification was performed from cell culture supernatant using an Enzyme-Linked ImmunoSorbent Assay kit (Demeditec Diagnostic GmbH, Germany), following the instructions of the manufacturer. OCN and ALP data were normalized against total cell number, as evaluated measuring LDH activity.

## 6.2.8 Bioprinting of MC-laden GelMA

Models of the constructs were obtained using Computer Aided Design (CAD) software (Rhinoceros, McNeel, Seattle, WA, USA). The CAD files were loaded in Computer Aided Manufacturing (CAM) software (PrimCAM, Einsiedeln, Switzerland), and printed with the Bioscaffolder system (SYS+ENG, Salzgitter-Bad, Germany), which has been described previously [11]. GelMA-GG hydrogels loaded with MCs, tested for printability, and used as a bioink. While 50 mg mL$^{-1}$ was the highest printable MC suspension, a concentration of 40 mg mL$^{-1}$ MCs was chosen to maximize the amount of MCs and loaded cells, while simultaneously maintain a safety margin to prevent nozzle clogging by formation of MC-MSCs complexes during the pre-culture period. The optimal settings for printing were found to be an extrusion velocity of 2.40 (adimensional number) and a printing speed of 475 mm/min, at room temperature. The dispensing tip was a 20G conical nozzle. Distance between the hydrogel strands was set at 2.25 mm in the CAM model, while layer-to-layer spacing was set to 0.4 mm. Printed constructs were then UV cured for 5 minutes (λ = 320–500 nm, intensity of 6 mWcm$^2$ at 365 nm, Superlite S-UV 2001AV lamp, Lumatec, Germany), and the immediately captured with an Olympus DP70 camera connected to a stereomicroscope. MC-MSCs complexes were introduced into the GelMA-GG hydrogels in order to assess the effect on cell viability and printability. MSCs were either pre-cultured on MCs under static conditions (12h) or in a spinner flask bioreactor for 5 days. For these assays, cylindrical, single-layered constructs were produced (diameter 16 mm, height 2.5 mm), using the settings described previously. To test cell viability, the constructs were cultured for 1 and 3 days in proliferation medium and then were analyzed with a LIVE/DEAD assay. Cell distribution in the printed constructs was observed with a fluorescence microscope (Olympus BX51, Olympus, USA), after staining cells for actin. In the samples, a total of $10 \cdot 10^6$ cells mL$^{-1}$ was encapsulated, with or without 40 mg mL$^{-1}$ of MCs.

## 6.2.9 Fabrication of bilayered osteochondral models

Cylindrical, bilayered constructs with anatomically relevant size (diameter 16 mm, height 5 + 5 mm) were fabricated, composed of two different bioinks. GelMA-GG encapsulating 40 mg mL$^{-1}$ MCs was used to

represent the bone compartment, while the cartilage layer was printed using the GelMA-GG without MCs. The optimal conditions to print the hydrogel without MCs were found to be an extrusion velocity of 3.80, a printing speed of 600 mm/min, and 34°C temperature.

## *6.2.10 Statistical analysis*

Each experiment was performed in three or five replicates (n=3 or 5). Data are presented as mean and standard deviation of the replicates. Statistical significance was assessed performing Student's t-test using Origin 8.0 Software (OriginLab, USA).

## 6.3 Results

### *6.3.1 Cell viability in MC-laden bioinks*

Non-viscous suspensions of MSC-loaded microcarriers in PBS (30 mg mL$^{-1}$) where successfully dispensed without clogging of the syringe needle. After dispensing, 80% of the cells were viable 1 day and more than 90% after 3 days (Figures 6.1A, 6.1B and 6.1E). MCs, cells and MC-MCS complexes suspended in GelMA-GG were homogeneously distributed in the gel matrix and showed good cell viability (Figures 6.1C-G). Pre-seeded particles suspended in the gels had the lowest number of viable cells (60%) after 1 day of culture, which recovered to 90% after 3 days, indicating a high proliferation rate. Interestingly, MSCs that were separately mixed with MCs into GelMA-GG hydrogels, without a pre-seeding step, were found attached to the MCs surface. After 4h, in presence of GelMA, MSCs were found in an early stage of adhesion onto MCs, whereas they already expressed organized actin fibers if seeded directly on the MCs (Figures 6.2A and 6.2B).
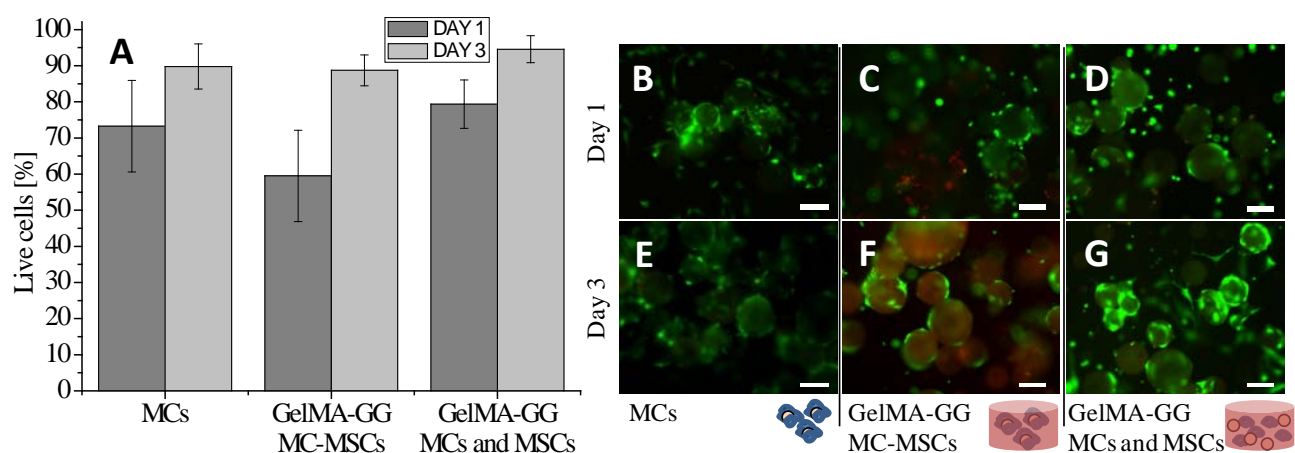


**Figure 6.1: (A) Viability of MSCs after dispensing; (B,E) Non-encapsulated cells cultured on MCs; (C,F) gels loaded with pre-cultured MC-MSC complexes and (D,G) with cells and MCs separately. Scale bar represents 50 μm.**

GelMA-GG
MCs and MSCs

MCs
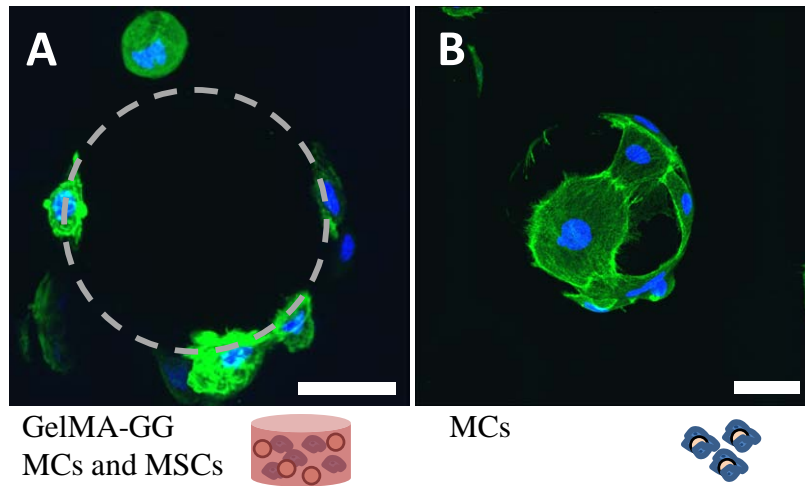
**Figure 6.2: (A) Morphology of MSCs 4 hours after mixing with cell-free microcarriers in GelMA-GG (dashed circle indicates a MC) and (B) seeded directly on the MCs in absence of the gel. Scale bar is 40 μm. Cytoskeleton stained in green, nuclei in blue.**

*6.3.2 Mechanical properties of MC-laden GelMA*

The incorporation of MCs into the GelMA-GG hydrogels resulted in an increment of the compressive modulus (Figure 6.3). The stiff PLA MCs reinforced the softer hydrogel matrix, and the compression modulus increased along with the MC concentration. For the highest concentration tested, stiffness was 2-fold higher than for MC-free gels.
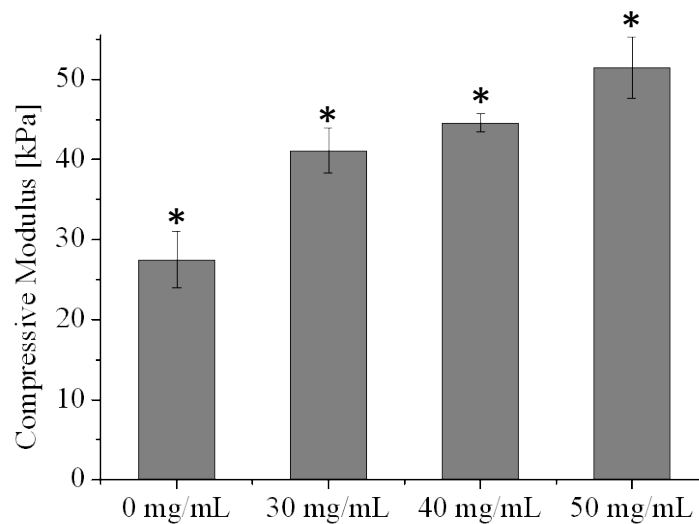


**Figure 6.3: Compression modulus of GelMA-GG with different concentrations of MCs. The four samples show significantly different moduli (p<0.05).**

*6.3.3 Osteogenic differentiation of MSCs*

Cell number was monitored along the culture time (7, 14 and 21 days) using the LDH assay, and cell amounts were comparable between all the experimental groups, ranging between $2 \cdot 10^5$ and $2.5 \cdot 10^5$ cells/sample. When MSCs were cultured in proliferation medium, no significant change in the expression of

bone markers was observed during culture for all samples, suggesting the absence of spontaneous differentiation. In presence of osteogenic medium, ALP activity increased over time and was considerably higher for 2D monolayer cultures compared to 3D MC culture (Figure 6.4A). However, MC-MSC complexes displayed enhanced OCN secretion, while histological analysis of both samples revealed the deposition of mineralized matrix, thus suggesting a consistent MSCs differentiation. MC culture also showed areas of alizarin red positive staining (Figure 6.5), in case standard proliferation medium was used.

During long-term culture of hydrogel samples under osteogenic conditions, GelMA and GelMA-GG samples induced higher levels of active ALP, when compared to the gels with incorporated MCs (either pre-seeded with cells or not). On the other hand, encapsulated MC-MSC complexes secreted more OCN compared to the other experimental groups, indicating cell differentiation and a production of mature components of bone matrix. In all experimental samples cultured in osteogenic medium, MSCs deposited calcified matrix. However, both in GelMA and GelMA-GG samples, the mineralized ECM appeared as discrete and small alizarin red stained areas, more likely in the proximity of the cells suspended into the gel matrix (Figure 6.6). Instead, GelMA-GG MC-MSCs samples displayed a diffuse staining surrounding the MCs.
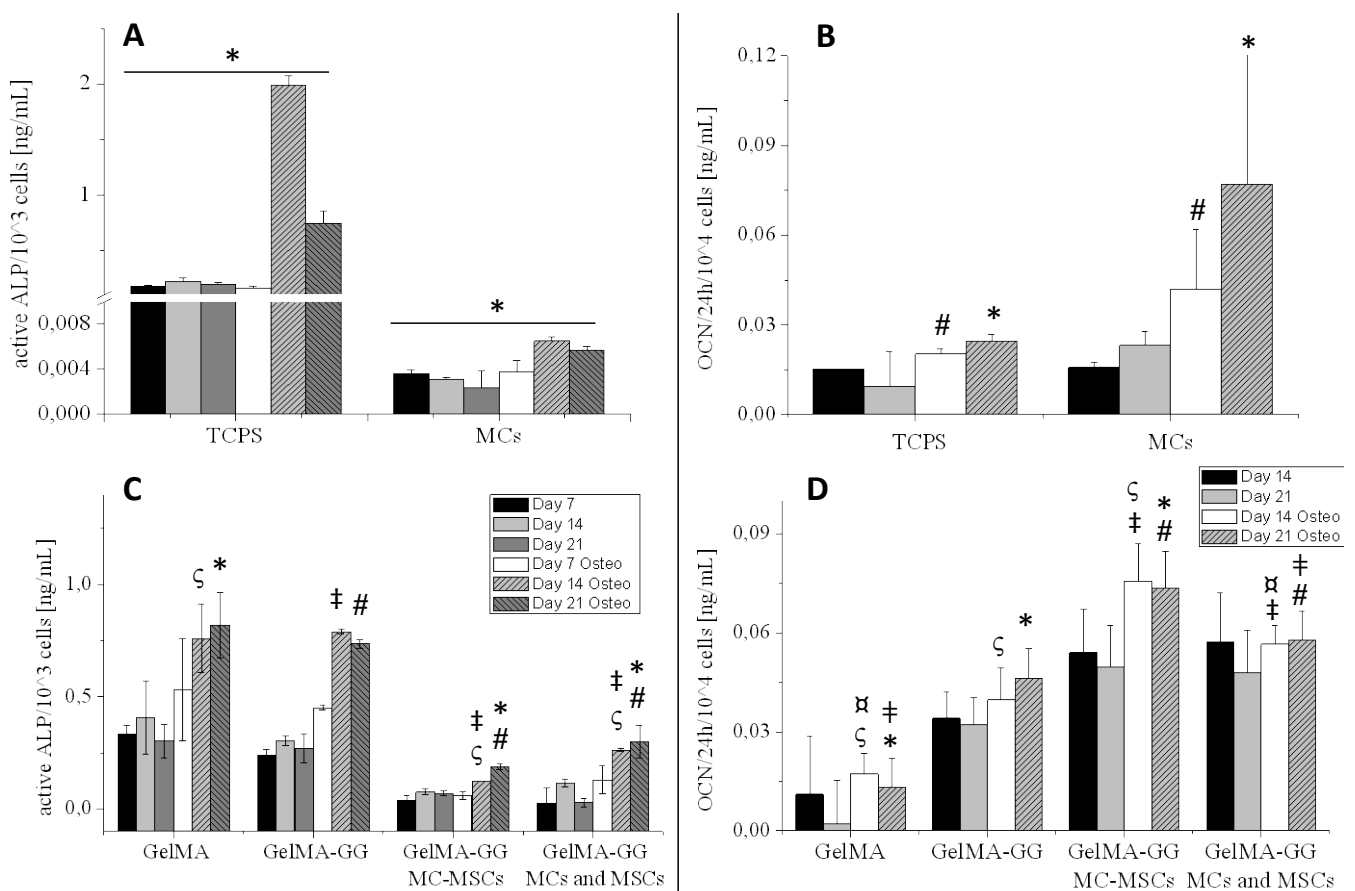


**Figure 6.4: (A) ALP and (B) OCN produced by MSCs in 2D culture (TCPS) and MCs. Quantification of (C) ALP and (D) OCN from GelMA-based hydrogels with or without MCs. The symbols group together samples that display statistically significant differences between them (p<0.05).**
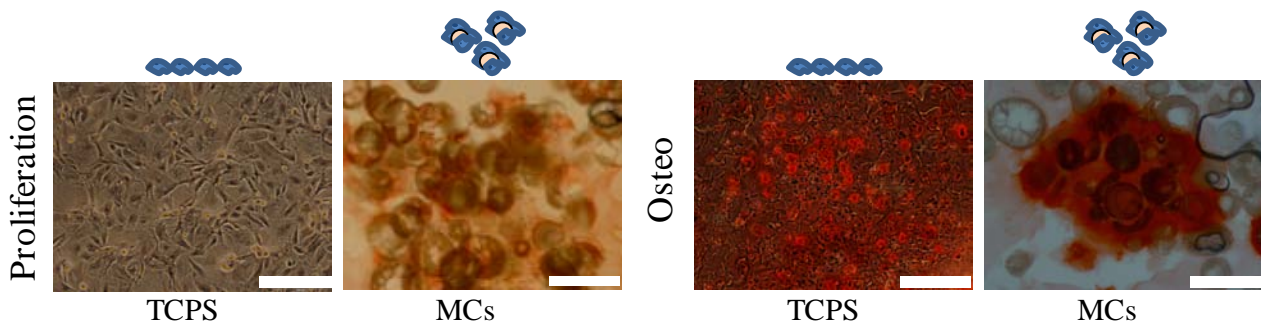
**Figure 6.5: Alizarin red staining of monolayer cell cultures on TCPS and static MC culture after 21 days. Scale bar is 200 μm.**
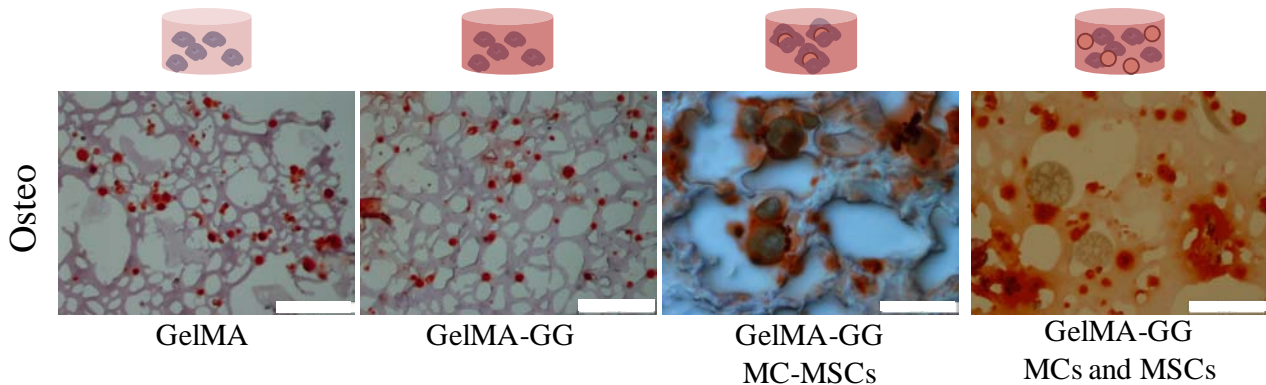


**Figure 6.6: Alizarin red staining on hydrogel samples after 21 days of culture in osteogenic medium. Scale bar is 200 μm.**

### 6.3.5   Bioprinting of MC-MSC constructs

MC-MSC laden bioinks were printable, meaning that they formed strands upon extrusion able to retain their shape. Cell laden constructs were fabricated with a strand diameter of $715 \pm 86$ and pore width of $1006 \pm 121$ μm. MSCs and MC-MSC complexes displayed a high viability after the automated printing process, both following static seeding and dynamic MC culture (Figure 6.7). MC-MSCs were cultured in a spinner flask, and excessive aggregation of the MCs was prevented. Viability values at day 1 and 3 after printing and photocrosslinking were comparable to those observed when MC-MSCs were dispensed manually. For all tested modalities, constructs were fabricated with homogeneous distribution of cells and MCs through the gel matrix, comparable geometry to the cell-free constructs (overall dimensions, strands orientation, struts and pore sizes), and a good fidelity to the original CAD design (Figure 6.8).
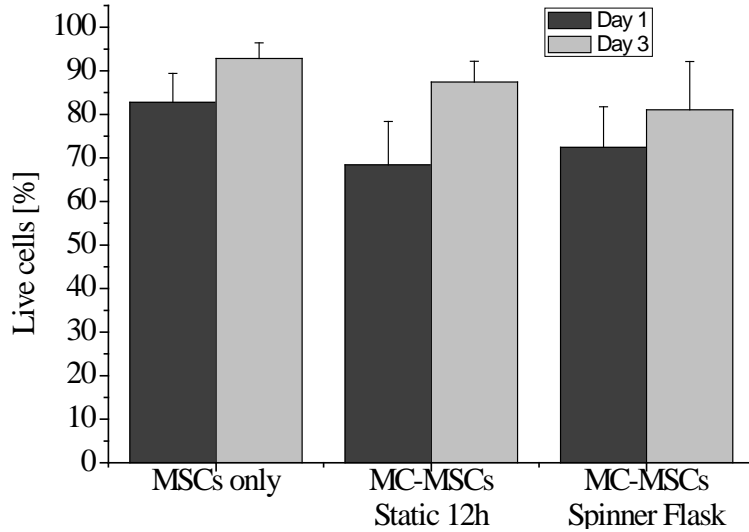
**Figure 6.7: Viability of MSCs encapsulated in GelMA-GG hydrogels after printing.**
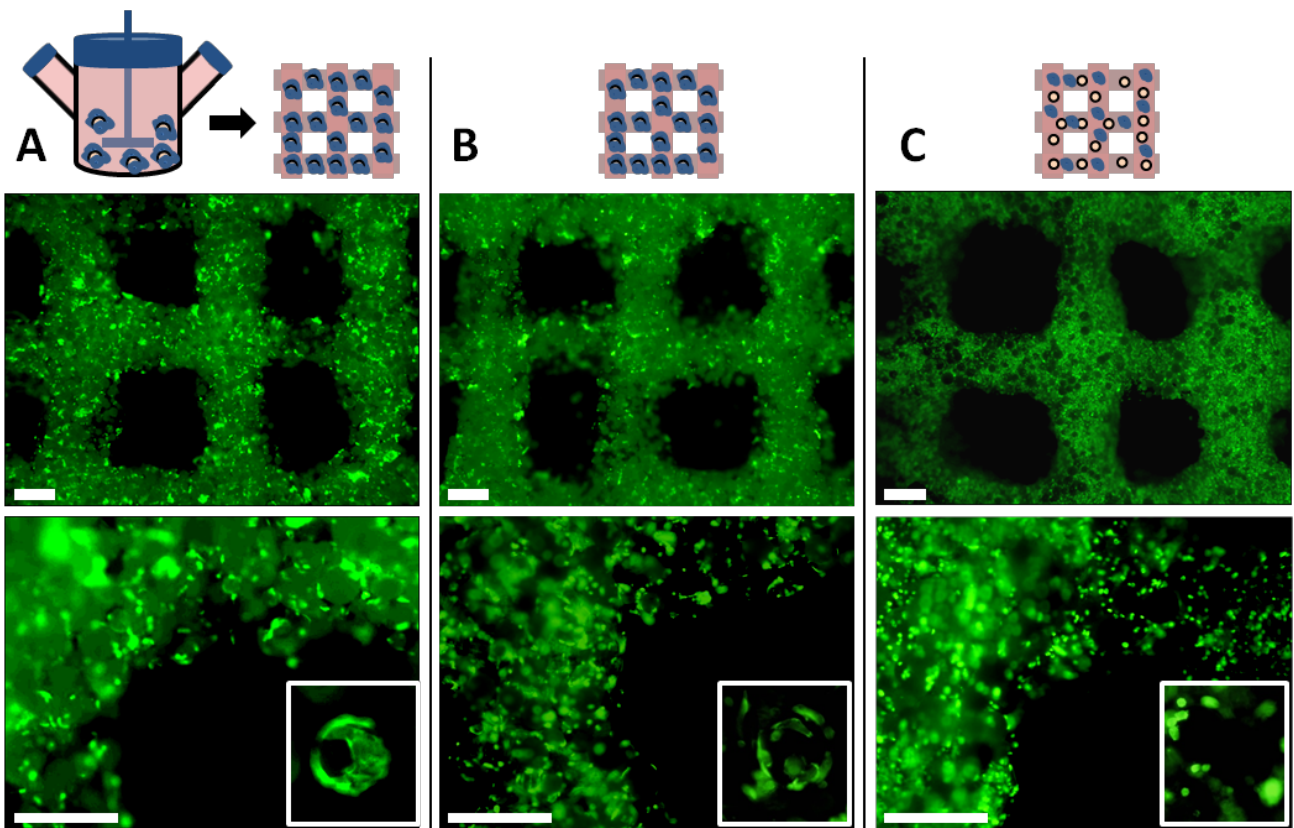


**Figure 6.8: Immunofluorescence staining for actin cytoskeleton (green) on bioprinted GelMA-GG hydrogels with encapsulated cells and MCs. (A) MSCs were precultured on MCs either in a spinner flask bioreactor for 5 days; (B), under static conditions for 12 h or (C) directly mixed together in the hydrogel solution without preculture. Lower panels and inserts show higher magnification of the constructs. Scale bar is 500 μm.**

*6.3.6 Printing of osteochondral models*

Using the MC-based biofabrication approach, it was feasible to fabricate bilayered osteochondral graft models of clinically relevant size. The cartilage region was printed with GelMA-GG and the bone region was represented by GelMA-GG with encapsulated MCs. MC-laden gels flowed smoothly through the dispensing nozzle and strands retained their rounded shape better than the gel-only bioink, possibly due to the increased rigidity of the composite material. As a result, the constructs showed a strand diameter of $682 \pm 74$ µm (with an average pore width of about $1226 \pm 83$ µm) for the MC-laden gel and $755 \pm 92$ µm for the gel-only ink (with an average pore width of $1020 \pm 80$ µm).The two compartments were well aligned and no delamination was observed during the manipulation of the construct. There was a consistent axial porosity that can be observed in figure 6.9A and 6.9B. The MC-laden region showed a homogenous distribution of the PLA particles throughout the structure and appeared optically opaque (opposed to the translucent hydrogel-only section, figures 6.9A and 6.9C). As quite common with hydrogel printing, no significant lateral porosity was introduced into the construct, as the bioinks tend to lean on the underlying layer (Figure 6.9D).
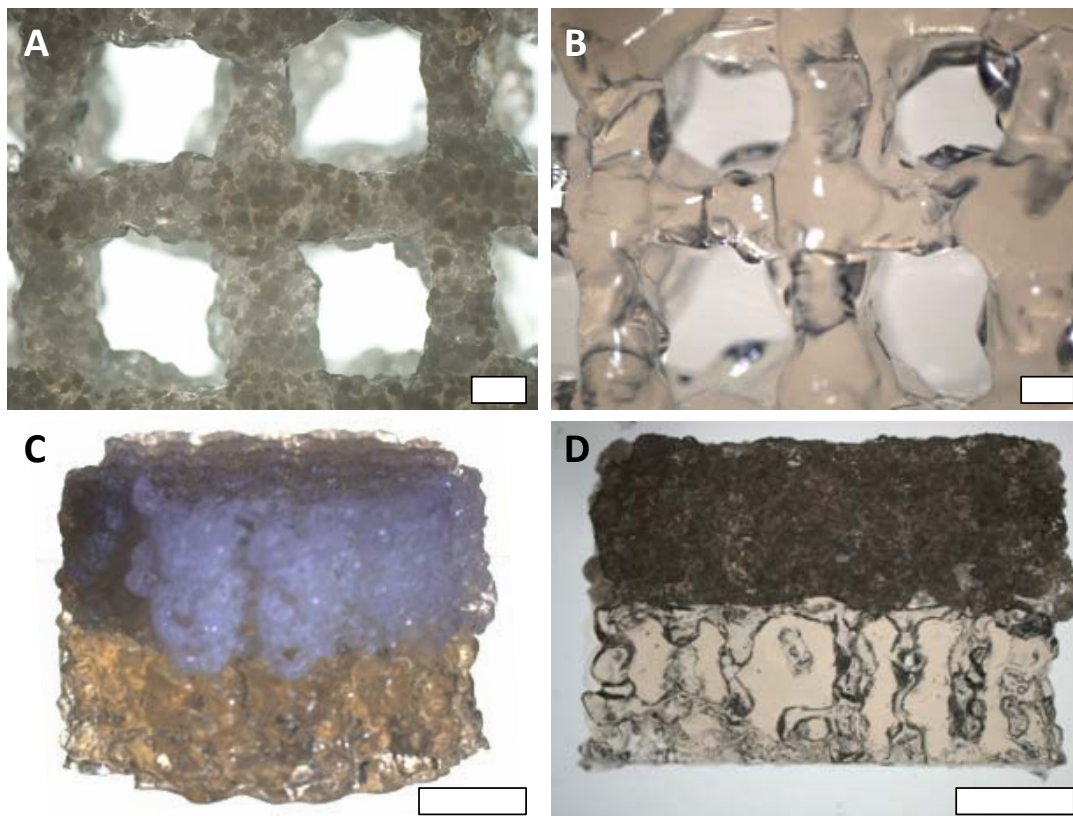


**Figure 6.9: Bilayered GelMA-GG cylindrical osteochondral graft model (16 mm diameter, 1 cm height). (A) MC-laden layer top view, (B) GelMA-GG layer top view, (C) perspective, (D) cross-section. Scale bars are (A, B) 400 µm and (C, D) 4 mm.**

**6.4 Discussion**

In this study, living 3D structures containing MC-MSCs complexes were fabricated using bioprinting technology. MCs were found to be suitable substrates to for cell adhesion and osteogenic differentiation and acted as reinforcing material to the hydrogel. Furthermore, high cells concentrations could be obtained by pre-culturing MSCs on MCs.

GelMA-GG was chosen as a bioink for bioprinting. Due to its shear-thinning behavior, it can be easily extruded into filaments, which then maintain their shape once deposited on the printing substrate, thus allowing the generation of 3D printed structures with good shape fidelity [6, 13]. Finally, the obtained scaffolds can be irreversibly crosslinked after mild UV-exposure. We found this procedure had little impact on cell viability, which is in line with previous research [31-33]. It should be noted that human MSCs may show different survival rates compared to rat MSCs in response to mechanical stresses and UV radiation, although previous work reported reassuring results regarding MSCs differentiation (hence survival) after UV-encapsulation in collagenous hydrogels [34].

Another issue regarding the current crosslinking set-up, is that constructs were UV cured after the printing process, may limit the size of the constructs, since UV may not penetrate deeply into larger grafts. However, this can be solved by inducing photocrosslinking during the printing process. Such technology has been recently described by Cui et al., and could be adapted to our system by a hardware modification [35].

In this work, cells and MCs were either suspended as precultured MC-MSCs complexes or mixed separately into the hydrogel. The first approach is preferable, since such aggregates have been shown to promote cell viability, biomolecules synthesis and differentiation [26], due to the establishment of cell-cell contacts and actin cytoskeleton reorganization [36]. However, since large aggregates can easily clog the injection nozzle, expansion periods under static culture should be limited. As an interesting alternative, MCs and MSCs can be separately mixed, without preculture steps. The current work showed that such suspensions can easily be dispensed, and once suspended in the bioink, cells were able to migrate through the hydrogel matrix to adhere, spread and proliferate on the MC surface. Although it could be possible to use this approach to tune MSCs adhesion and response, the amount of cells that could be loaded into the gel would be limited by standard 2D proliferation protocols. Therefore, 3D-expansion methods are required. To retain a printable bioink, cells should be expanded on individual MCs or small aggregates, a condition that can be achieved in a stirring bioreactor, as also shown in this study.

Composite bioinks were thus created, in which MCs, made of a mechanically stiff polymer, were dispersed in the softer hydrogel matrix. It is known that hydrogel stiffness can be improved increasing the polymer concentration or the crosslinking degree (UV exposure, temperature) [12]. A high crosslink density however is less desirable, as it can hamper the migration of encapsulated cells and their ability to homogeneously colonize the hydrogel with newly synthesized extracellular matrix [37]. Instead, incorporation of MCs does not alter the nature of the hydrogel network, and construct stiffness was shown to increase along with the concentration of MCs. However, it should be considered that stress at failure may be reduced, although this was not evident in our mechanical assay. MC reinforcement of hydrogels does not lead to compressive

moduli similar to hard tissues. When hydrogel-based constructs are implanted in load-bearing locations, external fixation will be required to reduce weight on the implant. Another strategy that can be implemented to improve the mechanical properties of hydrogel constructs, is co-printing of a supportive thermoplastic polymer network [12, 38]. Still, in all regenerative approaches, the final mechanical properties should be provided by the neo-tissue that is secreted by the embedded cells [39].

To further enhance the hydrogel compression modulus and match the stiffness of hard tissues, it may be feasible to encapsulate particles made of different materials (e.g. calcium phosphates) [40], provided that they do not sediment over the time scale of the printing process and their size allows the extrusion of the bioink. However, an advantage of MCs encapsulation is to use them as devices to efficiently expand MSCs and then print MC-MSCs aggregates with improved biological behavior and bone forming potential [23]. For this reason, MCs with a highly porous core made from low density materials and suitable for spinner flask culture were chosen.

The potential to improve the osteogenic differentiation of MSCs by encapsulating them with MCs into GelMA hydrogels was studied *in vitro*. All the samples cultured with differentiation medium displayed calcified matrix deposition, and MSC commitment towards osteogenic lineage, thus supporting the suitability to use GelMA-based gels for bone bioprinting. Alizarin red staining, which appeared as discrete spots surrounding cells without MCs, intensely marked diffused areas around MC-MSCs complexes. This indicates strongly mineralized regions, probably due to the fact that local cell density is higher on cell-colonized MCs, a factor affecting cell behavior and differentiation [23]. At a molecular level, MC-laden samples showed markedly reduced ALP activity compared to their respective controls. This was accompanied by a higher secretion of OCN, which is a late marker for maturation of osteoblasts, and key component of bone extracellular matrix [41]. MC-MSCs gels gave the best results regarding the secretion of OCN, and at the same time induced matrix calcification, suggesting that they are able to form a mature bone-like tissue. This discrepancy of ALP levels *in vitro* and bone-forming capacity of MSCs was recently described by Goh et al. who compared the bone forming potential of human fetal MSCs cultured as monolayers with Cytodex 3 MCs. Despite a 45-fold reduction in ALP activity on MCs, MSCs cultured on MCs and MC-MSCs complexes induced better and more consistent bone formation *in vitro* and *in vivo* (in a rodent model), indicating that MC culture can improve the potential of MSCs in bone tissue engineering [42].

Eventually, it is worthwhile to underline that the addition of gellan gum to the bioink formulation did not have a relevant effect on osteogenic differentiation of MSCs. Gellan gum, may thus be safely mixed with GelMA for printing of bone tissue in order to increase the solution viscosity and improve the printability of the bioink [13]. The results of the differentiation assay also suggest that it is not advisable to use solely MSCs in GelMA-based hydrogels for the cartilage region, since they can easily differentiate towards osteoblastic lineage. For this reason, it would be preferable to use chondrocytes, which have shown capable of chondrogenic differentiation in GelMA *in vitro* and *in vivo* [11, 38]. MSCs can play an important role in maintaining chondrocyte phenotype in co-cultures [43-45], although the mechanism underlying this crosstalk

is not fully understood, and cases of downregulation of chondrocytes differentiation have also been reported [46]. However, co-cultures of MSCs and chondrocytes in hydrogel systems have been reported, suggesting the beneficial effect of the combination of such cell types in generating bone and cartilage tissues. For instance, Mo et al. demonstrated that MSCs and chondrocytes interacted in an alginate matrix, possibly due to trophic factors secretion, determining an enhancement of GAGs secretion by chondrocytes and an initiation of osteogenesis of MSCs, which induced osteocalcin production [47]. These effects were found to be dependent on the MSC/chondrocyte ratio [47].

Proven that MC-laden GelMA-GG can be a matrix for bone tissue engineering, the material was used as a bioink to construct model of an osteochondral graft. Recently, calcium phosphate particles (size 100-212 µm) have been introduced at low concentrations (up to 15 mg mL$^{-1}$) into alginate bioinks to promote bone regeneration [48]. Poldervaart et al. also printed gelatin microparticles for controlled release of Bone Morphogenic Protein-2. Both cases showed promising results in terms of *in vivo* osteoinduction, however low amounts of particles where encapsulated [49]. We found that the addition of high concentrations of MCs to GelMA-GG hydrogels did not reduce the printability of the ink, nor did it affect the size of the extruded strands and the porosity. Living constructs were obtained by adding MC-MSCs to the bioink mixture, either after a short period of static culture (12h) or longer culture (5 days) in a spinner flask bioreactor. Both approaches generated viable MC-MSCs complexes, but the latter has a clear advantage, as dynamic culture allows cell proliferation while preventing formation of large, difficult to extrude, aggregates. Furthermore, spinner flask culture has the great potential to combine 3D printing with a well-established cell expansion technology. To date, bioprinting of cell aggregates was prevalently performed by producing tissue spheroids and using them as bioink components [50]. Despite of the interesting biological performance, spheroid generation methods are still time consuming and not suitable for mass production, thus limiting the size of printable tissues [50]. Conversely, microcarrier culture is a simple, industrially scalable technology to achieve large cell numbers, with precise control over cell culture conditions [51]. MSCs aggregates have been demonstrated to improve cell proliferation, survival and multilineage differentiation, especially when the endogenous ECM produced in the aggregates is preserved [52]. Such matrix preservation is a characteristic of MC-MSCs complexes [19] which are profitable to induce cell differentiation and build tissue engineered constructs [53]. Additionally, to further exploit the advantage of 3D cell-cell connections, MCs with an open porous structure could be used, so that cells can colonize the inside of the carrier and display a 3D organization in it [16]. MC culture opens promising possibilities when combined with bioprinting technologies.

In tissue constructs fabricated from all MC-bioinks (short-term static culture, dynamic culture, and without preseeding), the complexes or the free cells and particles were homogeneously distributed in the printed graft with shape fidelity comparable to that of the cell-free constructs, thus proving the printability of MC-MSCs complexes. Under these conditions, zonal constructs composed of MC-laden and MC-free layers of gels with clinically relevant size were obtained. The size of the strand was not significantly affected by the presence of the MCs, thus allowing a good stacking and alignment of the two compartments, which generated a

consistent and well-aligned axial porosity all through the construct. The high viability of MSCs, and the results of the multimaterial printing process demonstrates the feasibility of a combined MC culture-bioprinting strategy to generate large, living constructs, with potential applications in osteochondral tissue engineering and as 3D tissue models.

## 6.5 Conclusions and future perspectives

MC-laden GelMA-based bioink was shown to be a promising composite material for bioprinting. PLA MCs acted as a mechanical reinforcement to the soft GelMA matrix, without compromising the printability of GelMA bioinks. Additionally, encapsulation of MC-MSCs complexes - with improved cell adhesion and cell-cell contacts – supported bone matrix deposition, and hence is of great interest for the engineering of bone tissue. Finally, MC-MSC-rich living construct where obtained using bioprinting combined with microcarrier dynamic expansion. These are key findings to build advanced constructs for bone and cartilage tissue engineering. Furthermore, the printability of bioinks with high MC concentrations opens possibilities for the fabrication of biomedical screening models. Drug-encapsulating MCs could be used, adding an additional level of complexity in the bioprinting of living tissues. Co-delivery of cells and growth factors with control over the spatial and temporal distributions would be possible, and constitutes another promising trend that can be explored in the area of biofabrication.

## 6.6 References

[1]     Rowkema J, Gibbs S, Lutolf MC, Martin I, Vunjak-Novakovic G and Malda J. In vitro platforms for tissue engineering: implications to basic research and clinical translation. J Tissue Eng Reg Med. 5(8) (2011) 164-7.

[2]     Mironov V, Trusk T, Kasyanov V, Little S, Swaja R and Markwald R. Biofabrication: a 21st century manufacturing paradigm. Biofabrication .1 (2009) 022001.

[3]     Kang KH, Hockaday LA, Butcher JT . Quantitative optimization of solid freeform deposition of aqueous hydrogels. Biofabrication. 5  (2013) 035001.

[4]     Miller SJ, Stevens KR, Yang MT, Baker BM, Nguyen DHT, Cohen DM, Toro E, Chen AA, Galie PA, Yu X, Chaturvedi R, Bhatia SN, Chen CS. Rapid casting of patterned vascular networks for perfusable engineered three-dimensional tissues. Nat Mater .11 (2013) 768-74.

[5]     Kolesky DB, Truby RL, Gladman AS, Busbee TA, Homan KA, Lewis JA. 3D Bioprinting of Vascularized, Heterogeneous Cell-Laden Tissue Constructs. Adv Mat. (2014) doi: 10.1002/adma.201305506.

[6]     Visser J, Peters B, Burger TJ, Boomstra J, Dhert WJ, Melchels FP, Malda J. Biofabrication of multi-material anatomically shaped tissue constructs. Biofabrication. (2013) 5 035007.

[7]     Klein TJ, Rizzi SC, Reichert JC, Georgi N, Malda J, Schuurman W, Crawford RW, Hutmacher DW. Strategies for Zonal Cartilage Repair using Hydrogels. Macromol Biosci. 9 (2009) 1049-58.

[8]     Xu T, Binder KW, Albanna MZ, Dice D, Zhao W, Yoo JJ, Atala A. Hybrid printing of mechanically and biologically improved constructs for cartilage tissue engineering applications. Biofabrication. 5 (2013) 015001.

[9]     Malda J, Visser J, Melchels FP, Jüngst T, Hennink WE, Dhert WJ, Groll J, Hutmacher DW. 25th anniversary article: Engineering hydrogels for biofabrication. Adv Mater. 25(36)  (2013) 5011-28.

[10]   Billiet T, Vandenhaute M, Schelfhout J, Van Vlierberghe S, Dubruel P. A review of trends and limitations in hydrogel-rapid prototyping for tissue engineering. Biomaterials. 33 (2012) 6020-41.

[11]   Levett PA, Melchels FP, Schrobback K, Hutmacher DW, Malda J, Klein TJ. A biomimetic extracellular matrix for cartilage tissue engineering centered on photocurable gelatin, hyaluronic acid and chondroitin ulfate. Acta Biomater. 10(1) (2014) 214-23.

[12]   Schuurman W, Levett PA, Pot MW, van Weeren PR, Dhert WJA, Hutmacher DW, Melchels FPW, Klein TJ, Malda J. Gelatin-Methacrylamide Hydrogels as Potential Biomaterials for Fabrication of Tissue-Engineered Cartilage Constructs. Macromol Biosci. (2012) 13(5) 551-61.

[13]   Melchels FPW, Dhert WJA, Hutmacher D, Malda J. Development and  Characterisation of a New Bioink for Additive Tissue Manufacturing. J Mater Chem B. (2014) doi: 10.1039/C3TB21280G.

[14]   Wang C, Gong Y, Zhong Y, Yao Y, Sui K, Wang DA. The control of anchorage-dependent cell behavior within a hydrogel/microcarrier system in an osteogenic model. Biomaterials 30 (2009) 2259-69.

[15]  Zhu Y, Liu T, Song K, Fan X, Ma X, Cui Z. Ex vivo expansion of adipose tissue-derived stem cells in spinner flasks. Biotechnol J. 4(8) (2009) 1198-209.

[16]  Chang J, Lei H, Liu Q, Qin S, Ma K, Luo S, Zhang X, Huang W, Zuo Z, Fu H, Xia Y. Optimization of culture of mesenchymal stem cells: a comparison of conventional plate and microcarrier cultures. Cell Prolif. 45(5) (2012) 430-37.

[17]  Sart S, Agathos SN, Li Y. Engineering stem cell fate with biochemical and biomechanical properties of microcarriers. Biotechnol Prog. 29(6) (2013) 1354-66.

[18]  Ayyildiz-Tamis D, Avcı K, Deliloglu-Gurhan SI. Comparative investigation of the use of various commercial microcarriers as a substrate for culturing mammalian cells. In Vitro Cell Dev Biol Anim. (2013) doi:10.1007/s11626-013-9717-y.

[19]  Urciuolo F, Imparato G, Palmiero C, Trilli A, Netti PA. Effect of Process Conditions on the Growth of Three-Dimensional Dermal-Equivalent Tissue Obtained by Microtissue Precurson Assembly. Tissue Eng Part C. 17(2) (2011) 155-64.

[20]  Malda J, Frondoza CG. Microcarriers in the engineering of cartilage and bone.
Trends Biotechnol. 24(7) (2006) 299-304.

[21]  Borg DJ, Dawson RA, Leaveslet DI, Hutmacher DW, Upton Z, Malda J. Functional and phenotypic characterization of human keratinocytes expandaded in microcarrier culture. J Biomed Mater Res A. 88(1) (2009) 184-94.

[22]  Stich S, Schulze-Tanzil G, Ibold Y, Stoll C, Abbas A, Kohl B, Ullah M, John T, Sittinger M, Ringe J. Continuous cultivation of human hamstring tenocytes on microcarriers in a spinner flask bioreactor system. Biotechnol Prog. (2013) doi:10.1002/btpr.1815.

[23]  Tseng PC, Young TH, Wang TM, Peng HW, Hou SM, Yen ML. Spontaneous osteogenesis of MSCs cultured on 3D microcarriers through alteration of cytoskeletal tension. Biomaterials. 33(2) (2012) 556-64.

[24]  Bouffi C, Thomas O, Bony C, Giteau A, Venier-Julienne MC, Jorgensen C, Montero-Menei C, Noël D. The role of pharmacologically active microcarriers releasing TGF-beta3 in cartilage formation in vivo by mesenchymal stem cells. Biomaterials. 31(25) (2010) 6485-93.

[25]  Delcroix GJ, Garbayo E, Sindji L, Thomas O, Vanpouille-Box C, Schiller PC, Montero-Menei CN. The therapeutic potential of human multipotent mesenchymal stromal cells combined with pharmacologically active microcarriers transplanted in hemi-parkinsonian rats. Biomaterials. 32(6) (2011) 1560-73.

[26]  Martin Y, Eldardiri M, Lawrence-Watt DJ, Sharpe JR. Microcarriers and their potential in tissue regeneration. Tissue Eng Part B Rev. 17(1) (2011)71-80.

[27]  Zhang Q, Tanb K, Yeb Z, Tanb W, Lang M. Preparation of open porous polycaprolactone microspheres and their applications as effective cell carriers in hydrogel system. Mater Sci Eng C. 32 (2012) 2589–95.

[28] Kim BS, Choi JS, Kim JD, Yeo TY, Cho YW. Improvement of Stem Cell Viability in Hyaluronic Acid Hydrogels Using Dextran Microspheres. J Biomater Sci Polym Ed. 21(13) (2010) 1701-11.

[29] Puñet X, Machauffé R, Giannotti MI, Rodríguez-Cabello JC, Sanz F, Engel E, Mateos-Timoneda MA, Planell JA. Enhanced cell-material interactions through the biofunctionalization of polymeric surfaces with engineered peptides. Biomacromolecules 14(8) (2013) 2690-702.

[30] Gonzalez-Vazquez AG, Planell JA, Engel E. Extracellular calcium and CaSR drive osteoinduction in mesenchymal stromal cells Acta Biomater. (2014) doi:10.1016/j.actbio.2014.02.004.

[31] Fedorovich NE, Oudshoorn MH, van Geemen D, Hennink WE, Alblas J, Dhert WJ. The effect of photopolymerization on stem cells embedded in hydrogels. Biomaterials. 30(3) (2009) 344-53

[32] Hwang NS, Varghese S, Li H, Elisseeff J. Regulation of osteogenic and chondrogenic differentiation of mesenchymal stem cells in PEG-ECM hydrogels. Cell Tissue Res. 344(3) (2011) 499-509.

[33] Shin H, Olsen BD, Khademhosseini A. The mechanical properties and cytotoxicity of cell-laden double-network hydrogels based on photocrosslinkable gelatin and gellan gum biomacromolecules. Biomaterials. 33(11) (2012) 3143-52.

[34] Rowland CR, Lennon DP, Caplan AI, Guilak F. The effects of crosslinking of scaffolds engineered from cartilage ECM on the chondrogenic differentiation of MSCs. Biomaterials. 34(24) (2013) 5802-12.

[35] Cui X, Breitenkamp K, Finn MG, Lotz M, D'Lima DD. Direct human cartilage repair using three-dimensional bioprinting technology. Tissue Eng Part A. 18(11-12) (2012) 1304-12.

[36] Sart S, Errachid A, Schneider YJ, Agathos SN. Modulation of mesenchymal stem cell actin organization on conventional microcarriers for proliferation and differentiation in stirred bioreactors. J Tissue Eng Regen Med. 7(7) (2013) 537-51.

[37] DeForest CA, Anseth KS. Advances in Bioactive Hydrogels to Probe and Direct Cell Fate. Annu Rev Chem Biomol Eng. 3 (2012) 421-44.

[38] Boere KW, Visser J, Seyednejad H,Rahimian S, Gawlitta D, van Steenbergen MJ, Dhert WJ, Hennink WE, Vermonden T, Malda J. Covalent attachment of a three-dimensionally printed thermoplast to a gelatin hydrogel for mechanically enhanced cartilage constructs. Acta Biomater. 10(6) (2014) 2602-11.

[39] Naito H, Dohi Y, Zimmermann WH, Tojo T, Takasawa S, Eschenhagen T, Taniguchi S. The effect of mesenchymal stem cell osteoblastic differentiation on the mechanical properties of tissue engineered bone-like tissue. Tissue Eng Part A. 17(17-18) (2011) 2321-9.

[40] Marelli B, Ghezzi CE, Stark WJ, Barralet JE, Boccaccini AR, Nazhat SN. Accelerated mineralization of dense collagen-nano bioactive glass hybrid gels increases scaffold stiffness and regulates osteoblastic function. Biomaterials. 32(34) (2011) 8915-26.

[41] Christenson RH. Biochemical Markers of Bone Metabolism: An Overview. Clinical Biochemistry. 30(8) (1997) 573-93

[42] Goh TKP, Zhang ZY, Chen AKL, Reuveny S, Choolani M, Chan JKY, Oh SKW. Microcarrier Culture for Efficient Expansion and Osteogenic Differentiation of Human Fetal Mesenchymal Stem Cells. BioRes Open Access. 2(2) (2013) 84-96.

[43] Nakaoka R, Hsiong SX, Mooney DJ. Regulation of chondrocyte differentiation level via co-culture with osteoblasts. Tissue Eng. 12(9) (2006) 2425-33.

[44] Dahlin RL, Meretoja VV, Ni M, Kasper FK, Mikos AG. Chondrogenic Phenotype of Articular Chondrocytes in Monoculture and Co-Culture with Mesenchymal Stem Cells in Flow Perfusion. Tissue Eng Part A. (20014) doi:10.1089/ten.tea.2014.0107.

[45] Wu L, Prins HJ, Helder MN, van Blitterswijk CA, Karperien M. Trophic effects of mesenchymal stem cells in chondrocyte co-cultures are independent of culture conditions and cell sources. Tissue Eng Part A. 18(15-16) (2012) 1542-51.

[46] Xu L, Wang Q, Xu F, Ye Z, Zhou Y, Tan WS. Mesenchymal stem cells downregulate articular chondrocyte differentiation in noncontact coculture systems: implications in cartilage tissue regeneration. Stem Cells Dev. 22(11) (2013) 1657-69.

[47] Mo XT, Guo SC, Xie HQ, Deng L, Zhi W, Xiang Z, Li XQ, Yang ZM. Variations in the ratios of co-cultured mesenchymal stem cells and chondrocytes regulate the expression of cartilaginous and osseous phenotype in alginate constructs. Bone 45(1) (2009) 42-51.

[48] Federovich NE, Schuurman W, Wijnberg HM, Prins HJ, van Weeren PR, Malda J, Alblas J, Dhert WJ. Biofabrication of osteochondral tissue equivalents by printing topologically defined, cell-laden hydrogel scaffolds. Tissue Eng Part C. 18(1) (2011) 33-44

[49] Poldervaart MT, Wang H, van der Stok J, Weinans H, Leeuwenburgh SC, Oner FC, Dhert WJ, Alblas J. Sustained Release of BMP-2 in Bioprinted Alginate for Osteogenicity in Mice and Rats. PLoS ONE. 8(8) (2013) e72610 doi:10.1371/journal.pone.0072610.

[50] Mironov V, Kasyanow V, Markwald RR. Organ printing: from bioprinter to organ biofabrication line. Curr Opin Biotechnol. 22(5) (2011) 667-73

[51] Rafiq QA, Brosnan KM, Coopman K, Nienow AW, Hewitt CJ. Culture of human mesenchymal stem cells on microcarriers in a 5 l stirred-tank bioreactor. Biotechnol Lett 35(8) (2013) 1233-45.

[52] Kim J, Ma T. Endogenous extracellular matrices enhance human mesenchymal stem cell aggregate formation and survival. Biotechnol Prog. 29(2) (2013) 441-51.

[53] Chen M, Wang X, Ye Z, Zhang Y, Tan WS. A Modular approach to the engineering of a centimeter-sized bone tissue construct with human amniotic mesenchymal stem cells-laden microcarrier. Biomaterials 32(30) (2011) 7532-42.

# Chapter 7

# Conclusions and future perspectives

## 7.1 Conclusions

This Thesis is an extensive study on the development of novel nano- and microcarriers, and demonstrates the versatility and high potential of such carriers. Below are summarized the main conclusions of the work reported in the experimental chapters (Chapters 3-6).

### 7.1.1 Chapter 3 – MCs fabrication

- A novel method to process PLA and fabricate MCs was developed and characterized.
- This method involves the use of chemicals that are non-harmful, green and biodegradable, thus improving the biocompatibility of the device and fabrication procedure. Furthermore, the method can be potentially scaled up and poses no significant harm to the environment and the workers involved in the MCs fabrication.
- MCs size can be controlled by adjusting experimental parameters such as polymeric solution viscosity, and aero- and hydrodynamic parameters such flow velocity of the polymer phase and the nitrogen phase.
- Additionally, the method can be adapted to generate MCs made of different materials, modifying the choice of solvent and coagulation bath.
- The MCs production and solidification technique is suitable to encapsulate bioactive compound of both hydrophobic and hydrophilic nature, by loading them either into the coagulation bath or into the polymeric phase.
- The PLA-EtLac system can be of potential interest for green fabrication routes to generate devices for other types of applications (scaffolds and films for tissue engineering, membranes for separation technology and films for packing purposes).

### 7.1.2 Chapter 4 – Antimicrobial NPs

- The green approach to particles fabrication presented in Chapter 3 was adapted to fabricate NPs made of PLGA. The EtLac-polymer system was used in a nanoprecipitation-based processing method to successfully generate monodisperse NPs. CPX, an antibiotic, was encapsulated in the particles.
- These spherical NPs have size ranging between 200 and 300 nm, suitable for drug delivery to bacterial biofilms established into the airways.
- PLGA NPs could be prepared unmodified, thus bearing a negative surface charge or in presence of PL, to endow them with a positively charged coating.

- Positively charged NPs could also be functionalized with DNase I, and the enzyme coated on the NPs surface retained its capability to degrade DNA.

- The drug loading into the NPs is low, although this is comparable with other studies reported in the literature, as the nanoprecipitation method is most effective for encapsulating hydrophobic compounds, rather than hydrophilic.

- The CPX release profile, with a high burst in the first hours and a slower release until complete depletion of the loaded drug is compatible with the application of antibiotic delivery to biofilms, and, as suggested in the literature, can be suitable to reduce insurgence of resistant bacterial strains.

- All the NPs formulation loaded with CPX (unmodified, PL coated and PL-DNase I coated) were active against planktonic *P. aeruginosa,* a biofilm-forming bacteria involved in infections related to cystic fibrosis, and the encapsulated antibiotic retained its antimicrobial potential. The NPs were also able to prevent biofilm formation by planktonic bacterial cells.

- NPs functionalized with DNase I were the most effective at eradicating established biofilm infections. With this approach, both the bacterial cell and the matrix they produce are targeted in the treatment of persistent bacterial infections,.

- Degradation of the bacterial ECM composing the biofilm with enzyme-functionalized NPs appears as a promising strategy to improve controlled drug delivery into biofilms. Combination of functionalized NPs and antibiotic release can thus help to treat persistent bacterial infections.

### 7.1.3 Chapter 5 – Cell delivery and migration from MCs

- PLA MCs fabricated according to the method proposed in Chapter 3 were successfully functionalized with RGD short peptides and collagen type I, either via coavalent bonding or physisorption. These MCs were demonstrated to be suitable carriers for MSCs homing and proliferation.

- The highest values for cell adhesion and proliferation were found on MCs covalently functionalized with collagen that thus offered a suitable environment for cell survival, homing and expansion.

- Surface functionalization does not only modulate cell adhesion and proliferation, but also allows acting on MSCs migratory behavior in response to chemokines, and directly affects SDF1-α/CXCR4 axis.

- These effects are dependent on surface functionalization, both in terms of nature of the coating (bio)molecule and mode of surface modification (physisorption vs. covalent), together with cues given by cell culture on MCs 3D spherical devices.

- Culture on 3D MCs, in comparison to 2D surfaces and modification of material chemistry by collagen coatings, induced higher CXCR4 expression in MSCs. This is especially important as MSCs tend to lose functional CXCR4 expression when expanded *in vitro*, and thus MCs can be an

advantageous substrate for cell proliferation, cell delivery and to improve cell grafting after transplantation.

- Simplified molecules such as RGD peptides can promote cell adhesion and proliferation, but do not trigger the biological pathways that improve CXCR4 expression.
- Covalent modification reduce the basal level of MSCs migration in absence of chemokine stimulation, and may therefore be used to prevent cell non-triggered release from the MCs and to limit cell migration. On the other hand, physisorbed coatings permit higher cell migration from the carrier. These findings can help to choose properly biomaterial devices that can balance SDF-1α mediated MSCs recruitment towards specific target tissues. Furthermore, they highlight the importance of considering the effect of biomaterial carrier properties on cell migration, in order to design devices for efficient and controllable cell delivery.

## 7.1.4 Chapter 6 – Cell-laden MCs bioprinting

- PLA MCs prepared with the method described in Chapter 3 can be used as injectable cell carriers, and the injection of MSCs-laden MCs causes no negative impact on cell viability.
- Cell-laden MCs can be suspended in a hydrogel to be injected. In this study, MCs loaded in a GelMA-GG solution could be suspended and injected. Furthermore, the mixture showed good extrudability properties, meaning that it was injectable and formed strands upon extrusion.
- MSCs-laden MCs encapsulated in GelMA-GG can be used as a composite bioink for bioprinting, via layer by layer deposition of spatially-organized MC-hydrogel strands.
- PLA MCs acted as a mechanical reinforcement to the soft GelMA-GG matrix, without compromising the printability of GelMA-based bioinks.
- MSCs formed complexes on MCs that supported osteogenic differentiation and bone matrix deposition.
- MC-laden bioinks can be suitable as components to generate complex bone and cartilage tissue engineering constructs by means of bioprinting. As a proof-of-concept of such an approach, an osteochondral graft model was printed using a MC-laden bioink to fabricate the bone compartment and a GelMA-GG only bioink to build the cartilage region.
- MCs can be used to expand under dynamic conditions MSCs and then to print cell-rich living constructs with potential applications in tissue engineering, as well as *in vitro* 3D tissue models, disease models and platforms for drug screening.

## 7.2 Future perspectives

The work developed in this Thesis shows the versatility of MCs and NPs that can be applied for drug delivery, cell therapy, tissue engineering and *in vitro* 3D tissue modeling applications, among many possibilities. As several important implications of the use of particulate carriers in such applications have been investigated and deepened (*i.e.* impact of fabrication processes on materials properties, surface modification and functionalization, interaction with biological milieu, cell-materials interface and its influence on cell behavior, generation of advanced biomaterial devices with cutting-edge technologies), the work presented herein opens a wide array of possibility for future research. At the same time the topics developed in this Thesis could also be faced with alternative approaches and further aspects of particulate carriers development and applications could be explored. In this section, a non-exhaustive list of possible future development of the work presented in this Thesis is provided.

The fabrication procedure exposed in Chapter 3, on one hand can be adapted to generate MCs made of different type of materials, according to the type of desired application. On the other hand, considering PLA-based polymers, in terms of MCs fabrication and design, there are several interesting aspect that may be researched. As already mentioned in the previous chapters, solid spheres MCs can be loaded with drugs (in the inside), while carrying seeded cells on their surface, allowing for a compartmental separation of the drug and the cells component. This strategy, as already shown in the literature [1, 2], can be used, for instance, to guide cell behavior via controlled release of growth factors. There is a huge spectrum of the possible drug-cell pairing, and the proper choice of these components, of course, depends on the type of target tissue to regenerate/disease to treat (i.e. bone morphogenic proteins and MSCs/osteoblasts for bone tissue engineering). MCs with open porosity are also widely studied as substrate for cell expansion and as cell carriers [3]. It could be of interest to study the introduction of porogens during the MC fabrication step, in order to modulate pore size, shape and interconnectivity. Open porosity allows for higher surface available for cell proliferation and also for improved formation of 3D cell-cell communication and aggregate in the inside of the MC [4]. This would permit to study the effect of this greater extend of 3D cell-cell organization on parameters such as stem cells differentiation, ECM deposition, biomarkers expression, secretion of paracrine factors. Both drug- and cell-loaded solid sphere MCs and open porous MCs would provide appealing approaches for MCs bioprinting of living tissues, as suggested in Chapter 6.

Regarding the work presented in Chapter 4, the proposed NPs system, it would be interesting to test DNase I functionalized NPs *in vivo* in animal models of persistent infections due to established *P. areuginosa* biofilms. This would be an especially important step, due to the fact that currently only a very limited number of *in vivo* studies concerning antibacterial nano/microscale delivery systems are reported in the literature [5].

Moreover, *in vivo* studies would also be a natural development of the research described in Chapters 5. An interesting investigation would be that of MSC-MCs complexes injection *in vivo*, with or without chemokine stimulation, followed by live tracking of MSCs localization and number (for instance using cells modified to

express luciferase). Finally, the next step for the study described in chapter 6 would be that of evaluating the tissue deposition from long term co-cultures of MSC-laden MCs and chondrocytes, encapsulated in different compartment of a hydrogel system, in order to recapitulate the bone-cartilage transition in osteochondral tissues. Bioprinted, bilayered and cell- and MC encapsulating osteochondral grafts could be evaluated for *in vitro* tissue formation in a dynamic culture system (i.e. bioreactor providing mechanical compression stimulation) and *in vivo* tissue regeneration after implantation of the graft.

## 7.3 References

[1]    Bouffi C, Thomas O, Bony C, Giteau A, Venier-Julienne MC, Jorgensen C, Montero-Menei C, Noël D. The role of pharmacologically active microcarriers releasing TGF-beta3 in cartilage formation in vivo by mesenchymal stem cells. Biomaterials. 31(25) (2010) 6485-93.

[2]    Delcroix GJ, Garbayo E, Sindji L, Thomas O, Vanpouille-Box C, Schiller PC, Montero-Menei CN. The therapeutic potential of human multipotent mesenchymal stromal cells combined with pharmacologically active microcarriers transplanted in hemi-parkinsonian rats. Biomaterials. 32(6) (2011) 1560-73.

[3]    Chung HJ, Park TG. Injectable cellular aggregates prepared from biodegradable porous microspheres for adipose tissue engineering. Tissue Eng Part A. 15(6) (2009) 1391-400.

[4]    Sart S, Errachid A, Schneider YJ, Agathos SN. Modulation of mesenchymal stem cell actin organization on conventional microcarriers for proliferation and differentiation in stirred bioreactors. J Tissue Eng Regen Med. 7(7) (2013) 537-51.

[5]    Forier K, Raemdonck K, De Smedt SC, Demeester J, Coenye T, Braeckmans K. Lipid and polymer nanoparticles for drug delivery to bacterial biofilms. J Control Release. (2014) doi: 10.1016/j.jconrel.2014.03.055.

# APPENDIX A

# List of publications

- **Riccardo Levato**, Miguel Angel Mateos-Timoneda, Josep A Planell. Preparation of Biodegradable Polylactide Microparticles via a Biocompatible Procedure. Macromol Biosci. 12 (2012) 557-66.

- Aurelio Salerno, **Riccardo Levato**, Miguel Angel Mateos-Timoneda, Elisabeth Engel, Paolo Netti, Josep A Planell. Modular polylactic acid microparticle-based scaffolds prepared via microfluidic emulsion/solvent displacement process: fabrication, characterization, and in vitro mesenchymal stem cells interaction study. J Biomed Mater Res A. 101A (2013) 720-32.

- **Riccardo Levato**, Jetze Visser, Josep A Planell, Elisabeth Engel, Jos Malda, Miguel Angel Mateos-Timoneda. Biofabrication of tissue constructs by 3D bioprinting of cell-laden microcarriers. Biofabrication. 6 (2014) 035020.

- **Riccardo Levato**, Josep A Planell, Miguel Angel Mateos-Timoneda, Elisabeth Engel. Role of ECM/peptide coatings on SDF-1α triggered cell migration from microcarriers for cell therapy. *In preparation.*

- Anna Crespo, **Riccardo Levato**, Esther Julian, Elisabeth Engel, Miguel Angel Mateos-Timoneda, Eduard Torrents. Degrading bacterial ECM with DNase-coated nanoparticles to enhance antibiotic delivery in biofilm infections. *In preparation.*

# APPENDIX B

# List of contributions to congresses and conferences

- **Riccardo Levato**, Miguel A. Mateos-Timoneda, Josep A. Planell. "Novel Preparation of Polylactic Acid Microparticles for Cell and Drug Delivery Using a Green Solvent". 24th European Conference on Biomaterials. 4th – 9th September 2011, Dublin, Ireland. Oral Presentation.

- Aurelio Salerno, **Riccardo Levato**, Miguel A. Mateos-Timoneda, Elisabeth Engel, Paolo A. Netti, Josep A. Planell. "Design and fabrication of porous scaffolds via microfluidic and bottom-up assembly integrated processes". 24th European Conference on Biomaterials. 4th – 9th September 2011, Dublin, Ireland. Oral Presentation.

- **Riccardo Levato**, David Miranda-Nieves, Elisabeth Engel, Miguel A. Mateos-Timoneda, Josep A. Planell. "Improving biological response of PLA microcarriers via covalent surface grafting of collagen". 9th World Biomaterials Congress. 1st – 5th June 2012, Chengdu, China. Poster.

- **Riccardo Levato**, Eduard Torrents, Antonio Juárez, Josep A Planell Miguel A Mateos-Timoneda. "Antimicrobial PLGA nanoparticles releasing ciprofloxacin produced using non-toxic reagents". 9th World Biomaterials Congress. 1st – 5th June 2012, Chengdu, China. Poster.

- **Riccardo Levato**, Elisabeth Engel, Miguel A. Mateos-Timoneda, Josep A. Planell. "Influence of bioadhesive coatings on cells migration from polylactide microcarriers for cell therapy". 3rd TERMIS World Congress "Tissue Engineering and Regenerative Medicine", 5th – 8th September 2012, Vienna, Austria. Oral Presentation.

- **Riccardo Levato**, Elisabeth Engel, Nuria Rubio, Jeronimo Blanco, Miguel A. Mateos-Timoneda, Josep A. Planell. "Surface Functionalization Role on Cell Delivery from Microcarriers for Cell Therapy". 25th European Conference on Biomaterials, 8th – 12th September, 2013, Madrid, Spain. Oral Presentation.

- **Riccardo Levato**, Jetze Visser, Josep A. Planell, Elisabeth Engel, Jos Malda, Miguel A. Mateos-Timoneda. "Biofabrication of osteochondral grafts via 3D printing of cell-laden microcarriers in a gelatin methacrylamide/gellan gum bioink". 26th European Conference on Biomaterials, 31st August – 3rd September 2014, Liverpool, UK. Oral Presentation.

# Acknowledgments

This doctoral thesis represents my work of the past four years. In this timespan, a lot of things happened and I shared this journey with many people whose contribution has been fundamental to get through the challenges of life and research. I will try to put into words the feelings I have, and although nothing I can write here can fully explain the importance you have for me, I hope these short thoughts can stay as a nice memory for you, whenever you will open this book again.

First of all, I owe my most sincere thankfulness to my director Dr. Miguel Ángel Mateos-Timoneda. Miguel always had an open ear for me and his stimulating suggestions and encouragement helped me throughout the entire research and writing. At the same time he gave me full support and freedom to explore my creativity and scientific interests. I am really glad for sharing these years with you, Miguel, that besides being an excellent director, are very good friend, always present whenever needed.

I want to thank Dr. Elisabeth Engel, the group leader of the Biomaterials for Regenerative Therapies group at IBEC, and tutor of this thesis. The door of her office was always open for me, and I owe her a special gratitude for her support and fruitful conversations. Early in my career path, since I stepped into the world of cell assays and biology, her expertise and open-mindedness helped me to learn and grow as a scientist in the field of Tissue Engineering.

I deeply acknowledge the help of Prof. Josep Planell for accepting me in the lab. His full support has been fundamental in these years and his wise and earnest criticism helped to improve my research. I am also really thankful to Dr. Oscar Castaño for sharing his passion for research and his keen suggestions.

One of the things I am most grateful of is the friendly environment in the Biomaterials lab and at IBEC that made every day of work amazing. Tiziano, Xavi, Nad, Arlyng, Aitor, Zaida, Andrea and Asma it was awesome to find great friends as you once I arrived in Barcelona, and Cris, Laura, Sole, Claudia, Joan, Irene, Doug and everyone that I get to know or came later made (and is making) things even nicer. Thanks also to Pablo, Yassine, Sara and David, and the members of the BIBITE group lead by Dr. Maria Pau Ginebra for the good moments spent together.

I also would like to give a special thank to Dr. Jos Malda from the University Medical Center Utrecht for the great collaboration and the research stay at his lab. His friendly attitude made me feel welcomed from the very beginning, and his commitment to the project and constructive criticism had a great impact over my experience, as well as his innovative scientific vision had over the development of my research. Together with Jos, all the amazing staff of the Orthopaedic Department of UMC made me feel at home in their team and in Holland, since the very beginning of my stay. Dank je wel Jetze, Mattie, Debby, Vivian, Loek, Emile,